ISTANBUL TECHNICAL UNIVERSITY ★ GRADUATE SCHOOL

QUANTUM CORRECTED CORRELATION FUNCTIONS AND POWER SPECTRA OF SPECTATOR SCALAR AND INFLATON FIELDS DURING INFLATION

Ph.D. THESIS

Gülay KARAKAYA

Department of Physics Engineering

Physics Engineering Programme

MAY 2022

ISTANBUL TECHNICAL UNIVERSITY ★ GRADUATE SCHOOL

QUANTUM CORRECTED CORRELATION FUNCTIONS AND POWER SPECTRA OF SPECTATOR SCALAR AND INFLATON FIELDS DURING INFLATION

Ph.D. THESIS

Gülay KARAKAYA
(509132104)

Department of Physics Engineering

Physics Engineering Programme

Thesis Advisor: Asst. Prof. Vakıf Kemal ÖNEMLİ

MAY 2022

İSTANBUL TEKNİK ÜNİVERSİTESİ ★ LİSANSÜSTÜ EĞİTİM ENSTİTÜSÜ

ENFLASYON SÜRECİNDE İZLEYİCİ SKALER VE İNFLATON ALANLARININ KUANTUM DÜZELTİLİ KORELASYON FONKSİYONLARI VE GÜÇ TAYFLARI

DOKTORA TEZİ

Gülay KARAKAYA
(509132104)

Fizik Mühendisliği Anabilim Dalı

Fizik Mühendisliği Programı

Tez Danışmanı: Dr. Öğr. Üyesi Vakıf Kemal ÖNEMLİ

MAYIS 2022

Gülay KARAKAYA, a Ph.D. student of ITU Graduate School with ID number 509132104, successfully defended the thesis entitled "QUANTUM CORRECTED CORRELATION FUNCTIONS AND POWER SPECTRA OF SPECTATOR SCALAR AND INFLATON FIELDS DURING INFLATION", which she prepared after fulfilling the requirements specified in the associated legislations, before the jury whose signatures are below.

Thesis Advisor :	**Asst. Prof. Vakıf Kemal ÖNEMLİ** Istanbul Technical University	....
Jury Members :	**Assoc. Prof. Özgür AKARSU** Istanbul Technical University	....
	Assoc. Prof. Tolga BİRKANDAN Istanbul Technical University	....
	Prof. Vedat Nefer ŞENOĞUZ Mimar Sinan Fine Arts University	....
	Assoc. Prof. Ayşe Nihan KATIRCI Doğuş University	....

Date of Submission : 26 April 2022
Date of Defense : 31 May 2022

To my dear parents,

FOREWORD

I would like to thank my advisor, Dr. Vakıf Kemal ÖNEMLİ. He is a very hardworking person. It's very nice to know and work with someone who has such good and different ideas. I am very lucky to be his student. I want to thank him for his endless support throughout my PhD studies.

I would like to thank Assoc. Prof. Tolga BİRKANDAN for his supports.

I would like to thank my committee members Assoc. Prof. Özgür AKARSU and Prof. Vedat Nefer ŞENOĞUZ for the constructive and helpful comments during my PhD studies. It is a pleasure to express my thanks to the other members of my supervisory committee: Prof. Abdurrahman Savaş ARAPOĞLU, Assoc. Prof. Tolga BİRKANDAN, Assoc. Prof. Ayşe Nihan KATIRCI and Asst. Prof. Barış YAPIŞKAN. I have been honored by their presence on my committee.

I would like to thank my father Yusuf KARAKAYA, my mother Hanım KARAKAYA and my brother Akman KARAKAYA for constantly encouraging me the job i want to do during my education.

I would like to thank my friends Sevtap KARGIN, Şeyma BAYRACI, Tansu ERSOY and Elif PEKSU.

May 2022 Gülay KARAKAYA
(Physicist)

TABLE OF CONTENTS

Page

ABBREVIATIONS

FRW	**:** Friedmann-Robertson-Walker
QFT	**:** Quantum Field Theory
VEV	**:** Vacuum Expectation Value
IR	**:** Infrared
MMC	**:** Massless Minimally Coupled
SK	**:** Schwinger-Keldish Formalism

SYMBOLS

∂_μ	:	Partial Derivative
$g_{\mu\nu}$	:	Covariant Components of the Metric Tensor
R	:	Ricci Scalar
H	:	Hubble Parameter
ε	:	Slow-roll Parameter
ϕ	:	Spectator Scalar Field
φ	:	Inflaton Field
m	:	Mass
λ	:	Self-coupling Strength
Δ^2	:	Power Spectrum
n	:	Spectral Index
α	:	Running of the Spectral Index
σ^2	:	Variance

LIST OF TABLES

Page

LIST OF FIGURES

Page

QUANTUM CORRECTED CORRELATION FUNCTIONS AND POWER SPECTRA OF SPECTATOR SCALAR AND INFLATON FIELDS DURING INFLATION

SUMMARY

The inflationary cosmology not only explains apparently mysterious features of the universe like the flatness, horizon, and relic particle abundance problems, but also provides a natural mechanism to produce primordial density fluctuations that eventually lead to the cosmic structure formation. The primordial density perturbations are generated spontaneously from the quantum fluctuations of a scalar field, called inflaton, that drives the inflation. The physical origin of quantum fluctuations is the uncertainty principle that manifests itself as the virtual particle pair production out of vacuum. The observed anisotropies in the cosmic microwave background (CMB) are believed to be the amplified imprints of the fluctuations of an inflaton which later grow, due to gravitational instability, to become galaxies and clusters of galaxies. Variation of the amplitudes of fields with length scales is measured by the spectral index n. Predictions of the inflation models for the spectral index and its variation with scale, quantified the by running of the spectral index α, can be compared with observations to discriminate between the alternative inflation models. It is, therefore, important to study the correlation function and power spectrum Δ^2 of the quantum fluctuations to understand the distribution and the origin of large scale structure in the universe.

During inflationary expansion, physical length scales grow much more rapidly than the horizon size, therefore the scales continuously exit the horizon. After the end of inflation though the horizon size grows more rapidly than the physical length scales, hence the scales begin to reenter the horizon. The quantum fluctuation modes that get caught up in the inflationary expansion are also stretched, with their wavelengths increased in proportion to the scale factor $a(t)$, across a wide range of length scales. In the history of each fluctuation mode of cosmological interest with comoving wavenumber k, there exists a comoving time t_k at which the mode exits the horizon. The fluctuation mode k is therefore a subhorizon [ultraviolet (UV)] mode when $t < t_k$ but becomes a superhorizon [infrared (IR)] mode when $t > t_k$. After the time t_k, the amplitude of the mode remains constant and the mode retains the same form—hence, the fluctuation mode is converted to classical perturbation until it reenters the horizon to induce structure formation in the universe. Different fluctuation modes go through the horizon crossing at different times. In fact, the modes that exit latest reenter earliest. The modes that exited the horizon at late times during inflation, reenter long before the modes that exited at early times during inflation and hence play the key role in seeding the structure formation. The modes which are reentering the horizon around the current epoch that are observed via large-angle CMB anisotropies exited the horizon at late times when the universe e-folded about fifty times. Since the UV modes are irrelevant for the late time behaviour of scalar potential models, using the IR truncated fields and the stochastic formalism, introduced by Starobinsky, gets the exact leading terms that the Schwinger-Keldish formalism gives at each loop order.

The outline of the thesis is as follows. In Sec. 1, we introduce the formalism we use and define the physical quantities we compute throughout the thesis.

In Sec. 2, we consider an IR truncated spectator scalar field $\bar{\phi}(t,\vec{x})$ with potential $V(\phi)=\frac{m^2}{2}\phi^2\pm\frac{\lambda}{4!}\phi^4$ during a cosmological constant driven de Sitter inflation hence, the expansion rate H is a constant. The model, not only provides us an opportunity to predict observable cosmological characteristics of a yet hypothetical scalar which does not participate in driving inflation but also mimics the behaviour of an inflaton which drives the inflation so that one can draw qualitative conclusions about the quantum dynamics and fluctuations of a self-interacting inflaton. We compute the quantum corrected two-point correlation function of the IR truncated scalar at two-loop order. The tree-order correlator is positive. For a fixed physical distance, in the massless limit, it grows like $\ln a$ at late times. The growth is suppressed for massive scalars. As the mass increases, so does the suppression. The one-loop correlator, on the other hand, is negative. For a fixed physical distance, in the massless limit, it grows like $-\lambda\ln^3 a$ at late times. The growth, however, is suppressed for massive scalars. The suppression is sensitive to increase in mass. (In fact, for $m>\frac{H}{2}$, it asymptotes to zero.) In this section, we propose a method to compute the stochastic contributions to the quantum corrected Δ^2, n and α. The results show that, the spectrum of fluctuations of a massive scalar is red tilted at tree and one-loop order. As the mass decreases, so does the tilt. In the massless limit, although the tilt vanishes at tree-order—hence the tree-order spectrum is scale invariant—the one-loop correction still implies a red tilt. Physically, this means that the amplitudes of fluctuations, in both massive and massless cases, grow toward the larger scales. Then, we compare our numerical predictions for the n_ϕ and α_ϕ with the measurements of Planck 2018 Collaboration obtained by analyzing the CMB data. Finally, we compute the variance of the field variation at tree and one-loop order. The result implies that the tree-order variance decreases when the quantum corrections are included. Physically, this means that the difference between the actual effect perceived by a local observer in the field strength and the average effect, as fluctuations happen, is not as large as the tree-order variance implies.

In Sec. 3, we consider an IR truncated inflaton field $\bar{\varphi}(t,\vec{x})$ with the same potential $V(\varphi)=\frac{m^2}{2}\varphi^2\pm\frac{\lambda}{4!}\varphi^4$ which drives the inflation, during a slow-roll inflation—hence the H is necessarily time dependent—and study the quantum dynamics and fluctuations of the field. We decompose the inflaton $\varphi(t,\vec{x})$ into an unperturbed (averaged) background field $\bar{\varphi}(t)$ which is a function of time only and a quantum fluctuation field $\delta\varphi(t,\vec{x})$ with a completely different time evaluation coupled to the background field that evolves independently. As the classical restoring force pushes the $\bar{\varphi}(t)$ back down to the configuration where the potential is minimum and therefore the inflaton rolls downhill, the $\delta\varphi(t,\vec{x})$ engenders eventually the density perturbations required for the structure formation in the universe. We solve the equations of motion of the fields and Einstein's field equation and get the scale factor $a(t)$, expansion rate $H(t)$, slow-roll parameter $\varepsilon(t)$ and the background field $\bar{\varphi}(t)$ in terms of initial values H_{i0} and ε_{i0} with $\mathcal{O}(\lambda)$ corrections that arise as a backreaction of interactions. We then obtain, in the $\lambda\to 0$ limit, the free field mode expansion for the tree-order fluctuation field $\delta\varphi_0(t,\vec{x})$ and express the full fluctuation field $\delta\varphi(t,\vec{x})$ in terms of $\delta\varphi_0(t,\vec{x})$. We compute the quantum corrected two-point correlation function for the IR truncated fluctuation field. The correlation function is evaluated at the full solution of the effective field equation. Therefore, the tree-order and one-loop correlators respectively get $\mathcal{O}(\lambda)$ and $\mathcal{O}(\lambda^2)$

corrections due to the backreaction of interactions on the dynamics of spacetime geometry. The tree-order correlator in the $\lambda \to 0$ limit for a fixed physical distance grows at early times and asymptotes to a constant at late times. The growth is reduced as the ε_{i0} increases. For the $+$ $(-)$ sign choice in the interaction potential, the $\mathcal{O}(\lambda)$ correction at tree-order enhances (reduces) the growth whereas the $\mathcal{O}(\lambda)$ correction at one-loop order reduces (enhances) the growth. The figures given in this section imply that the amplitudes of fluctuations do not grow forever during inflation—which would lead to proliferation of ever newer regions of the universe. The inflaton, therefore, cannot continue rolling up its potential but comes to a half eventually. At this stage, the classical rolling of the inflaton down its potential, due to the push of the restoring force, start to dominate the motion rather the random up and down jigglings of the field, due to the quantum fluctuations. As the inflaton rolls downhill, in this regime, the fluctuations engender the density perturbations, as pointed out earlier. Generalizing the method we introduced in Sec. 2 to the case of inflaton driven inflation, where the H is time dependent, we compute the stochastic contributions to the $\Delta^2_{\delta\bar{\varphi}}$, $n_{\delta\bar{\varphi}}$ and $\alpha_{\delta\bar{\varphi}}$ of the fluctuation at tree and one-loop order. The $\mathcal{O}(\lambda)$ correction to the spectrum of inflaton fluctuations is enhanced significantly, due to the terms involving huge factors of ε_{i0}^{-2} and ε_{i0}^{-1} that are not present in the spectrum of the spectator scalar during cosmological constant driven inflation considered in Sec. 2. (The $\mathcal{O}(\lambda)$ correction to the $n_{\delta\bar{\varphi}}$, on the other hand, gets enhanced by the terms involving the factor ε_{i0}^{-1}.) The $\Delta^2_{\delta\bar{\varphi}}$, in the $\lambda \to 0$ limit, is red tilted. The $\mathcal{O}(\lambda)$ correction to the $n_{\delta\bar{\varphi}}$ enhances (reduces) the red tilt for the $+$ $(-)$ sign choice in the self-interaction potential. Our numerical predictions for the $n_{\delta\bar{\varphi}}$ and $\alpha_{\delta\bar{\varphi}}$ of the inflaton fluctuations are in accordance with the cosmological measurements by the Planck 2018 Collaboration. Comparing the predictions for the n and α in Secs. 2 and 3 with the observed values, we conclude that the data favor the inflaton model more.

Sec. 4 is on the problems that are left open in this thesis. The quantum corrected power spectrum can be defined in two different ways: (i) as the Fourier transform of quantum corrected two-point correlation function or (ii) as the norm square of quantum corrected mode function. Although at tree-order these alternative definitions give exactly the same result, they differ at loop orders. We implemented the first alternative to define the stochastic power spectrum that we introduced to the literature. Computing the fully renormalized quantum corrected power spectrum of fields using the Schwinger-Keldish (SK) formalism is an extremely formidable task which has not been done yet. The stochastic power spectrum is an approximation which only gets the dominant leading terms at each loop order but it misses the suppressed subleading terms. The deviation of the stochastic power spectrum from the exact result is an open problem. To estimate the deviation, we considered the simplest model: massless minimally coupled (MMC) scalar with a quartic self-interaction in de Sitter spacetime. To compute the exact fully renormalized quantum corrected power spectrum, via definition (i), we attempted to compute the one-loop two-point correlator using the SK formalism. We managed to reduce the computation into the evaulation of four integrals and even computed one of them. The result, however, is too long to give in a paper. Thus, estimating the deviation of the stochastic power spectrum from the exact result—even in a simplest possible model—is still an issue to be resolved. We, however, compute the quantum corrected power spectrum for the scalar in the simplest model considered in this section at one-loop order via the alternative definition (ii). We summarize the conclusions in Sec. V.

ENFLASYON SÜRECİNDE İZLEYİCİ SKALER VE İNFLATON ALANLARININ KUANTUM DÜZELTİLİ KORELASYON FONKSİYONLARI VE GÜÇ TAYFLARI

ÖZET

Şişme kozmolojisi, yalnızca düzlük, ufuk, ve kalıntı parçacık bolluğu problemleri gibi evrenin gizemli görünen özelliklerini açıklamakla kalmaz, aynı zamanda sonuç da kozmik yapı oluşumuna yol açan ilkel yoğunluk pertürbasyonlarını üreten doğal bir mekanizma sağlar. İlkel yoğunluk pertürbasyonları, evreni şişiren ve inflaton adı verilen skaler alanın kuantum dalgalanmalarından kendiliğinden üretilir. Kuantum dalgalanmalarının fiziksel kaynağı, vakumdan sanal parçacık üretimi olarak kendini gösteren belirsizlik ilkesidir. Kozmik mikrodalga fonunda gözlemlenen anizotropilerin bir inflaton alanının, sonradan gravitasyonel kararsızlık vasıtasıyla, galaksiler ve galaksi kümeleri haline gelecek olan, kuantum dalgalanmalarının büyümüş izleri olduğuna inanılmaktadır. Alanların genliklerinin uzunluk ölçeğine göre değişimi tayf indeksi ile ölçülür. Şişme modellerinin tayf indeksi ve tayf indeksinin ölçekle değişimi olan tayfın indeksinin akışı için verdiği öngörüler gözlemlerle kıyaslanabilir ve farklı modeller arasında ayıklama yapılabilir. Öyleyse kuantum dalgalanmalarının korelasyon fonksiyonunu ve güç tayfını Δ^2 çalışmak evrendeki büyük ölçekli yapıların kökenini ve dağılımını anlamak için önemlidir.

Şişerek genişleme sürecinde, fiziksel uzunluk ölçekleri ufuk boyundan çok daha hızlı uzarlar, bu yüzden de ölçekler, sürekli bir şekilde, ufkun dışına çıkarlar. Şişme sona erdikten sonra, ufuk boyu fiziksel uzunluk ölçeklerinden daha hızlı uzar, ve dolayısıyla ölçekler ufuktan içeri yeniden girmeye başlarlar. Şişerek genişlemeye yakalanan kuantum dalgalanma modları da, dalga boyları ölçek faktörü $a(t)$ ile orantılı bir şekilde, geniş yelpazeli bir uzunluk ölçek aralığında uzarlar. Kozmolojinin ilgi alanına giren her bir k eşhareketli dalgasayılı dalgalanma modunun geçmişinde, bu modun ufkun dışına çıktığı bir eşhareketli zaman t_k vardır. Öyleyse, dalgalanma modu k, $t < t_k$ iken bir ufukaltı [ultraviyole (UV)] moddur, ama $t > t_k$ olduğunda ufuküstü [kızılötesi (KÖ)] bir mod haline gelir. t_k anından sonra, modun genişliği sabit kalır ve mod formunu aynen korur—yani dalgalanma modu evrende yapı oluşumunu indüklemek için tekrar ufuktan içeri girene kadar klasik pertürbasyona dönüşürülmüş olur. Farklı dalgalanma modları ufuk geçişlerini, geç çıkan önce girecek şekilde, farklı zamanlarda yaparlar. Bundan dolayı şişmenin geç zamanlarında ufuktan çıkan modlar, şişmenin erken zamanlarında ufuktan çıkan modlardan çok daha önce ufuktan içeri girerek, evrende yapı oluşumunu tetiklemede anahtar rol oynarlar. Evrenin biz gözlemcilerin yaşamakta olduğu evresinde ufuktan giren ve kozmik mikrodalga fonunda geniş açı anizotropileri olarak gözlemlenen modlar, evrenin yaklaşık e^{50} kat büyüdüğü geç zamanlarında ufuktan çıkmış olan modlarıdır. UV modları, skaler potansiyel modellerinin geç zamanlardaki davranışları açısından önemsiz olduklarından, hesaplarda kuantum alanlarının UV modları kesilip atılarak yalnızca KÖ modları tutulacak şekilde kullanılmaları (stokastik formülasyon), her bir

ilmek mertebesinde Schwinger-Keldish formülasyonu ile elde edilen sonucun baskın öncü terimini aynen elde etmek için yeterli olmaktadır.

Ana hatlarıyla tezin içeriği şöyle özetlenebilir. Bölüm 1'de tezde kullanılan formulasyon tanıtılmakta ve hesaplanan fiziksel nicelikler tanımlanmaktadır.

Bölüm 2'de, kozmolojik sabitin evreni şişirdiği dolayısıyla, H'nın sabit olduğu bir de Sitter şişmesi sürecinde $V(\phi)=\frac{m^2}{2}\phi^2\pm\frac{\lambda}{4!}\phi^4$ potansiyeline sahip, UV modları kesilip atılarak KÖ modları tutulmuş bir izleyici skaler alan incelenmektedir. Bu model bize henüz yalnızca varsayımsal olan bir skaler alanın gözlemlenebilir kozmolojik karakteristiklerini öngörme fırsatı sağlamakla kalmaz aynı zamanda şişmeyi sağlayan inflaton alanı modeline benzer davrandığı için, kendisiyle etkileşen bir inflaton alanının kuantum dinamiği ve dalgalanmaları hakkında niteliksel çıkarımlarda bulunabilmemizi sağlar. Bu bölümde, önce ele alınan izleyici skaler alan için kuantum düzeltili iki-nokta korelasyon fonksiyonu iki-ilmek mertebesinde hesaplanmaktadır. Ağaç mertebesinde iki-nokta korelatör pozitiftir. Sabit bir eşhareketli uzaysal (yani artan fiziksel) mesafe için bu korelatör geç zamanlarda kütlesiz durumda bir sabite yakınsarken, kütle arttıkça bu sabit sıfıra gider. Sabit bir fiziksel mesafe için ise bu korelatör, geç zamanlarda, kütlesiz durumda $\ln a$ gibi büyürken, kütle arttıkça bu büyüme bastırılmaktadır. Bir-ilmek korelatör ise negatiftir. Sabit bir eşhareketli uzaysal mesafe için bu korelatör, geç zamanlarda, kütlesiz durumda $-\lambda\ln^2 a$ gibi büyürken kütleli durumda sıfıra yakınsar. Sabit bir fiziksel mesafe için ise bu korelatör, geç zamanlarda, kütlesiz durumda $-\lambda\ln^3 a$ gibi büyürken, kütle arttıkça bu büyüme şiddetli bir şekilde bastırılmaktadır. (Hatta $m>\frac{H}{2}$ için sıfıra yakınsar.) Yine bu bölümde kuantum düzeltili Δ^2, n ve α için stokastik katkıları veren bir metot önerilmekte ve bu nicelikler ağaç, bir- ve iki-ilmek mertebelerinde hesaplanmaktadır. Sonuçlar, skaler alanın dalgalanmalarının ağaç ve bir-ilmek mertebelerinde kızıla eğildiğini, kütle azaldıkça eğikliğin de azaldığını göstermektedir. Kütlesiz limitte, eğiklik ağaç mertebesinde sıfıra giderken, bir-ilmek mertebesinde kızıla kaymaktadır. Fiziksel olarak bu, skaler alan dalgalanmalarının genliklerinin dalga boyları (ölçek) büyüdükçe arttığı anlamına gelir. Daha sonra bu modelde hesaplanan n ve α'nın sayısal değerleri kozmik mikrodalga fonu verileri analiz edilerek elde edilen Planck 2018 sonuçlarıyla kıyaslanmaktadır. Son olarak, skaler alandaki değişimin varyansı hesaplanmaktadır. Bir-ilmek mertebesindeki varyans göstermektedir ki kuantum düzeltiler ağaç mertebesindeki varyansı azaltmaktadır. Yani yerel bir gözlemcinin alan dalgalandıkça algıladığı alan şiddetindeki gerçek etkinin ortalama etkiden farkı, ağaç mertebesindeki varyansın ima ettiğinden azdır.

Bölüm 3'te, $V(\varphi)=\frac{m^2}{2}\varphi^2\pm\frac{\lambda}{4!}\varphi^4$ potansiyeline sahip bir φ inflaton alanının evreni şişirdiği—dolayısıyla H'nın zamanla değiştiği—bir yavaş-yuvarlanma şişmesi sürecinde, bu φ alanının kuantum dinamiği ve dalgalanmaları incelenmektedir. Model çalışılırken φ alanı sadece zamanın fonksiyonu olan ortalama bir $\bar{\varphi}(t)$ fon alanı ile bu fon üzerindeki uzayzamanın fonksiyonu olan küçük $\delta\varphi(t,\vec{x})$ kuantum dalgalanmalarının toplamı olarak düşünülmektedir. Şişme sürecinde $\bar{\varphi}(t)$, klasik geri çağırıcı kuvvetin etkisiyle potansiyelin minimumuna doğru inerken $\delta\varphi(t,\vec{x})$ dalgalanmaları ileride evrendeki yapı oluşumunu sağlayacak olan yoğunluk perturbasyonlarının kökenini üretirler. $\bar{\varphi}$ ve $\delta\varphi$ alanlarının hareket denklemleri birbirlerinden farklıdır. ($\bar{\varphi}$'ın hareket denklemi $\delta\varphi$'den bağımsız olup, $\delta\varphi$'nin denklemi $\bar{\varphi}$'ye bağlıdır.) Bu hareket denklemleri, Einstein'ın alan denklemleriyle birlikte çözülerek modelde uzayın ölçek faktörü $a(t)$, genişleme oranı $H(t)$, inflatonun yavaş-yuvarlanma parametresi $\varepsilon(t)$ ve fon alanı $\bar{\varphi}(t)$, λ–mertebesindeki düzeltileriyle birlikte H_{i0} ve ε_{i0} başlangıç değerleri cinsinden elde edilmektedir. (Düzeltiler, inflatonun kendisiyle etkileşiminin, uzayzaman geometrisinin dinamiğine olan geri tepkisinden dolayıdır.) Sonra, $\lambda \to 0$ limitinde, $\delta\varphi_0$ kuantum dalgalanmalarının mod açılımı elde edilmektedir. Etkileşimlerin dahil edildiği durumda ise $\delta\varphi$ tam alanı $\delta\varphi_0$ cinsinden ifade edilmekte ve UV-modları atılarak, şişme sürecinde, $\delta\varphi$ tam alanının kuantum düzeltili iki-nokta fonksiyonu elde edilmektedir. (İki-nokta fonksiyonu alan denklemlerinden elde edilen, a, H, ε ve $\bar{\varphi}$ çözümleri kullanılarak hesaplandığından ağaç mertebesindeki korelatör, inflatonun kendisiyle etkileşiminden kaynaklı, λ–mertebesinde düzelti alırken, bir-ilmek korelatör λ^2-mertebesinde düzelti alır.) Ağaç mertebesindeki korelatör, $\lambda \to 0$ limitinde, sabit bir fiziksel mesafe için erken zamanlarda büyüyerek geç zamanlarda bir sabite yakınsar. Bu büyüme ε_{i0} arttıkça zayıflamaktadır. λ'nın sıfırdan farklı olduğu durumda, kendisiyle etkileşme teriminde $+$ $(-)$ işaret seçimi için ağaç korelatör kaynaklı λ–mertebeli düzelti bu büyümeyi güçlendirir (zayıflatır). Bir-ilmek korelatör kaynaklı λ–mertebeli düzelti ise bu büyümeyi zayıflatır (güçlendirir). Verilen dört grafik, dalgalanma genliklerinin sürekli artmadığını, bir sabite yakınsadığını göstermektedir. Bu yapı oluşumu için önemlidir çünkü, dalgalanma genliklerinin sürekli artması, evrende dalgalanmaların yapı oluşumunu tetiklemek yerine sürekli büyüyen yeni yeni bölgeler doğurmasına sebep olurdu. Modelde inflaton alanının genliği şişme sürecinde vakumdan parçacık, üretilmesi (dalgalanmalar) dolayısıyla artar ancak bu artış sonsuza kadar sürmez ve sonunda durur. Yani inflaton potansiyelinde yukarı yuvarlanır ve durur. Daha önce de belirtildiği gibi, bu aşamada klasik geri çağırıcı kuvvet baskın gelmeye başlar ve inflaton, potansiyelin minimumuna doğru aşağı yuvarlanırken küçük genlikli dalgalanmaların yol açtığı yukarı-aşağı tedirginlikler, sonuçta yapı oluşumu için gerekli olan yoğunluk pertürbasyonları doğururlar. Bu bölümde, daha sonra Bölüm 2'de önerilen metot, genişleme oranı H'nın zamana bağlı olduğu, inflaton tarafından şişirilen uzayzamana genelleştirilerek, dalgalanmalar için Δ^2, n ve α ağaç ve bir-ilmek mertebelerinde hesaplanmaktadır. Sonuçlar, inflaton dalgalanmalarının güç tayfına gelen λ–mertebesindeki kuantum katkısının, Bölüm 2'de incelenen izleyici skalerin güç tayfında bulunmayan, çok büyük ε_{i0}^{-2} ve ε_{i0}^{-1} faktörlerini içeren terimler sebebiyle güçlendiğini göstermektedir. Tayf indeksine gelen λ–mertebesindeki kuantum katkısı ise ε_{i0}^{-1} faktörünü içeren terimler sebebiyle büyümektedir. Güç tayfı, $\lambda \to 0$ limitinde, kızıla eğiktir. Yani izleyici skaler alan modelinde olduğu gibi, burada da inflaton dalgalanmalarının genlikleri dalgalanmanın dalgaboyu (ölçek) büyüdükçe artmaktadır. λ'nın sıfırdan farklı olduğu durumda, kendisiyle etkileşme teriminde $+$ $(-)$ işaret seçimi için, λ mertebeli düzelti bu eğikliği arttırmaktadır (azaltmaktadır). Hesaplanan n ve α'nın öngördüğü sayısal değerler Planck 2018 ölçümleriyle uyumludur. Bu ölçümler, izleyici skaler alan modelinden ziyade, inflaton alanını desteklemektedir.

Bölüm 4, tezdeki çalışmaların işaret ettiği henüz açıklığa kavuşmamış problemler üzerinedir. Kuantum düzeltmeli güç tayfı iki farklı şekilde tanımlanabilir: (i) Kuantum düzeltili iki-nokta korelasyon fonksiyonunun Fourier dönüşümü veya (ii) Kuantum düzeltili mod fonksiyonunun normun karesi olarak. Bu alternatif tanımlar ağaç mertebesinde tam olarak aynı sonucu vermelerine rağmen, ilmek mertebelerinde farklılık gösterirler. Bu tezde, literatüre ilk defa sunulan stokastik güç tayfını tanımlamak için ilk tanım kullanılmaktadır. Kuantum alanlarının, tamamıyla renormalize edilmiş kuantum düzeltili güç tayfını SK formalizmini kullanarak hesaplamak son derece zorlu, henüz başarılmamış bir problemdir. Stokastik güç tayfı ise, her ilmek mertebesindeki baskın öncü terimleri veren ancak bastırılmış diğer terimleri vermeyen bir yaklaşımdır. Stokastik güç tayfının tam sonuçtan sapması hesaplanmamış açık bir problemdir. Sapmayı hesaplamak için, bu bölümde, basit bir model olan kütlesiz, minimal bağlı, kendisiyle dördüncü dereceden etkileşim potansiyeline sahip skaler alan ele alınmıştır. Tamamıyla renormalize edilmiş, kuantum düzeltili güç tayfı için tam sonuç tanım (i) vasıtasıyla, SK formülasyonu kullanılarak hesaplanmaya başlanmış ve bir-ilmek korelatör hesabı dört tane uzayzaman integralin alınması problemine indirgenmiştir. Integrallerin birinin hesabı tamamlanmış ancak sonuç bu tezde verilmeyecek kadar uzundur. Şu aşamada, bu basit modelde bile stokastik güç tayfının tam sonuçtan sapmasını hesaplamak hala çözülmesi gereken bir problem olarak durmaktadır. Bununla birlikte, bu bölümde, ele alınan basit modelde skaler alanın güç tayfı için tam sonuç tanım (ii) kullanılarak bir-ilmek mertebesinde elde edilebilmiştir. Bu tezde yapılan çalışmaların sonuçlarını Bölüm 5'te özetlenmektedir.

1. INTRODUCTION

Physicists typically imagine that the universe began with a big bang (an initial singularity) followed by a brief period of inflation [1–20], when the universe was about 10^{-36} sec. old, that lasted only about 10^{-34} sec. during which the universe expanded by at least a factor of e^{60} and the universe became spatially flat, almost homogeneous and isotropic. The origin of the big bang, in the language of QFT was fluctuations [21–23] in a primordial wave functional of probabilities and potentialities. Out of one of these fluctuations, it is believed, that the primordial substance for the universe emerged as an outcome reality. It is assumed that a field which has negative pressure—known as scalar field in field theory—drives the expansion in this primordial substance.

At some stage in this earliest epoch, the inflationary scalar field φ, called inflaton, with potential $V(\varphi)$ and density $\rho = \frac{1}{2}\dot{\varphi}^2 + V(\varphi)$ that evolves slowly and becomes dominant while the density of other fields diminish rapidly during expansion. As the inflaton rolls down its potential slowly, it drives the inflationary expansion with a huge rate $H \propto \sqrt{V(\varphi)}$ that evolves slowly, hence at this stage, the inflaton behaves like a cosmological constant in driving the expansion. The process of inflation can be eternal. It can start at a highly energetic stage where the quantum fluctuations of the inflaton dominate the classical rolling down motion of the inflaton in its potential. In such a stage, inflaton can roll up its potential, where the expansion rate $H \propto \sqrt{V(\varphi)}$ is larger, creating more space. Hence, the locations where inflaton fluctuates up remarkably, and hence the energy is high, lead to endless profileration of ever newer regions (pocket universes) in a multiverse. As the inflaton executes a drunkard's walk due to the fluctuations, the energy in the regions jitters up and down in response. Therefore, by chance, the inflaton can find itself in a region of lower energy where the amplitude of fluctuations is smaller and hence the classical rolling down of the inflaton in its potential dominates the motion. In such a region, the same fluctuations that lead to profileration of pocket universes in regions where the energy is high, engender, here, the density perturbations, as the inflaton rolls down its potential, that ultimately evolve and lead to the formation of large scale structure—clusters of galaxies, galaxies, stars, planets animals that populate the present universe.

As pointed out in the preceding paragraph, fluctuations are responsible for (i) popping up of the primordial universe into existence out of potentialities in a wave functional, (ii) creating pocket universes and (iii) generating large scale structure in our universe out of vacuum fluctuations of a scalar field. We study case (iii), adopting the natural units where $\hbar = c = 1$, in this thesis.

The vacuum fluctuations correspond to the inflationary particle-antiparticle pair production out of vacuum, persisting for a time Δt and then annihilating. Persistance time Δt obeys the Heisenberg's uncertainty principle according to which the minimum time to resolve an energy change ΔE satisfies $\Delta E\,\Delta t \geq 1$. Therefore, to not resolve such an energy change, the persistence time should satisfy $\Delta E\,\Delta t \leq 1$. Emergence of a particle of mass m and comoving wavenumber k out of vacuum implies a change in energy from zero to $E = \sqrt{m^2+k^2}$. Hence, not to detect such a violation of energy conservation, a virtual particle that emerges out of vacuum should annihilate in $\Delta t \leq 1/\sqrt{m^2+k^2}$. Thus, the lightest virtual particles with longest wavelengths have the longest persistence time hence, they induce greatest field strength and cause strongest quantum effects. In an expanding universe, energy of a particle is time dependent: $E(t,\vec{k}) = \sqrt{m^2+k^2/a^2(t)}$ where $a(t)$ is the scale factor. Therefore, a virtual particle of comoving wavenumber k which emerges out of vacuum at time t can persist [24, 25] for a time Δt satisfying $\int_t^{t+\Delta t} \sqrt{m^2+k^2/a^2(t')}\,dt' \leq 1$. Thus, the expansion causes the virtual particles to persist longer and therefore enhances their quantum effects. For massive fields, the integral grows with Δt and ultimately the inequality is violated which implies that massive particles have finite persistence time. As the mass decreases, the Δt increases. Just as in Minkowski spacetime, massless virtual particles that pop up with sufficiently long wavelengths, can persist forever and therefore have strongest quantum effects. This can be seen [25] easily by considering the uncertainty principle for virtual particles during a de Sitter phase of inflation where $a(t) = e^{Ht}$ and H is constant:

$$\lim_{m\to 0}\int_t^{t+\Delta t} \sqrt{m^2+k^2/a^2(t')}\,dt' = k\int_t^{t+\Delta t} e^{Ht'}dt' = \frac{k}{Ha(t)}[1-e^{-H\Delta t}] \leq 1\,. \qquad (1.1)$$

Therefore, the modes with $k < Ha(t)$ at time t, the inequality is never violated, even for $\Delta t \to \infty$, hence, they persist forever and exhibit strong quantum effects. The inequality

$k < Ha(t)$ implies $\lambda a(t) = \lambda_{\text{phys}} > 1/H$ at time t, where λ is the comoving wavelength and $1/H$ is the horizon size (Hubble length). During inflation, therefore, physical length scales grow more rapidly than the horizon size. Hence, the physical wavelengths are stretched and the modes with $\lambda_{\text{phys}} < 1/H(t)$ at time t are continuously shifted to the modes with $\lambda_{\text{phys}} > 1/H(t)$ as time evolves. Therefore, in the history of each fluctuation mode with comoving wavenumber k, there exits a comoving time t_k at which the scale exits the horizon $[k = H(t_k)a(t_k)]$. The mode k of the fluctuation field is, therefore, a subhorizon [ultraviolet (UV)] mode $[k > H(t_k)a(t_k)]$ when $t < t_k$. But becomes a superhorizon [infrared (IR)] mode $[k < H(t_k)a(t_k)]$ when $t > t_k$. It is at time t_k that inflationary perturbations are imprinted on the universe providing the inhomogeneties that eventually engender the large scale structure formation. This is because, as soon as a particular mode exits the horizon, the crest of the mode loses causal contact with the through and hence, cannot propagate. Its amplitude remains constant and the mode retains the same form—it does not behave like a wave at all. Thus the mode "freezes in" after it exits the horizon and becomes superhorizon. The fluctuation mode is, therefore, converted to classical perturbation. After the end of inflation, the horizon size grows more rapidly than the physical length scales, and the modes that exited the horizon during inflation start reentering the horizon with the same amplitudes as they were when exited—except for a small factor that depends on the ratio of pressure to energy density in the universe when they exit and reenter—and the crests and throughs of the reentering mode regain causal contact and propagate; they start to behave like a wave. The modes that exit the horizon latest during inflation reenter earliest, after the end of inflation, long before the modes that exited at early times during inflation, and play the key role in inducing the structure formation. In fact, the large-scale CMB anisotropies which we observe on the sky are due to the fluctuation modes reentering in the present era that exited the horizon when $a(t_k) = e^{50}$.

It was Starobinsky [26, 27] who realized that the UV modes are irrelevant for the late time behaviour of scalar potential models during inflation and amputated them. An IR truncated field comprised of the modes whose physical wavelengths, at a particular time t, are longer than the horizon size at that time, can be obtained by introducing a time dependent cutoff via a dynamical window function. Starobinsky introduced the Heaviside step function $\Theta(Ha(t) - k)$ in the free field mode expansion of a scalar field to obtain the IR truncated free scalar field and used it to compute stochastic contributions to some observables in scalar potential models. Starobinsky's stochastic approach yields exactly the same leading secular terms [28–36] that the SK (in-in) formalism [37, 38] gives at each perturbative order.

There has been a recent revival of interest in IR dynamics of scalar potential models with various approaches [39–55]. We use the Starobinsky's approach in this thesis to compute the quantum corrected two-point correlation function for an IR truncated self-interacting spectator scalar [56] at two-loop order during a cosmological constant driven inflation where the expansion rate H is constant and for the fluctuations of an IR truncated self-interacting inflaton [57] during slow-roll inflation where the expansion rate H is naturally time dependent. We then introduce [56, 57] a new method to compute the stochastic contributions to the quantum corrected power spectrum Δ^2 [58, 59], spectral index n, and running of the spectral index α in these two cases.

Two-point correlation function $\langle\Omega|\phi(t,\vec{x})\phi(t',\vec{x}')|\Omega\rangle$ of a quantum field ϕ is an average measure of how the amplitude of the field at one event $(t,\vec{x})$ is related to the amplitude of the same field at another event $(t',\vec{x}')$ as the field fluctuates randomly in spacetime. The fluctuation spectrum contains wide range of fluctuations of different length scales (wavelengths) at a particular time t. (The fluctuation generated at early times during inflation are stretched to the scales much larger than our present observable universe whereas the ones generated at late times during inflation are much smaller than our present universe.) Spatial correlation between simultaneous values of the field measured at two spatial points $\vec{x}$ and $\vec{x}'$ and power spectrum $P(t,k)$, which quantifies information about the probability of how many random quantum fluctuations of each size ought to contribute to the spectrum at a given time t, form a Fourier transform pair of each other (Wiener-Khinchin theorem):

$$\langle\Omega|\phi(t,\vec{x})\phi(t,\vec{x}')|\Omega\rangle = \int \frac{d^{D-1}k}{(2\pi)^{D-1}} P_{\phi}(t,k) e^{i\vec{k}(\vec{x}-\vec{x}')} \;, \tag{1.2}$$

in D-dimensions. We call Eq. (1.2) as the first definition of the quantum corrected power spectrum. At tree-order $P_{\phi_0}(t,k)$ is the amplitude square of fluctuations, more correctly the norm square of mode function, i.e.,

$$P_{\phi_0}(t,k) = |u_0(t,k)|^2, \tag{1.3}$$

hence, the name power. (Recall that in quantum mechanics amplitude square is interpreted as probability.) The second definition of the quantum corrected power spectrum is given generalizing Eq. (1.3) to the case of interacting (full) fields,

$$P_\phi(t,k) = |u(t,k)|^2 \,, \tag{1.4}$$

where $u(t,k)$ is the quantum corrected mode function. Note that the two alternative definitions of quantum corrected power spectrum given in Eqs. (1.2) and (1.4) agree with each other at tree-order, but differ at loop orders.

It is, in general, physically more meaningful to define a normalized measure of power

$$\Delta^2_\phi(t,k) \equiv \frac{k^{D-1}}{\pi^{\frac{D}{2}}} \frac{\Gamma(\frac{D}{2})}{\Gamma(D-1)} P_\phi(t,k) \,, \tag{1.5}$$

so that

$$\langle \Omega | \phi(t,\vec{x}) \phi(t,\vec{x}\,') | \Omega \rangle = \int_0^\infty \frac{dk}{k} \frac{\sin(k\Delta x)}{k\Delta x} \Delta^2_\phi(t,k), \tag{1.6}$$

where the measure $\frac{dk}{k}$ is logarithmic. The usual time-independent power spectrum $\Delta^2_\phi(k) = \lim_{t>>t_k} \Delta^2_\phi(t,k)$ can be obtained as a time derivative of the coincident correlation function evaulated at time t_k of the first horizon crossing of the mode k, as we show in this thesis.

If there are more fluctuations of long wavelengths in the spectrum, like the large waves on the surface of a sea in a stormy day, the power is accumulated at long wavelengths and the spectrum is said to be red tilted. If, on the other hand, there are more fluctuations of short wavelengths in the spectrum, like the densely populated ripples on the surface of a sea in a calm sunny day, the power is accumulated at short wavelengths and the spectrum is said to be blue tilted. If there are equal number of fluctuations at all length scales, the spectrum is said to be scale-invariant. (Harrison-Zeldovich spectrum.)

The spectral index n is a measure of how the power (amplitude square) of fluctuations varies with length scale, i.e., with wavenumber k. If the $\Delta^2_\phi(k)$ is assumed to have the simple power-law form $\Delta^2_\phi(k) \propto k^n$ then the spectral is the power of k, which can be obtained as $\frac{d\ln\Delta^2_\phi(k)}{d\ln k}$ for a constant n. If n depends on k, on the other hand, Taylor expanding the $\ln(\Delta^2_\phi(k))$ around the $\ln(k_p)$, where k_p is a pivotal wavenumber, yields

$$\ln(\Delta^2_\phi(k)) = \ln(\Delta^2_\phi(k_p)) + n(k_p)\ln\left(\frac{k}{k_p}\right) + \frac{1}{2!}\alpha(k_p)\ln^2\left(\frac{k}{k_p}\right) + \cdots \,, \tag{1.7}$$

where the expansion coefficients

$$n(k_p) \equiv \frac{d\ln(\Delta^2(k))}{d\ln(k)}\Big|_{k=k_p}, \tag{1.8}$$

and

$$\alpha(k_p) \equiv \frac{d^2\ln(\Delta^2(k))}{d(\ln(k))^2}\Big|_{k=k_p} = \frac{dn(k)}{d\ln(k)}\Big|_{k=k_p}. \tag{1.9}$$

Conventionally, the scale invariant Harrison-Zeldovich spectrum is defined for a n inflaton field so that the corresponding expansion coefficient, the spectral index n_φ, equals 1 rather than more logical 0, as in the case of graviton fluctuations. Thus n_φ is defined as

$$n_\varphi(k) = 1 + \frac{d\ln(\Delta_\varphi^2(k))}{d\ln(k)}, \tag{1.10}$$

which, indeed, equals 1 when the Δ^2 is k independent. In Ref. [56], however, we define the spectral index n_ϕ of our spectator scalar field ϕ the same way as for the graviton:

$$n_\phi(k) = \frac{d\ln(\Delta_\phi^2(k))}{d\ln(k)}. \tag{1.11}$$

In this thesis, on the other hand, to be able to compare our predictions for the n_ϕ with the cosmological measurements provided by the Planck 2018 Collaboration [60], we adopt definition (1.10) for our spectator scalar fluctuations. The tilt, mentioned earlier, is, therefore, quantified for the spectator scalar in this thesis as $n_\phi - 1$. Thus, if the n_ϕ is less than 1, then the spectrum is called red tilted because that implies $\frac{d\ln\Delta_\phi^2(k)}{d\ln k} < 0$ hence, fluctuations with longer wavelengths are dominant in amplitude in the spectrum. Conversely, if the n_φ is larger than 1, then the spectrum is called blue tilted, because the shorter wavelength fluctuations are dominant in amplitude in the spectrum. We quantify the tilt for our spectator scalar with the n_ϕ—the same way as for the graviton.

The second coefficient $\alpha(k_p)$ defined in Eq. (1.9) is a measure of how the spectral index varies with length scale, i.e., with wavenumber k. Hence, we define the running of spectral index

$$\alpha_\phi(k) \equiv \frac{dn(k)}{d\ln(k)}. \tag{1.12}$$

The spectral index $n_{\delta\varphi}$ and its running $\alpha_{\delta\varphi}$ of inflaton fluctuations are the two physical parameters that can be measured from the power spectrum of the CMB which provides the size distribution of temperature fluctuations, i.e., how many hot and cold spots there are of each angular scale on the background. The exact values of the n and α depend on the potential and the details of the inflaton model, hence they can be used to discriminate between the models. We compute and estimate the quantum corrected n and α in the models we consider in Secs. 2 and 3 and compare the results with the measurements [60] in Secs. 2 and 3, respectively.

As a field fluctuates in spacetime, the magnitude of the field strength increases at some locations, at others it decreases. The actual effect that a local observer perceives, therefore, is not an average value measured by a VEV like the two-point correlation function we compute [56, 57] but either an increase or a decrease in the field strength. This is the main reason why some cosmologists doubt about the implications of VEVs. Some cosmologists, however, counterargue [61,62] claiming that, while there is spatial and temporal variation in the actual effects, one can roughly trust the implications of VEVs under certain conditions. We compute the quantum corrected variance for the fluctuations in Sec. 2.7 and show that the tree-order variance decreases if the quantum corrections are taken into account. Thus, the difference between the actual effect perceived by a local observer and the averaged effect measured by a VEV, as the field fluctuates, is not as large as the tree-order variance implies.

1.1 Purpose of the Thesis

As pointed out earlier, not only the origin of our observable universe was a quantum fluctuation—with a large amplitude—of a scalar field, but also the origin of structure formation in our universe was quantum fluctuations—with low amplitudes—of the same field during inflation. Inflation enhances quantum effects which engender the density perturbations that eventually lead to the structure formation in the universe, as explained in the preceding section. Correlations of these quantum fluctuations are therefore important to understand the distrubutions of large scale structure and the cold dark matter in our present universe. The Fourier transform of the two-point correlation function of the fluctuations, the power spectrum, is a measure of how the amplitude square—at tree-order—of fluctuations vary with scale. The two charachteristics of the power spectrum, the spectral index n and its running α can be measured from the power spectrum of the CMB anisotropies which are the amplified imprints of the quantum fluctuations of a scalar field. The predictions for the n and α in different inflation models can, therefore, be used to discriminate between the alternative scenarios.

The purpose of this thesis is to compute the quantum corrected two-point correlation function, power spectrum Δ^2, spectral index n and its running α for the quantum fluctuations of self-interacting, massive, spectator scalar [56]—that exhibits intriguing enhanced quantum effects in the massless limit—and inflaton [57] fields during inflation. Motivated by the fact that inflation enhances quantum effects, we wanted to find out how the quantum corrections during inflation alter these physical quantities. Computing the fully renormalized quantum corrected correlation function, even at one-loop order, is a very difficult endeavor which has not been accomplished yet. We, however, recognized [56, 57] that Starobinsky's stochastic formalism, which yields only the leading secular terms at each perturbative order, simplifies the computation of the quantum corrected two-point correlation function, and that the time derivative of the coincident stochastic correlation function evaluated at time t_k of the first horizon crossing of a mode k yields the stochastic power spectrum, which motivated us further.

1.2 Literature Review

Observed homogeneity, isotropy, flatness and relic particle abundances were the deficiencies of standard big bang cosmology. The idea of inflation [1–20] not only explains such apparently puzzling aspects of our universe, but also introduces an intrinsically quantum mechanical mechanism for the creation of our observed pocket universe out of a vacuum fluctuation. The same mechanism, during inflation, engenders [9–12] density perturbations—out of vacuum fluctuations—required for the structure formation in our pocket universe.

Tyron [21] was the first to propose the origin of the universe with its matter content, as a quantum fluctuation out of vacuum state in spacetime. Vilenkin [22] developed the Tyron's idea, suggesting that not only the matter but also the background spacetime itself was created from absolute nothingness by a quantum tunneling. Hartle and Hawking [23] further extended the idea speculating that the universe appeared as 'Objective reality' out of a fluctuation in a wave functional of the universe.

The energy-time uncertainty relation in an expanding universe [24, 25] implies that lighter virtual particles with sufficiently long wavelengths (IR modes of fluctuations) can have longer persistence time hence can engender strong quantum effects. Inflation continously shifts subhorizon modes to the superhorizon scales, streching their wavelengths beyond the horizon size. Starobinsky [26] was the first to realize that all that matters, for the late time behaviour of scalar potential models during inflation are the IR modes of the field. He obtains [26] an IR truncated scalar field comprised of the IR modes at any time t by introducing a time dependent cutoff via Heaviside Θ–function in the mode expansion of the free field and uses it to compute quantum contributions to some observables in scalar potential models during de Sitter inflation. Starobinsky conjectured that his stochastic formalism reproduces leading logarithmic terms at each perturbative order. With Yokoyama [27] he utilized this conjecture to nonperturbatively solve for the late time limit of a MMC scalar model endowing a self-interaction potential. Starobinsky's stochastic formalism gives exactly the same leading terms [28–36] that the SK [37, 38] in-in formalism—an extension of the Feynman's formulation of QFT developed to produce expectation values rather than in-out matrix elements—gives at each perturbative order. For example, the coincidence limit of the two-point correlation function of a MMC scalar computed by applying [28,29] the Schwinger-Keldish formalism and by applying [29] Starobinsky's formalism yield the same leading terms at one- and two-loop order. Other examples indicating the exact agreement include scalars interacting with fermions [30,31], scalar quantum electrodynamics [32, 33] and scalar with derivative interactions [34–36].

To study the IR dynamics of scalar potential models, there have been various approaches that include: employing stochastic spectral expansion [39], extending the stochastic formalism [40], applying complementary and principal series analysis [41, 42], computing effective actions [43–46], using Schwinger-Keldish formalism [47], implementing Fokker-Planck equation and δN formalism [48], employing $1/N$ expansion [49], adopting reduced density matrix method [50, 51], applying renormalization group analysis [52] and computing effective potentials [53]. Influence of fermions on scalar field fluctuations has been studied in Refs. [54,55]. We employed Strobinsky's approach in Refs [56, 57] which are the papers upon which this thesis is based. In Ref. [56], we consider a spectator scalar field model with potential

$V(\phi) = \frac{m^2}{2}\phi^2 + \frac{\lambda}{4!}\phi^4$ during a cosmological constant driven (de Sitter) inflation where the expansion rate H is constant. We compute the quantum corrected two-point correlation function for the IR truncated scalar at two-loop order and introduce a method to obtain stochastic contributions to the quantum corrected power spectrum Δ^2_ϕ, spectral index n_ϕ and running of the spectral index α_ϕ. Note that alternative definitions [58,59] of the quantum corrected Δ^2_ϕ can be given via the Fourier transform of quantum corrected two-point correlation function or via the quantum corrected mode function squared. We adapt the first alternative in our method. In Ref. [57] we consider an inflaton field model with the same potential which drives the inflation hence the expansion rate H is naturally time dependent. Generalizing the method we introduced in Ref. [56], we compute the same observables for the inflaton fluctuations. We compare our predictions for the n and α obtained in Refs. [56, 57] with the measurements [60] of Planck 2018 Collaboration obtained by analyzing the CMB data.

Some cosmologists argue that an expectation value, like the correlation function we compute, is a measure of average effect and therefore can be misleading since the actual effect perceived by any local observer, as the field fluctuates, is either an increase or a decrease in the field strength. References [56,57], however, argue that while there is spatial and temporal variation in the actual effects, under certain conditions, we can roughly trust what the expectation values imply.

The model we consider is of interest because it predicts, in the massless limit, intriguing enhanced quantum effects. The renormalized energy density and pressure of the scalar field violate [63, 64] the weak energy condition $(\rho + p > 0)$ on cosmological scales at two-loop order. This implies that the expansion of the universe is superaccelerated. As the fluctuations, i.e., inflationary particle production out of vacuum amplifies the field strength, the scalar rises up its potential and develops [28] a self-mass squared which, in turn, reduces the particle production rate. Moreover, the classical restoring force pushes the scalar back down to the configuration where the potential is minimum. The scalar, therefore, cannot continue rolling up its potential forever; as Figs. 2.1-2 in this thesis imply, it eventually comes to a halt. Thus, the model is stable [29]. In many QFT computations—involving UV modes—in cosmology, quantum corrections have to involve changes in the initial state. Without the initial state corrections, the effective field equations diverge on the initial value surface. The model, in the massless limit, also provides [65] a nice example of how perturbative initial state corrections can absorb the initial value divergences. Moreover, the scalar makes [66] a time-dependent contributions to the amplitudes of curvature fluctuations at two-loop order. Using the Starobinsky's formalism, the two-loop corrected two-point correlation function of the scalar and the variance of the fluctuations, in the massless limit, are computed first in Ref. [67]. The mode function for a massive noninteracting inflaton during a slow-roll regime of chaotic inflation in a spatially flat Friedmann-Robertson-Walker spacetime is computed in $D = 4$ in Ref. [68]. We follow the method given in this paper to obtain the tree-order mode function in our model in D–dimensions. The authors study [68] the renormalized stress-energy tensor of the inflaton fluctuations and obtain a scale invariant tree-order power spectrum for the fluctuations. They show that the renormalized stress-energy tensor of the fluctuations grows at early times during inflation but saturates to an almost constant value at late times which implies inflationary particle production out of vacuum. The Feynmann rules for gravity in a spatially flat Friedmann-Robertson-Walker background are derived in Ref. [69] where the authors give explicit expressions for the propagators during inflation, radiation domination and matter domination regimes of cosmic expansion. In our computation of the tree-order correlator, in Sec. 4.3.1, for a MMC scalar, we benefited from the results of the integrals that arise in the computation [69] of the propagators. The authors also compute the quantum corrections to the Newtonian gravitational force in the present matter dominated era and conclude that the corrections are negligible except for the large scales.

2. SPECTATOR SCALAR FIELD DURING DE SITTER INFLATION[1]

As is pointed out earlier, the structure in our universe is believed to be engendered by quantum fluctuations during inflation driven by a scalar field called inflaton, which we study in the next section. In this section, we consider [56] a massive self-interacting spectator scalar field, which does not participate in driving the inflation, during de Sitter phase of an inflation where the expansion rate H is constant. In this model, the cosmological constant drives the inflation. Fluctuations of the spectator scalar mimic the behaviour of inflaton fluctuations qualitatively. Hence, one can draw conclusions about the quantum dynamics and statistics of a self-interacting inflaton fluctuations. Furthermore, such a spectator scalar can still be present during an inflaton driven inflation, therefore, computing its cosmological characteristics provides us the opportunity to predict possible observable effects of a yet hypothetical scalar field. In Sec. 2.1, we present the background spacetime and the Lagrangian of the model. In Secs. 2.2-3, we analyze the model following the Starobinsky's approach and applying the standard techniques of perturbative QFT. In Sec. 2.4, we compute the two-point correlation function of the IR truncated scalar field in our model at tree, one- and two-loop order. Using the two-point correlation function, we compute the stochastic contributions to the power spectrum Δ^2_ϕ, spectral index n_ϕ and the running of the spectral index α_ϕ in Sec. 2.5. In Sec. 2.6, we compare our numerical predictions for the n_ϕ and α_ϕ with the measurements [60] of the Planck 2018 Collaboration. We study the statistics of fluctuations in Sec. 2.7.

2.1 The Model

We work in the de-Sitter spacetime and consider a self-interacting massive, minimally coupled, spectator scalar field during inflation. Lagrangian density of the model

$$\mathcal{L} = -\frac{1}{2}\,\partial_\mu\Phi\,\partial_\nu\Phi\,g^{\mu\nu}\sqrt{-g} - \frac{1}{2}m_0^2\Phi^2\sqrt{-g} - V(\Phi)\sqrt{-g}\,, \tag{2.1}$$

[1] This chapter is based on the paper Karakaya, G. and Onemli, V. K. (2018). Quantum effects of mass on scalar field correlations, power spectrum and fluctuations during inflation, *Physical Review D*, *97*(12), 123531.

where $\Phi(x)$ and m_0 represent the bare field and the bare mass, respectively. The $V(\Phi)$ is specified as the quartic self-interaction potential. The $g_{\mu\nu}$ are chosen as the metric tensor components of a locally de Sitter spacetime. The g denotes the determinant of the metric. Therefore, the invariant line element is

$$ds^2 = g_{\mu\nu} dx^\mu dx^\nu = -dt^2 + a^2(t) d\vec{x} \cdot d\vec{x} \,, \tag{2.2}$$

where the scale factor with a constant expansion rate H is $a(t) = e^{Ht}$. We work in a D-dimensional spacetime and adopt the convention that a Greek index $\mu = 0, 1, ..., (D-1)$, hence $x^\mu = (x^0, \vec{x})$, $x^0 \equiv t$ and $\partial_\mu = (\partial_0, \vec{\nabla})$. The model is interesting because it predicts, in the massless limit, intriguing enhanced quantum effects. The renormalized energy density and pressure of the scalar field violate [63, 64] the weak energy condition on cosmological scales at two-loop order. This, implies that the expansion of the universe is superaccelerated. As the fluctuations i.e., inflationary particle production out of vacuum amplifies the field strength, the scalar rises up its potential and develops [28] a self-mass squared which, in turn, reduces the particle production rate. Moreover, the classical restoring force pushes the scalar back down to the configuration where the potential is minimum. The scalar, therefore, cannot continue rolling up its potential forever; as the Figs. 2.1-2 imply, it eventually comes to a halt. Thus, the model is stable [29].

In this section, we first get the renormalized Lagrangian density of the model from bare Lagrangian density (2.1) with a quartic self-interaction. The usual procedure can be outlined as the follows. The renormalized field $\phi(x)$ is defined by the field strength renormalization of the bare field as $\phi(x) \equiv \frac{1}{\sqrt{Z}} \Phi(x)$. Then the bare mass squared m_0^2 and bare coupling strength λ_0 are expressed in terms of the renormalized parameters as $m_0^2 Z \equiv m^2 Z + \delta m^2$ and $\lambda_0 Z^2 \equiv \lambda + \delta\lambda$, where δm^2 and $\delta\lambda$ denote the mass renormalization and coupling strength renormalization counterterms, respectively. Finally, defining $Z \equiv 1 + \delta Z$, where δZ is the field strength renormalization counterterm, the renormalized Lagrangian density is obtained as

$$\mathcal{L} = -\frac{1}{2}(1+\delta Z)\left[\partial_\mu \phi \, \partial_\nu \phi \, g^{\mu\nu} + m^2 \phi^2\right]\sqrt{-g} - V(\phi)\sqrt{-g} \,, \tag{2.3}$$

where the renormalized potential

$$V(\phi) = \frac{1}{2}\delta m^2 \phi^2 + \frac{1}{4!}(\lambda + \delta\lambda)\phi^4 \,. \tag{2.4}$$

Varying the Lagrangian with metric (2.2), density (2.3) and interaction potential (2.4), yields the scalar field equation

$$\ddot{\phi}(t,\vec{x})+(D-1)H\dot{\phi}(t,\vec{x})-\left[\frac{\nabla^2}{a^2}-m^2\right]\phi(t,\vec{x})=-\frac{V'(\phi)(t,\vec{x})}{1+\delta Z}\ , \tag{2.5}$$

where an overdot denotes derivative with respect to comoving time t and prime denotes derivative with respect to the argument. Therefore,

$$V'(\phi)(t,\vec{x})=\delta m^2\phi+\frac{1}{6}(\lambda+\delta\lambda)\phi^3. \tag{2.6}$$

The solution of Eq. (2.5) can be written as

$$\phi(t,\vec{x})=\phi_0(t,\vec{x})-\int_0^t dt' a^{D-1}(t')\int d^{D-1}x' G(t,\vec{x};t',\vec{x}')\frac{V'(\phi)(t',\vec{x}')}{1+\delta Z}\ , \tag{2.7}$$

where the free field $\phi_0(t,\vec{x})$ in Eq. (2.7) obeys the homogeneous field equation and agrees with the interacting (full) field at initial comoving time $t=t_i=0$. The free field can be expressed as a linear combination of Hankel functions of the first and second kind which we use in Sec. 2.2. The Green's function $G(t,\vec{x};t',\vec{x}')$ in Eq. (2.7), on the other hand, is any solution of the field equation with a Dirac-delta source term $\delta(t-t')\delta^{D-1}(\vec{x}-\vec{x}')$ which obeys the retarded boundary conditions. It can be given in terms of the commutator function as

$$G(t,\vec{x};t',\vec{x}')=i\Theta(t-t')\left[\phi_0(t,\vec{x}),\phi_0(t',\vec{x}')\right]\ . \tag{2.8}$$

We use Eq. (2.8) to compute the Green's function and its IR limit in Sec. 2.3.

One can iterate Eq. (2.7) to obtain the full field in terms of the free field and the Green's function, perturbatively. The first iteration, for example, yields

$$\begin{aligned}\phi(t,\vec{x})=\phi_0(t,\vec{x})&-\frac{1}{1+\delta Z}\int_0^t dt' a^{D-1}(t')\int d^{D-1}x' G(t,\vec{x};t',\vec{x}')\Bigg\{\delta m^2\Bigg[\phi_0(t',\vec{x}')-\frac{1}{1+\delta Z}\\
&\times\int_0^{t'} dt'' a^{D-1}(t'')\int d^{D-1}x'' G(t',\vec{x}';t'',\vec{x}'')\left[\delta m^2\phi(t'',\vec{x}'')+\frac{\lambda+\delta\lambda}{6}\phi^3(t'',\vec{x}'')\right]\Bigg]+\frac{\lambda+\delta\lambda}{6}\\
&\times\Bigg[\phi_0(t',\vec{x}')-\frac{1}{1+\delta Z}\int_0^{t'} dt'' a^{D-1}(t'')\int d^{D-1}x'' G(t',\vec{x}';t'',\vec{x}'')\Bigg[\delta m^2\phi(t'',\vec{x}'')+\frac{\lambda+\delta\lambda}{6}\\
&\times\phi^3(t'',\vec{x}'')\Bigg]\Bigg]^3\Bigg\}\ .\end{aligned} \tag{2.9}$$

Successive iterations give the higher order corrections in λ and yield the full field as an expansion. We obtain the free-field mode expansion of the scalar in Sec. 2.2 and use it to study the interacting theory in Sec. 2.3.

2.2 Free Theory

As pointed out in Sec. 2.1, we work on a conformal coordinate patch with a topology $\mathcal{T}^{D-1}\times\Re$. Since the manifold is spatially compact, the modes of fields are discrete. Thus, the comoving wave vector and wave number are defined as

$$\vec{k}\equiv 2\pi H\vec{n} \;\text{ and }\; k\equiv\|\vec{k}\|=2\pi H\|\vec{n}\| \;, \tag{2.10}$$

respectively. Here $\vec{n}$ denotes a $(D–1)$-dimensional vector with integer components. To express the scalar $\phi_0(t,\vec{x})$ as a sum over its modes, we, therefore, expand it in a spatial Fourier series.

The spatially Fourier transformed free field equation is obtained as

$$\ddot{\widetilde{\phi}}_0(t,\vec{k})+(D-1)H\dot{\widetilde{\phi}}_0(t,\vec{k})+\left[\frac{k^2}{a^2}+m^2\right]\widetilde{\phi}_0(t,\vec{k})=0\,. \tag{2.11}$$

The canonical quantization condition $[\phi_0(t,\vec{x}),\Pi_0(t,\vec{x}')]=i\delta^{D-1}(\vec{x}-\vec{x}')$, where $\Pi_0(t,\vec{x}')=a^{D-1}(t)\dot{\phi}_0(t,\vec{x}')$ is the conjugate momentum, implies

$$[\widetilde{\phi}_0(t,\vec{k}),\dot{\widetilde{\phi}}_0(t,\vec{k}')]=\frac{i\delta_{\vec{n},-\vec{n}'}}{a^{D-1}(t)H^{D-1}}\;, \tag{2.12}$$

in mode space. To express $\widetilde{\phi}_0(t,\vec{k})$ satisfying Eq. (2.12), in terms of the amplitude for each mode $\vec{k}$ of the field—the so called mode function and the mode coordinates, we need to solve Eq. (2.13). In order to solve it, however, one needs to distinguish between the case of zero mode and the case of nonzero modes.

Let us consider the case of zero mode first.

Equation (2.13) for $\vec{k}=0$,

$$\ddot{\widetilde{\phi}}_0(t,0)+(D-1)H\dot{\widetilde{\phi}}_0(t,0)+m^2\widetilde{\phi}_0(t,\vec{k})=0\,, \tag{2.13}$$

has two linearly independent solutions,

$$u_1(t,0)=a^{-\frac{D-1}{2}+\nu}(t) \;\text{ and }\; u_2(t,0)=\frac{-i}{2\nu H}a^{-\frac{D-1}{2}-\nu}(t)\,, \tag{2.14}$$

where

$$\nu\equiv\sqrt{\left(\frac{D-1}{2}\right)^2-\left(\frac{m}{H}\right)^2} \;\text{ with }\; \frac{m}{H}\leq\frac{D-1}{2}\,, \tag{2.15}$$

obeying the Wronskian normalization

$$u_1(t,0)\dot{u}_2(t,0)-u_2(t,0)\dot{u}_1(t,0)=\frac{i}{a^{D-1}(t)}\,. \tag{2.16}$$

In mode space, the zero mode of the free field is expressed in terms of the zero mode functions $u_1(t,0)$ and $u_2(t,0)$ and the self-adjoint zero mode coordinates $\hat{Q}$ and $\hat{P}$ as

$$\widetilde{\phi}_0(t,0) = H^{-\frac{D-1}{2}} \left[\hat{Q}u_1(t,0) - i\hat{P}u_2(t,0)\right] \ . \tag{2.17}$$

Canonical commutation (2.12) and Wronskian normalization (2.16), together, imply

$$[\hat{Q},\hat{P}] = i \ . \tag{2.18}$$

Therefore, the zero mode field in momentum space is

$$\widetilde{\varphi}_0(t,0) = H^{-\frac{D-1}{2}} \left[\frac{\hat{Q}}{a^{\frac{D-1}{2}-\nu}(t)} - \frac{\hat{P}}{2\nu H a^{\frac{D-1}{2}+\nu}(t)}\right] \ . \tag{2.19}$$

The operators $\hat{Q}$ and $\hat{P}$ can be expressed in terms of the initial values of the spatial Fourier transforms of the field and its first time derivative for $\vec{k}=0$,

$$\hat{Q} \ = \ H^{\frac{D-1}{2}} \left[\widetilde{\phi}_0(0,0)\frac{1}{2}\left(1+\frac{D-1}{2\nu}\right) + \frac{\widetilde{\dot{\phi}}_0(0,0)}{2\nu H}\right] , \tag{2.20}$$

$$\hat{P} \ = \ H^{\frac{D-1}{2}} \left[\widetilde{\phi}_0(0,0)\left(\frac{D-1}{2}-\nu\right)H + \widetilde{\dot{\phi}}_0(0,0)\right] \ . \tag{2.21}$$

Let us now consider the case of nonzero modes. Two linearly independent solutions of Eq. (2.11) for the nonzero modes ($\vec{k}\neq 0$) can be given in terms of the Hankel function of the first kind $\mathcal{H}_\nu^{(1)}$ and its complex conjugate. The solution obeying the Wronskian normalization

$$u_0(t,k)\,\dot{u}_0^*(t,k) - u_0^*(t,k)\,\dot{u}_0(t,k) = \frac{i}{a^{D-1}(t)} \ , \tag{2.22}$$

is known as the Bunch-Davies mode function

$$u_0(t,k) = i\sqrt{\frac{\pi}{4Ha^{D-1}(t)}}\,\mathcal{H}_\nu^{(1)}\Big(\frac{k}{Ha(t)}\Big) \ . \tag{2.23}$$

which is the amplitude of the normal mode with wave number $\vec{k}$. In momentum space, a nonzero mode of the free field is represented in terms of the mode function $u(t,k)$, its complex conjugate, and mode coordinates $\hat{A}_{\vec{n}}$ and $\hat{A}^\dagger_{-\vec{n}}$ as

$$\widetilde{\phi}_0(t,\vec{k}\neq 0) = H^{-\frac{D-1}{2}} \left[u_0(t,k)\hat{A}_{\vec{n}} + u_0^*(t,k)\hat{A}^\dagger_{-\vec{n}}\right] \ . \tag{2.24}$$

Canonical commutation relation (2.12) and Wronskian normalization (2.22) together imply that the operators $\hat{A}_{\vec{n}}$ and $\hat{A}^\dagger_{\vec{n}}$ satisfy the commutation relation

$$\left[\hat{A}_{\vec{n}}, \hat{A}^\dagger_{\vec{m}}\right] = \delta_{\vec{n},\vec{m}} \ . \tag{2.25}$$

They can be expressed in terms of the initial values of the spatial Fourier transforms of the field and its first time derivative,

$$\begin{aligned}
\hat{A}_{\vec{n}} &= -iH^{\frac{D-1}{2}}\left[\dot{u}^*(0,k)\widetilde{\phi}_0(0,\vec{k})-u^*(0,k)\widetilde{\dot{\phi}}_0(0,\vec{k})\right] , \\
\hat{A}^\dagger_{\vec{n}} &= iH^{\frac{D-1}{2}}\left[\dot{u}(0,k)\widetilde{\phi}_0(0,-\vec{k})-u(0,k)\widetilde{\dot{\phi}}_0(0,-\vec{k})\right] .
\end{aligned} \tag{2.26}$$

Note that the state $|\Omega\rangle$ annihilated by all $\hat{A}_{\vec{n}}$ is known as Bunch-Davies vacuum.

Next, we obtain the free field mode expansion of the scalar field.

Inverse Fourier transforming Eqs. (2.19) and (2.24) back to position space and combining the outcomes, we yield the expansion as

$$\phi_0(t,\vec{x}) = H^{\frac{D-1}{2}}\left\{\frac{\hat{Q}}{a^{\frac{D-1}{2}-\nu}(t)}-\frac{\hat{P}}{2\nu H a^{\frac{D-1}{2}+\nu}(t)}+\sum_{\vec{n}\neq 0}\left[u_0(t,k)e^{i\vec{k}\cdot\vec{x}}\hat{A}_{\vec{n}}+u_0^*(t,k)e^{-i\vec{k}\cdot\vec{x}}\hat{A}^\dagger_{\vec{n}}\right]\right\} \tag{2.27}$$

Free field mode expansion (2.27) includes arbitrarily large wave numbers. The physical size, grows more rapidly than the horizon size during inflation. In fact, the scale factor grows exponentially whereas the horizon size remains constant during de Sitter inflation. Hence, at comoving time $t=t_k$ the scale with comoving wave number

$$k \equiv H\,a(t_k) = He^{Ht_k}, \tag{2.28}$$

exits the horizon. In other words, the mode k is a subhorizon (UV) mode when $t<t_k$ but becomes a superhorizon (IR) mode at $t=t_k$. During the later phases of expansion after the end of inflation (radiation domination and matter domination) though, the horizon size grows more rapidly than the physical size, as pointed out in Sec. 1 1, and the superhorizon modes start reentering the horizon as the horizon size successively reaches their wavelengths and engender the density perturbations required for the structure formation in the early Universe.

To study the IR physics during inflation, one cuts out [27] the UV modes with wave number $k > Ha(t)$ in mode expansion Eq. (2.27) using a dynamical Heaviside step function Θ in Fourier space,

$$\phi_0(t,\vec{x}) = H^{\frac{D-1}{2}}\sum_{\vec{n}\neq 0}\Theta(Ha(t)-k)\left[u_0(t,k)e^{i\vec{k}\cdot\vec{x}}\hat{A}_{\vec{n}}+u_0^*(t,k)e^{-i\vec{k}\cdot\vec{x}}\hat{A}^\dagger_{\vec{n}}\right] . \tag{2.29}$$

The zero mode is neglected in Eq. (2.29) because it is just one mode as opposed to ever increasing number of nonzero modes. Note also that the two zero mode solutions,

$1/a^{\frac{D-1}{2}\mp\nu}$ decay exponentially fast in time. Therefore, the zero mode cannot have any significant effect in late time cosmology. In Eq. (2.29) one can further take the IR limit of mode function (2.29) given in terms of the Hankel function

$$\mathcal{H}_\nu^{(1)}(z) = J_\nu(z) + iY_\nu(z) \; , \tag{2.30}$$

where $z \equiv \frac{k}{Ha(t)}$, $J_\nu(z)$ is the Bessel function of order ν and

$$Y_\nu(z) = J_\nu(z)\cot(\nu\pi) - J_{-\nu}(z)\csc(\nu\pi) \; , \tag{2.31}$$

is the Neumann function of order ν. The right side of Eq. (2.31) is replaced by its limiting value if ν is an integer or zero. Using the series expansion of the Bessel function

$$J_\nu(z) = \left(\frac{z}{2}\right)^\nu \frac{1}{\nu\Gamma(\nu)}\left[1 - \frac{1}{\nu+1}\left(\frac{z}{2}\right)^2 + \mathcal{O}(z^4)\right] \; , \tag{2.32}$$

the reflection formula for the Gamma function $\pi\csc(p\pi) = \Gamma(1-p)\Gamma(p)$ for $p=\nu$ and $p=\nu+\frac{1}{2}$, and the duplication identity $\Gamma(\nu) = \frac{\sqrt{\pi}}{2^{2\nu-1}}\frac{\Gamma(2\nu)}{\Gamma(\nu+\frac{1}{2})}$, one gets the leading IR limit of the mode function as

$$u_0(t,k) \longrightarrow \frac{1}{\sqrt{Ha^{D-1}(t)}}\frac{\Gamma(2\nu)}{\Gamma(\nu+\frac{1}{2})}\left(\frac{2k}{Ha(t)}\right)^{-\nu}\left\{1 + \mathcal{O}\left(\left(\frac{k}{Ha(t)}\right)^{2\beta}\right)\right\} . \tag{2.33}$$

Here $\beta = \nu$ if $\frac{1}{2}\sqrt{(D-3)(D+1)} < \frac{m}{H} < \frac{1}{2}(D-1)$ or $\beta = 1$ if $\frac{m}{H} < \frac{1}{2}\sqrt{(D-3)(D+1)} < \frac{1}{2}(D-1)$. Thus, inserting $u(t,k)$ in Eq. (2.33) into Eq. (2.29), we finally obtain the IR truncated massive free field as

$$\bar{\phi}_0(t,\vec{x}) = H^{\nu+\frac{D}{2}-1}\frac{\Gamma(2\nu)}{\Gamma(\nu+\frac{1}{2})2^\nu}\, a^{\nu-\frac{D-1}{2}}(t)\sum_{\vec{n}\neq 0}\frac{\Theta\left(Ha(t)-k\right)}{k^\nu}\left[e^{i\vec{k}\cdot\vec{x}}\hat{A}_{\vec{n}} + e^{-i\vec{k}\cdot\vec{x}}\hat{A}^\dagger_{\vec{n}}\right] . \tag{2.34}$$

Note that, in the massless limit, Eq. (2.34) gives the form obtained in Ref. [67]. The IR truncated massive full field $\bar{\phi}$ is given in terms of the IR truncated massive free field $\bar{\phi}_0$ in the next section.

2.3 Interacting Theory

Recall that the full field $\phi(t,\vec{x})$ in de Sitter background with an interaction potential $V(\phi)$ satisfying equation of motion (2.11) is given in Eq. (2.7). Obtaining the full field—even perturbatively—by iterating Eq. (2.7) for potential (2.4), Green's function (2.8), mode function (2.23) and free field (2.29) is a difficult task. Amputating the ultraviolet modes, however, to study the IR limit of the theory, simplifies the computation. In this limit, the mode function and the free field are already obtained in Eqs. (2.33) and (2.34), respectively. To obtain the IR truncated full field $\bar{\phi}(t,\vec{x})$, the last ingredient we need is the IR limit of Green's function (2.8) given in terms of the commutator function

$$\left[\phi_0(t,\vec{x}),\phi_0(t',\vec{x}')\right]=H^{D-1}\sum_{\vec{n}\neq 0}\left\{u_0(t,k)u_0^*(t',k)-u_0^*(t,k)u_0(t',k)\right\}e^{i\vec{k}\cdot(\vec{x}-\vec{x}')}$$

$$=i\frac{\pi}{2}H^{D-2}\frac{\csc(\nu\pi)}{\sqrt{a^{D-1}(t)\,a^{D-1}(t')}}\sum_{\vec{n}\neq 0}\Big[J_\nu(z)J_{-\nu}(z')-J_{-\nu}(z)J_\nu(z')\Big]e^{i\vec{k}\cdot(\vec{x}-\vec{x}')}\,. \quad (2.35)$$

We used Eqs. (2.23) and (2.29)-(2.33) to obtain Eq. (2.34). Combining Eqs. (2.8), (2.32), (2.35) and $H^{D-1}\sum_{\vec{n}}e^{i\vec{k}\cdot(\vec{x}-\vec{x}')}=\delta^{D-1}(\vec{x}-\vec{x}')$ yields the retarded Green's function, in leading order,

$$G(t,\vec{x};t',\vec{x}')\longrightarrow\frac{\Theta(t-t')}{2H\nu}\left[\frac{a^{2\nu}(t)-a^{2\nu}(t')}{[a(t)\,a(t')]^{\nu+\frac{D-1}{2}}}\right]\delta^{D-1}(\vec{x}-\vec{x}')\,. \quad (2.36)$$

Substituting Eq. (2.36) into Eq. (2.7), we obtain the IR truncated full field as

$$\bar{\phi}(t,\vec{x})=\bar{\phi}_0(t,\vec{x})-\frac{1}{2\nu H}\int_0^t dt'\left[\left(\frac{a(t)}{a(t')}\right)^{\nu-\frac{D-1}{2}}-\left(\frac{a(t')}{a(t)}\right)^{\nu+\frac{D-1}{2}}\right]\frac{V'(\bar{\phi})(t',\vec{x})}{1+\delta Z}\,, \quad (2.37)$$

where the potential is given in Eq. (2.4). The latter term in the square brackets can be neglected next to the former which dominates throughout the range of integration. Moreover, the counterterms in potential (2.4) cannot contribute [33] in the leading order we consider. One can see this by comparing the powers of the fields and orders of λ involved in various counterterms in the model: $\delta\lambda\sim\mathcal{O}(\lambda^2)$, $\delta m^2\sim\mathcal{O}(\lambda)$ and $\delta Z\sim\mathcal{O}(\lambda^2)$ [28]. Firstly, compare the contributions involving $\lambda\phi^4$ and the contributions involving $\delta\lambda\phi^4$ terms. Powers of the fields are the same, so the former and the latter have the same structure of leading terms. The latter, however, are suppressed by at least one extra factor of λ (with $\delta\lambda\sim\mathcal{O}(\lambda^2)$), they can never be in leading order. Secondly, compare the contributions involving $\lambda\phi^4$ and the contributions involving $\delta m^2\phi^2$ terms. Although the former and the latter are linear in λ (with $\delta m^2\sim\mathcal{O}(\lambda)$), the former are quartic in the field, whereas the latter are quadratic in the field. Therefore, at a given order in λ, the latter can never have as high order leading terms as the former. Finally, the field strength counterterm δZ appears in Eq. (2.37) in the form

$$\frac{V'(\bar{\phi})(t',\vec{x})}{1+\delta Z}=V'(\bar{\phi})\left[1-\delta Z+(\delta Z)^2-\cdots\right]\,, \quad (2.38)$$

with $\delta Z\sim\mathcal{O}(\lambda^2)$. Hence, exactly the same leading order contributions that Eq. (2.37) would yield are obtained from its simplified version without the counterterms, i.e., from

$$\bar{\phi}(t,\vec{x})=\bar{\phi}_0(t,\vec{x})-\frac{\lambda}{6(2\nu)H}\,a^{-\frac{\delta}{2}}(t)\int_0^t dt' a^{\frac{\delta}{2}}(t')\,\bar{\phi}^3(t',\vec{x})\,, \tag{2.39}$$

where we define

$$\delta\equiv D-1-2\nu\,. \tag{2.40}$$

The infrared truncated full field $\bar{\phi}(t,\vec{x})$ can be expressed in terms of the IR truncated free field $\bar{\phi}_0(t,\vec{x})$, at any order of λ by iterating Eq. (2.39) successively. Iterating it twice, for example, yields

$$\begin{aligned}\bar{\phi}(t,\vec{x})=\bar{\phi}_0(t,\vec{x})&-\frac{\lambda}{6(2\nu)H}\,a^{-\frac{\delta}{2}}(t)\int_0^t dt' a^{\frac{\delta}{2}}(t')\,\bar{\phi}_0^3(t',\vec{x})+\frac{\lambda^2}{12(2\nu)^2H^2}\,a^{-\frac{\delta}{2}}(t)\\ &\times\int_0^t dt'\bar{\phi}_0^2(t',\vec{x})\int_0^{t'}dt'' a^{\frac{\delta}{2}}(t'')\bar{\phi}_0^3(t'',\vec{x})-\frac{\lambda^3}{24(2\nu)^3H^3}\,a^{-\frac{\delta}{2}}(t)\Bigg\{\int_0^t dt'\bar{\phi}_0^2(t',\vec{x})\\ &\times\int_0^{t'}dt''\bar{\phi}_0^2(t'',\vec{x})\int_0^{t''}dt''' a^{\frac{\delta}{2}}(t''')\bar{\phi}_0^3(t''',\vec{x})+\frac{1}{3}\int_0^t dt' a^{-\frac{\delta}{2}}(t')\,\bar{\phi}_0(t',\vec{x})\\ &\times\left[\int_0^{t'}dt'' a^{\frac{\delta}{2}}(t'')\,\bar{\phi}_0^3(t'',\vec{x})\right]^2\Bigg\}+\mathcal{O}(\lambda^4)\,. \end{aligned}\tag{2.41}$$

In the next section, we use Eq. (2.41) to compute the quantum corrected two-point correlation function of the IR truncated full field up to $\mathcal{O}(\lambda^3)$.

2.4 Two-Point Correlation Function

The two-point correlation function of the IR truncated full field for two distinct events

$$\begin{aligned}\langle\Omega|\bar{\phi}(t,\vec{x})\bar{\phi}(t',\vec{x}')|\Omega\rangle=&\langle\Omega|\bar{\phi}(t,\vec{x})\bar{\phi}(t',\vec{x}')|\Omega\rangle_{\rm tree}+\langle\Omega|\bar{\phi}(t,\vec{x})\bar{\phi}(t',\vec{x}')|\Omega\rangle_{1-{\rm loop}}\\ &+\langle\Omega|\bar{\phi}(t,\vec{x})\bar{\phi}(t',\vec{x}')|\Omega\rangle_{2-{\rm loop}}+\mathcal{O}(\lambda^3)\,,\end{aligned}\tag{2.42}$$

with $t'\leq t$ and $\vec{x}'\neq\vec{x}$, can be obtained for the field with a quartic self-interaction using Eq. (2.41). At tree-order, the two-point correlator

$$\langle\Omega|\bar{\phi}(t,\vec{x})\bar{\phi}(t',\vec{x}')|\Omega\rangle_{\rm tree}=\langle\Omega|\bar{\phi}_0(t,\vec{x})\bar{\phi}_0(t',\vec{x}')|\Omega\rangle\,. \tag{2.43}$$

The one-loop quantum correction

$$\begin{aligned}\langle\Omega|\bar{\phi}(t,\vec{x})\bar{\phi}(t',\vec{x}')|\Omega\rangle_{1-{\rm loop}}=&-\frac{\lambda}{6(2\nu)H}\Bigg[a^{-\frac{\delta}{2}}(t')\langle\Omega|\bar{\phi}_0(t,\vec{x})\int_0^{t'}d\tilde{t}\,a^{\frac{\delta}{2}}(\tilde{t})\,\bar{\phi}_0^3(\tilde{t},\vec{x}')|\Omega\rangle\\ &+a^{-\frac{\delta}{2}}(t)\langle\Omega|\int_0^t dt'' a^{\frac{\delta}{2}}(t'')\bar{\phi}_0^3(t'',\vec{x})\bar{\phi}_0(t',\vec{x}')|\Omega\rangle\Bigg]\,,\end{aligned}\tag{2.44}$$

is not hard to compute. The two-loop quantum correction

$$\langle\Omega|\bar{\phi}(t,\vec{x})\bar{\phi}(t',\vec{x}')|\Omega\rangle_{2-\text{loop}}=\frac{\lambda^2}{12(2\nu)^2H^2}\Bigg[a^{-\frac{\delta}{2}}(t')\langle\Omega|\bar{\phi}_0(t,\vec{x})\int_0^{t'}d\tilde{t}\,\bar{\phi}_0^2(\tilde{t},\vec{x}')\int_0^{\tilde{t}}d\tilde{\tilde{t}}$$

$$\times a^{\frac{\delta}{2}}(\tilde{\tilde{t}})\bar{\phi}_0^3(\tilde{\tilde{t}},\vec{x}')|\Omega\rangle+a^{-\frac{\delta}{2}}(t)\langle\Omega|\int_0^t dt''\bar{\phi}_0^2(t'',\vec{x})\int_0^{t''}dt'''\,a^{\frac{\delta}{2}}(t''')\bar{\phi}_0^3(t''',\vec{x})\bar{\phi}_0(t',\vec{x}')|\Omega\rangle$$

$$+\frac{1}{3}\Big[a(t)\,a(t')\Big]^{-\frac{\delta}{2}}\langle\Omega|\int_0^t dt''\,a^{\frac{\delta}{2}}(t'')\bar{\phi}_0^3(t'',\vec{x})\int_0^{t'}d\tilde{t}\,a^{\frac{\delta}{2}}(\tilde{t})\bar{\phi}_0^3(\tilde{t},\vec{x}')|\Omega\rangle\Bigg]\,, \tag{2.45}$$

where $0\le t'''\le t''\le t$, $0\le\tilde{\tilde{t}}\le\tilde{t}\le t'$ and $t'\le t$, however, is not easy to compute because it involves three VEVs each of which has a double time integral without a definite time ordering in the integrand. Note that the two-point correlation function for equal time, equal space and equal spacetime events can be obtained as the corresponding limits of Eq. (2.42). Note also that perturbation theory breaks down when $\ln(a(t))=Ht\sim 1/\sqrt{\lambda}$ [63]. Thus, for $\lambda\ll 1$, the perturbation theory and hence Eq. (2.42) are accurate for an arbitrarily long period of time. The correlation function, at tree, one- and two-loop order is computed in Secs. 2.4.1, 2.4.2 and 2.4.3, respectively.

2.4.1 Tree-Order Correlator

We obtain the tree-order two-point correlation function of the IR truncated massive scalar using Eqs. (2.25), (2.34) and (2.40) as

$$\langle\Omega|\bar{\phi}(t,\vec{x})\bar{\phi}(t',\vec{x}')|\Omega\rangle_{\text{tree}}=\langle\Omega|\bar{\phi}_0(t,\vec{x})\bar{\phi}_0(t',\vec{x}')|\Omega\rangle=\frac{\Gamma^2(2\nu)}{\Gamma^2(\nu+\frac{1}{2})}\frac{H^{D-2}}{(4\pi)^{2\nu}}\big[a(t)\,a(t')\big]^{-\frac{\delta}{2}}$$

$$\times\sum_{\vec{n}\neq 0}\frac{\Theta(Ha(t)-H2\pi n)\Theta(Ha(t')-H2\pi n)}{n^{2\nu}}\,e^{i2\pi H\vec{n}\cdot(\vec{x}-\vec{x}')}\,, \tag{2.46}$$

where $t'\le t$ and $\vec{x}'\neq\vec{x}$. The discrete sum over $\vec{n}$ in Eq. (2.46) can be approximated as a $(D-1)$-dimensional integral in the continuum limit,

$$\sum_{\vec{n}\neq 0}\frac{\Theta(Ha(t)-H2\pi n)\,\Theta(Ha(t')-H2\pi n)}{n^{2\nu}}\,e^{i2\pi H\vec{n}\cdot(\vec{x}-\vec{x}')}$$

$$\simeq\frac{1}{(2\pi H)^{\delta}}\int d\Omega_{D-1}\int_0^\infty\frac{dk}{k^{1-\delta}}\,\Theta(Ha(t)-k)\,\Theta(Ha(t')-k)\,e^{ik\Delta x\cos(\theta)}\,, \tag{2.47}$$

where $\Delta x\equiv\|\Delta\vec{x}\|=\|\vec{x}-\vec{x}'\|$ and θ is the angle between the vectors $\vec{n}$ and $\Delta\vec{x}$. Because $0\le t'\le t$, we have $Ha(t')\le Ha(t)$ which implies $\Theta(Ha(t)-k)\,\Theta(Ha(t')-k)=\Theta(Ha(t')-k)$. The right side of Eq. (2.47), after angular integrations and a change of variable $y\equiv k\Delta x$, yields

$$\frac{\Gamma\left(\frac{D}{2}\right)}{\Gamma(D-1)}2^{2\nu}\pi^{2\nu-\frac{D}{2}}H^{-\delta}(\Delta x^2)^{-\frac{\delta}{2}}\int_{H\Delta x}^{Ha(t')\Delta x}dy\frac{\sin(y)}{y^{2-\delta}}\,. \tag{2.48}$$

The remaining integral in Eq. (2.48) is

$$\int dy \frac{\sin(y)}{y^{2-\delta}} = -\frac{i}{2} y^{-1+\delta} \left[E_{2-\delta}(iy) - E_{2-\delta}(-iy) \right] , \tag{2.49}$$

where $E_\beta(z)$ is the exponential integral function defined in Eq. (A.1). Substituting Eq. (2.49) into Eq. (2.48) yields a result for sum (2.47) and hence, for tree-order correlator (2.46). However, using the identity

$$E_\beta(z) = z^{\beta-1} \Gamma(1-\beta, z) , \tag{2.50}$$

where $\Gamma(\beta, z)$ is the incomplete gamma function defined in Eq. (A.4), gives a more useful result for sum (2.47) and hence for the tree-order correlator. We find

$$\langle \Omega | \bar{\phi}_0(t, \vec{x}) \bar{\phi}_0(t', \vec{x}') | \Omega \rangle \simeq \mathcal{A} f_0(t, t', \Delta x) , \tag{2.51}$$

where the constant

$$\mathcal{A} \equiv \frac{\Gamma^2(2\nu)}{\Gamma^2\left(\nu+\frac{1}{2}\right)} \frac{\Gamma\left(\frac{D}{2}\right)}{\Gamma(D-1)} \frac{H^{D-2}}{2^{2\nu} \pi^{\frac{D}{2}}} , \tag{2.52}$$

and the spacetime and mass dependent function

$$f_0(t, t', \Delta x) = \frac{1}{2} \left[-\alpha(t)\, \alpha(t') \right]^{-\frac{\delta}{2}} \Big\{ \Gamma\left(-1+\delta, i\alpha(t')\right) - \Gamma(-1+\delta, iH\Delta x) + (-1)^{-\delta}$$
$$\times \Big[\Gamma\left(-1+\delta, -i\alpha(t')\right) - \Gamma(-1+\delta, -iH\Delta x) \Big] \Big\} , \tag{2.53}$$

with

$$\alpha(t) \equiv \alpha(t, \Delta x) \equiv a(t) H \Delta x . \tag{2.54}$$

Note that the tree-order correlator for a massless scalar can be obtained by taking the $m \to 0$ limit of Eq. (2.51); see Appendix A.2. Note also that Eq. (2.51) can also be used to infer the behavior of the tree-order correlator for a fixed comoving separation at late t' when $a(t')$ [hence $a(t)$] becomes large; see Appendix A.3. Asymptotic form (A.23) of the tree-order correlator implies that it asymptotes to zero for the massive case whereas to a nonzero constant [Eq. (A.24)] in the massless limit.

Using power series representation of the incomplete gamma function, Eq. (A.6) in Eq. (2.53) we obtain

$$f_0(t, t', \Delta x) = \Big[a(t)\, a(t') \Big]^{-\frac{\delta}{2}} \sum_{n=0}^{\infty} \frac{(-1)^n (H\Delta x)^{2n}}{(2n+1)!} \frac{a^{2n+\delta}(t') - 1}{2n+\delta} . \tag{2.55}$$

Alternatively, summing up the infinite sum in Eq. (2.55) we find

$$f_0(t,t',\Delta x)=a^{-\frac{\delta}{2}}(t)\Bigg\{\frac{a^{\frac{\delta}{2}}(t')}{\delta}\,{}_1\mathcal{F}_2\Big(\frac{\delta}{2};\frac{3}{2},1+\frac{\delta}{2};-\frac{\alpha^2(t')}{4}\Big)$$
$$-\frac{a^{-\frac{\delta}{2}}(t')}{\delta}\,{}_1\mathcal{F}_2\Big(\frac{\delta}{2};\frac{3}{2},1+\frac{\delta}{2};-\frac{(H\Delta x)^2}{4}\Big)\Bigg\}\,, \tag{2.56}$$

where ${}_1\mathcal{F}_2$ is the generalized hypergeometric function whose power series representation is given in Eq. (A.8). Form (2.55) or (2.56) of f_0 can be used to figure out the behaviors of tree-order correlator (i) at a fixed comoving separation Δx at late times—as in Eq. (A.23)— and (ii) for a fixed physical distance $a(t')\Delta x$. In case (i), f_0 asymptotes to

$$f_0(t,t',\Delta x)\to$$
$$\Big[a(t)\,a(t')\Big]^{-\frac{\delta}{2}}\Bigg\{\frac{\sqrt{\pi}\,\Gamma(\frac{\delta}{2})}{2^{2-\delta}\Gamma(\frac{3-\delta}{2})}\frac{1}{(H\Delta x)^{\delta}}-\frac{1}{\delta}\,{}_1\mathcal{F}_2\Big(\frac{\delta}{2};\frac{3}{2},1+\frac{\delta}{2};-\frac{(H\Delta x)^2}{4}\Big)\Bigg\}\,. \tag{2.57}$$

which implies, as pointed out earlier, that the tree-order correlator asymptotes to zero as $\mathcal{O}((a(t)\,a(t'))^{-\frac{\delta}{2}})$ for a massive scalar. In the massless ($\delta\to 0$) limit though the tree-order correlator asymptotes to a nonzero constant. To see this, it is useful to rewrite Eq. (2.55) singling out $n=0$ term in the infinite sum

$$f_0(t,t',\Delta x)=\Big[a(t)\,a(t')\Big]^{-\frac{\delta}{2}}\Bigg\{\frac{a^{\delta}(t')-1}{\delta}+\sum_{n=1}^{\infty}\frac{(-1)^n(H\Delta x)^{2n}}{(2n+1)!}\frac{a^{2n+\delta}(t')-1}{2n+\delta}\Bigg\}\,. \tag{2.58}$$

The $n=0$ term in the curly brackets gives a $0/0$ ambiguity in the $\delta\to 0$ limit. Expanding the $a^{\delta}(t')=e^{\delta\ln(a(t'))}$ in this term around $\delta=0$ and then taking the massless limit of Eq. (2.58) we find

$$\lim_{m\to 0}f_0(t,t',\Delta x)=\ln(a(t'))+\sum_{n=1}^{\infty}\frac{(-1)^n(H\Delta x)^{2n}}{(2n+1)!}\frac{a^{2n}(t')-1}{2n}\,. \tag{2.59}$$

Summing up the terms in the infinite sum in Eq. (2.59), using Eq. (A.10), yields

$$\lim_{m\to 0}f_0(t,t',\Delta x)=\mathrm{ci}(\alpha(t'))-\frac{\sin(\alpha(t'))}{\alpha(t')}-\mathrm{ci}(H\Delta x)+\frac{\sin(H\Delta x)}{H\Delta x}\,, \tag{2.60}$$

where $\mathrm{ci}(z)$ is the cosine integral function defined in Eq. (A.9). Employing Eq. (A.11) in the time dependent terms in Eq. (2.60) implies that $\mathrm{ci}(\alpha(t'))-\frac{\sin(\alpha(t'))}{\alpha(t')}\to 0+\mathcal{O}\big(\alpha^{-2}(t')\big)$. Thus, the tree-order correlator, in the massless limit, asymptotes to a nonzero constant:

$$\lim_{m\to 0}\langle\Omega|\bar{\phi}_0(t,\vec{x})\bar{\phi}_0(t',\vec{x}')|\Omega\rangle\longrightarrow\frac{\Gamma(D-1)}{\Gamma(\frac{D}{2})}\frac{H^{D-2}}{2^{D-1}\pi^{\frac{D}{2}}}\Bigg\{\frac{\sin(H\Delta x)}{H\Delta x}-\mathrm{ci}(H\Delta x)\Bigg\}\,. \tag{2.61}$$

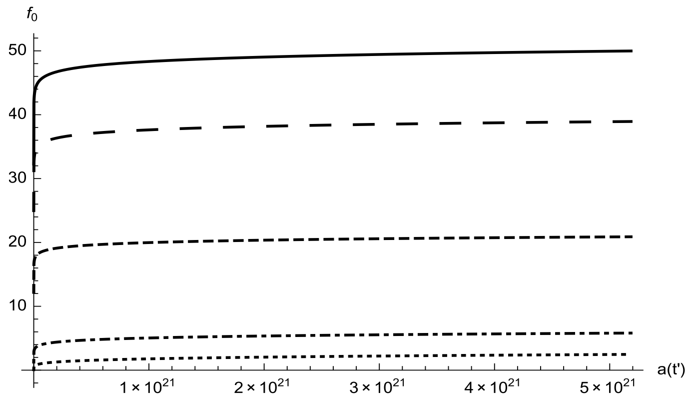

Figure 2.1 : Plots of $f_0(t,t',K)$, defined in Eq. (2.55) with separation (2.62), versus $a(t')$ for different values of mass, $K{=}1/2$ and $a(t) = e^{50}$. $a(t')$ runs from 1 to $a(t)$. The solid, large-dashed, dashed, dot-dashed and dotted lines are for $m{=}0, H/8, H/4, H/2$ and $3H/4$, respectively.

In case (ii), choosing the comoving separation in Eq. (2.55) as

$$\Delta x = \frac{K}{Ha(t')} \ , \tag{2.62}$$

to keep the physical distance $a(t')\Delta x$ a constant fraction K of the Hubble length, yields $f_0(t,t',K)$ which grows logarithmically for a massless scalar. This growth, however, is suppressed for massive scalars; see Fig. 2.1. To see the logarithmic growth and the effect of mass analytically, consider massless form (2.59) of f_0 with a Δx given in Eq. (2.62),

$$\lim_{m\to 0} f_0(t,t',K) = \ln(a(t')) + \sum_{n=1}^{\infty} \frac{(-1)^n K^{2n}}{(2n{+}1)!} \, \frac{1-a^{-2n}(t')}{2n} \ , \tag{2.63}$$

and compare it with the corresponding massive form of f_0 given in Eq. (2.58),

$$f_0(t,t',K) = \Big[a(t)\,a(t')\Big]^{-\frac{\delta}{2}} \left\{ \frac{a^{\delta}(t')-1}{\delta} + \sum_{n=1}^{\infty} \frac{(-1)^n K^{2n}}{(2n{+}1)!} \frac{a^{\delta}(t')-a^{-2n}(t')}{2n{+}\delta} \right\} . \tag{2.64}$$

Notice that the time dependent terms in the infinite sum in Eq. (2.63) decay rapidly, at least as fast as $\mathcal{O}(a^{-2}(t'))$. The time independent part of the infinite sum in Eq. (2.63) adds up to a constant,

$$\sum_{n=1}^{\infty} \frac{(-1)^n K^{2n}}{(2n{+}1)!2n} = \mathrm{ci}(K) - \frac{\sin(K)}{K} - \ln(K) - \gamma + 1 \ , \tag{2.65}$$

where γ is the Euler-Mascheroni number. Hence, the tree-order correlator at a fixed physical distance grows logarithmically with the scale factor $a(t')$ in the massless limit. Physically, this is because more and more scalar particles are created out of vacuum, the local field strength enhances. In the massive case, on the other hand, the time dependent terms that are also mass (or δ) dependent in Eq. (2.64) imply that the mass suppresses the logarithmic growth in Eq. (2.63). This is because $\frac{a^{\delta}(t')-1}{\delta} \leq \ln(a(t'))$, where the equality holds in the massless limit and $a^{\delta}(t') \leq [a(t)\,a(t')]^{\frac{\delta}{2}}$ where the equality holds in the equal time limit.

The simultaneous tree-order correlator is trivial to read off using either Eq. (2.53) or Eq. (2.55). The latter, for example, gives

$$\langle\Omega|\bar{\varphi}_0(t,\vec{x})\bar{\varphi}_0(t,\vec{x}')|\Omega\rangle \simeq \mathcal{A}\,a^{-\delta}(t)\sum_{n=0}^{\infty}\frac{(-1)^n(H\Delta x)^{2n}}{(2n+1)!}\,\frac{a^{2n+\delta}(t)-1}{2n+\delta}\;, \tag{2.66}$$

the required correlator as a power series expansion.

The equal space limit of Eq. (2.55) yields

$$\langle\Omega|\bar{\varphi}_0(t,\vec{x})\bar{\varphi}_0(t',\vec{x})|\Omega\rangle \simeq \mathcal{A}\big[a(t)\,a(t')\big]^{-\frac{\delta}{2}}\,\frac{a^{\delta}(t')-1}{\delta}\;. \tag{2.67}$$

The coincident tree-order correlator, can be obtained either from Eq. (2.66) or from Eq. (2.67). Taking the equal space limit of Eq. (2.66) [or the equal time limit of Eq. (2.67)] leads to

$$\langle\Omega|\bar{\varphi}_0^2(t,\vec{x})|\Omega\rangle \simeq \mathcal{A}\frac{1-a^{-\delta}(t)}{\delta}\;. \tag{2.68}$$

In the massless limit, Eqs. (2.51)-(2.55) yield the tree-order correlator for a massless IR truncated scalar in analytic function and power series forms; see Eqs. (A.15)-(A.20).

The tree-order correlator is the basic entity in the computation of quantum corrected correlation function in a self-interacting theory perturbatively. We employ results (2.51), (2.52), (2.55), and (2.66)-(2.68) in Secs. 2.4.2-3 to compute one- and two-loop correlator in the $\lambda\bar{\varphi}^4$ theory.

2.4.2 One-Loop Correlator

The calculation of one-loop contribution (2.44) to two-point correlation (2.42) involves evaluations of two VEVs. The first one is

$$\langle\Omega|\bar{\phi}_0(t,\vec{x})\int_0^{t'} d\tilde{t}\,a^{\frac{\delta}{2}}(\tilde{t})\,\bar{\phi}_0^3(\tilde{t},\vec{x}')|\Omega\rangle\;. \tag{2.69}$$

It can be expressed, in terms of topologically inequivalent field pairs, as

$$\int_0^{t'} d\tilde{t}\,a^{\frac{\delta}{2}}(\tilde{t})\,3\cdot 1\langle\Omega|\bar{\phi}_0(t,\vec{x})\,\bar{\phi}_0(\tilde{t},\vec{x}')|\Omega\rangle\langle\Omega|\bar{\phi}_0^2(\tilde{t},\vec{x}')|\Omega\rangle\;. \tag{2.70}$$

Using Eqs. (2.51), (2.52), (2.55) with $\tilde{t}\leq t$, and Eq. (2.68) in Eq. (2.70) yields

$$-\mathcal{A}^2\,\frac{a^{-\frac{\delta}{2}}(t)}{\delta}\,3\int_0^{t'}d\tilde{t}\Big[1-a^{-\delta}(\tilde{t})\Big]\sum_{n=0}^{\infty}\frac{(-1)^n(H\Delta x)^{2n}}{(2n+1)!}\,\frac{[1-a^{2n+\delta}(\tilde{t})]}{2n+\delta}\,. \tag{2.71}$$

Evaluating the integral in Eq. (2.70), the first VEV is obtained as

$$\begin{aligned}\langle\Omega|\bar{\phi}_0(t,\vec{x})\int_0^{t'}d\tilde{t}\,a^{\frac{\delta}{2}}(\tilde{t})\,\bar{\phi}_0^3(\tilde{t},\vec{x}')|\Omega\rangle=&-\frac{\mathcal{A}^2}{H}\,\frac{a^{-\frac{\delta}{2}}(t)}{\delta}\,3\sum_{n=0}^{\infty}\frac{(-1)^n(H\Delta x)^{2n}}{(2n+1)!(2n+\delta)}\\&\times\Big[\ln(a(t'))+\frac{1-a^{2n+\delta}(t')}{2n+\delta}-\frac{1-a^{2n}(t')}{2n}-\frac{1-a^{-\delta}(t')}{\delta}\Big]\,.\end{aligned} \tag{2.72}$$

The second VEV that contributes at one-loop order in Eq. (2.44) is

$$\begin{aligned}&\langle\Omega|\int_0^{t}dt''a^{\frac{\delta}{2}}(t'')\bar{\phi}_0^3(t'',\vec{x})\bar{\phi}_0(t',\vec{x}')|\Omega\rangle\\&=\int_0^{t}dt''a^{\frac{\delta}{2}}(t'')3\cdot1\langle\Omega|\bar{\phi}_0(t'',\vec{x})\bar{\phi}_0(t',\vec{x}')|\Omega\rangle\langle\Omega|\bar{\phi}_0^2(t'',\vec{x})|\Omega\rangle\,,\end{aligned} \tag{2.73}$$

where we have $0\leq t''\leq t$ and $t'\leq t$. The coincident tree-order correlator in the integrand is as given in Eq. (2.68). To evaluate the remaining VEV in the integrand we need to break up the integral into two as $\int_0^t dt''=\int_0^{t'}dt''+\int_{t'}^t dt''$. In the first integral $t''\leq t'$, whereas in the second $t'\leq t''$. Hence, appropriate use of Eqs. (2.51), (2.52) and (2.55) in Eq. (2.73), and evaluating the integrals give

$$\begin{aligned}\langle\Omega|\int_0^{t}dt''a^{\frac{\delta}{2}}(t'')\bar{\phi}_0^3(t'',\vec{x})\bar{\phi}_0(t',\vec{x}')|\Omega\rangle=&-\frac{\mathcal{A}^2}{H}\,\frac{a^{-\frac{\delta}{2}}(t')}{\delta}\,3\sum_{n=0}^{\infty}\frac{(-1)^n(H\Delta x)^{2n}}{(2n+1)!(2n+\delta)}\\&\times\Bigg\{\ln(a(t))-a^{2n}(t')\Bigg[a^{\delta}(t')\Big(\ln(a(t))-\ln(a(t'))+\frac{a^{-\delta}(t)}{\delta}\Big)-\frac{1}{\delta}\Bigg]\\&-\frac{1-a^{-\delta}(t)}{\delta}+\frac{1-a^{2n+\delta}(t')}{2n+\delta}-\frac{1-a^{2n}(t')}{2n}\Bigg\}\,.\end{aligned} \tag{2.74}$$

Combining Eqs. (2.72) and (2.74) in Eq. (2.44) yields the one-loop correlator for the massive scalar as

$$\langle\Omega|\bar{\phi}(t,\vec{x})\bar{\phi}(t',\vec{x}')|\Omega\rangle_{1-\mathrm{loop}}\simeq-\frac{\lambda}{2\nu}\frac{\mathcal{A}^2}{H^2}f_1(t,t',\Delta x)\,, \tag{2.75}$$

where we define the spacetime and mass dependent function

$$\begin{aligned}f_1(t,t',\Delta x)=&\frac{[a(t)\,a(t')]^{-\frac{\delta}{2}}}{2\,\delta}\sum_{n=0}^{\infty}\frac{(-1)^n(H\Delta x)^{2n}}{(2n+1)!(2n+\delta)}\Bigg\{a^{2n}(t')\Bigg[a^{\delta}(t')\Bigg(\ln(a(t))\\&-\ln(a(t'))+\frac{a^{-\delta}(t)}{\delta}\Bigg)-\frac{1}{\delta}\Bigg]-\ln(a(t))-\ln(a(t'))+\frac{1-a^{-\delta}(t)}{\delta}\\&+\frac{1-a^{-\delta}(t')}{\delta}-2\Bigg[\frac{1-a^{2n+\delta}(t')}{2n+\delta}\Bigg]+\frac{1-a^{2n}(t')}{n}\Bigg\}\,.\end{aligned} \tag{2.76}$$

Taking the $m \to 0$ limit of Eq. (2.75) gives the one-loop correlator for the massless scalar,

$$\lim_{m\to 0}\langle\Omega|\bar{\phi}(t,\vec{x})\bar{\phi}(t',\vec{x}')|\Omega\rangle_{1-\text{loop}} \simeq -\frac{\lambda}{(D-1)}\frac{H^{2D-6}}{2^{2D-2}\pi^{D}}\frac{\Gamma^2(D-1)}{\Gamma^2\left(\frac{D}{2}\right)}\lim_{m\to 0} f_1(t,t',\Delta x)\ , \quad (2.77)$$

where the massless limit of f_1, defined in Eq. (2.76), is

$$\lim_{m\to 0} f_1(t,t',\Delta x) = \frac{1}{4}\Bigg\{\ln^2(a(t))\ln(a(t')) + \frac{\ln^3(a(t'))}{3} + \frac{1}{2}\sum_{n=1}^{\infty}\frac{(-1)^n(H\Delta x)^{2n}}{n(2n+1)!}\Bigg[a^{2n}(t')$$
$$\times\Big[\ln^2(a(t)) - \ln^2(a(t')) + \frac{2\ln(a(t'))}{n} - \frac{1}{n^2}\Big] - \ln^2(a(t)) - \ln^2(a(t')) + \frac{1}{n^2}\Bigg]\Bigg\}\ . \quad (2.78)$$

Using the coincidence limit of Eq. (2.75) yields the VEV of the field strength squared

$$\langle\Omega|\bar{\phi}^2(t,\vec{x})|\Omega\rangle_{1-\text{loop}} \simeq -\frac{\lambda}{2\nu}\frac{\mathcal{A}^2}{H^2}\frac{a^{-\delta}(t)}{\delta^2}\left[\frac{a^{\delta}(t) - a^{-\delta}(t)}{\delta} - 2\ln(a(t))\right]\ . \quad (2.79)$$

A constraint on the coupling constant λ can immediately be deduced here. Magnitude of one-loop correction (2.79) ought to remain less than the magnitude of tree-order correlator (2.51) for the perturbation theory to be valid. This implies that the inequality

$$\lambda < \frac{H^2}{\mathcal{A}}2\nu\delta\left[\frac{1+a^{-\delta}(t)}{\delta} - \frac{2\ln(a(t))}{a^{\delta}(t)-1}\right]^{-1}\ , \quad (2.80)$$

must hold during inflation. Massless limit of Eq. (2.80) yields $\lambda < 36\pi^2/\ln^2(a(t))$ in $D=4$, in agreement with the note—stated in Sec. 2.4—that the perturbation theory breaks down when $\ln(a(t)) \sim 1/\sqrt{\lambda}$.

We can examine the behaviors of one-loop correlator (i) at a fixed comoving separation at late times and (ii) for a fixed physical distance using Eqs. (2.75)-(2.76), as in the tree-order computations in Sec. 2.4.1. In case (i), the asymptotic limit of Eq. (2.76) at a fixed comoving separation Δx, is

$$f_1(t,t',\Delta x) \to \frac{1}{\delta}\frac{\sqrt{\pi}}{2^{3-\delta}}\frac{\Gamma\left(\frac{\delta}{2}\right)}{\Gamma\left(\frac{3-\delta}{2}\right)}\left[\alpha(t)\,\alpha(t')\right]^{-\frac{\delta}{2}}\Bigg\{\ln\Big(a(t)a(t')\Big) - \frac{1-a^{-\delta}(t)}{\delta}$$
$$+\frac{1-a^{-\delta}(t')}{\delta} + \mathcal{C}_1\Bigg\} - \frac{1}{2\delta^2}\left[a(t)a(t')\right]^{-\frac{\delta}{2}}\Bigg\{\Bigg[\ln\Big(a(t)a(t')\Big) - \frac{1-a^{-\delta}(t)}{\delta} - \frac{1-a^{-\delta}(t')}{\delta}\Bigg]$$
$$\times {}_1\mathcal{F}_2\Big(\frac{\delta}{2};\frac{3}{2},1+\frac{\delta}{2};-\frac{(H\Delta x)^2}{4}\Big) + 2\mathcal{C}_2\Bigg\}, \quad (2.81)$$

where

$$\mathcal{C}_1(\Delta x) = \ln\left(\frac{(H\Delta x)^2}{4}\right) - \psi\left(\frac{\delta}{2}\right) - \psi\left(\frac{3-\delta}{2}\right) , \tag{2.82}$$

$$\mathcal{C}_2(\Delta x) = \ln(H\Delta x) - \mathrm{ci}(H\Delta x) + \frac{1+\delta}{\delta}\left[\frac{\sin(H\Delta x)}{H\Delta x} - 1\right] + \frac{1}{\delta} + \gamma + \frac{1}{\delta^2}$$

$${}_2\mathcal{F}_3\left(\frac{\delta}{2},\frac{\delta}{2};\frac{3}{2},1+\frac{\delta}{2},1+\frac{\delta}{2};-\frac{(H\Delta x)^2}{4}\right) + \frac{(H\Delta x)^2}{3\delta(2+\delta)}\,{}_1\mathcal{F}_2\left(1+\frac{\delta}{2};\frac{5}{2},2+\frac{\delta}{2};-\frac{(H\Delta x)^2}{4}\right) . \tag{2.83}$$

The digamma function $\psi(z)$ is the logarithmic derivative of the gamma function, $\psi(z) = \Gamma'(z)/\Gamma(z)$. Equation (2.81) implies that the one-loop correlator of a massive scalar for a fixed comoving separation asymptotes to zero during inflation. For the massless scalar, Eq. (2.75) and the asymptotic limit of Eq. (2.78),

$$\lim_{m\to 0} f_1 \to \frac{1}{4}\left[\ln^2(a(t)) + \ln^2(a(t'))\right]\left[\frac{\sin(H\Delta x)}{H\Delta x} - \mathrm{ci}(H\Delta x)\right] + \mathcal{C}_0 , \tag{2.84}$$

where

$$\mathcal{C}_0(\Delta x) = \frac{1}{6}\ln^3(H\Delta x) - \frac{1}{2}[1-\gamma]\ln^2(H\Delta x) + \left[1-\gamma+\frac{\gamma^2}{2}-\frac{\pi^2}{24}\right]\ln(H\Delta x) - \frac{(H\Delta x)^2}{48}$$

$$\times {}_4\mathcal{F}_5\left(1,1,1,1;2,2,2,2,\frac{5}{2};-\frac{(H\Delta x)^2}{4}\right) - \frac{5}{6} + \frac{\pi^2}{24}(1-\gamma) + \frac{1}{3}\zeta(3) + \frac{\gamma}{2} - \frac{1}{6}(1-\gamma)^3 , \tag{2.85}$$

imply that the one-loop correlator grows negatively and proportional to $\ln^2(a)$ during inflation even for a Δx of order the horizon size $1/H$ because $\frac{\sin(H\Delta x)}{H\Delta x} - \mathrm{ci}(H\Delta x) > 0$. Thus, tree-order result (2.61) decreases when quantum corrections are included.

In case (ii), to obtain the one-loop correlator for a fixed physical distance, we choose $a(t')\Delta x$ as a constant fraction K of the Hubble length, as in the corresponding tree-order computation given in Sec. 2.4.1. The function $f_1(t,t',K)$, obtained by employing Eq. (2.62) in Eq. (2.76), is positive definite and grows in time. [It grows logarithmically with the scale factor in the massless limit; see Eq. (2.78).] Hence one-loop correlator (2.75), at fixed physical distance, grows negatively during inflation. This growth, however, is suppressed for massive scalars; see Fig. 2.2. As can be seen in the plots of the function $f_1(t=\frac{50}{H},t',K=\frac{1}{2})$ for $m = 0, H/8, H/4$ and $H/2$, the suppression is very sensitive to an increase in mass. In fact, for masses $m \geq H/2$ the one-loop correlator is effectively zero at late times. One can also infer the late time behavior of one-loop correlator from the asymptotic form of $f_1(t,t',K)$. For the

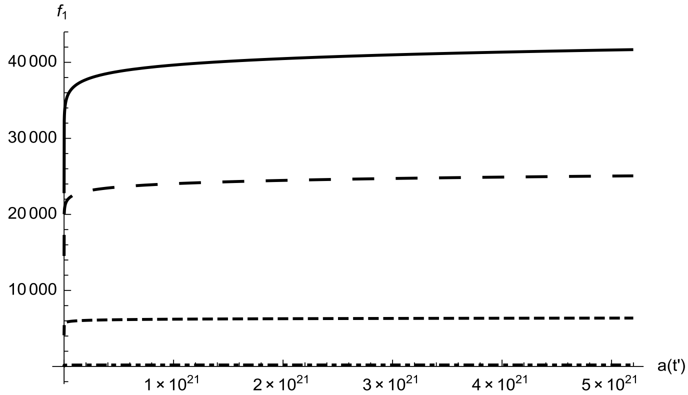

Figure 2.2 : Plots of $f_1(t,t',K)$, defined in Eq. (2.76) with separation (2.62), versus $a(t')$. The ranges of parameters K, $a(t)$, $a(t')$, m and styles of the lines are chosen same as in Fig. 2.1 except that here the $m\!=\!3H/4$ case is not plotted.

massive scalars,

$$f_1 \to \frac{1}{\delta^2}\left[\frac{a(t')}{a(t)}\right]^{\frac{\delta}{2}}\left\{\frac{1}{2}\left[\ln(a(t))-\ln(a(t'))+\frac{a^{-\delta}(t)}{\delta}-\frac{a^{-\delta}(t')}{\delta}\right]{}_1\mathcal{F}_2\Big(\frac{\delta}{2};\frac{3}{2},1+\frac{\delta}{2};-\frac{K^2}{4}\Big)\right.$$
$$+\frac{1}{\delta}\,{}_2\mathcal{F}_3\Big(\frac{\delta}{2},\frac{\delta}{2};\frac{3}{2},1+\frac{\delta}{2},1+\frac{\delta}{2};-\frac{K^2}{4}\Big)\Bigg\}-\frac{[a(t)\,a(t')]^{-\frac{\delta}{2}}}{\delta^2}\left\{\frac{1}{2}\left[\ln(a(t))+3\ln(a(t'))\right.\right.$$
$$\left.+\frac{1+a^{-\delta}(t)}{\delta}+\frac{1+a^{-\delta}(t')}{\delta}\right]+\mathrm{ci}(K)-\left[1+\frac{1}{\delta}\right]\frac{\sin(K)}{K}-\ln(K)-\gamma+1-\frac{K^2}{3\delta(2+\delta)}$$
$$\left.\times{}_1\mathcal{F}_2\Big(1+\frac{\delta}{2};\frac{5}{2},2+\frac{\delta}{2};-\frac{K^2}{4}\Big)\right\}. \tag{2.86}$$

Asymptotic form (2.86) consists of two kinds of terms: (i) the ones with the overall factor of $[a(t')/a(t)]^{\delta/2}$ minus (ii) the ones with the overall factor of $[a(t)a(t')]^{-\delta/2}$. For large masses $\left(\frac{1}{2}\lesssim\frac{m}{H}\leqslant\frac{3}{2}\right)$ in $D\!=\!4$) the both kinds are small; in fact, the latter is entirely negligible next to the former, as the overall factors indicate. As the mass decreases both (i) and (ii) grow rapidly. The latter, however, grows faster and becomes comparable to the former so that the asymptotic form of f_1 agrees with the—almost constant—values that can be read off from Fig. 2.2 at late times. In the massless limit, the asymptotic form,

$$\lim_{m\to 0} f_1 \to \frac{1}{4}\left\{\ln^2(a(t))\ln(a(t'))+\frac{\ln^3(a(t'))}{3}+\Big[\ln^2(a(t))-\ln^2(a(t'))\Big]\Big[\mathrm{ci}(K)\right.$$
$$-\frac{\sin(K)}{K}-\ln(K)-\gamma+1\Big]-\frac{K^2}{6}\,{}_3\mathcal{F}_4\Big(1,1,1;2,2,2,\frac{5}{2};-\frac{K^2}{4}\Big)\ln(a(t'))$$
$$\left.+\frac{K^2}{12}\,{}_4\mathcal{F}_5\Big(1,1,1,1;2,2,2,2,\frac{5}{2};-\frac{K^2}{4}\Big)\right\}, \tag{2.87}$$

implies a stronger—though logarithmic— growth compared to the massive case.

In the next section, we compute the two-loop contribution to the correlation function of the IR truncated scalar field in our model.

2.4.3 Two-Loop Correlator

Computation of two-loop contribution (2.45) in two-point correlation function (2.42) involves evaluations of three VEVs each of which has a double time integral without a definite time ordering in the integrand. Hence the computation is more intricate than that of the one-loop correlator which required evaluations of two VEVs each of which had a single time integral with a trivial time ordering in the integrand. Let us start to calculate the first VEV in Eq. (2.45),

$$\begin{aligned}
&\langle\Omega|\bar{\phi}_0(t,\vec{x})\int_0^{t'} d\tilde{t}\,\bar{\phi}_0^2(\tilde{t},\vec{x}')\int_0^{\tilde{t}} d\tilde{\tilde{t}}\,a^{\frac{\delta}{2}}(\tilde{\tilde{t}})\bar{\phi}_0^3(\tilde{\tilde{t}},\vec{x}')|\Omega\rangle \\
&=\int_0^{t'} d\tilde{t}\int_0^{\tilde{t}} d\tilde{\tilde{t}}\,a^{\frac{\delta}{2}}(\tilde{\tilde{t}})\Big\{2\cdot 3\cdot 1\,\langle\Omega|\bar{\phi}_0(t,\vec{x})\bar{\phi}_0(\tilde{t},\vec{x}')|\Omega\rangle\langle\Omega|\bar{\phi}_0(\tilde{t},\vec{x}')\bar{\phi}_0(\tilde{\tilde{t}},\vec{x}')|\Omega\rangle\langle\Omega|\bar{\phi}_0^2(\tilde{\tilde{t}},\vec{x}')|\Omega\rangle \\
&\quad +3\cdot 1\cdot 1\,\langle\Omega|\bar{\phi}_0(t,\vec{x})\bar{\phi}_0(\tilde{\tilde{t}},\vec{x}')|\Omega\rangle\langle\Omega|\bar{\phi}_0^2(\tilde{t},\vec{x}')|\Omega\rangle\langle\Omega|\bar{\phi}_0^2(\tilde{\tilde{t}},\vec{x}')|\Omega\rangle \\
&\quad +3\cdot 2\cdot 1\,\langle\Omega|\bar{\phi}_0(t,\vec{x})\bar{\phi}_0(\tilde{\tilde{t}},\vec{x}')|\Omega\rangle\left[\langle\Omega|\bar{\phi}_0(\tilde{t},\vec{x}')\bar{\phi}_0(\tilde{\tilde{t}},\vec{x}')|\Omega\rangle\right]^2\Big\}\,, \qquad (2.88)
\end{aligned}$$

where we have $0\leq\tilde{\tilde{t}}\leq\tilde{t}\leq t'$ and $t'\leq t$. This time ordering makes it easy to read off the VEVs in the integrand from Eqs. (2.51), (2.52), (2.55), (2.67), and (2.68). Substituting the outcomes into Eq. (2.88) turns the computation into the evaluations of three double integrals,

$$\begin{aligned}
&\langle\Omega|\bar{\phi}_0(t,\vec{x})\int_0^{t'} d\tilde{t}\bar{\phi}_0^2(\tilde{t},\vec{x}')\int_0^{\tilde{t}} d\tilde{\tilde{t}}\,a^{\frac{\delta}{2}}(\tilde{\tilde{t}})\bar{\phi}_0^3(\tilde{\tilde{t}},\vec{x}')|\Omega\rangle \\
&=\mathcal{A}^3\frac{a^{-\frac{\delta}{2}}(t)}{\delta^2}6\sum_{n=0}^{\infty}\frac{(-1)^n(H\Delta x)^{2n}}{(2n+1)!(2n+\delta)}\Big\{\int_0^{t'} d\tilde{t}\Big[a^{2n}(\tilde{t})-a^{-\delta}(\tilde{t})\Big]\int_0^{\tilde{t}} d\tilde{\tilde{t}}\Big[a^{\delta}(\tilde{\tilde{t}})+a^{-\delta}(\tilde{\tilde{t}})-2\Big] \\
&\quad +\frac{1}{2}\int_0^{t'} d\tilde{t}\Big[1-a^{-\delta}(\tilde{t})\Big]\int_0^{\tilde{t}} d\tilde{\tilde{t}}\Big[a^{2n+\delta}(\tilde{\tilde{t}})-a^{2n}(\tilde{\tilde{t}})+a^{-\delta}(\tilde{\tilde{t}})-1\Big] \\
&\quad +\int_0^{t'} d\tilde{t}a^{-\delta}(\tilde{t})\int_0^{\tilde{t}} d\tilde{\tilde{t}}\Big[a^{2n}(\tilde{\tilde{t}})-a^{-\delta}(\tilde{\tilde{t}})\Big]\Big[a^{\delta}(\tilde{\tilde{t}})-1\Big]^2\Big\}\,. \qquad (2.89)
\end{aligned}$$

The results of the double integrals in Eq. (2.89) are given in Appendix A.4.1. Using Eqs. (A.25)-(A.27) in Eq. (2.89) we obtain the first VEV in the two-loop correlator as

$$\begin{aligned}
&\langle\Omega|\bar{\phi}_0(t,\vec{x})\int_0^{t'} d\tilde{t}\,\bar{\phi}_0^2(\tilde{t},\vec{x}')\int_0^{\tilde{t}} d\tilde{\tilde{t}}\,a^{\frac{\delta}{2}}(\tilde{\tilde{t}})\bar{\phi}_0^3(\tilde{\tilde{t}},\vec{x}')|\Omega\rangle=-\frac{\mathcal{A}^3}{H^2}\frac{a^{-\frac{\delta}{2}}(t)}{\delta^2}6\sum_{n=0}^{\infty}\frac{(-1)^n(H\Delta x)^{2n}}{(2n+1)!(2n+\delta)} \\
&\times\Big\{\frac{\ln^2(a(t'))}{4}-\Big[\frac{1-a^{2n}(t')}{n}+\frac{9}{2}\Big[\frac{1-a^{-\delta}(t')}{\delta}\Big]-\frac{6}{\delta}-\frac{3}{4n}-\frac{1}{2(2n+\delta)}\Big]\ln(a(t'))
\end{aligned}$$

$$
\begin{aligned}
&+\left[\frac{1}{\delta}+\frac{1}{2(n+\delta)}+\frac{1}{2(2n+\delta)}\right]\left[\frac{1-a^{2n+\delta}(t')}{2n+\delta}\right]+\left[\frac{3}{4n}-\frac{5}{2(2n+\delta)}\right]\left[\frac{1-a^{2n}(t')}{2n}\right] \\
&-\left[\frac{1}{\delta}-\frac{3}{4n}\right]\left[\frac{1-a^{2n-\delta}(t')}{2n-\delta}\right]-\left[\frac{7}{2\delta}-\frac{3}{4n}-\frac{1}{2(n+\delta)}+\frac{5}{2(2n+\delta)}\right]\left[\frac{1-a^{-\delta}(t')}{\delta}\right] \\
&\left.-\frac{5}{2\delta}\left[\frac{1-a^{-2\delta}(t')}{2\delta}\right]\right\} . \qquad (2.90)
\end{aligned}
$$

Note that the $n=0$ term in the infinite sum in Eq. (2.90) is finite—though it includes terms proportional to n^{-1} and n^{-2}; see Eq. (A.28).

The second VEV that contributes at two-loop order in Eq. (2.45) is calculated similarly,

$$
\begin{aligned}
&\langle\Omega|\int_0^t dt''\bar{\phi}_0^2(t'',\vec{x})\int_0^{t''}dt'''a^{\frac{\delta}{2}}(t''')\bar{\phi}_0^3(t''',\vec{x})\bar{\phi}_0(t',\vec{x}')|\Omega\rangle \\
&=\int_0^t dt''\int_0^{t''}dt'''a^{\frac{\delta}{2}}(t''')\Big\{2\cdot3\cdot1\,\langle\Omega|\bar{\phi}_0(t'',\vec{x})\bar{\phi}_0(t',\vec{x}')|\Omega\rangle\,\langle\Omega|\bar{\phi}_0(t'',\vec{x})\bar{\phi}_0(t''',\vec{x})|\Omega\rangle \\
&\times\langle\Omega|\bar{\phi}_0^2(t''',\vec{x})|\Omega\rangle+1\cdot3\cdot1\,\langle\Omega|\bar{\phi}_0^2(t'',\vec{x})|\Omega\rangle\,\langle\Omega|\bar{\phi}_0(t''',\vec{x})\bar{\phi}_0(t',\vec{x}')|\Omega\rangle\,\langle\Omega|\bar{\phi}_0^2(t''',\vec{x})|\Omega\rangle \\
&+3\cdot2\cdot1\Big[\langle\Omega|\bar{\phi}_0(t'',\vec{x})\bar{\phi}_0(t''',\vec{x})|\Omega\rangle\Big]^2\langle\Omega|\bar{\phi}_0(t''',\vec{x})\bar{\phi}_0(t',\vec{x}')|\Omega\rangle\Big\}\,, \qquad (2.91)
\end{aligned}
$$

where $0\le t'''\le t''\le t$ and $t'\le t$. Substituting Eqs. (2.66), (2.67) and (2.68) into Eq. (2.91), brings it to a simpler form which includes three-double integrals each of which with a single VEV in the integrand:

$$
\begin{aligned}
&\langle\Omega|\int_0^t dt''\bar{\phi}_0^2(t'',\vec{x})\int_0^{t''}dt'''a^{\frac{\delta}{2}}(t''')\bar{\phi}_0^3(t''',\vec{x})\bar{\phi}_0(t',\vec{x}')|\Omega\rangle \\
&=\frac{\mathcal{A}^2}{\delta^2}6\Big\{\int_0^t dt''\int_0^{t''}dt'''a^{\frac{\delta}{2}}(t''')\langle\Omega|\bar{\phi}_0(t'',\vec{x})\bar{\phi}_0(t',\vec{x}')|\Omega\rangle\Big[a(t'')\,a(t''')\Big]^{-\frac{\delta}{2}}\Big[a^{\delta}(t''')-1\Big] \\
&\times\Big[1-a^{-\delta}(t''')\Big]+\frac{1}{2}\int_0^t dt''\int_0^{t''}dt'''a^{\frac{\delta}{2}}(t''')\langle\Omega|\bar{\phi}_0(t''',\vec{x})\bar{\phi}_0(t',\vec{x}')|\Omega\rangle\Big[1-a^{-\delta}(t'')\Big] \\
&\times\Big[1-a^{-\delta}(t''')\Big]+\int_0^t dt''\int_0^{t''}dt'''a^{\frac{\delta}{2}}(t''')\langle\Omega|\bar{\phi}_0(t''',\vec{x})\bar{\phi}_0(t',\vec{x}')|\Omega\rangle\Big[a(t'')\,a(t''')\Big]^{-\delta} \\
&\times\Big[a^{\delta}(t''')-1\Big]^2\Big\}\,. \qquad (2.92)
\end{aligned}
$$

Because the orderings between t' and t'' and between t' and t''' are unknown in the double integrals, we cannot just read off the VEVs from Eqs. (2.51), (2.52), and (2.55). We can, however, decompose the double integrals so that a definite ordering between the time parameters exists. That makes the evaluation of the integrals, using Eqs. (2.51), (2.52) and (2.55), possible; see Appendix A.4.2. Substituting Eqs. (A.31), (A.34) and (A.36) into Eq. (2.92), we find

$$
\begin{aligned}
&\langle\Omega|\int_0^t dt''\bar{\phi}_0^2(t'',\vec{x})\int_0^{t''}dt'''a^{\frac{\delta}{2}}(t''')\bar{\phi}_0^3(t''',\vec{x})\bar{\phi}_0(t',\vec{x}')|\Omega\rangle \\
&=-\frac{\mathcal{A}^3}{H^2}\frac{a^{-\frac{\delta}{2}}(t')}{\delta^2}3\sum_{n=0}^{\infty}\frac{(-1)^n(H\Delta x)^{2n}}{(2n+1)!(2n+\delta)}\Bigg\{\left[\frac{1-a^{2n+\delta}(t')}{2}\right]\ln^2(a(t))+a^{2n+\delta}(t') \\
&\times\left[\ln(a(t))-\frac{\ln(a(t'))}{2}\right]\ln(a(t'))+\left[\left[\frac{1-a^{2n+\delta}(t')}{\delta}\right]\left[9a^{-\delta}(t)+\frac{\delta}{2n+\delta}+4\right]\right. \\
&\left.-\left[\frac{1-a^{2n}(t')}{\delta}\right]\left[1+\frac{\delta}{2n}\right]\right]\ln(a(t))+\left[\frac{a^{2n}(t')}{\delta}\left[2a^{\delta}(t')+\frac{3\delta}{2n}+3\right]+\frac{a^{2n+\delta}(t')}{\delta}\right. \\
&\left.\times\left[5a^{-\delta}(t)+\frac{\delta}{2n+\delta}+2\right]\right]\ln(a(t'))-\left[\frac{1-a^{2n+2\delta}(t')}{\delta}\right]\left[\frac{a^{-\delta}(t)}{\delta}\left[\frac{\delta}{n+\delta}-2\right]\right. \\
&\left.-\frac{a^{-\delta}(t')}{n+\delta}\right]+\left[\frac{1-a^{2n+\delta}(t')}{\delta}\right]\left[\frac{a^{-\delta}(t)}{\delta}\left[\frac{5a^{-\delta}(t)}{2}+\frac{5\delta}{2n+\delta}+8\right]+\frac{a^{-\delta}(t')}{\delta}\right. \\
&\left.\times\left[a^{-\delta}(t')-\frac{4\delta}{2n+\delta}\right]+\frac{\delta}{2n+\delta}\left[\frac{1}{2n+\delta}+\frac{1}{n+\delta}+\frac{2}{\delta}\right]-\frac{2}{\delta}\right]-\left[\frac{1-a^{2n}(t')}{\delta}\right] \\
&\times\left[\frac{a^{-\delta}(t)}{\delta}\left[\frac{3\delta}{2n}+3\right]-\frac{3a^{-\delta}(t')}{2n}+\frac{1}{2n+\delta}\left[\frac{5\delta}{2n}+1\right]-\frac{3\delta}{4n^2}+\frac{8}{\delta}\right]+\left[\frac{1-a^{2n-\delta}(t')}{\delta}\right] \\
&\times\left[\frac{\delta}{2n-\delta}\left[\frac{3}{2n}-\frac{2}{\delta}\right]-\frac{1}{2\delta}\right]+\left[\frac{1-a^{-\delta}(t')}{\delta}\right]\left[\frac{a^{-\delta}(t')}{\delta}+\frac{3}{2n}+\frac{1}{n+\delta}-\frac{4}{2n+\delta}+\frac{1}{\delta}\right]\Bigg\}\,. \qquad (2.93)
\end{aligned}
$$

Note that the $n=0$ term in the infinite sum in Eq. (2.93) is finite—though it includes terms proportional to n^{-1} and n^{-2}; see Eq. (A.37).

Finally, the third VEV that contributes at two-loop order in Eq. (2.45) is

$$
\begin{aligned}
&\langle\Omega|\int_0^t dt''a^{\frac{\delta}{2}}(t'')\bar{\phi}_0^3(t'',\vec{x})\int_0^{t'}d\tilde{t}\,a^{\frac{\delta}{2}}(\tilde{t})\bar{\phi}_0^3(\tilde{t},\vec{x}')|\Omega\rangle \\
&=\int_0^t dt''\,a^{\frac{\delta}{2}}(t'')\int_0^{t'}d\tilde{t}\,a^{\frac{\delta}{2}}(\tilde{t})\Bigg\{3\cdot1\cdot1\,\langle\Omega|\bar{\phi}_0(t'',\vec{x})\bar{\phi}_0(\tilde{t},\vec{x}')|\Omega\rangle\,\langle\Omega|\bar{\phi}_0^2(t'',\vec{x})|\Omega\rangle \\
&\times\langle\Omega|\bar{\phi}_0^2(\tilde{t},\vec{x}')|\Omega\rangle+2\cdot3\cdot1\,\langle\Omega|\bar{\phi}_0^2(t'',\vec{x})|\Omega\rangle\,\langle\Omega|\bar{\phi}_0(t'',\vec{x})\bar{\phi}_0(\tilde{t},\vec{x}')|\Omega\rangle\,\langle\Omega|\bar{\phi}_0^2(\tilde{t},\vec{x}')|\Omega\rangle \\
&\qquad+3\cdot2\cdot1\left[\langle\Omega|\bar{\phi}_0(t'',\vec{x})\bar{\phi}_0(\tilde{t},\vec{x}')|\Omega\rangle\right]^3\Bigg\}\,, \qquad (2.94)
\end{aligned}
$$

where $0\leq t''\leq t$, $0\leq\tilde{t}\leq t'$, and $t'\leq t$. The integrand on the right of Eq. (2.94) consists of three terms that are added together. Notice that the second term is twice the first term. Using Eqs. (2.66), (2.67), and (2.68) in Eq. (2.94) we get

$$
\begin{aligned}
&\langle\Omega|\int_0^t dt''a^{\frac{\delta}{2}}(t'')\bar{\phi}_0^3(t'',\vec{x})\int_0^{t'}d\tilde{t}\,a^{\frac{\delta}{2}}(\tilde{t})\bar{\phi}_0^3(\tilde{t},\vec{x}')|\Omega\rangle \\
&=\int_0^t dt''a^{\frac{\delta}{2}}(t'')\int_0^{t'}d\tilde{t}\,a^{\frac{\delta}{2}}(\tilde{t})\Bigg\{9\langle\Omega|\bar{\phi}_0(t'',\vec{x})\bar{\phi}_0(\tilde{t},\vec{x}')|\Omega\rangle\mathcal{A}^2\left[\frac{1-a^{-\delta}(t'')}{\delta}\right]\left[\frac{1-a^{-\delta}(\tilde{t})}{\delta}\right]
\end{aligned}
$$

$$+6\left[\langle\Omega|\bar{\phi}_0(t'',\vec{x})\bar{\phi}_0(\tilde{t},\vec{x}\,')|\Omega\rangle\right]^3\Bigg\}\,. \tag{2.95}$$

At this stage, we break up the double integral into two parts: $\int_0^t dt''\int_0^{t'}d\tilde{t}=\int_0^{\tilde{t}}dt''\int_0^{t'}d\tilde{t}+\int_{\tilde{t}}^t dt''\int_0^{t'}d\tilde{t}$, where in the first part we have $t''\leq\tilde{t}$ whereas $\tilde{t}\leq t''$ in the second. Then, we employ Eqs. (2.51), (2.52), and (2.55) to obtain

$$\langle\Omega|\int_0^t dt''\,a^{\frac{\delta}{2}}(t'')\bar{\phi}_0^3(t'',\vec{x})\int_0^{t'}d\tilde{t}\,a^{\frac{\delta}{2}}(\tilde{t})\bar{\phi}_0^3(\tilde{t},\vec{x}\,')|\Omega\rangle=\mathcal{A}^3\Bigg\{\frac{9}{\delta^2}\sum_{n=0}^{\infty}\frac{(-1)^n(H\Delta x)^{2n}}{(2n+1)!(2n+\delta)}$$
$$\times\Bigg[\int_0^{t'}d\tilde{t}\left[1-a^{-\delta}(\tilde{t})\right]\Bigg[\int_0^{\tilde{t}}dt''\left[1-a^{-\delta}(t'')\right]\left[a^{2n+\delta}(t'')-1\right]+\left[a^{2n+\delta}(\tilde{t})-1\right]$$
$$\times\int_{\tilde{t}}^t dt''\left[1-a^{-\delta}(t'')\right]\Bigg]\Bigg]+6\int_0^{t'}d\tilde{t}\,a^{-\delta}(\tilde{t})\Bigg[\int_0^{\tilde{t}}dt''a^{-\delta}(t'')\Bigg[\sum_{n=0}^{\infty}\frac{(-1)^n(H\Delta x)^{2n}}{(2n+1)!(2n+\delta)}$$
$$\times\left[a^{2n+\delta}(t'')-1\right]\Bigg]^3+\int_{\tilde{t}}^t dt''a^{-\delta}(t'')\Bigg[\sum_{n=0}^{\infty}\frac{(-1)^n(H\Delta x)^{2n}}{(2n+1)!(2n+\delta)}\left[a^{2n+\delta}(\tilde{t})-1\right]\Bigg]^3\Bigg]\Bigg\}\,. \tag{2.96}$$

The results of the four double integrals in Eq. (2.96) are given in Appendix A.4.3. Substituting Eqs. (A.38)-(A.40) and (A.42) into Eq. (2.96), we obtain

$$\langle\Omega|\int_0^t dt''\,a^{\frac{\delta}{2}}(t'')\bar{\phi}_0^3(t'',\vec{x})\int_0^{t'}d\tilde{t}\,a^{\frac{\delta}{2}}(\tilde{t})\bar{\phi}_0^3(\tilde{t},\vec{x}\,')|\Omega\rangle=-\frac{\mathcal{A}^3}{H^2}9\Bigg\{\frac{1}{\delta^2}\sum_{n=0}^{\infty}\frac{(-1)^n(H\Delta x)^{2n}}{(2n+1)!(2n+\delta)}$$
$$\times\Bigg[\ln(a(t))\ln(a(t'))+\Bigg[\frac{1-a^{2n+\delta}(t')}{2n+\delta}-\frac{1-a^{2n}(t')}{2n}-\frac{1-a^{-\delta}(t')}{\delta}\Bigg]\ln(a(t))-\Bigg[\frac{1-a^{-\delta}(t)}{\delta}$$
$$-\frac{1+a^{2n+\delta}(t')}{2n+\delta}+\frac{1+a^{2n}(t')}{2n}\Bigg]\ln(a(t'))+\frac{1-a^{2n+\delta}(t')}{2n+\delta}\Bigg[\frac{a^{-\delta}(t)}{\delta}+\frac{2}{2n+\delta}\Bigg]-\frac{1-a^{2n}(t')}{2n}$$
$$\times\Bigg[\frac{1+a^{-\delta}(t)}{\delta}+\frac{1}{n}+\frac{1}{2n+\delta}\Bigg]+\frac{1-a^{2n-\delta}(t')}{2n-\delta}\Bigg[\frac{1}{\delta}+\frac{1}{2n}\Bigg]+\frac{1-a^{-\delta}(t')}{\delta}\Bigg[\frac{1-a^{-\delta}(t)}{\delta}$$
$$+\frac{1}{2n}-\frac{1}{2n+\delta}\Bigg]\Bigg]-\frac{2}{3}\sum_{q=0}^{\infty}\sum_{p=0}^{q}\sum_{n=0}^{p}\Gamma_{qpn}(H\Delta x)^{2q}\Bigg[\frac{a^{-\delta}(t)}{\delta}\Bigg[\frac{1-a^{2(q+\delta)}(t')}{2(q+\delta)}$$
$$-3\Bigg[\frac{1-a^{2p+\delta}(t')}{2p+\delta}\Bigg]+3\Bigg[\frac{1-a^{2(q-p)}(t')}{2(q-p)}\Bigg]\Bigg]-\frac{1-a^{2q+\delta}(t')}{2q+\delta}\Bigg[\frac{1}{2(q+\delta)}+\frac{1}{\delta}\Bigg]$$
$$+3\Bigg[\frac{1-a^{2p}(t')}{2p}\Bigg]\Bigg[\frac{1}{2p+\delta}+\frac{1}{\delta}\Bigg]-3\Bigg[\frac{1-a^{2(q-p)-\delta}(t')}{2(q-p)-\delta}\Bigg]\Bigg[\frac{1}{2(q-p)}+\frac{1}{\delta}\Bigg]$$
$$-\frac{1-a^{-\delta}(t')}{\delta}\Bigg[\frac{1-a^{-\delta}(t)}{\delta}+\frac{1}{2(q+\delta)}-\frac{3}{2p+\delta}+\frac{3}{2(q-p)}\Bigg]\Bigg]\Bigg\}\,, \tag{2.97}$$

where the δ-dependent coefficients Γ_{qpn} are defined in Eq. (A.41) which we copy here,

$$\Gamma_{qpn}\equiv\frac{(-1)^q}{[2(q-p)+1]![2(q-p)+\delta][2(p-n)+1]![2(p-n)+\delta][2n+1]![2n+\delta]}\,.$$

Note that the $n=0$ term in the first infinite sum in Eq. (2.97) is finite—though the sum includes terms proportional to n^{-1} and n^{-2}; see Eq. (A.43). Note also that the $p=0$ and $p=q$ terms in the triple infinite sum in Eq. (2.97) are finite—though the sum includes terms proportional to p^{-1} and $(q-p)^{-1}$; see Eqs. (A.44) and (A.45).

We have completed evaluating each of the three VEVs that yields an $\mathcal{O}(\lambda^2)$ contribution to two-point correlation function (2.42). Hence, substitution of VEVs (2.90), (2.93), and (2.97) into Eq. (2.45) yields the two-loop correlator which can be expressed as

$$\langle\Omega|\bar{\varphi}(t,\vec{x})\bar{\varphi}(t',\vec{x}')|\Omega\rangle_{2-\text{loop}} \simeq \frac{\lambda^2}{(2\nu)^2}\frac{\mathcal{A}^3}{H^4}f_2(t,t',\Delta x)\,. \tag{2.98}$$

To save space we don't write the explicit form of the function $f_2(t,t',\Delta x)$.

The reader can add up tree, one- and two-loop correlators (2.51), (2.75), and (2.98) and obtain one- and two-loop corrected two-point correlation function (2.42) of the IR truncated full field. Coincidence limit of the quantum corrected two-point correlation function (2.42) of the IR truncated full field

$$\begin{aligned}\langle\Omega|\bar{\varphi}^2(t,\vec{x})|\Omega\rangle =& \mathcal{A}\frac{1-a^{-\delta}(t)}{\delta} - \frac{\lambda}{2\nu}\frac{\mathcal{A}^2}{H^2}\frac{a^{-\delta}(t)}{\delta^2}\left[\frac{a^{\delta}(t)-a^{-\delta}(t)}{\delta}-2\ln(a(t))\right]\\ &+\frac{\lambda^2}{(2\nu)^2}\frac{\mathcal{A}^3}{H^4}\frac{a^{-\delta}(t)}{\delta^3}2\times\left\{\frac{4}{3}\left[\frac{a^{\delta}(t)-1}{\delta^2}\right]-\ln^2(a(t))-\left[\frac{3+4a^{-\delta}(t)}{\delta}\right]\ln(a(t))\right.\\ &\left.+4\left[\frac{1-a^{-\delta}(t)}{\delta^2}\right]+\frac{5}{6}\left[\frac{1-a^{-2\delta}(t)}{\delta^2}\right]\right\}+\mathcal{O}(\lambda^3)\,.\end{aligned} \tag{2.99}$$

We employed Eqs. (2.68), (2.79), and the equal spacetime limit of Eq. (2.98) to get Eq. (2.99) from which one can obtain the leading contributions to the induced self-mass squared by the curvature of the potential, $\lambda\langle\Omega|\bar{\varphi}^2(t,\vec{x})|\Omega\rangle/2$, at each order up to $\mathcal{O}(\lambda^4)$. To estimate the induced self-mass squared, we choose $D=4$ and $m=H/2$ in Eq. (2.99) and find, up to $\mathcal{O}(\lambda^3)$,

$$\begin{aligned}\frac{\lambda}{2}\langle\Omega|\bar{\varphi}^2(t,\vec{x})|\Omega\rangle =& \frac{\lambda\,\Gamma^2(2\nu)}{\Gamma^2(\nu+\frac{1}{2})}\frac{H^2}{2^{2\nu+2}\pi^2}\\ &\times\left\{\frac{1-a^{-\delta}}{\delta}-\frac{\lambda\,\Gamma^2(2\nu)}{\nu\Gamma^2(\nu+\frac{1}{2})}\frac{a^{-\delta}(t)}{2^{2\nu+2}\pi^2\delta^2}\left[\frac{a^{\delta}(t)-a^{-\delta}(t)}{\delta}-2\ln(a(t))\right]\right\},\end{aligned} \tag{2.100}$$

where $\nu=\sqrt{2}$ and $\delta=3-2\sqrt{2}$. The only dimensional parameter in Eq. (2.100) is the Hubble parameter H. Inserting back the Planckian units $H\to(Ht_P)M_P=H\hbar/\mathrm{c}^2$

where the Planck time $t_P \simeq 5.4\times10^{-44}$s and the Planck mass $M_P \simeq 1.22\times10^{19}\mathrm{GeV}/\mathrm{c}^2$. An upper limit for the Hubble parameter during inflation is $H \sim 10^{38}$Hz. Thus, for the scalar with $m^2 = H^2/4$, an upper bound for the effective mass is estimated by taking the $a = e^{50}$ as

$$m_{\mathrm{eff}} \sim \left(3.3+\lambda\,0.43-\lambda^2\,0.14\right)\times10^{13}\,\frac{\mathrm{GeV}}{\mathrm{c}^2}\left(\frac{H}{10^{38}\mathrm{Hz}}\right)\,. \tag{2.101}$$

Let us note that the massless limit of Eq. (2.99),

$$\lim_{m\to0}\langle\Omega|\bar{\phi}^2(t,\vec{x})|\Omega\rangle = \frac{H^{D-2}}{2^{D-1}\pi^{D/2}}\frac{\Gamma(D-1)}{\Gamma\left(\frac{D}{2}\right)}\ln(a(t)) - \frac{\lambda}{(D-1)}\frac{H^{2D-6}}{2^{2D-2}\,3\,\pi^{D}}\frac{\Gamma^2(D-1)}{\Gamma^2\left(\frac{D}{2}\right)}$$
$$\times\ln^3(a(t)) + \frac{\lambda^2}{(D-1)^2}\frac{H^{3D-10}}{2^{3D-3}\,5\,\pi^{3D/2}}\frac{\Gamma^3(D-1)}{\Gamma^3\left(\frac{D}{2}\right)}\ln^5(a(t)) + \mathcal{O}(\lambda^3)\,, \tag{2.102}$$

reproduces the result found in Ref. [67]. Note also that, the renormalized $\langle\Omega|\phi^2(t,\vec{x})|\Omega\rangle$ for the massless full field $\phi(t,\vec{x})$ with a quartic self interaction in de Sitter background was computed in Ref. [29] using the results calculated in Ref. [28] applying the Schwinger-Keldish formalism. Limit (2.102) agrees with it in leading logaritm order, as it should. Equation (2.102) can be used to estimate the self-mass squared induced by the curvature of the potential for a massless scalar. For $D = 4$,

$$\lim_{m\to0}\frac{\lambda}{2}\langle\Omega|\bar{\phi}^2(t,\vec{x})|\Omega\rangle = \lambda\frac{H^2}{8\pi^2}\ln(a(t))\left\{1-\lambda\frac{\ln^2(a(t))}{2^2 3^2\pi^2}+\lambda^2\frac{\ln^4(a(t))}{2^4 3^2 5\pi^4}+\mathcal{O}(\lambda^3)\right\} \tag{2.103}$$

which implies an upper bound for the effective mass as,

$$m_{\mathrm{eff}} \sim \sqrt{\lambda}\,(5.2-\lambda\,18.4)\times10^{13}\,\frac{\mathrm{GeV}}{\mathrm{c}^2}\left(\frac{H_I}{10^{38}\mathrm{Hz}}\right)\,. \tag{2.104}$$

Next, we use Eq. (2.99) to compute the stochastic contributions to the power spectrum at tree, one- and two-loop order.

2.5 Power Spectrum

Using the free-field mode expansion $\phi_0(t,\vec{x})$ in Eq. (1.4) yields the tree-order power spectrum as,

$$\Delta^2_{\phi_0}(t,k) = \frac{k^{D-1}}{\pi^{\frac{D}{2}}}\frac{\Gamma\left(\frac{D}{2}\right)}{\Gamma(D-1)}|u_0(t,k)|^2\,, \tag{2.105}$$

where $u_0(t,k)$ is the tree-order mode function, which agrees with Eq. (1.5) at tree-order. The quantum corrected field $\phi(t,\vec{x})$ is an interacting quantum field; hence, it does not have a free-field expansion. Using the full field $\phi(t,\vec{x})$ in Eq. (1.6) and using [59] the full (quantum corrected) mode function $u(t,k)$ in Eq. (2.105) do not give the same result exactly. One can, therefore, define [58] the quantum corrected power spectrum Δ^2_ϕ either (i) using the full field $\phi(t,\vec{x})$ in Eq. (1.6) or (ii) using [54] the quantum corrected mode function $u(t,k)$ in Eq. (2.105). We use [56,57] definition (i) to compute the loop corrections to the power spectrum. The equal space limit of Eq. (1.6) implies for the coincident correlator

$$\langle\Omega|\phi^2(t,\vec{x})|\Omega\rangle \equiv \int_0^\infty \frac{dk}{k}\Delta^2_\phi(t,k) \; . \tag{2.106}$$

The stochastic contributions to the coincident correlator ought to involve the usual, time-independent power spectrum $\Delta^2_\phi(k) \equiv \lim_{t\gg t_k}\Delta^2_\phi(t,k)$ where t_k is the time of first horizon crossing defined by Eq. (2.28). Thus, we obtain [56]

$$\langle\Omega|\bar{\phi}^2(t,\vec{x})|\Omega\rangle_{\rm stoch} \equiv \int_0^\infty \frac{dk}{k}\Theta\left(Ha(t)-k\right)\Delta^2_\phi(k) = \int_{k_i=H}^{Ha(t)} \frac{dk}{k}\Delta^2_\phi(k) \; . \tag{2.107}$$

Taking the derivative with respect to time, yields the power for the horizon-sized mode k at time $t=t_k$:

$$\Delta^2_{\bar{\phi}}\left(k=Ha(t)\right) = \frac{1}{H}\frac{d}{dt}\langle\Omega|\bar{\phi}^2(t,\vec{x})|\Omega\rangle_{\rm stoch} \; . \tag{2.108}$$

One can, however, look at the power at and time t and that time corresponds to a mode k through the relation $a(t)=k/H$. Therefore, by considering in Eq. (2.108) at different times one can access the power for different modes (k values). Using our quantum corrected coincident correlator (2.99) in Eq. (2.108) we obtain the quantum corrected power spectrum. In $D=4$, we find

$$\begin{aligned}\Delta^2_{\bar{\phi}}(k=Ha(t)) = {} & \frac{\Gamma^2(2\nu)}{\Gamma^2(\nu+\frac{1}{2})}\frac{H^2}{2^{2\nu+1}\pi^2}\Bigg\{a^{-\delta}(t) - \frac{\lambda}{\nu}\frac{\Gamma^2(2\nu)}{\Gamma^2(\nu+\frac{1}{2})}\frac{a^{-\delta}(t)}{2^{2\nu+1}\pi^2\delta} \\ & \times\left[\ln(a(t)) - \frac{1-a^{-\delta}(t)}{\delta}\right] + \frac{\lambda^2}{\nu^2}\frac{\Gamma^4(2\nu)}{\Gamma^4(\nu+\frac{1}{2})}\frac{a^{-\delta}(t)}{2^{4\nu+3}\pi^4\delta^2}\left[\ln^2(a(t)) + \left[\frac{1+8a^{-\delta}(t)}{\delta}\right]\right. \\ & \left.\times\ln(a(t)) - 4\left[\frac{1-a^{-\delta}(t)}{\delta^2}\right] - \frac{5}{2}\left[\frac{1-a^{-2\delta}(t)}{\delta^2}\right]\right] + \mathcal{O}(\lambda^3)\Bigg\} \; . \end{aligned} \tag{2.109}$$

Here and in the rest of this section $\nu=\sqrt{9/4-(m/H)^2}$, $\delta=3-2\nu$ and $a(t)=k/H$, i.e. $t=t_k$. Power (2.109) is scale dependent. At tree-order, $\Delta^2_{\bar{\varphi}_{\rm tree}} = \frac{\Gamma^2(2\nu)}{\Gamma^2(\nu+\frac{1}{2})}\frac{H^2}{2^{2\nu+1}\pi^2}\left(\frac{k}{H}\right)^{-\delta}$. As the comoving wave number k increases, i.e. as the scale decreases, the tree-order power decreases. That means that the power increases as the scale increases and the spectrum is said to be red-tilted. At one-loop order,

$$\Delta^2_{\bar{\varphi}_{1-\rm loop}} = -\frac{\lambda}{\nu}\frac{\Gamma^4(2\nu)}{\Gamma^4(\nu+\frac{1}{2})}\frac{H^2}{2^{4\nu+2}\pi^4\delta}\left(\frac{k}{H}\right)^{-\delta}\left[\ln\left(\frac{k}{H}\right) - \frac{1}{\delta}\left[1-\left(\frac{k}{H}\right)^{-\delta}\right]\right] \; .$$

As the scale decreases the one-loop power decreases (grows negatively) and hence enhances the tree-order red-tilt. For a given mode, on the other hand, one-loop correction implies that the power is less than the tree-order power implies.

The massless limit of Eq. (2.109) is

$$\lim_{m\to 0}\Delta^2_{\bar\varphi}(k=Ha(t))=\frac{H^2}{4\pi^2}\left\{1-\lambda\frac{\ln^2(a(t))}{2^2\,3\,\pi^2}+\lambda^2\frac{\ln^4(a(t))}{2^4\,3^2\,\pi^4}+\mathcal{O}(\lambda^3)\right\}\ . \tag{2.110}$$

Thus, unlike the massive scalar, the power spectrum is scale invariant, and therefore, has zero tilt at tree-order in this limit. At one-loop order $\Delta^2_{\bar\varphi_{1-\mathrm{loop}}}=-\lambda\frac{H^2}{48\pi^4}\ln^2\left(\frac{k}{H}\right)$, hence the spectrum is red-tilted. Like in the massive case, the power for a given mode decreases when the loop corrections are included.

In the next section, we compute the quantum corrected spectral index for a massive spectator scalar using the quantum corrected power spectrum.

2.5.1 Spectral Index n_ϕ of the Spectator Scalar

The spectral index $n_{\bar\phi}$ which measures variation of power spectrum $\Delta^2_{\bar\phi}(k)$ with scale, for the spectator scalar in this thesis, is defined as that of the inflaton given in Eq. (1.10). Hence,

$$n_{\bar\phi}(k=Ha(t))\equiv 1+\frac{d\ln\left(\Delta^2_{\bar\phi}(k=Ha(t))\right)}{d\ln(k)}=1+\frac{a(t)}{\Delta^2_{\bar\phi}(k=Ha(t))}\frac{\partial\Delta^2_{\bar\phi}(k=Ha(t))}{\partial a(t)}. \tag{2.111}$$

Using Eq. (2.109) in Eq. (2.111), the quantum corrected spectral index for the massive scalar in our model is obtained as

$$n_{\bar\phi}(k=Ha(t))=1-\delta-\frac{\lambda}{\nu}\frac{\Gamma^2(2\nu)}{\Gamma^2(\nu+\frac{1}{2})}\frac{1}{2^{2\nu+1}\pi^2}\left[\frac{1-a^{-\delta}(t)}{\delta}\right]$$
$$+\frac{\lambda^2}{\nu^2}\frac{\Gamma^4(2\nu)}{\Gamma^4(\nu+\frac{1}{2})}\frac{3}{2^{4\nu+3}\pi^4\delta}\left[\frac{1-a^{-2\delta}(t)}{\delta^2}-2\frac{a^{-\delta}(t)}{\delta}\ln(a(t))\right]+\mathcal{O}(\lambda^3)\ , \tag{2.112}$$

which implies a red-tilted ($n_{\bar\phi}<0$) primordial spectrum in accordance with the above discussion. Thus, the amplitudes of fluctuations grow toward the larger scales.

The massless limit of Eq. (2.112)

$$\lim_{m\to 0}n_{\bar\phi}(k=Ha(t))=1-\lambda\frac{\ln(a(t))}{2\,3\,\pi^2}+\lambda^2\frac{\ln^3(a(t))}{2^3\,3^2\,\pi^4}+\mathcal{O}(\lambda^3)\ , \tag{2.113}$$

implies a scale invariant ($n_{\bar\varphi}=0$) tree-order primordial spectrum for the fluctuations of the massless spectator scalar. Loop corrections, however, red-tilt the spectrum. Data obtained from CMB, galaxy power spectra and gravitational lensing survey correlation function provides evidence for a primordial power spectrum with a red-tilt. In the next section, we study the variaton of the n_ϕ with scale measured by the running of the spectral index.

2.5.2 Running of the Spectral Index α_ϕ of the Spectator Scalar

The running of the spectral index is defined in Eq. (1.12). Hence,

$$\alpha_{\bar{\phi}}(k=Ha(t)) \equiv \frac{d\,n_{\bar{\phi}}(k=Ha(t))}{d\ln(k)} = a(t)\frac{\partial n_{\bar{\phi}}(k=Ha(t))}{\partial a(t)} \,. \tag{2.114}$$

Employing Eq. (2.112) in Eq. (2.114), the running of the massive scalar is obtained as

$$\begin{aligned}\alpha_{\bar{\phi}}(k=Ha(t)) = & -\frac{\lambda}{\nu}\frac{\Gamma^2(2\nu)}{\Gamma^2(\nu+\frac{1}{2})}\frac{a^{-\delta}(t)}{2^{2\nu+1}\pi^2}+\frac{\lambda^2}{\nu^2}\frac{\Gamma^4(2\nu)}{\Gamma^4(\nu+\frac{1}{2})}\frac{3a^{-\delta}(t)}{2^{4\nu+2}\pi^4\delta} \\ & \times\left[\ln(a(t))-\frac{1-a^{-\delta}(t)}{\delta}\right] .\end{aligned} \tag{2.115}$$

The massless limit of Eq. (2.115)

$$\lim_{m\to 0}\alpha_{\bar{\phi}}(k=Ha(t)) = -\frac{\lambda}{2\,3\,\pi^2}+\lambda^2\frac{\ln^2(a(t))}{2^3\,3\,\pi^4}+\mathcal{O}(\lambda^3) \,. \tag{2.116}$$

Eqs (2.115) and (2.116) imply that the spectral index increases as the scale changes from the scale at which the index is measured to a larger scale for both the massive and massless scalars. In the next section, we compare the measurements of the Planck 2018 Collaboration for the n and α with our predictions for the n_ϕ and α_ϕ of the spectator scalar field fluctuations.

2.6 Comparison of Our Predictions for the $n_{\delta\varphi}$ and $\alpha_{\delta\varphi}$ with Measurements

The cosmological measurements [60] for the n and α, obtained by analyzing three data sets, are given in Table 2.1. The $n_{\bar{\phi}}$ and $\alpha_{\bar{\phi}}$ for the fluctuations of a spectator

Table 2.1 : Planck 2018 Collaboration constraints on the n and α.

	Planck Collaboration Constraints	
Data Sets	n	α
TT,TE,EE+lowEB+lensing	0.9647 ± 0.0044	-0.0085 ± 0.0073
TT,TE,EE+lowE+lensing+BK15	0.9639 ± 0.0044	-0.0069 ± 0.0069
TT,TE,EE+lowE+lensing+BK15+BAO	0.9658 ± 0.0040	-0.0066 ± 0.0070

scalar with potential (2.4) during de Sitter inflation are given in Eqs. (2.112) and

(2.115), respectively. Since the H is constant, the slow-roll parameter ε is not defined in de Sitter spacetime. However, using the equality $\varepsilon = \frac{m^2}{3H^2}$ (Eq. (3.11)), we may identify the ratio $\frac{m^2}{3H^2}$ as a new parameter ε in de Sitter, corresponding to the initial value of the slow-roll parameter for the inflaton ε_{i0}, to make predictions for the $n_{\bar{\phi}}$ and $\alpha_{\bar{\phi}}$ and compare the results with the measured values in Table 2.1. Defining $\nu \equiv \sqrt{9/4-3\varepsilon}$ and $\delta \equiv 3-2\nu$ in Eqs. (2.112) and (2.115), yield, for $a(t_k)=e^{50}$, the predictions given in Table 2.2, up to $\mathcal{O}(\lambda^2)$. The values for $\frac{m^2}{3H^2}\equiv\varepsilon$ are chosen to yield the same measured mean values for the $n_{\delta\varphi}$ given in Table 2.1. Notice that the required ε's are about 5.5 times the ε_{i0}'s of the inflaton in Table 3.1.

Table 2.2 : Predictions for the n_{ϕ} and α_{ϕ} of the spectator scalar.

	Predictions	
Parameter $\frac{m^2}{3H^2}\equiv\varepsilon$	$n_{\bar{\phi}}$	$\alpha_{\bar{\phi}}$
0.017545	$0.9647\mp\lambda\,0.3911$	$\mp\lambda\,0.0028$
0.017940	$0.9639\mp\lambda\,0.3855$	$\mp\lambda\,0.0027$
0.017002	$0.9658\mp\lambda\,0.3992$	$\mp\lambda\,0.0030$

Recall that the Planck TT,TE,EE+lowEB+lensing data in Table 2.1 constrains the spectral index as $0.9603 < n_{\delta\bar{\varphi}} < 0.9691$. Using these limits in Eq. (2.112) implies $0.01537 < \frac{m^2}{3H^2} = \varepsilon < 0.01972$. Employing these bounds on the ε in Eq. (2.115) yields $-0.0036\lambda < \alpha_{\bar{\phi}} < -0.0023\lambda$. Since $\lambda < 10^{-14}$, this result is incompatible with the measured constraint $-0.0158 < \alpha_{\delta\bar{\varphi}} < -0.0012$.

The Planck TT,TE,EE+lowE+lensing+BK15 data in Table 2.1, on the other hand, constrains the spectral index as $0.9595 < n_{\delta\bar{\varphi}} < 0.9683$. Using these limits in Eq. (2.112) implies $0.015765 < \frac{m^2}{3H^2} = \varepsilon < 0.02011$. Employing these bounds on the ε, in Eq. (2.115) yields, $-0.0034\lambda < \alpha_{\bar{\phi}} < -0.0022\lambda$, i.e., $\alpha_{\bar{\varphi}} \approx 0$, as before. Such an $\alpha_{\bar{\varphi}}$, however, lies just at the upper bound of the measured constraint $-0.0138 < \alpha_{\delta\bar{\varphi}} < 0$; see Table 2.1. [Inclusion of BAO data to this data set somewhat improves the case, slightly shifting the measured constraint on $\alpha_{\delta\bar{\varphi}}$ to $-0.0136 < \alpha_{\delta\bar{\varphi}} < 0.0004$. The measured constraint $0.9618 < n_{\delta\bar{\varphi}} < 0.9698$ implies, via Eq. (2.112), $0.015023 < \frac{m^2}{3H^2} = \varepsilon < 0.018975$ and hence, $-0.0037\lambda < \alpha_{\bar{\phi}} < -0.0025\lambda$, i.e., $\alpha_{\bar{\phi}} \approx 0$ again, which is close to the upper bound 0.0004 allowed by the data.] Thus, overall, the data sets seem to favor more an inflaton driven inflation rather than a spectator scalar in a cosmological constant driven de Sitter inflation.

We pointed out in the Introduction that as a field fluctuates in spacetime, the magnitude of the field strength increases at some locations while it decreases at others. Therefore, the actual effect perceived by a local observer is not an average value measured by a VEV like the correlation function but either an increase or a decrease in the field strength. The mean squared deviation, i.e., variance, of the field variation from its average provides information about the magnitude of the actual effect. In the next section, we use our two-point correlation function (2.42) and its coincidence limit (2.99) to compute the variance of fluctuations at tree and one-loop order and examine how the tree-order contrast between the VEV and the actual effect changes when the quantum corrections are included.

2.7 Statistics of Fluctuations in Spacetime

The variation field $\Delta\bar{\varphi}$ of the IR truncated scalar $\bar{\varphi}$ is defined as the difference of fields at two events,

$$\Delta\bar{\phi}(t,t';\vec{x},\vec{x}') \equiv \bar{\phi}(t,\vec{x}) - \bar{\phi}(t',\vec{x}') \; . \tag{2.117}$$

Because the mean field $\langle\Omega|\bar{\phi}(t,\vec{x})|\Omega\rangle$ is zero at any event, the VEV of variation $\Delta\bar{\phi}$ vanishes. Therefore, the fluctuation field is

$$\delta\bar{\phi}(t,t';\vec{x},\vec{x}') \equiv \Delta\bar{\phi}(t,t';\vec{x},\vec{x}') - \langle\Omega|\Delta\bar{\phi}(t,t';\vec{x},\vec{x}')|\Omega\rangle = \Delta\bar{\phi}(t,t';\vec{x},\vec{x}') \; . \tag{2.118}$$

Thus, the mean squared fluctuations, or the variance, defined as,

$$\begin{aligned}
\sigma^2_{\Delta\bar{\phi}}(t,t';\vec{x},\vec{x}') &\equiv \langle\Omega|\big(\delta\bar{\phi}\big)^2|\Omega\rangle = \langle\Omega|\big(\Delta\bar{\phi}\big)^2|\Omega\rangle \\
= \langle\Omega|\bar{\phi}^2(t,\vec{x})|\Omega\rangle &- \langle\Omega|\bar{\phi}(t,\vec{x})\bar{\phi}(t',\vec{x}')|\Omega\rangle - \langle\Omega|\bar{\phi}(t',\vec{x}')\bar{\phi}(t,\vec{x})|\Omega\rangle \\
&+ \langle\Omega|\bar{\phi}^2(t',\vec{x}')|\Omega\rangle \; ,
\end{aligned} \tag{2.119}$$

does not necessarily vanish. We obtain the tree-order variance as

$$\sigma^2_{\Delta\bar{\phi}_{\text{tree}}}(t,t';\vec{x},\vec{x}') = \mathcal{A} g_0(t,t';\vec{x},\vec{x}') \; , \tag{2.120}$$

where

$$\begin{aligned}
g_0(t,t';\vec{x},\vec{x}') = \frac{1-a^{-\delta}(t)}{\delta} + \frac{1-a^{-\delta}(t')}{\delta} + 2\Big[a(t)\,a(t')\Big]^{-\frac{\delta}{2}} \\
\times \sum_{n=0}^{\infty} \frac{(-1)^n (H\Delta x)^{2n}}{(2n+1)!} \frac{1-a^{2n+\delta}(t')}{2n+\delta} \; ,
\end{aligned} \tag{2.121}$$

and the one-loop variance as

$$\sigma^2_{\Delta\bar{\phi}_{1-\mathrm{loop}}}(t,t';\vec{x},\vec{x}')=-\frac{\lambda}{2\nu}\frac{\mathcal{A}^2}{H^2}g_1(t,t';\vec{x},\vec{x}')\ , \tag{2.122}$$

where

$$g_1(t,t';\vec{x},\vec{x}')=\frac{1}{\delta}\Bigg\{\Big[a(t)\,a(t')\Big]^{-\frac{\delta}{2}}\sum_{n=0}^{\infty}\frac{(-1)^n(H\Delta x)^{2n}}{(2n+1)!(2n+\delta)}\Bigg\{\ln(a(t))+\ln(a(t'))$$
$$-\frac{1-a^{-\delta}(t)}{\delta}-\frac{1-a^{-\delta}(t')}{\delta}-a^{2n}(t')\Bigg[a^{\delta}(t')\Bigg(\ln(a(t))-\ln(a(t'))+\frac{a^{-\delta}(t)}{\delta}\Bigg)-\frac{1}{\delta}\Bigg]$$
$$+2\Bigg[\frac{1-a^{2n+\delta}(t')}{2n+\delta}\Bigg]-\frac{1-a^{2n}(t')}{n}\Bigg\}-\Bigg\{\Bigg[\frac{a^{-\delta}(t)}{\delta}\Bigg(2\ln(a(t))-\frac{a^{\delta}(t)-a^{-\delta}(t)}{\delta}\Bigg)\Bigg]$$
$$+\Bigg[a(t)\rightarrow a(t')\Bigg]\Bigg\}\Bigg\}+\mathcal{O}(\lambda^2). \tag{2.123}$$

In the next two sections, we consider equal time and equal space limits of the variance.

2.7.1 Statistics of Fluctuations in Space

The spatial variation of the IR truncated scalar is the difference of field strengts at equal time events $\Delta\bar{\varphi}(t,\vec{x},\vec{x}')=\bar{\varphi}(t,\vec{x})-\bar{\varphi}(t,\vec{x}')$. The field strength is positive at some places, at others it is negative. Moreover, the inflationary particle production is a quantum mechanical random process. At some places the field strength is positive, at others it is negative. While the magnitude of the field strength increases at some places, at others it decreases. Hence, the expectation value of the spatial variation $\Delta\bar{\varphi}(t,\vec{x},\vec{x}')$ vanishes, but the spatial variance $\sigma^2_{\Delta\bar{\varphi}}(t,\vec{x},\vec{x}')$, which we compute next, does not.

2.7.1.1 Tree-Order Variance in Space

For a massive scalar, we employ the equal time limits of Eqs. (2.42) and (2.99) in Eq. (2.119) to get

$$\sigma^2_{\Delta\bar{\phi}_{\mathrm{tree}}}(t,\vec{x},\vec{x}')=\mathcal{A}g_0(t,\vec{x},\vec{x}')\ , \tag{2.124}$$

where

$$g_0(t,\vec{x},\vec{x}')=2a^{-\delta}(t)\sum_{n=1}^{\infty}\frac{(-1)^n(H\Delta x)^{2n}}{(2n+1)!}\frac{1-a^{2n+\delta}(t)}{2n+\delta}\ . \tag{2.125}$$

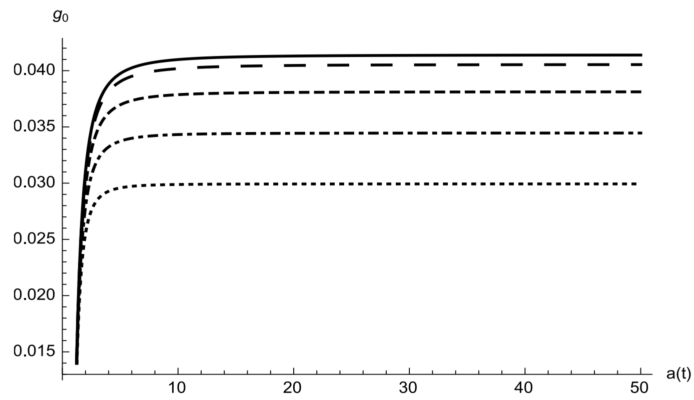

Figure 2.3 : Plots of $g_0(t,K)$, defined in Eq. (2.125) with separation (2.62), versus $a(t')$ for different values of mass and $K{=}1/2$. $a(t)$ runs from 1 to 50. Extending it to e^{50} does not alter the plots significantly. The solid, large-dashed, dashed, dot-dashed and dotted lines are for $m{=}0, H/4, H/2, 3H/4$ and H, respectively.

In the late time limit, for a fixed comoving separation, Eq. (2.125) asymptotes to

$$g_0(t,\vec{x},\vec{x}') \to 2\Bigg[\frac{1-a^{-\delta}(t)}{\delta}+\frac{a^{-\delta}(t)}{\delta}\Bigg[\frac{\sin(H\Delta x)}{H\Delta x}+\frac{(H\Delta x)^2}{3(2+\delta)} \times {}_1\mathcal{F}_2\Big(1+\frac{\delta}{2};\frac{5}{2},2+\frac{\delta}{2};-\frac{(H\Delta x)^2}{4}\Big)\Bigg]\Bigg]. \tag{2.126}$$

For a massless scalar ($\delta=0$), on the other hand, Eq. (2.125) asymptotes to

$$\lim_{m\to 0} g_0(t,\vec{x},\vec{x}') \to 2\Big\{\ln(a(t))+\mathrm{ci}(H\Delta x)-\frac{\sin(H\Delta x)}{H\Delta x}\Big\} . \tag{2.127}$$

The growth in tree-order variance implied by Eqs. (2.125)-(2.127) means that the *magnitude* of spatial variation increases in time. This fact is a main argument of some cosmologists against putting trust in results obtained from the VEVs. They argue that the average effect measured by a VEV may be misleading because the actual effect observed by any local observer is either a decrease or an increase in field strength as fluctuations happen. As we show in Sec. 2.7.1.2, however, the dominant quantum correction to the tree-order variance comes with a minus sign. Thus, the quantum corrected variance does not grow as large as the tree-order result implies.

To interpret result (2.124) for a fixed physical distance we take comoving spatial separation $\Delta x{=}K/Ha(t)$ in Eq. (2.125) and obtain $g_0(t,K)$. Figure 2.3 shows that $g_0(t,K)$ rapidly grows and asymptotes to a constant during inflation. One can see this behavior of $g_0(t,K)$ analytically by computing its asymptotic form,

$$g_0(t,K)=\frac{2}{\delta}\left\{1-a^{-\delta}(t)-\frac{\sin(K)}{K}+a^{-\delta}(t)\frac{\sin(Ka^{-1}(t))}{Ka^{-1}(t)}-\frac{K^2}{3(2+\delta)}\right.$$
$$\left.\times\left[{}_1\mathcal{F}_2\left(1+\frac{\delta}{2};\frac{5}{2},2+\frac{\delta}{2};-\frac{K^2}{4}\right)-a^{-2-\delta}(t)\,{}_1\mathcal{F}_2\left(1+\frac{\delta}{2};\frac{5}{2},2+\frac{\delta}{2};-\frac{K^2}{4a^2(t)}\right)\right]\right\}.(2.128)$$

which is a constant.

Numerical values of $g_0(t,K)$, for a given K and δ, can be obtained from Eq. (2.128) at any time t during inflation. Figure 2.3 shows that it rapidly grows and asymptotes to a constant during inflation. This late time behaviour of $g_0(t,K)$ can be shown analytically by computing its asymptotic form:

$$g_0(t,K)\to\frac{2}{\delta}\left\{1-\frac{\sin(K)}{K}-\frac{K^2}{3(2+\delta)}\,{}_1\mathcal{F}_2\left(1+\frac{\delta}{2};\frac{5}{2},2+\frac{\delta}{2};-\frac{K^2}{4}\right)\right\}, \qquad (2.129)$$

which is a constant.

2.7.1.2 One-Loop Variance in Space

We obtain one-loop equal time variance of a massive scalar as,

$$\sigma^2_{\Delta\bar{\phi}_{1-\text{loop}}}(t,\vec{x},\vec{x}')=-\frac{\lambda}{2\nu}\frac{\mathcal{A}^2}{H^2}g_1(t,\vec{x},\vec{x}'), \qquad (2.130)$$

where

$$g_1(t,\vec{x},\vec{x}')=2\frac{a^{-\delta}(t)}{\delta}\sum_{n=1}^{\infty}\frac{(-1)^n(H\Delta x)^{2n}}{(2n+1)!(2n+\delta)}$$
$$\times\left\{\ln(a(t))-\frac{1-a^{-\delta}(t)}{\delta}+\frac{1-a^{2n+\delta}(t)}{2n+\delta}-\frac{1-a^{2n}(t)}{2n}\right\}. \qquad (2.131)$$

Hence, the one-loop spatial variance $\sigma^2_{\Delta\bar{\phi}_{1-\text{loop}}}(t,\vec{x},\vec{x}')<0$, contrary to the positive tree-order spatial variance, as pointed out in Sec. 2.7.1.1. In the late time limit, for a fixed comoving separation, $g_1(t,\vec{x},\vec{x}')$ asymptotes to

$$2\frac{a^{-\delta}(t)}{\delta^2}\left\{\left[\ln(a(t))+\frac{1+a^{-\delta}(t)}{\delta}\right]\left[\frac{\sin(H\Delta x)}{H\Delta x}-1+\frac{(H\Delta x)^2}{3(2+\delta)}\right.\right.$$
$$\left.\times{}_1\mathcal{F}_2\left(1+\frac{\delta}{2};\frac{5}{2},2+\frac{\delta}{2};-\frac{(H\Delta x)^2}{4}\right)\right]-\ln(a(t))+\frac{1+a^{\delta}(t)}{\delta}-\text{ci}(H\Delta x)$$
$$\left.+\frac{\sin(H\Delta x)}{H\Delta x}+\frac{(H\Delta x)^2}{3(2+\delta)^2}\,{}_2\mathcal{F}_3\left(1+\frac{\delta}{2},1+\frac{\delta}{2};\frac{5}{2},2+\frac{\delta}{2},2+\frac{\delta}{2};-\frac{(H\Delta x)^2}{4}\right)\right\}.(2.132)$$

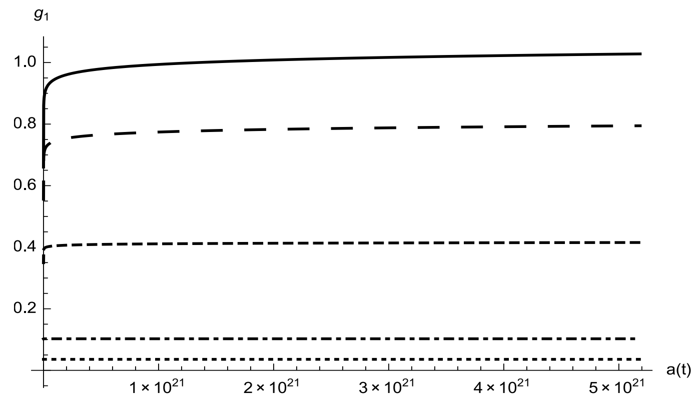

Figure 2.4 : Plots of $g_1(t,K)$, defined in Eq. (2.131) with separation (2.62), versus $a(t)$. The ranges of parameters K, $a(t)$, m and styles of the lines are chosen same as in Fig. 2.1

In massless limit,

$$\lim_{m\to 0} g_1(t,\vec{x},\vec{x}') = \sum_{n=1}^{\infty} \frac{(-1)^n (H\Delta x)^{2n}}{(2n+1)!2n} \Big\{ \ln^2(a(t)) - \frac{a^{2n}(t)}{n} \ln(a(t)) - \frac{1-a^{2n}(t)}{2n^2} \Big\} , \quad (2.133)$$

on the other hand, $g_1(t,\vec{x},\vec{x}')$ asymptotes to

$$\lim_{m\to 0} g_1(t,\vec{x},\vec{x}') \to \frac{2}{3}\ln^3(a(t)) + \Big[\mathrm{ci}(H\Delta x) - \frac{\sin(H\Delta x)}{H\Delta x} \Big] \ln^2(a(t)) - \frac{1}{3}\Big[\ln(H\Delta x) + \gamma - 1 \Big]^3$$
$$- \Big[1 - \frac{\pi^2}{12} \Big] \Big[\ln(H\Delta x) + \gamma - 1 \Big] - \frac{2}{3}\Big[\zeta(3) - 1 \Big] . \quad (2.134)$$

Figure 2.4 shows that $g_1(t,K)$ grows logarithmically for the massless scalar and that the growth is suppressed for massive scalars. As the mass increases, the suppression gets stronger. To interpret one-loop equal time variance (2.130) for a fixed physical distance we take $\Delta x = K/Ha(t)$ in Eq. (2.131) and obtain

$$g_1(t,K) = 2\frac{a^{-\delta}(t)}{\delta^2} \Bigg\{ \Big[\ln(a(t)) - \frac{1-a^{-\delta}(t)}{\delta} \Big] \Big[\frac{\sin(Ka^{-1}(t))}{Ka^{-1}(t)} - 1 + \frac{K^2 a^{-2}(t)}{3(2+\delta)}$$
$$\times {}_1\mathcal{F}_2\Big(1+\frac{\delta}{2}; \frac{5}{2}, 2+\frac{\delta}{2}; \frac{-K^2}{4a^2(t)} \Big) \Big] - \frac{a^{\delta}(t)}{\delta} \Bigg[\Bigg\{ \frac{\sin(K)}{K} - 1 + \frac{K^2}{3(2+\delta)} \Big[{}_1\mathcal{F}_2\Big(1+\frac{\delta}{2}; \frac{5}{2}, 2+\frac{\delta}{2}; -\frac{K^2}{4} \Big)$$
$$+ \frac{\delta}{2+\delta}\, {}_2\mathcal{F}_3\Big(1+\frac{\delta}{2}, 1+\frac{\delta}{2}; \frac{5}{2}, 2+\frac{\delta}{2}, 2+\frac{\delta}{2}; -\frac{K^2}{4} \Big) \Big] \Bigg\} - a^{-\delta}(t) \Big\{ K \to \frac{K}{a(t)} \Big\} \Bigg] + \Bigg[\Bigg\{ \mathrm{ci}(K) - \frac{\sin(K)}{K}$$
$$- \ln(K) - \frac{1}{\delta} \Big[\frac{\sin(K)}{K} + \frac{K^2}{3(2+\delta)}\, {}_1\mathcal{F}_2\Big(1+\frac{\delta}{2}; \frac{5}{2}, 2+\frac{\delta}{2}; -\frac{K^2}{4} \Big) \Big] \Bigg\} - \Big\{ K \to \frac{K}{a(t)} \Big\} \Bigg] \Bigg\} . \quad (2.135)$$

Figure 2.4 shows that $g_1(t,K)$ grows logarithmically for the massless scalar and the growth is suppressed for massive scalars. At the mass increases, the suppression gets stronger. This late time behaviour of from the asymptotic form of $g_1(t,K)$ can be shown analytically by comparing its asymptotic form in the massless limit

$$\lim_{m\to 0} g_1(t,K) \to \frac{K^2}{12}\,{}_3\mathcal{F}_4\left(1,1,1;2,2,2,\frac{5}{2};-\frac{K^2}{4}\right)\ln(a(t)) - \frac{K^2}{24}\,{}_4\mathcal{F}_5\left(1,1,1,1;2,2,2,2,\frac{5}{2};-\frac{K^2}{4}\right), \quad (2.136)$$

which implies a logarithmic growth at late times, and its asymptotic form for a finite mass,

$$g_1(t,K) \to \frac{2}{\delta^2}\left\{a^{-\delta}(t)\left[\mathrm{ci}(K) - \frac{\sin(K)}{K} - \ln(K) - \gamma + 1 - \frac{1}{\delta}\left[\frac{\sin(K)}{K} - 1 + \frac{K^2}{3(2+\delta)}\right.\right.\right.$$
$$\left.\left.\times\,{}_1\mathcal{F}_2\left(1+\frac{\delta}{2};\frac{5}{2},2+\frac{\delta}{2};-\frac{K^2}{4}\right)\right]\right] - \frac{1}{\delta}\left[\frac{\sin(K)}{K} - 1 + \frac{K^2}{3(2+\delta)}\left[{}_1\mathcal{F}_2\left(1+\frac{\delta}{2};\frac{5}{2},2+\frac{\delta}{2};-\frac{K^2}{4}\right)\right.\right.$$
$$\left.\left.\left. + \frac{\delta}{2+\delta}\,{}_2\mathcal{F}_3\left(1+\frac{\delta}{2},1+\frac{\delta}{2};\frac{5}{2},2+\frac{\delta}{2},2+\frac{\delta}{2};-\frac{K^2}{4}\right)\right]\right]\right\}. \quad (2.137)$$

Equation (2.137) shows suppression of some constant terms by the factor $\frac{a^{-\delta}(t)}{\delta^2}$, which becomes stronger as the mass increases.

2.7.2 Statistics of Fluctuations in Time

The temporal variation is the difference of fields at equal space events $\Delta\bar{\phi}(t,t',\vec{x}) \equiv \bar{\phi}(t,\vec{x}) - \bar{\phi}(t',\vec{x})$ whose VEV vanishes. The temporal variance

$$\begin{aligned}\sigma^2_{\Delta\bar{\phi}}(t,t') &= \langle\Omega|\left[\Delta\bar{\phi}(t,t',\vec{x}) - \langle\Omega|\Delta\bar{\phi}(t,t',\vec{x})|\Omega\rangle\right]^2|\Omega\rangle \\ &= \langle\Omega|\left[\bar{\phi}(t,\vec{x}) - \bar{\phi}(t',\vec{x})\right]^2|\Omega\rangle\,, \end{aligned} \quad (2.138)$$

can be obtained by taking the equal space limit of Eq. (2.119).

2.7.2.1 Tree-Order Variance in Time

Using Eqs. (2.120) and (2.121), we obtain the tree-order temporal variance as

$$\sigma^2_{\Delta\bar{\phi}_{\mathrm{tree}}}(t,t') = \mathcal{A}g_0(t,t')\,, \quad (2.139)$$

where

$$g_0(t,t') = \frac{1-a^{-\delta}(t)}{\delta} + \frac{1-a^{-\delta}(t')}{\delta} + 2\left[a(t)\,a(t')\right]^{-\frac{\delta}{2}}\frac{1-a^{\delta}(t')}{\delta}\,. \quad (2.140)$$

Note that $\lim_{t'\to t} g_0(t,t') = 0$, hence $\sigma^2_{\Delta\bar{\phi}_{\mathrm{tree}}}(t,t)$ vanishes, as it should. For $t' < t$, on the other hand, we have $g_0(t,t') > 0$, hence the tree-order temporal variance $\sigma^2_{\Delta\bar{\phi}_{\mathrm{tree}}}(t,t') > 0$.

Note also that the massless limit of the tree-order temporal variance

$$\lim_{m\to 0}\sigma^2_{\Delta\bar{\phi}_{\rm tree}}(t,t')=\frac{\Gamma(D-1)}{\Gamma\left(\frac{D}{2}\right)}\frac{H^{D-2}}{2^{D-1}\pi^{\frac{D}{2}}}\Big[\ln(a(t))-\ln(a(t'))\Big]\ ,$$

is positive and grows logarithmically. Next, we calculate the one-loop quantum correction to the tree-order temporal variance.

2.7.2.2 One-Loop Variance in Time

Using Eqs. (2.122) and (2.123) we find the one-loop temporal variance

$$\sigma^2_{\Delta\bar{\phi}_{1-{\rm loop}}}(t,t')=-\frac{\lambda}{2\nu}\frac{\mathcal{A}^2}{H^2}g_1(t,t')\ , \tag{2.141}$$

where

$$\begin{aligned}g_1(t,t')=&\Big[a(t)\,a(t')\Big]^{-\frac{\delta}{2}}\frac{1}{\delta^2}\Bigg\{\ln(a(t))+3\ln(a(t'))-a^{\delta}(t')\\&\times\left[\ln(a(t))-\ln(a(t'))+\frac{1+a^{-\delta}(t)}{\delta}\right]+\frac{1-a^{\delta}(t')}{\delta}+\frac{a^{-\delta}(t)+a^{-\delta}(t')}{\delta}\Bigg\}\\&-\left\{\left[\frac{a^{-\delta}(t)}{\delta^2}\left(2\ln(a(t))-\frac{a^{\delta}(t)-a^{-\delta}(t)}{\delta}\right)\right]+\Big[a(t)\to a(t')\Big]\right\}\ .\end{aligned} \tag{2.142}$$

At equal time, we have $\lim_{t'\to t}g_1(t,t')=0$, hence $\sigma^2_{\Delta\bar{\phi}_{1-{\rm loop}}}(t,t)$ vanishes. For $t'<t$, however, $g_1(t,t')>0$, hence the one-loop temporal variance $\sigma^2_{\Delta\bar{\phi}_{1-{\rm loop}}}(t,t')<0$ contrary to positive tree-order temporal variance (2.120). Thus, the temporal variation does not grow as fast as the $\sigma^2_{\Delta\bar{\phi}_{\rm tree}}$ implies. Let us note finally that the massless limit of the one-loop variance yields

$$\begin{aligned}\lim_{m\to 0}\sigma^2_{\Delta\bar{\phi}_{1-{\rm loop}}}(t,t')=-\frac{\lambda}{(D-1)}\frac{\Gamma^2(D-1)}{\Gamma^2\left(\frac{D}{2}\right)}\frac{H^{2D-6}}{2^{2D-1}\pi^{D}}\Bigg[&\frac{2\ln^3(a(t))}{3}-\ln^2(a(t))\ln(a(t'))\\&+\frac{\ln^3(a(t'))}{3}\Bigg]\ ,\end{aligned} \tag{2.143}$$

which is the same result computed in Ref. [67] for a massless scalar. At this point, we end our discussion on the self-interacting spectator scalar field during cosmological constant driven de Sitter inflation where the expansion rate H is constant. In the next section, we study self-interacting inflaton field which drives inflation, hence the expansion rate H is necessarily time dependent.

3. INFLATON FIELD DURING SLOW-ROLL INFLATION[1]

In this section, we extend the method we used to study a self-interacting spectator scalar field during a cosmological constant driven inflation where the expansion rate H is constant—hence the spacetime is a de Sitter spacetime—to study a self-interacting inflaton field which drives the inflation where the expansion rate H is naturally time dependent—hence the spacetime is a Friedman-Robertson-Walker spacetime. We consider an inflaton φ with the same potential $V(\varphi) = \frac{m^2}{2}\varphi^2 \pm \frac{\lambda}{4!}\varphi^4$ where $0 < \lambda \ll 1$. The $+(-)$ sign in the quartic self-interaction implies a steeper (flattened) feature. We first compute the quantum corrected two-point correlation function for the inflaton fluctuations at tree and one-loop order, including also the $\mathcal{O}(\lambda)$ correction to the tree-order correlator that arise as a backreaction of the self-interactions on the geometry—that is calculating the $\mathcal{O}(\lambda)$ corrections to the $a(t)$, $H(t)$, $\varepsilon(t)$ and using these corrected parameters in our computations—first time ever in the literature. Applying the method we introduce [56] in Sec. 2 and using the coincidence limit of the quantum corrected correlation function, we compute the quantum corrected $\Delta^2_{\delta\varphi}$, $n_{\delta\varphi}$ and $\alpha_{\delta\varphi}$ for the inflaton fluctuations. We show that the one-loop power spectrum gets enhanced by the terms involving huge factors of ε_{i0}^{-2} and ε_{i0}^{-1} which do not exist in the spectrum [56] of the spectator scalar in de Sitter spacetime. The one-loop spectral index, on the other hand, gets enhanced by the terms involving the factor ε_{i0}^{-1}. We compare the numerical estimates of our predictions for the $n_{\delta\varphi}$ and $\alpha_{\delta\varphi}$ with the cosmological measurements [60] of Planck 2018 Collaboration and show that the data favor the inflaton model rather than the spectator scalar model.

3.1 The Model

The renormalized Lagrangian density of the inflaton model

$$\mathcal{L} = \left[\frac{R}{16\pi G} - \frac{1+\delta Z}{2}\partial_\mu\varphi\,\partial_\nu\varphi\,g^{\mu\nu} - V(\varphi)\right]\sqrt{-g}\,, \tag{3.1}$$

[1] This chapter is based on the paper Karakaya, G. and Onemli, V. K. Quantum Fluctuations of a Self-interacting Inflaton, *arXiv:1912.07963*

where the R represent the Ricci scalar. The renormalized potential

$$V(\varphi) = \frac{1+\delta Z}{2} m^2 \varphi^2 + V_{\rm pert}(\varphi) \; , \tag{3.2}$$

where the part of the potential that we treat perturbatively,

$$V_{\rm pert}(\varphi) \equiv \frac{\delta m^2}{2} \varphi^2 \pm \frac{\lambda + \delta\lambda}{4!} \varphi^4 \; . \tag{3.3}$$

Recall that the orders of λ of the counterterms are $\delta Z \sim \mathcal{O}(\lambda^2)$, $\delta m^2 \sim \mathcal{O}(\lambda)$ and $\delta\lambda \sim \mathcal{O}(\lambda^2)$. The components of metric tensor $g_{\mu\nu}$ are chosen as that of a spatially flat Friedmann-Robertson-Walker spacetime with no metric perturbations which are suppressed. Therefore the invariant line element, $ds^2 = -dt^2 + a^2(t) d\vec{x} \cdot d\vec{x}$ where the scale factor $a(t)$ is to be solved for in Sec. 3.1.2. The inflaton in this background obeys the field equation,

$$\ddot{\varphi}(x) + (D-1)H(t)\dot{\varphi}(x) - \left[\frac{\nabla^2}{a^2} - m^2\right]\varphi(x) = -\frac{V'_{\rm pert}(\varphi)(x)}{1+\delta Z} \; , \tag{3.4}$$

where the prime denotes derivative with respect to the argument, hence, $V'_{\rm pert}(\varphi) = \delta m^2 \varphi \pm \frac{1}{6}(\lambda + \delta\lambda)\varphi^3$. We consider the inflaton field $\varphi(x)$ as a sum of an unperturbed (averaged) background field $\bar{\varphi}(t)$ that depends only on time and a small perturbation $\delta\varphi(x)$ on this background,

$$\varphi(x) = \bar{\varphi}(t) + \delta\varphi(x) \; . \tag{3.5}$$

Thus, Eq. (3.4) yields the following equations for the homogenous part $\bar{\varphi}(t)$ and for the fluctuations $\delta\varphi(t, \vec{x})$ around it are

$$\ddot{\bar{\varphi}}(t) + (D-1)H(t)\dot{\bar{\varphi}}(t) + m^2\bar{\varphi}(t) = -\frac{1}{1+\delta Z}\left\{\delta m^2 \bar{\varphi}(t) \pm \frac{\lambda+\delta\lambda}{6}\bar{\varphi}^3(t)\right\} \; , \tag{3.6}$$

$$\delta\ddot{\varphi}(x) + (D-1)H(t)\,\delta\dot{\varphi}(x) - \left[\frac{\nabla^2}{a^2} - m^2\right]\delta\varphi(x) = -\frac{V'_{\rm pert}(\delta\varphi)(x)}{1+\delta Z} \; , \tag{3.7}$$

where

$$V'_{\rm pert}(\delta\varphi) \equiv \delta m^2 \delta\varphi(x) \pm \frac{\lambda+\delta\lambda}{6}\left[3\bar{\varphi}^2(t)\,\delta\varphi(x) + 3\bar{\varphi}(t)\,(\delta\varphi(x))^2 + (\delta\varphi(x))^3\right]. \tag{3.8}$$

Using two non-trivial Einstein's field equations—corresponding to purely temporal and purely spatial components we find

$$\dot{\bar{\varphi}}^2(t) = \frac{(D-2)H^2(t)}{8\pi G}\,\varepsilon(t) \; , \tag{3.9}$$

$$V(\bar{\varphi}) = \frac{(D-2)H^2(t)}{16\pi G}\left[D-1-\varepsilon(t)\right] , \tag{3.10}$$

where the slow-roll parameter

$$\varepsilon(t) \equiv -\frac{\dot{H}(t)}{H^2(t)} \ll 1 \, . \tag{3.11}$$

Substituting Eqs. (3.2) and (3.3) into Eq. (3.10), yields

$$H^2 = \frac{8\pi G}{(D-2)(D-1-\varepsilon)} \left[\left(m^2 + \delta m^2\right) \bar{\varphi}^2 \pm \frac{\lambda}{12} \bar{\varphi}^4 + \mathcal{O}(\lambda^2) \right] . \tag{3.12}$$

The mass counterterm δm^2, which is of $\mathcal{O}(\lambda)$, is multiplied by $\bar{\varphi}^2$. Hence, it is suppressed by a factor of $\bar{\varphi}^2$ compared to the quartic self-interaction term which is also of $\mathcal{O}(\lambda)$. Because $4 \lesssim \bar{\varphi} \lesssim 10^5$ in Planckian units, the former cannot contribute as significant as the latter. Therefore, we have

$$H = \sqrt{\frac{8\pi G}{(D-2)(D-1)}} m^2 \frac{\bar{\varphi}}{m} \left[1 \pm \frac{\lambda}{24} \left(\frac{\bar{\varphi}}{m}\right)^2 + \mathcal{O}(\varepsilon) + \mathcal{O}(\lambda^2) \right] . \tag{3.13}$$

Recall that the quartic self-interaction term $\frac{\lambda}{4!}\bar{\varphi}^4$ is treated perturbatively next to the the mass term $\frac{m^2}{2}\bar{\varphi}^2$. Hence, $1 \gg \frac{\lambda}{12}\frac{\bar{\varphi}^2}{m^2}$ in Eq. (3.13).

To get the expansion rate H from Eq. (3.13), as a function of time and initial values H_{i0} and ε_{i0}, we first need to solve field equation (3.6) for $\bar{\varphi}(t)$. In the slow-roll regime where $|\ddot{\bar{\varphi}}| \ll H|\dot{\bar{\varphi}}|$, and at $\mathcal{O}(\lambda)$, Eq. (3.6) implies

$$(D-1)H\dot{\bar{\varphi}} + m^2\bar{\varphi} \simeq \mp \frac{\lambda}{6} \bar{\varphi}^3 \, . \tag{3.14}$$

We neglected the other $\mathcal{O}(\lambda)$ term—$\delta m^2 \bar{\varphi}$—suppressed by a factor of $\bar{\varphi}^2$ on the right side of Eq. (3.6), as we did in obtaining Eq. (3.13). Employing Eq. (3.13) in Eq. (3.14) yields

$$\dot{\bar{\varphi}} \simeq -\frac{m}{\sqrt{8\pi G}} \sqrt{\frac{D-2}{D-1}} \left[1 \pm \frac{\lambda}{8} \left(\frac{\bar{\varphi}}{m}\right)^2 + \mathcal{O}(\varepsilon) + \mathcal{O}(\lambda^2) \right] . \tag{3.15}$$

The solution of Eq. (3.15), for the plus sign choice in the $\mathcal{O}(\lambda)$-term, can be given as

$$\bar{\varphi}(t) \simeq \sqrt{\frac{8}{\lambda}} m \tan\left(-\sqrt{\frac{\lambda}{8} \frac{D-2}{(D-1)8\pi G}} \, t + \arctan\left(\sqrt{\frac{\lambda}{8}} \frac{\bar{\varphi}_i}{m} \right) \right) . \tag{3.16}$$

For the minus sign choice in Eq. (3.15), taking $\lambda \to -\lambda$ and analytically continuing the tangent function in Eq. (3.16), yields the background field solution as

$$\bar{\varphi}(t) \simeq \sqrt{\frac{8}{\lambda}} m \tanh\left(-\sqrt{\frac{\lambda}{8} \frac{D-2}{(D-1)8\pi G}} \, t + \operatorname{arctanh}\left(\sqrt{\frac{\lambda}{8}} \frac{\bar{\varphi}_i}{m} \right) \right) . \tag{3.17}$$

Using the addition formulae for the $\tan(x)$ and $\tanh(x)$ functions in Eqs. (3.16) and (3.17) respectively and then expanding the results in series, up to $\mathcal{O}(\lambda^2)$, leads to

$$\bar{\varphi}(t) \simeq \bar{\varphi}_i \left\{ 1 - \sqrt{\frac{D-2}{(D-1)8\pi G}} \left[\frac{m}{\bar{\varphi}_i} \pm \frac{\lambda}{8} \frac{\bar{\varphi}_i}{m} \right] t \pm \frac{\lambda}{8} \frac{D-2}{(D-1)8\pi G} t^2 \right\} , \tag{3.18}$$

where $\bar{\varphi}_i$ is the initial value of $\bar{\varphi}(t)$ at $t = t_i = 0$. Note that $\bar{\varphi}_i = \bar{\varphi}_{i0}$ where the subscript 0 denotes the result in the noninteracting ($\lambda \to 0$) limit. Note also that, in this limit, one recovers

$$\lim_{\lambda \to 0} \bar{\varphi}(t) \simeq -m\sqrt{\frac{D-2}{(D-1)8\pi G}}\, t + \bar{\varphi}_i, \tag{3.19}$$

the well known solution in the chaotic inflation. The fluctuation field $\delta\varphi(x)$ in Eq. (3.5), on the other hand, is obtained by solving Eq. (3.7) as

$$\delta\varphi(x) = \delta\varphi_0(x) - \int_0^t dt' a^{D-1}(t') \int d^{D-1}x' G_{\rm ret}(x;x') \frac{V'_{\rm pert}(\delta\varphi)(x')}{1+\delta Z} , \tag{3.20}$$

where $V'_{\rm pert}(\delta\varphi)$ is given in Eq. (3.8) and the retarded Green's function is computed in Eq. (3.62). In the rest of this section, we use background solution (3.18) to express the $H(t)$, $a(t)$, $\varepsilon(t)$ and $\bar{\varphi}(t)$, with $\mathcal{O}(\lambda)$ corrections, in terms of the initial values H_{i0} and ε_{i0}. The results are employed, in Sec. 3.3, to compute the quantum corrected two-point correlation function for the IR truncated inflaton fluctuations $\delta\bar{\varphi}(x)$.

3.1.1 The Expansion Rate $H(t)$ in Terms of Initial Values H_{i0} and ε_{i0}

Employing Eq. (3.18) in Eq. (3.13) we obtain the expansion rate $H(t)$ in terms of the initial values in the $\lambda \to 0$ limit,

$$H_{i0} = \sqrt{\frac{8\pi G}{(D-2)(D-1)}}\, m\bar{\varphi}_i \qquad \text{and} \qquad \dot{H}_{i0} = -\frac{m^2}{D-1} . \tag{3.21}$$

Expressing the initial value of the background field, using the first equation in Eq. (3.21), as

$$\bar{\varphi}_i = \bar{\varphi}_{i0} = \varepsilon_{i0}^{-1} \sqrt{\xi}\, m , \tag{3.22}$$

where $\varepsilon_{i0} = -\frac{\dot{H}_{i0}}{H_{i0}^2} = \frac{m^2}{(D-1)H_{i0}^2}$ is the initial value of the $\varepsilon(t)$ in the $\lambda \to 0$ limit and

$$\xi \equiv \frac{D-2}{(D-1)8\pi G H_{i0}^2}, \tag{3.23}$$

is a dimensionless number, we obtain the expansion rate as

$$H(t)=H_{i0}\left[1-\varepsilon_{i0}H_{i0}t\pm\frac{\lambda\xi}{4!}\left[\varepsilon_{i0}^{-2}-6\,\varepsilon_{i0}^{-1}H_{i0}t+6\,(H_{i0}t)^{2}-\varepsilon_{i0}\,(H_{i0}t)^{3}\right]+\mathcal{O}(\lambda^{2})\right] . \quad (3.24)$$

Among the $\mathcal{O}(\lambda)$ terms in Eq. (3.24), the first two dominate for $0<\varepsilon_{i0}<\frac{1}{2(H_{i0}t)}[\sqrt{5/3}-1]$. This means that for $0<\varepsilon_{i0}<0.0025$ they remain as leading terms during the first 60 e-foldings. For a larger ε_{i0}, the third term, $6\,(H_{i0}t)^{2}$, becomes of order the sum of the first two ones during the last epochs of inflation. The forth term, $\varepsilon_{i0}\,(H_{i0}t)^{3}$, is suppressed during inflation for an $\varepsilon_{i0}<6/(H_{i0}t)$; thus, for $\varepsilon_{i0}\ll 0.1$, it can be neglected during the first 60 e-foldings.

At this stage, using Eq. (3.24), we express time t in terms of the scale factor a which will provide us the change of variable essential for evaluating the integrals of one-loop correlator in Sec. 3.3.2. Integrating Eq. (3.24)—neglecting the suppressed fourth term—we find

$$(H_{i0}t)^{3}\mp\frac{6}{\lambda\xi}\varepsilon_{i0}\left[1\pm\frac{\lambda\xi}{4}\varepsilon_{i0}^{-2}\right](H_{i0}t)^{2}\pm\frac{12}{\lambda\xi}\left[1\pm\frac{\lambda\xi}{4!}\varepsilon_{i0}^{-2}\right](H_{i0}t)\mp\frac{12}{\lambda\xi}\ln(a)\cong 0\,, \quad (3.25)$$

which has three distinct real roots; see Appendix B.1. We define a new variable

$$q\equiv\sqrt{1-2\varepsilon_{i0}\ln(a)}\,. \quad (3.26)$$

and express the relevant root of polynomial (3.25) in terms of q in Eq. (B.5) which implies that the comoving time

$$t\cong\varepsilon_{i0}^{-1}\frac{1-q}{H_{i0}}\left[1\pm\frac{\lambda\xi}{4!}\varepsilon_{i0}^{-2}\left[1-2q\right]+\mathcal{O}(\lambda^{2})\right]\,. \quad (3.27)$$

Substituting Eq. (3.27) into Eq. (3.24)—without neglecting the fourth term—yields the expansion rate as

$$H(t)=H_{i0}\left[q\pm\frac{\lambda}{4!}\xi\,\varepsilon_{i0}^{-2}\left[q^{3}+q^{2}-1\right]+\mathcal{O}(\lambda^{2})\right]\,. \quad (3.28)$$

Thus, Eq. (3.28) implies

$$H_{0}(t)=H_{i0}q_{0}(t)\,, \quad (3.29)$$

where

$$q_{0}=\sqrt{1-2\varepsilon_{i0}\ln(a_{0})}\,. \quad (3.30)$$

Hence, $\dot{H}_{0}=H_{i0}\dot{q}_{0}=-\varepsilon_{i0}H_{i0}^{2}=\dot{H}_{i0}=$const., in agreement with the definition of ε_{i0}.

3.1.2 The Scale Factor $a(t)$ in Terms of Initial Values H_{i0} and ε_{i0}

The logarithm of the scale factor is obtained by integrating expansion rate (3.28) via making change of variable (3.27) which implies

$$dt = -\frac{dq}{H_{i0}}\varepsilon_{i0}^{-1}\left[1\pm\frac{\lambda}{8}\xi\varepsilon_{i0}^{-2}\left[1-\frac{4}{3}q\right]+\mathcal{O}(\lambda^2)\right] . \tag{3.31}$$

The result of the integral, upon exponentiation, yields

$$\begin{aligned} a(t) &= a_0(t)\exp\left(\mp\frac{\lambda}{4!}\frac{\xi}{4}\varepsilon_{i0}^{-3}[1-q_0]^4+\mathcal{O}(\lambda^2)\right) \\ &= a_0(t)\left[1\mp\frac{\lambda}{4!}\frac{\xi}{4}\varepsilon_{i0}^{-3}[1-q_0]^4+\mathcal{O}(\lambda^2)\right] , \end{aligned} \tag{3.32}$$

where

$$a_0(t) = \exp\left(H_{i0}t_0\left[1-\frac{\varepsilon_{i0}}{2}H_{i0}t_0\right]\right) = \exp\left(\varepsilon_{i0}^{-1}\frac{\mathcal{E}_0}{2}\right) , \tag{3.33}$$

is the scale factor in the $\lambda \to 0$ limit. Here, we define

$$\mathcal{E}_0(t) \equiv 1-q_0^2(t) = 2\varepsilon_{i0}\ln(a_0(t)) . \tag{3.34}$$

The scale factor reaches its maximum value at $t = t_{\mathrm{m}} \cong (\varepsilon_{i0}H_{i0})^{-1}$. Inflation, however, ends at $t_{\mathrm{e}} \cong t_{\mathrm{m}}[1-\sqrt{\varepsilon_{i0}}] = t_{\mathrm{m}} - (\sqrt{\varepsilon_{i0}}H_{i0})^{-1}$. Note that the condition $a(t_{\mathrm{e}}) \gtrsim e^{60}$ and the fact that $q = \sqrt{1-2\varepsilon_{i0}\ln(a)} > 0$ imply that $\varepsilon_{i0} < 0.0083$. A more stringent constraint, however, is obtained as $\varepsilon_{i0} < 0.0041$; see Sec. 3.5.1. Hence, the mass $m = \sqrt{3\varepsilon_{i0}}H_{i0} < 0.111H_{i0}$ for $D = 4$. Note also that using Eq. (3.32) in Eq. (3.28) yields

$$H(t) = H_{i0}\left[q_0\pm\frac{\lambda}{4!}\xi\varepsilon_{i0}^{-2}\left[q_0^3+q_0^2-1+q_0^{-1}\frac{[1-q_0]^4}{4}\right]+\mathcal{O}(\lambda^2)\right] . \tag{3.35}$$

Next, we similarly obtain the slow-roll parameter, which characterizes the flatness of the potential that drives the inflation.

3.1.3 The Slow-Roll Parameter $\varepsilon(t)$ in Terms of Initial Values H_{i0} and ε_{i0}

Using $\frac{d}{dt} = -\varepsilon_{i0}q^{-1}H\frac{d}{dq}$ in Eq. (3.11) yields $\varepsilon = \frac{\varepsilon_{i0}}{qH}\frac{dH}{dq}$. For the $H(t)$ given in Eq. (3.28),

$$\begin{aligned} \varepsilon &= \varepsilon_{i0}\left[q^{-2}\pm\frac{\lambda}{4!}\xi\varepsilon_{i0}^{-2}q^{-3}\left[2q^3+q^2+1\right]\right] \\ &= \varepsilon_{i0}\left[q_0^{-2}\pm\frac{\lambda}{4!}\xi\varepsilon_{i0}^{-2}q_0^{-3}\left[2q_0^3+q_0^2+1-q_0^{-1}\frac{[1-q_0]^4}{2}\right]\right] , \end{aligned} \tag{3.36}$$

up to $\mathcal{O}(\lambda^2)$. With this result, we end our study on the dynamics of spacetime geometry. In the next section, we obtain the solution of background field $\bar{\varphi}(t)$ in the interacting theory.

3.1.4 The Background Inflaton Field $\bar{\varphi}(t)$ in Terms of Initial Values H_{i0} and ε_{i0}

Substituting Eqs. (3.22) and (3.25) into Eq. (3.18), yields the background field in our model as,

$$\bar{\varphi}(t) \simeq \bar{\varphi}_{i0}\left[1-\varepsilon_{i0}H_{i0}t \mp \frac{\lambda}{8}\xi\left[\varepsilon_{i0}^{-1}(H_{i0}t)-(H_{i0}t)^2\right]+\mathcal{O}(\lambda^2)\right] . \tag{3.37}$$

Using Eq. (3.27) in Eq. (3.37) gives

$$\begin{aligned}\bar{\varphi}(t) &\simeq \bar{\varphi}_{i0}\left[q \mp \frac{\lambda}{4!}\xi\varepsilon_{i0}^{-2}\left[1-q^2\right]+\mathcal{O}(\lambda^2)\right] \\ &= \bar{\varphi}_{i0}\left[q_0 \mp \frac{\lambda}{4!}\xi\varepsilon_{i0}^{-2}\left[\mathcal{E}_0-q_0^{-1}\frac{[1-q_0]^4}{4}\right]+\mathcal{O}(\lambda^2)\right] .\end{aligned} \tag{3.38}$$

Recall that the initial value $\bar{\varphi}_{i0}$ is given in terms of ε_{i0} in Eq. (3.22). We study the fluctuations $\delta\varphi(x)$ of the self-interacting inflaton in the remainder of this section.

3.2 Inflaton Fluctuations

If the $\delta\varphi$ is neglected, the evolution of the inflaton with potential (3.2) is trivial: The homogeneous inflaton $\bar{\varphi}(t)$ rolls down its potential as the classical restoring force pushes it down to the configuration $\bar{\varphi}=0$, where the potential is minimum. Recall that we treat the self-interaction term perturbatively next to the mass term; i.e., we require $\frac{\lambda}{12}(\frac{\bar{\varphi}}{m})^2<1$ in our analysis. This implies an upper bound $\bar{\varphi}_{\max}$ on the amplitude $|\bar{\varphi}| < \bar{\varphi}_{\max} \equiv \sqrt{\frac{12}{\lambda}}\,m$. One can deduce the range of $\bar{\varphi}_{\max}$ as follows. Planck 2018 data [60] imply $H \sim 2.5\cdot 10^{-5}$ at the end of inflation and hence, an inflaton mass scale $m=\sqrt{3\varepsilon}H \sim 3\cdot 10^{-6}$. The level of inhomogeneity $\frac{\delta\rho}{\rho}\sim 10^{-5}$ in the distribution of matter implies $\lambda \lesssim 10^{-14}$ for an inflaton with potential (3.2). The estimate for m and the constraint for λ together yields $\bar{\varphi}_{\max} \gtrsim 10^2$. An upper bound $\bar{\varphi}_{\max} \lesssim 10^5$, on the other hand, is required to make sure that the quantum gravity effects can safely be disregarded. Thus, depending on the value of λ, we can have $10^2 \lesssim \bar{\varphi}_{\max} \lesssim 10^5$.

When the $\delta\varphi$ is taken into account, the particle production out of vacuum enhances the field strength and causes the inflaton to undergo a random walk such that its average distance from the minimum of the potential increases. The $\delta\varphi$ can have severe influences on the evolution of the inflaton as long as the amplitude $|\delta\varphi|$ is larger than the change $\Delta\bar{\varphi} \equiv \bar{\varphi}_i - \bar{\varphi}(\Delta t)$ in the strength of the background field $\bar{\varphi}$ in a typical time scale $\Delta t = H^{-1}(\varphi)$. This implies a certain value φ_* for the inflaton amplitude $|\varphi|$ such that if $|\varphi| > \varphi_*$ then the $\delta\varphi$ is of large amplitude ($|\delta\varphi| > \Delta\bar{\varphi}$) which cause the $|\varphi|$ to fluctuate remarkably, rolling the inflaton up its potential forever, and hence leading to endless proliferation of ever newer regions in a multiverse. For $\frac{1}{3} < |\varphi| < \varphi_*$, however, the $\delta\varphi$ is of relatively low amplitude ($|\delta\varphi| < \Delta\bar{\varphi}$) and, as the inflaton rolls downhill, the $\delta\varphi$ engenders the density inhomogeneities required for the structure formation in the universe. In Secs. 3.2.1-2 we give the mode expansion for the $\delta\varphi_0$ and obtain the $\delta\varphi$. The two-point correlation function of the $\delta\varphi$ that we compute and plot in Secs. 3.3.1-2 shows that the amplitude $|\delta\varphi|$ does not grow without a bound; it asymptotes to a constant at late-times. Thus, the inflaton cannot continue rolling up its potential forever; it eventually comes to a halt and therefore, as it rolls downhill, the $\delta\varphi$ can generate the inhomogeneteis.

3.2.1 Fluctuations of the Tree-Order Inflaton Field

Fluctuation field $\delta\varphi(x)$ of the full inflaton satisfies Eq. (3.7) whose solution is given in Eq. (3.20) in terms of the fluctuation field $\delta\varphi_0(x)$ of the tree-order inflaton and the retarded Green's function $G_{\rm ret}(x;x')$. The mode expansion for the fluctuation field of the tree-order inflaton

$$\delta\varphi_0(x) = \int \frac{d^{D-1}k}{(2\pi)^{D-1}} \left\{ \delta\Phi_0(x,\vec{k})A(\vec{k}) + \delta\Phi_0^*(x,\vec{k})A^*(\vec{k}) \right\} , \tag{3.39}$$

where the mode function of the fluctuation field

$$\delta\Phi_0(x,\vec{k}) \equiv u_0(t,k)e^{i\vec{k}\cdot\vec{x}} , \tag{3.40}$$

is the spatial plane wave solution of the linearized effective field equation evaluated at the full solution of the background effective field equation. The tree-order amplitude function $u_0(t,k)$ obeys

$$\ddot{u}_0(t,k) + (D-1)H(t)\dot{u}_0(t,k) + \left[\frac{k^2}{a^2} + m^2\right] u_0(t,k) = 0 . \tag{3.41}$$

The mode coordinates $A(\vec{k})$ and $A^*(\vec{k})$ in Eq. (3.39) are functions of the spatial Fourier transforms of the $\delta\varphi_0(x)$ and its first time derivative evaluated on the initial value surface. Canonical quantization promotes the mode coordinates to the annihilation and creation operators $\hat{A}(\vec{k})$ and $\hat{A}^\dagger(\vec{k})$ satisfying the usual commutation relations

$$\left[\hat{A}(\vec{k}), \hat{A}(\vec{k}')\right] = 0 , \left[\hat{A}^\dagger(\vec{k}), \hat{A}^\dagger(\vec{k}')\right] = 0 , \left[\hat{A}(\vec{k}), \hat{A}^\dagger(\vec{k}')\right] = (2\pi)^{D-1}\delta^{D-1}(\vec{k}-\vec{k}'), \tag{3.42}$$

and imposes the Wronskian normalization condition on the amplitude function,

$$u_0(t,k)\,\dot{u}_0^*(t,k)-u_0^*(t,k)\,\dot{u}_0(t,k)=\frac{i}{a^{D-1}}\ . \tag{3.43}$$

Rescaling the amplitude function as $a^{\frac{D-1}{2}}(t)\,u_0(t,k)\equiv v_0(t,k)$ reduces differential equation (3.41) to the form of the harmonic oscillator equation with a time dependent frequency

$$\ddot{v}_0(t,k)+\left[\frac{k^2}{a^2(t)}+m^2-\frac{D-1}{2}\dot{H}(t)-\left(\frac{D-1}{2}H(t)\right)^2\right]v_0(t,k)=0\ . \tag{3.44}$$

To solve Eq. (3.44), following the approach by Finelli, Marozzi, Vacca, and Venturi given in Ref. [68], we make the ansatz

$$v_0(t,k)\equiv\zeta^{\mu}Z_{\nu}(\chi\zeta)\text{ with }\zeta=\frac{k}{Ha},\ \mu=\mu(H),\ \nu=\nu(H),\text{ and }\chi=\chi(H), \tag{3.45}$$

and express the time derivative as derivatives with respect to ζ and H,

$$\frac{\partial}{\partial t}=-H\left[(1-\varepsilon)\,\zeta\frac{\partial}{\partial\zeta}+\varepsilon H\frac{\partial}{\partial H}\right]\ . \tag{3.46}$$

Employing Eq. (3.46) in Eq. (3.44), neglecting the terms of $\mathcal{O}(\ddot{H})$ and $\mathcal{O}(\varepsilon^2)$, yields

$$\zeta^2\frac{\partial^2 Z_\nu}{\partial\zeta^2}+\zeta\frac{\partial Z_\nu}{\partial\zeta}+(\chi^2\zeta^2-\nu^2)Z_\nu=0\ , \tag{3.47}$$

with parameters

$$\mu=-\frac{\varepsilon}{2}+\mathcal{O}(\varepsilon^2)\ ,\ \ \chi=1+\varepsilon+\mathcal{O}(\varepsilon^2)\ , \tag{3.48}$$

and

$$\nu^2=\left(\frac{D-1}{2}\right)^2-\frac{m^2}{H^2}+\frac{(D-2)(D-1)}{2}\,\varepsilon+\mathcal{O}(\varepsilon^2)\ . \tag{3.49}$$

Equation (3.28) and $\varepsilon_{i0}=\frac{m^2}{(D-1)H_{i0}^2}$ imply

$$\frac{m^2}{H^2}=(D-1)\,\varepsilon+\mathcal{O}(\lambda\varepsilon)\ , \tag{3.50}$$

and hence

$$\nu^2=\left(\frac{D-1}{2}\right)^2\left[1+2\,\frac{D-4}{D-1}\,\varepsilon+\mathcal{O}(\varepsilon^2)\right]\ . \tag{3.51}$$

The solution of Bessel's equation (3.47) is given in terms of Hankel's function of the first kind and its complex conjugate

$$Z_\nu(\chi\zeta)=C_1H_\nu^{(1)}(\chi\zeta)+C_2H_\nu^{(2)}(\chi\zeta)\ . \tag{3.52}$$

Thus, the solution of Eq. (3.41) can be given as

$$u_0(t,k)=a^{-\frac{D-1}{2}}\zeta^{\mu}Z_{\nu}(\chi\zeta)$$
$$=a^{-\frac{D-1}{2}}\Big(\frac{k}{Ha}\Big)^{-\frac{\varepsilon}{2}}\Big[C_1H_{\nu}^{(1)}\Big(\frac{(1+\varepsilon)k}{Ha}\Big)+C_2H_{\nu}^{(2)}\Big(\frac{(1+\varepsilon)k}{Ha}\Big)\Big]. \tag{3.53}$$

Wronskian normalization (3.43) constrains the constants C_1 and C_2,

$$|C_1|^2-|C_2|^2=\frac{\pi}{4H}(1+\varepsilon)\left(\frac{k}{Ha}\right)^{\varepsilon}\left[1+\mathcal{O}(\varepsilon^2)\right]. \tag{3.54}$$

A solution which corresponds to Bunch-Davies mode function in de Sitter spacetime can be chosen, up to $\mathcal{O}(\varepsilon^2)$, as

$$C_1=i\left[\frac{\pi}{4H}(1+\varepsilon)\Big(\frac{k}{Ha}\Big)^{\varepsilon}\right]^{\frac{1}{2}} \qquad \text{and} \qquad C_2=0\,. \tag{3.55}$$

Inserting Eq. (3.55) into Eq. (3.53) yields the amplitude of mode function (3.40) up to $\mathcal{O}(\varepsilon^2)$,

$$u_0(t,k)=ia^{-\frac{D-1}{2}}\left[\frac{\pi}{4H}(1+\varepsilon)\right]^{\frac{1}{2}}H_{\nu}^{(1)}\Big(\frac{(1+\varepsilon)k}{Ha}\Big)\,. \tag{3.56}$$

Recall that, at comoving time $t=t_k$, the mode with wave number

$$k\equiv\frac{H(t_k)a(t_k)}{1+\varepsilon(t_k)}\,, \tag{3.57}$$

exits the horizon, becomes a superhorizon (IR) mode and "freezes in." At a given time t, we take into account superhorizon modes $k<\frac{Ha}{1+\varepsilon}$ for which the argument of the Hankel function $\frac{(1+\varepsilon)k}{Ha}<1$. Thus, using the power series expansion of the Hankel function we obtain the IR limit of the amplitude function as

$$u_0(t,k)\longrightarrow\frac{2^{\nu-1}\Gamma(\nu)}{\sqrt{\pi}a^{\frac{\delta}{2}}}\Big(\frac{H}{1+\varepsilon}\Big)^{\nu-\frac{1}{2}}k^{-\nu}\Big[1+\mathcal{O}\Big(\Big(\frac{(1+\varepsilon)k}{2Ha}\Big)^2\Big)\Big]\left[1+\mathcal{O}(\varepsilon^2)\right]. \tag{3.58}$$

Substituting Eq. (3.58) into Eq. (3.39) we obtain the IR truncated fluctuation field of the tree-order inflaton as

$$\delta\bar{\varphi}_0(t,\vec{x})=$$
$$\frac{2^{\nu-1}\Gamma(\nu)}{\sqrt{\pi}\,a^{\frac{\delta}{2}}}\Big(\frac{H}{1+\varepsilon}\Big)^{\nu-\frac{1}{2}}\int\frac{d^{D-1}k}{(2\pi)^{D-1}}\frac{\Theta\left(\frac{Ha}{1+\varepsilon}-k\right)}{k^{\nu}}\left[e^{i\vec{k}\cdot\vec{x}}\hat{A}(\vec{k})+e^{-i\vec{k}\cdot\vec{x}}\hat{A}^{\dagger}(\vec{k})\right]. \tag{3.59}$$

The ratio $\frac{Ha}{1+\varepsilon}$ in the argument of the Θ-function is monotonically increasing function of time until $t_{\rm f}\cong t_{\rm m}[1-3^{1/4}\sqrt{\varepsilon_{i0}}]$, which is slightly less than the t_e, time at which the inflation ends, defined in Sec 3.1.2. Hence, we consider inflation during $0<t<t_{\rm f}$ in the model we consider. Mode expansion (3.58) is used to obtain the fluctuations of the self-interacting inflaton, in the next section.

3.2.2 Fluctuations of the Full Inflaton Field

Fluctuations $\delta\varphi(x)$ of an interacting inflaton is given in Eq. (3.20) in terms of the fluctuations $\delta\varphi_0(x)$ of tree-order inflaton (3.39) and the retarded Green's function $G(x;x') = i\Theta(t-t')\,[\delta\varphi_0(x), \delta\varphi_0(x')]$, where the commutator function

$$\big[\delta\varphi_0(x), \delta\varphi_0(x')\big] = \int \frac{d^{D-1}k}{(2\pi)^{D-1}} \Big\{u(t,k)u^*(t',k) - u^*(t,k)u(t',k)\Big\} e^{i\vec{k}\cdot(\vec{x}-\vec{x}')} \,. \quad (3.60)$$

The terms inside the curly brackets in the integrand

$$\begin{aligned} u(t,k)u^*(t',k) - u^*(t,k)u(t',k) = i\frac{\pi}{2}[aa']^{-\frac{D-1}{2}} \left[\frac{(1+\varepsilon)(1+\varepsilon')}{HH'}\right]^{\frac{1}{2}} \Bigg\{ \Big[\cot(\nu\pi) - \cot\big(\nu'\pi\big)\Big] \\ \times J_\nu\Big(\frac{(1+\varepsilon)k}{Ha}\Big) J_{\nu'}\Big(\frac{(1+\varepsilon')k}{H'a'}\Big) + \csc\big(\nu'\pi\big) J_\nu\Big(\frac{(1+\varepsilon)k}{Ha}\Big) J_{-\nu'}\Big(\frac{(1+\varepsilon')k}{H'a'}\Big) \\ - \csc(\nu\pi) J_{-\nu}\Big(\frac{(1+\varepsilon)k}{Ha}\Big) J_{-\nu'}\Big(\frac{(1+\varepsilon')k}{H'a'}\Big) \Bigg\} \,. \end{aligned} \quad (3.61)$$

where $J_\nu(z)$ is the Bessel's function of order ν and the primes indicate quantities evaluated at t'. During slow-roll inflation, $\nu = \frac{D-1}{2} + \mathcal{O}(\varepsilon) = \nu'$ is just a constant, up to $\mathcal{O}(\varepsilon)$, in D-dimensions. (In $D=4$, $\nu = \frac{3}{2} + \mathcal{O}(\varepsilon^2) = \nu'$.) Therefore, we evaluate integral (3.60) taking ν constant and obtain the IR limit of Green's function as

$$G(x;x') \to \frac{\Theta(t-t')}{D-1} \left[\frac{HH'}{(1+\varepsilon)(1+\varepsilon')}\right]^{\frac{D}{2}-1} \left\{ \left[\frac{1+\varepsilon'}{H'a'}\right]^{D-1} - \left[\frac{1+\varepsilon}{Ha}\right]^{D-1} \right\} \delta^{D-1}(\vec{x}-\vec{x}') \,. \quad (3.62)$$

The full inflaton fluctuation field $\delta\varphi$, in the IR limit, can be obtained mingling Eqs. (3.8) and (3.62) in Eq. (3.20): In leading order, the latter term in the curly brackets in Eq. (3.62) can be neglected next to the former which dominates throughout the range of integration. Hence,

$$\delta\varphi(x) \simeq \delta\varphi_0(x) - \frac{1}{D-1}\left[\frac{H}{1+\varepsilon}\right]^{\frac{D}{2}-1} \int_0^t dt'\Theta(t-t') \left[\frac{1+\varepsilon'}{H'}\right]^{\frac{D}{2}} \frac{\frac{\partial V_{\rm pert}(\delta\varphi)}{\partial\delta\varphi}(t',\vec{x})}{1+\delta Z} \,. \quad (3.63)$$

Consider the terms in $\frac{1}{1+\delta Z}\frac{\partial V_{\rm pert}(\delta\varphi)}{\partial\delta\varphi}$ where the $\frac{\partial V_{\rm pert}}{\partial\delta\varphi}$ is given Eq. (3.8). δZ and $\delta\lambda$ can be neglected since they are of $\mathcal{O}(\lambda^2)$. Comparing the powers of $\bar{\varphi}$ and $\delta\varphi$ in various terms in Eq. (3.8) one can see that the term quadratic in $\bar{\varphi}$ is the dominant term. The fact that $|\delta\varphi| \ll |\bar{\varphi}|$ does not necessarily imply that $|\delta\varphi|$ is small by itself, since the $|\varphi|$ can be as large as 10^5. Hence, we keep the term linear in $\bar{\varphi}$ that is also quadratic in $\delta\varphi$ and the term cubic in $\delta\varphi$, but neglect the $\delta m^2\delta\varphi$ term next to the dominant term.

Thus

$$\delta\varphi(x)\simeq\delta\varphi_0(x)\mp\frac{\lambda}{6(D-1)}\left[\frac{H_0}{1+\varepsilon_0}\right]^{\frac{D}{2}-1}\int_0^t dt'\Theta(t-t')\left[\frac{1+\varepsilon_0'}{H_0'}\right]^{\frac{D}{2}}\Bigg\{3\bar{\varphi}_0^2(t')\delta\varphi_0(t',\vec{x})$$
$$+3\bar{\varphi}_0(t')\Big[\delta\varphi_0(t',\vec{x})\Big]^2+\Big[\delta\varphi_0(t',\vec{x})\Big]^3\Bigg\}+\mathcal{O}(\lambda^2)\,. \tag{3.64}$$

We use Eq. (3.64) to compute the two-point correlation function of the inflaton fluctuations at tree- and one-loop order in the next section.

3.3 Two-Point Correlation Function of the Fluctuations

The two-point correlation function of the IR truncated fluctuations of the full field

$$\langle\Omega|\delta\bar{\varphi}(x)\delta\bar{\varphi}(x')|\Omega\rangle$$
$$=\langle\Omega|\delta\bar{\varphi}(x)\delta\bar{\varphi}(x')|\Omega\rangle_{\rm tree}+\langle\Omega|\delta\bar{\varphi}(x)\delta\bar{\varphi}(x')|\Omega\rangle_{1-{\rm loop}}+\mathcal{O}(\lambda^2), \tag{3.65}$$

with $t'\leq t$ and $\vec{x}'\neq\vec{x}$, can be obtained for the inflaton in our model using Eq. (3.64). The tree-order correlator

$$\langle\Omega|\delta\bar{\varphi}(x)\delta\bar{\varphi}(x')|\Omega\rangle_{\rm tree}=\langle\Omega|\delta\bar{\varphi}_0(x)\delta\bar{\varphi}_0(x')|\Omega\rangle\,, \tag{3.66}$$

and the one-loop correlator

$$\langle\Omega|\delta\bar{\varphi}(x)\delta\bar{\varphi}(x')|\Omega\rangle_{1-{\rm loop}}=\mp\frac{\lambda}{6(D-1)}\Bigg\{\left[\frac{H_0'}{1+\varepsilon_0'}\right]^{\frac{D}{2}-1}\int_0^{t'}d\tilde{t}\left[\frac{1+\tilde{\varepsilon}_0}{\tilde{H}_0}\right]^{\frac{D}{2}}$$
$$\times\langle\Omega|\delta\bar{\varphi}_0(x)\Big[3\bar{\varphi}_0^2(\tilde{t})\delta\bar{\varphi}_0(\tilde{t},\vec{x}')+[\delta\bar{\varphi}_0(\tilde{t},\vec{x}')]^3\Big]|\Omega\rangle+\left[\frac{H_0}{1+\varepsilon_0}\right]^{\frac{D}{2}-1}\int_0^t dt''\left[\frac{1+\varepsilon_0''}{H_0''}\right]^{\frac{D}{2}}$$
$$\times\langle\Omega|\Big[3\bar{\varphi}_0^2(t'')\delta\bar{\varphi}_0(t'',\vec{x})+[\delta\bar{\varphi}_0(t'',\vec{x})]^3\Big]\delta\bar{\varphi}_0(x')|\Omega\rangle\Bigg\}\,, \tag{3.67}$$

are computed in Secs. 3.3.1 and 3.3.2, respectively.

3.3.1 Tree-Order Correlator

The tree-order correlator of the IR truncated fluctuations is obtained using Eq. (3.59),

$$\begin{aligned}\langle\Omega|\delta\bar{\varphi}(x)\delta\bar{\varphi}(x')|\Omega\rangle_{\rm tree}&=\langle\Omega|\delta\bar{\varphi}_0(x)\delta\bar{\varphi}_0(x')|\Omega\rangle\\ =\frac{1}{4\pi}\Big(\frac{H}{1+\varepsilon}\Big)^{\nu-\frac{1}{2}}&\Big(\frac{H'}{1+\varepsilon'}\Big)^{\nu'-\frac{1}{2}}\frac{2^{\nu}\Gamma(\nu)}{a^{\frac{\delta}{2}}}\frac{2^{\nu'}\Gamma(\nu')}{a'^{\frac{\delta'}{2}}}\int\frac{d^{D-1}k}{(2\pi)^{D-1}}\Theta\Big(\frac{Ha}{1+\varepsilon}-k\Big)\\ &\times\Theta\Big(\frac{H'a'}{1+\varepsilon'}-k\Big)\frac{e^{i\vec{k}\cdot(\vec{x}-\vec{x}')}}{k^{\nu+\nu'}}\,.\end{aligned}\tag{3.68}$$

For $0\leq t'\leq t$, we have $\frac{H'a'}{1+\varepsilon'}\leq\frac{Ha}{1+\varepsilon}$. Thus, defining $\Delta x\equiv\|\Delta\vec{x}\|=\|\vec{x}-\vec{x}'\|$ and θ as the angle between the vectors $\vec{k}$ and $\Delta\vec{x}$, the integral on the right side of Eq. (3.68) yields

$$\int\frac{d\Omega_{D-1}}{(2\pi)^{D-1}}\int_0^\infty dk\,\Theta\Big(\frac{H'a'}{1+\varepsilon'}-k\Big)\frac{e^{ik\Delta x\cos(\theta)}}{k^{1-\frac{\delta+\delta'}{2}}}=\frac{\Gamma(\frac{D}{2})}{\pi^{\frac{D}{2}}\Gamma(D-1)}(\Delta x^2)^{-\frac{\delta+\delta'}{4}}\int_{\alpha_i}^{\alpha'}dy\frac{\sin(y)}{y^{2-\frac{\delta+\delta'}{2}}}\,,\tag{3.69}$$

where we made a change of variable $y\equiv k\Delta x$. The remaining integral

$$\int dy\frac{\sin(y)}{y^{2-\frac{\delta+\delta'}{2}}}=-\frac{i}{2}y^{\frac{\delta+\delta'}{2}-1}\Big[E_{2-\frac{\delta+\delta'}{2}}(iy)-E_{2-\frac{\delta+\delta'}{2}}(-iy)\Big]\,,\tag{3.70}$$

where the exponential integral function $E_\beta(z)$ is defined in Eq. (A.1). The result is real for $y\in\mathbb{R}$. Combining Eqs. (3.69)-(3.70) in Eq. (3.68) yields the tree-order correlator,

$$\begin{aligned}&\langle\Omega|\delta\bar{\varphi}_0(x)\delta\bar{\varphi}_0(x')|\Omega\rangle\\ &=\frac{-i\Gamma(\frac{D}{2})}{8\pi^{\frac{D}{2}+1}\Gamma(D-1)}\Big(\frac{H}{1+\varepsilon}\Big)^{\frac{D}{2}-1}\Big(\frac{H'}{1+\varepsilon'}\Big)^{\frac{D}{2}-1}\frac{2^{\nu}\Gamma(\nu)}{\alpha^{\frac{\delta}{2}}}\frac{2^{\nu'}\Gamma(\nu')}{\alpha'^{\frac{\delta'}{2}}}\Big\{\alpha'^{\frac{\delta+\delta'}{2}-1}\Big[E_{2-\frac{\delta+\delta'}{2}}(i\alpha')\\ &\quad-E_{2-\frac{\delta+\delta'}{2}}(-i\alpha')\Big]-\alpha_i^{\frac{\delta+\delta'}{2}-1}\Big[E_{2-\frac{\delta+\delta'}{2}}(i\alpha_i)-E_{2-\frac{\delta+\delta'}{2}}(-i\alpha_i)\Big]\Big\}\,,\end{aligned}\tag{3.71}$$

where we define $\alpha\equiv\frac{Ha\Delta x}{1+\varepsilon}$ which implies $\alpha'=\frac{H'a'\Delta x}{1+\varepsilon'}$ and $\alpha_i=\frac{H_i\Delta x}{1+\varepsilon_i}$. Recalling the fact that $\nu=\frac{D-1}{2}+\mathcal{O}(\varepsilon)$, a simpler form of tree-order correlator, up to $\mathcal{O}(\varepsilon)$, can be given:

$$\begin{aligned}&\langle\Omega|\delta\bar{\varphi}_0(x)\delta\bar{\varphi}_0(x')|\Omega\rangle\\ &\simeq\frac{\Gamma(D-1)}{2^{D-1}\pi^{\frac{D}{2}}\Gamma(\frac{D}{2})}\Big[\frac{HH'}{(1+\varepsilon)(1+\varepsilon')}\Big]^{\frac{D}{2}-1}\Big[\mathrm{ci}(\alpha')-\frac{\sin(\alpha')}{\alpha'}-\mathrm{ci}(\alpha_i)+\frac{\sin(\alpha_i)}{\alpha_i}\Big],\end{aligned}\tag{3.72}$$

where the $\mathrm{ci}(z)$ is the cosine integral function defined in Eq. (A.9). Expansion (A.10) provides a useful form for the tree-order correlator. In $D=4$, since $\nu=\frac{3}{2}+\mathcal{O}(\varepsilon^2)$, we have, up to $\mathcal{O}(\varepsilon^2)$,

$$\begin{aligned}&\langle\Omega|\delta\bar{\varphi}_0(x)\delta\bar{\varphi}_0(x')|\Omega\rangle\\ &=\frac{HH'}{4\pi^2(1+\varepsilon)(1+\varepsilon')}\Big[\ln\Big(\frac{H'a'}{H_i}\Big)-\ln\Big(\frac{1+\varepsilon'}{1+\varepsilon_i}\Big)+\sum_{n=1}^{\infty}\frac{(-1)^n\big[\alpha'^{2n}-\alpha_i^{2n}\big]}{2n(2n+1)!}\Big]\,.\end{aligned}\tag{3.73}$$

The tree-order correlator is evaluated at the full solution of the background effective field equation. Because the H, a and ε in Eq. (3.73) have $\mathcal{O}(\lambda)$ corrections, it can be recast as

$$\begin{aligned}&\langle\Omega|\delta\bar{\varphi}_0(x)\delta\bar{\varphi}_0(x')|\Omega\rangle\\ &\equiv\langle\Omega|\delta\bar{\varphi}_0(x)\delta\bar{\varphi}_0(x')|\Omega\rangle_{\mathbf{0}}\pm\lambda\langle\Omega|\delta\bar{\varphi}_0(x)\delta\bar{\varphi}_0(x')|\Omega\rangle_{\lambda}+\mathcal{O}(\lambda^2).\end{aligned} \tag{3.74}$$

Employing Eqs. (3.28) and (3.36) in Eq. (3.73) yields

$$\begin{aligned}&\langle\Omega|\delta\bar{\varphi}_0(x)\delta\bar{\varphi}_0(x')|\Omega\rangle_{\mathbf{0}}\\ &=\frac{H_0H_0'}{4\pi^2(1+\varepsilon_0)(1+\varepsilon_0')}\left[\ln\Big(\frac{H_0'a_0'}{H_{i0}}\Big)-\ln\Big(\frac{1+\varepsilon_0'}{1+\varepsilon_{i0}}\Big)+\sum_{n=1}^{\infty}\frac{(-1)^n\left[\alpha_0'^{2n}-\alpha_{i0}^{2n}\right]}{2n(2n+1)!}\right].\end{aligned} \tag{3.75}$$

Substituting Eq. (3.29) into Eq. (3.75) yields

$$\langle\Omega|\delta\bar{\varphi}_0(x)\delta\bar{\varphi}_0(x')|\Omega\rangle_{\mathbf{0}}=\frac{H_{i0}^2}{4\pi^2}f_{00}(t,t',\Delta x)\ , \tag{3.76}$$

where

$$f_{00}\equiv\frac{(q_0q_0')^3}{(q_0^2+\varepsilon_{i0})(q_0'^2+\varepsilon_{i0})}\left[\varepsilon_{i0}^{-1}\frac{\mathcal{E}_0'}{2}-\ln\Big(\frac{q_0'^2+\varepsilon_{i0}}{q_0'^3(1+\varepsilon_{i0})}\Big)+\sum_{n=1}^{\infty}\frac{(-1)^n\left[\alpha_0'^{2n}-\alpha_{i0}^{2n}\right]}{2n(2n+1)!}\right]. \tag{3.77}$$

Here, $\alpha_0'\equiv\alpha_0(t')=\frac{a_0'H_0'\Delta x}{1+\varepsilon_0'}=\frac{q_0'^3H_{i0}\Delta x}{q_0'^2+\varepsilon_{i0}}\exp\Big(\varepsilon_{i0}^{-1}\frac{\mathcal{E}_0'}{2}\Big)$, which implies $\alpha_{i0}=\frac{H_{i0}\Delta x}{1+\varepsilon_{i0}}$. Choosing physical distance $a_0(t')\Delta x$ a constant fraction K of Hubble length so that the comoving separation

$$\Delta x=K/H_0(t')a_0(t')\ , \tag{3.78}$$

in Eq. (3.77) yields $f_{00}(t,t',K)$. The plots of the function $f_{00}(t,t',K)$ versus $a_0(t')$, for $K{=}1/2$ and four different values of the $\varepsilon_{i0}=\frac{m^2}{3H_{i0}^2}$, are given in Fig. 3.1. They show that correlation (3.76) grows at early times and asymptotes to an almost constant value at late times during inflation. This means that the amplitudes $|\delta\varphi_0|$ of fluctuations do not grow forever; they asymptote to constants. Thus, the inflationary particle production does not continue to drive the inflaton φ up its potential forever and the classical restoring force, which gets bigger as the field rolls up its potential, can push it back down. As the field rolls downhill, the $\delta\varphi_0$ engenders the density inhomogeneities, as pointed out earlier. Note also that the growth in the plots of Fig. 3.1 is sensitive to the value of ε_{i0}. Even a slight increase in the ε_{i0} causes a noticeable suppression in the growth. This is because the production rate and lifetime of virtual inflatons—the origin of fluctuations—are suppressed as the mass increases.

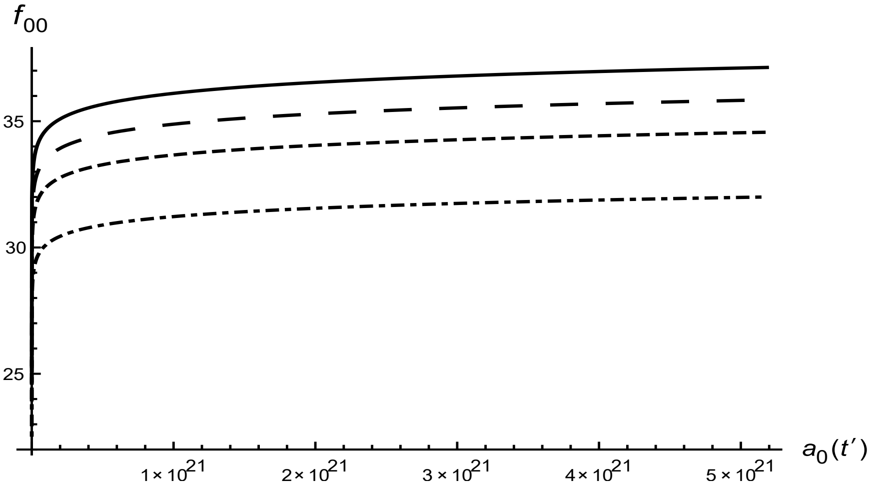

Figure 3.1 : Plots of $f_{00}(t,t',K)$, defined in Eq. (3.77) with separation (3.78), versus $a_0(t')$ for different values of ε_{i0}, $K{=}1/2$ and $a(t)=e^{50}$. $a_0(t')$ runs from 1 to $a_0(t)$. The solid, large-dashed, dashed and dot-dashed lines are for $\varepsilon_{i0}=0.0025, 0.00275, 0.003$ and 0.0035, respectively.

As for the $\mathcal{O}(\lambda)$ correction in Eq. (3.74), employing Eqs. (3.35) and (3.36) in Eq. (3.73)

$$\langle\Omega|\delta\bar{\varphi}_0(x)\delta\bar{\varphi}_0(x')|\Omega\rangle_\lambda=\frac{H_{i0}^2}{4\pi^2}\frac{\xi}{4!}f_{0\lambda}(t,t',\Delta x)\;, \tag{3.79}$$

where $\xi/4!\sim 700$ in a GUT scale inflation for which $H_{i0}\sim 10^{-3}M_{Pl}$ and the dimensionless function

$$\begin{aligned} f_{0\lambda}=\varepsilon_{i0}^{-2}\Bigg\{\Bigg\{&\Bigg[q_0^2+q_0-q_0^{-1}+q_0^{-2}\frac{[1-q_0]^4}{4}-\frac{\varepsilon_{i0}}{q_0^2+\varepsilon_{i0}}\Bigg(2q_0^2+q_0+q_0^{-1}-q_0^{-2}\frac{[1-q_0]^4}{2}\Bigg)\Bigg]\\ &+\Big[q_0\to q_0'\Big]\Bigg\}f_{00}+\frac{(q_0q_0')^3}{(q_0^2+\varepsilon_{i0})(q_0'^2+\varepsilon_{i0})}\Bigg\{\Bigg[q_0'^2+q_0'-q_0'^{-1}-\Big[\varepsilon_{i0}^{-1}-q_0'^{-2}\Big]\frac{[1-q_0']^4}{4}\\ &-\frac{\varepsilon_{i0}}{q_0'^2+\varepsilon_{i0}}\Big[2q_0'^2+q_0'+q_0'^{-1}-q_0'^{-2}\frac{[1-q_0']^4}{2}\Big]\Bigg]\sum_{n=0}^{\infty}\frac{(-1)^n\alpha_0'^{2n}}{(2n+1)!}-\Big[1-\frac{4\varepsilon_{i0}}{1+\varepsilon_{i0}}\Big]\\ &\times\sum_{n=0}^{\infty}\frac{(-1)^n\alpha_{i0}^{2n}}{(2n+1)!}\Bigg\}\Bigg\}\;. \end{aligned} \tag{3.80}$$

For Δx (3.78) and $K{=}1/2$, plots of the function $f_{0\lambda}(t,t',K)$ versus $a_0(t')$ are given in Fig. 3.2 considering the values of ε_{i0} chosen in Fig 3.1. The plots show that $\mathcal{O}(\lambda)$ correction (3.79), for a given ε_{i0}, grows at early times and asymptotes to a constant at late times during inflation. The asymptotic value is substantially suppressed as ε_{i0} increases even slightly.

The coincidence $x'\to x$ limit of two-point correlation function of the fluctuations is needed to compute the power spectrum in Sec. 3.5. In this limit, the tree-order

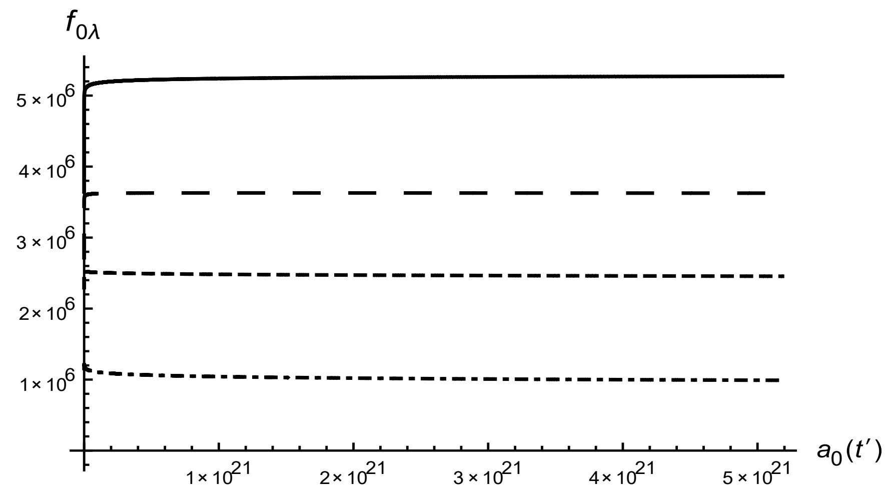

Figure 3.2 : Plots of $f_{0\lambda}(t,t',K)$, defined in Eq. (3.80) with separation (3.78), versus $a_0(t')$. The ranges of parameters K, $a_0(t)$, $a_0(t')$, ε_{i0} and styles of the lines are chosen same as in Fig. 3.1.

correlator (3.71) is

$$\langle\Omega|\delta\bar{\varphi}_0^2(x)|\Omega\rangle=\frac{\Gamma(\frac{D}{2})}{4\pi^{\frac{D}{2}+1}\Gamma(D-1)}\Big(\frac{H}{1+\varepsilon}\Big)^{D-2}\frac{2^{2\nu}\Gamma^2(\nu)}{\delta}\Big[1-\Big(\frac{\alpha_i}{\alpha}\Big)^{\delta}\Big]\,. \quad (3.81)$$

In $D=4$, yields

$$\langle\Omega|\delta\bar{\varphi}_0^2(x)|\Omega\rangle\cong\frac{H^2}{4\pi^2(1+\varepsilon)^2}\Big[\ln\Big(\frac{Ha}{H_i}\Big)-\ln\Big(\frac{1+\varepsilon}{1+\varepsilon_i}\Big)\Big]$$
$$=\frac{H_{i0}^2}{4\pi^2}\frac{q_0^6}{(q_0^2+\varepsilon_{i0})^2}\Bigg\{\varepsilon_{i0}^{-1}\frac{\mathcal{E}_0}{2}-\ln\Big(\frac{q_0^2+\varepsilon_{i0}}{q_0^3(1+\varepsilon_{i0})}\Big)\pm\frac{\lambda}{4!}\xi\varepsilon_{i0}^{-2}\Bigg[\Big[\varepsilon_{i0}^{-1}\mathcal{E}_0+1-2\ln\Big(\frac{q_0^2+\varepsilon_{i0}}{q_0^3(1+\varepsilon_{i0})}\Big)\Big]$$
$$\times\Big[q_0^2+q_0-q_0^{-1}+q_0^{-2}\frac{[1-q_0]^4}{4}-\frac{\varepsilon_{i0}}{q_0^2+\varepsilon_{i0}}\Big[2q_0^2+q_0+q_0^{-1}-q_0^{-2}\frac{[1-q_0]^4}{2}\Big]\Big]-\varepsilon_{i0}^{-1}\frac{[1-q_0]^4}{4}$$
$$-1+\frac{4\varepsilon_{i0}}{1+\varepsilon_{i0}}\Bigg]\Bigg\}. \quad (3.82)$$

Self-interactions of the inflaton yield quantum corrections to the tree-order correlator that are too long to give in arbitrary D in this thesis. The results are simplified in $D=4$. The one-loop correction at $\mathcal{O}(\lambda)$ is, therefore, computed in $D=4$, next.

3.3.2 One-Loop Correlator

The one-loop correlator at $\mathcal{O}(\lambda)$,

$$\langle\Omega|\delta\bar{\varphi}(x)\delta\bar{\varphi}(x')|\Omega\rangle_{1-\mathrm{loop}}\equiv\mp\lambda\,\Big\{\mathcal{V}_{\bar{\varphi}_0^2\delta\bar{\varphi}_0^2}+\mathcal{V}_{\delta\bar{\varphi}_0^4}\Big\}\,, \quad (3.83)$$

where $\mathcal{V}_{\bar{\varphi}_0^2\delta\bar{\varphi}_0^2}$ denotes the sum of the VEVs which are quadratic both in $\bar{\varphi}_0$ and $\delta\bar{\varphi}_0$, and $\mathcal{V}_{\delta\bar{\varphi}_0^4}$ denotes the sum of the VEVs which are quartic in $\delta\bar{\varphi}_0$. They are evaluated in Secs. 3.3.2.1-2.

3.3.2.1 The VEVs Quadratic in the Background and Fluctuation Fields

One-loop correlator (3.67) has two VEVs that are quadratic in $\bar{\varphi}_0$ and $\delta\bar{\varphi}_0$. In $D\!=\!4$,

$$\mathcal{V}_{\bar{\varphi}_0^2\delta\bar{\varphi}_0^2}(q_0,q_0',\Delta x)\equiv\mp\frac{\lambda}{6}\Bigg\{\frac{H_0'}{1\!+\!\varepsilon_0'}\langle\Omega|\delta\bar{\varphi}_0(x)\int_0^{t_0'}\!d\tilde{t}_0\left[\frac{1\!+\!\tilde{\varepsilon}_0}{\tilde{H}_0}\right]^2\bar{\varphi}_0^2(\tilde{t}_0)\,\delta\bar{\varphi}_0(\tilde{t}_0,\vec{x}')|\Omega\rangle_{\mathbf{0}}$$

$$+\frac{H_0}{1\!+\!\varepsilon_0}\langle\Omega|\int_0^{t_0}\!dt_0''\left[\frac{1\!+\!\varepsilon_0''}{H_0''}\right]^2\bar{\varphi}_0^2(t_0'')\,\delta\bar{\varphi}_0(t_0'',\vec{x})\,\delta\bar{\varphi}_0(x')|\Omega\rangle_{\mathbf{0}}\Bigg\}\,,$$

$$\simeq\mp\lambda\frac{H_{i0}^2}{192\pi^4}\frac{\pi}{GH_{i0}^2}f_{1\lambda\bar{\varphi}_0^2\delta\bar{\varphi}_0^2}(t,t',\Delta x)\,. \tag{3.84}$$

Here, we define

$$f_{1\lambda\bar{\varphi}_0^2\delta\bar{\varphi}_0^2}\!=\!\frac{q_0^3q_0'^3}{(q_0^2\!+\!\varepsilon_{i0})(q_0'^2\!+\!\varepsilon_{i0})}\Bigg\{\varepsilon_{i0}^{-3}\frac{\mathcal{E}_0'^2}{2}-\varepsilon_{i0}^{-2}[1\!+\!q_0'^2]\ln(q_0'^2)-\varepsilon_{i0}^{-1}2\Big[\ln^2(q_0')-\mathcal{E}_0'\Big]$$

$$+\Big[\varepsilon_{i0}^{-2}\mathcal{E}_0'\!-\!\varepsilon_{i0}^{-1}\ln(q_0'^2)\Big]2\Big[\ln(\alpha_{i0})\!-\!2\!+\!\gamma\Big]\!-\!\Big[\varepsilon_{i0}^{-2}[2\!-\!q_0^2\!-\!q_0'^2]\!-\!\varepsilon_{i0}^{-1}\Big[\ln(q_0^2)\!+\!\ln(q_0'^2)\Big]\Big]$$

$$\times\Big[\mathrm{ci}(\alpha_{i0})\!-\!\frac{\sin(\alpha_{i0})}{\alpha_{i0}}\Big]\!-\!\Big[\varepsilon_{i0}^{-2}\Big[q_0^2\!-\!q_0'^2\Big]+\varepsilon_{i0}^{-1}\Big[\ln(q_0^2)\!-\!\ln(q_0'^2)\Big]\Big]\Big[\mathrm{ci}(\alpha_0')\!-\!\frac{\sin(\alpha_0')}{\alpha_0'}\Big]$$

$$-2\ln(q_0'^2)\!-\!q_0'^{-2}\!+\!q_0'^2\!+\!\mathbf{A}(q_0',\Delta x)\!+\!\mathcal{O}(\varepsilon_{i0})\Bigg\}, \tag{3.85}$$

where

$$\mathbf{A}(q_0',\Delta x)\equiv\sum_{n=1}^{\infty}\frac{(-1)^n(H_{i0}\Delta x)^{2n}}{2n(2n\!+\!1)!}2e^{\frac{n}{\varepsilon_{i0}}}\Bigg\{\varepsilon_{i0}^{-2}\Big[q_0'^{2n+2}E_{-n}\Big(\frac{nq_0'^2}{\varepsilon_{i0}}\Big)\!-\!E_{-n}\Big(\frac{n}{\varepsilon_{i0}}\Big)\Big]-(2n\!-\!1)$$

$$\times\Big[\varepsilon_{i0}^{-1}\Big[q_0'^{2n}E_{1-n}\Big(\frac{nq_0'^2}{\varepsilon_{i0}}\Big)\!-\!E_{1-n}\Big(\frac{n}{\varepsilon_{i0}}\Big)\Big]\!-\!n\Big[q_0'^{2n-2}E_{2-n}\Big(\frac{nq_0'^2}{\varepsilon_{i0}}\Big)\!-\!E_{2-n}\Big(\frac{n}{\varepsilon_{i0}}\Big)\Big]\Big]\Bigg\}. \tag{3.86}$$

For comoving separation (3.78) and $K\!=\!1/2$, plots of the function $f_{1\lambda\bar{\varphi}_0^2\delta\bar{\varphi}_0^2}(t,t',K)$ versus $a_0(t')$ are given in Fig. 3.3. The values of ε_{i0} are chosen as in Figs. 3.1 and 3.2. The plots imply that, for a given ε_{i0}, the one-loop $\mathcal{O}(\lambda)$ correction $\mathcal{V}_{\bar{\varphi}_0^2\delta\bar{\varphi}_0^2}$ grows–and asymptotes to a constant at late times during inflation. The growth is suppressed as the ε_{i0} increases, though not as sensitively as in $\mathcal{O}(\lambda)$ correction (3.79) plotted in Fig. 3.2.

To complete the computation of one-loop correlator (3.67), we ought to evaluate the remaining VEVs that are quartic in the fluctuation field, in the next section.

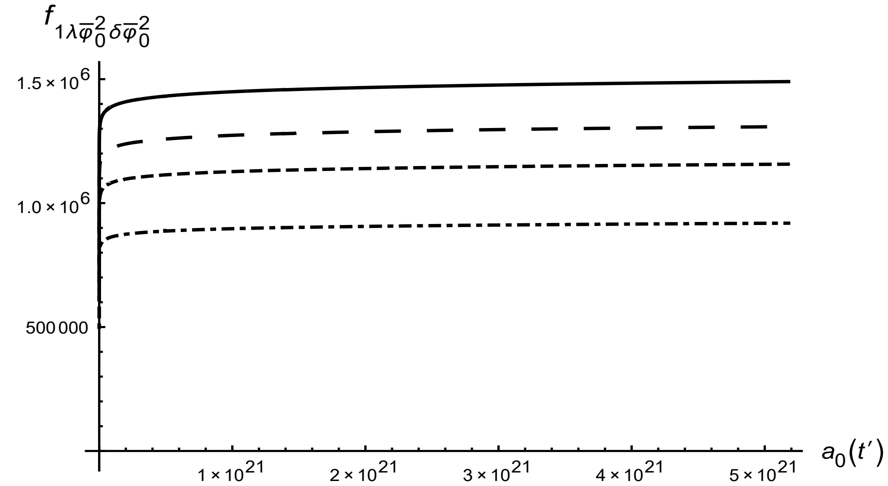

Figure 3.3 : Plots of $f_{1\lambda\bar{\varphi}_0^2\delta\bar{\varphi}_0^2}(t,t',K)$, defined in Eq. (3.85) with separation (3.78), versus $a_0(t')$. The ranges of parameters K, $a_0(t)$, $a_0(t')$, ε_{i0} and styles of the lines are chosen same as in Fig. 3.1.

3.3.2.2 The VEVs Quartic in the Fluctuation Field

The remaining VEVs that are quartic in the fluctuation field in one-loop correlator (3.67), for $D=4$, are

$$\begin{aligned}
\mathcal{V}_{\delta\bar{\varphi}_0^4}(q_0,q_0',\Delta x)\equiv&\mp\frac{\lambda}{18}\Bigg\{\frac{H_0'}{1+\varepsilon_0'}\langle\Omega|\delta\bar{\varphi}_0(x)\int_0^{t_0'}d\tilde{t}_0\Big[\frac{1+\tilde{\varepsilon}_0}{\tilde{H}_0}\Big]^2\delta\bar{\varphi}_0^3(\tilde{t}_0,\vec{x}')|\Omega\rangle\\
&+\frac{H_0}{1+\varepsilon_0}\langle\Omega|\int_0^{t_0}dt_0''\Big[\frac{1+\varepsilon_0''}{H_0''}\Big]^2\delta\bar{\varphi}_0^3(t_0'',\vec{x})\,\delta\bar{\varphi}_0(x')|\Omega\rangle\Bigg\}.\\
&\simeq\mp\lambda\frac{H_{i0}^2}{192\pi^4}f_{1\lambda\delta\bar{\varphi}_0^4}(t,t',\Delta x)\,. \qquad (3.87)
\end{aligned}$$

Here, we define

$$\begin{aligned}
f_{1\lambda\delta\bar{\varphi}_0^4}=&\frac{q_0^3q_0'^3}{(q_0^2+\varepsilon_{i0})(q_0'^2+\varepsilon_{i0})}\Bigg\{\varepsilon_{i0}^{-3}\frac{\mathcal{E}_0'^3}{6}+\varepsilon_{i0}^{-2}\mathcal{E}_0'^2\Big[\ln(q_0')-\frac{1-\gamma}{2}\Big]+\varepsilon_{i0}^{-1}\Big[\mathcal{E}_0'^2+2\mathcal{E}_0'\\
&\times\Big[\ln^2(q_0')+\gamma\ln(q_0')+1\Big]+\frac{q_0'^{-2}}{2}-\frac{q_0'^2}{2}+\Big[2+q_0'^2\Big]\ln(q_0'^2)\Big]-\frac{2}{3}+\frac{1-q_0'^{-4}}{4}-4\Big[1-q_0'^{-2}\Big]\\
&-2\mathcal{E}_0'-\frac{\mathcal{E}_0'^2}{2}+\Big[1+q_0'^{-2}-2q_0'^2\Big]\Big[\ln(q_0'^2)+\gamma\Big]+2\gamma\Big[\ln^2(q_0')+\ln(q_0'^3)\Big]+\frac{\ln^3(eq_0'^2)}{6}+\frac{\ln^2(eq_0'^2)}{2}\\
&+\Bigg\{\varepsilon_{i0}^{-2}\frac{\mathcal{E}_0'^2}{4}+\varepsilon_{i0}^{-1}\mathcal{E}_0'\ln(q_0')-\frac{1-q_0'^{-2}}{2}+\mathcal{E}_0'+\ln^2(q_0')+\ln(q_0'^3)\Bigg\}\ln(\alpha_{i0}^2)-\Bigg\{\frac{\varepsilon_{i0}^{-2}}{4}\Big[\mathcal{E}_0^2+\mathcal{E}_0'^2\Big]\\
&+\varepsilon_{i0}^{-1}\Big[\mathcal{E}_0\ln(q_0)+\mathcal{E}_0'\ln(q_0')\Big]+\frac{q_0^{-2}}{2}+\frac{q_0'^{-2}}{2}-\big[q_0^2+q_0'^2\big]+1+\ln^2(q_0)+\ln^2(q_0')+\ln(q_0^3)\\
&+\ln(q_0'^3)\Bigg\}\Big[\mathrm{ci}(\alpha_{i0})-\frac{\sin(\alpha_{i0})}{\alpha_{i0}}\Big]+\Bigg\{\frac{\varepsilon_{i0}^{-2}}{4}\Big[\mathcal{E}_0^2-\mathcal{E}_0'^2\Big]+\varepsilon_{i0}^{-1}\Big[\mathcal{E}_0\ln(q_0)-\mathcal{E}_0'\ln(q_0')\Big]+\frac{q_0^{-2}}{2}
\end{aligned}$$

$$-\frac{q_0'^{-2}}{2}-\big[q_0^2-q_0'^2\big]+\ln^2(q_0)-\ln^2(q_0')+\ln(q_0^3)-\ln(q_0'^3)\Bigg\}\Bigg[\mathrm{ci}(\alpha_0')-\frac{\sin(\alpha_0')}{\alpha_0'}\Bigg]$$

$$+\mathbf{B}(q_0',\Delta x)+\mathcal{O}(\varepsilon_{i0})\Bigg\}, \tag{3.88}$$

where

$$\mathbf{B}(q_0',\Delta x)\equiv\sum_{n=1}^{\infty}\frac{(-1)^n(H_{i0}\Delta x)^{2n}}{2n(2n+1)!}e^{\frac{n}{\varepsilon_{i0}}}\Bigg\{\varepsilon_{i0}^{-2}\Bigg[E_{-n-1}\Big(\frac{n}{\varepsilon_{i0}}\Big)-q_0'^{2n+4}E_{-n-1}\Big(\frac{nq_0'^2}{\varepsilon_{i0}}\Big)$$
$$-\Bigg\{E_{-n}\Big(\frac{n}{\varepsilon_{i0}}\Big)-q_0'^{2n+2}E_{-n}\Big(\frac{nq_0'^2}{\varepsilon_{i0}}\Big)\Bigg\}\Bigg]-\varepsilon_{i0}^{-1}\Bigg[(2n+1)\Bigg\{E_{-n}\Big(\frac{n}{\varepsilon_{i0}}\Big)-q_0'^{2n+2}E_{-n}\Big(\frac{nq_0'^2}{\varepsilon_{i0}}\Big)$$
$$-\Bigg[E_{1-n}\Big(\frac{n}{\varepsilon_{i0}}\Big)-q_0'^{2n}E_{1-n}\Big(\frac{nq_0'^2}{\varepsilon_{i0}}\Big)\Bigg]\Bigg\}-q_0'^{2n+2}E_{-n}\Big(\frac{nq_0'^2}{\varepsilon_{i0}}\Big)\ln(q_0'^2)+\frac{1}{(n+1)^2}$$
$$\times\Bigg\{{}_2\mathcal{F}_2\Big(n+1,n+1;n+2,n+2;-\frac{n}{\varepsilon_{i0}}\Big)-q_0'^{2n+2}{}_2\mathcal{F}_2\Big(n+1,n+1;n+2,n+2;-\frac{nq_0'^2}{\varepsilon_{i0}}\Big)\Bigg\}\Bigg]$$
$$-2\Bigg[E_{-n}\Big(\frac{n}{\varepsilon_{i0}}\Big)-q_0'^{2n+2}E_{-n}\Big(\frac{nq_0'^2}{\varepsilon_{i0}}\Big)-\Bigg\{E_{1-n}\Big(\frac{n}{\varepsilon_{i0}}\Big)-q_0'^{2n}E_{1-n}\Big(\frac{nq_0'^2}{\varepsilon_{i0}}\Big)\Bigg\}\Bigg]$$
$$+(2n+1)\Bigg[(n+1)\Bigg\{E_{1-n}\Big(\frac{n}{\varepsilon_{i0}}\Big)-q_0'^{2n}E_{1-n}\Big(\frac{nq_0'^2}{\varepsilon_{i0}}\Big)-\Bigg\{E_{2-n}\Big(\frac{n}{\varepsilon_{i0}}\Big)-q_0'^{2n-2}E_{2-n}\Big(\frac{nq_0'^2}{\varepsilon_{i0}}\Big)\Bigg\}\Bigg\}$$
$$-q_0'^{2n}E_{1-n}\Big(\frac{nq_0'^2}{\varepsilon_{i0}}\Big)\ln(q_0'^2)+\frac{1}{n^2}\Bigg\{{}_2\mathcal{F}_2\Big(n,n;n+1,n+1;-\frac{n}{\varepsilon_{i0}}\Big)$$
$$-q_0'^{2n}{}_2\mathcal{F}_2\Big(n,n;n+1,n+1;-\frac{nq_0'^2}{\varepsilon_{i0}}\Big)\Bigg\}\Bigg]\Bigg\}. \tag{3.89}$$

Plots of the function $f_{1\lambda\delta\bar{\varphi}_0^4}(t,t',K)$ versus $a_0(t')$, for comoving separation (3.78), $K=1/2$ and the four values of ε_{i0} that are used in the preceding figures, are given in Fig. 3.4. They imply that, for a chosen ε_{i0}, the one loop $\mathcal{O}(\lambda)$ correction $\mathcal{V}_{\delta\bar{\varphi}_0^4}$ grows—positively or negatively, depending on the sign choice in the potential—and asymptotes to an almost constant value at late times during inflation. The growth is only marginally suppressed as the ε_{i0} increases.

3.3.2.3 The Result

The one-loop correlator at $\mathcal{O}(\lambda)$ is obtained mingling contributions (3.84) and (3.87) in Eq (3.67), setting $D=4$, as

$$\langle\Omega|\delta\bar{\varphi}(t,\vec{x})\,\delta\bar{\varphi}(t',\vec{x}')|\Omega\rangle_{1-\mathrm{loop}}\simeq\mp\lambda\frac{H_{i0}^2}{192\pi^4}f_{1\lambda}(t,t',\Delta x)\,, \tag{3.90}$$

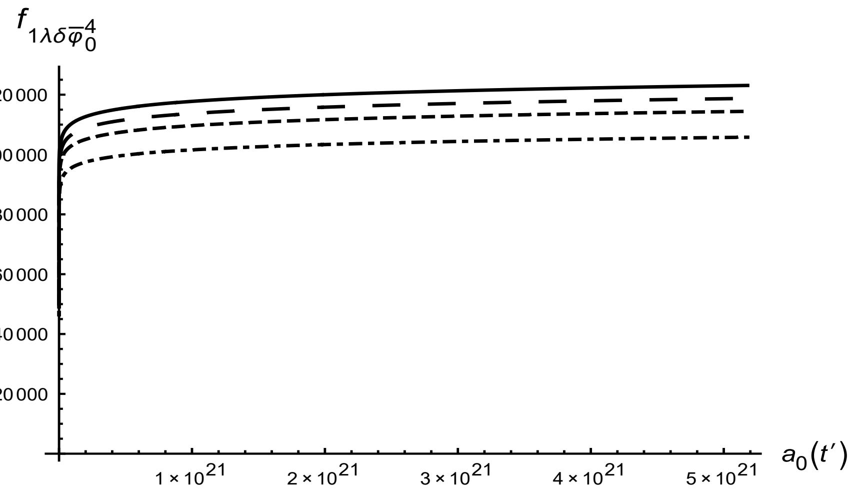

Figure 3.4 : Plots of $f_{1\lambda\delta\bar{\varphi}_0^4}(t,t',K)$, defined in Eq. (3.88) with separation (3.78), versus $a_0(t')$. The ranges of parameters K, $a_0(t)$, $a_0(t')$, ε_{i0} and styles of the lines are chosen same as in Fig. 3.1.

where

$$
\begin{aligned}
f_{1\lambda}=&\frac{q_0^3 q_0'^3}{(q_0^2+\varepsilon_{i0})(q_0'^2+\varepsilon_{i0})}\Bigg\{\frac{\pi}{GH_{i0}^2}\Bigg\{\varepsilon_{i0}^{-3}\frac{\mathcal{E}_0'^2}{2}-\varepsilon_{i0}^{-2}\big[1+q_0'^2\big]\ln(q_0'^2)-\varepsilon_{i0}^{-1}2\Big[\ln^2(q_0')-\mathcal{E}_0'\Big]\\
&+\Big[\varepsilon_{i0}^{-2}\mathcal{E}_0'-\varepsilon_{i0}^{-1}\ln(q_0'^2)\Big]\Big[\ln(\alpha_{i0}^2)-4+2\gamma\Big]-\Bigg[\varepsilon_{i0}^{-2}\big[2-q_0^2-q_0'^2\big]-\varepsilon_{i0}^{-1}\Big[\ln(q_0^2)+\ln(q_0'^2)\Big]\Bigg]\\
&\times\Big[\mathrm{ci}(\alpha_{i0})-\frac{\sin(\alpha_{i0})}{\alpha_{i0}}\Big]-\Bigg[\varepsilon_{i0}^{-2}\Big[q_0^2-q_0'^2\Big]+\varepsilon_{i0}^{-1}\Big[\ln(q_0^2)-\ln(q_0'^2)\Big]\Bigg]\Big[\mathrm{ci}(\alpha_0')-\frac{\sin(\alpha_0')}{\alpha_0'}\Big]\\
&-2\ln(q_0'^2)-q_0'^{-2}+q_0'^2+\mathbf{A}(q_0',\Delta x)\Bigg\}+\varepsilon_{i0}^{-3}\frac{\mathcal{E}_0'^3}{6}+\varepsilon_{i0}^{-2}\mathcal{E}_0'^2\Big[\ln(q_0')-\frac{1-\gamma}{2}\Big]\\
&+\varepsilon_{i0}^{-1}\Bigg[\mathcal{E}_0'^2+2\mathcal{E}_0'\Big[\ln^2(q_0')+\gamma\ln(q_0')+1\Big]+\frac{q_0'^{-2}-q_0'^2}{2}+\Big[2+q_0'^2\Big]\ln(q_0'^2)\Bigg]-\frac{2}{3}+\frac{1-q_0'^{-4}}{4}\\
&-4\Big[1-q_0'^{-2}\Big]-2\mathcal{E}_0'-\frac{\mathcal{E}_0'^2}{2}+\Big[1+q_0'^{-2}-2q_0'^2\Big]\Big[\ln(q_0'^2)+\gamma\Big]+2\gamma\Big[\ln^2(q_0')+\ln(q_0'^3)\Big]\\
&+\frac{\ln^3(eq_0'^2)}{6}+\frac{\ln^2(eq_0'^2)}{2}+\Bigg\{\varepsilon_{i0}^{-2}\frac{\mathcal{E}_0'^2}{4}+\varepsilon_{i0}^{-1}\mathcal{E}_0'\ln(q_0')-\frac{1-q_0'^{-2}}{2}+\mathcal{E}_0'+\ln^2(q_0')+\ln(q_0'^3)\Bigg\}\\
&\times\ln(\alpha_{i0}^2)-\Bigg\{\frac{\varepsilon_{i0}^{-2}}{4}\Big[\mathcal{E}_0^2+\mathcal{E}_0'^2\Big]+\varepsilon_{i0}^{-1}\Big[\mathcal{E}_0\ln(q_0)+\mathcal{E}_0'\ln(q_0')\Big]+\frac{q_0^{-2}+q_0'^{-2}}{2}-\big[q_0^2+q_0'^2\big]\\
&+1+\ln^2(q_0)+\ln^2(q_0')+\ln(q_0^3)+\ln(q_0'^3)\Bigg\}\Big[\mathrm{ci}(\alpha_{i0})-\frac{\sin(\alpha_{i0})}{\alpha_{i0}}\Big]+\Bigg\{\frac{\varepsilon_{i0}^{-2}}{4}\Big[\mathcal{E}_0^2-\mathcal{E}_0'^2\Big]\\
&+\varepsilon_{i0}^{-1}\Big[\mathcal{E}_0\ln(q_0)-\mathcal{E}_0'\ln(q_0')\Big]+\frac{q_0^{-2}-q_0'^{-2}}{2}-\big[q_0^2-q_0'^2\big]+\ln^2(q_0)-\ln^2(q_0')+\ln(q_0^3)\\
&-\ln(q_0'^3)\Bigg\}\Big[\mathrm{ci}(\alpha_0')-\frac{\sin(\alpha_0')}{\alpha_0'}\Big]+\mathbf{B}(q_0',\Delta x)+\mathcal{O}(\varepsilon_{i0})\Bigg\}\,. \qquad (3.91)
\end{aligned}
$$

Coincidence limit of Eq. 3.91 yields the coincident one-loop correlator at $\mathcal{O}(\lambda)$ as

$$\langle\Omega|\delta\bar{\varphi}^2(t,\vec{x})|\Omega\rangle_{1-\text{loop}} = \mp\lambda\frac{H_{i0}^2}{192\pi^4}\frac{q_0^6}{[q_0^2+\varepsilon_{i0}]^2}\Bigg\{\frac{\pi}{GH_{i0}^2}\Bigg[\varepsilon_{i0}^{-3}\frac{\mathcal{E}_0^2}{2}-\varepsilon_{i0}^{-2}2\Big[\ln(q_0^2)$$
$$+\mathcal{E}_0\Big[1-\frac{\ln(q_0^2)}{2}\Big]\Big]+\varepsilon_{i0}^{-1}2\Big[\ln(q_0^2)-\frac{\ln^2(q_0^2)}{4}+\mathcal{E}_0\Big]-2\ln(q_0^2)-q_0^{-2}\Big[2\mathcal{E}_0-\mathcal{E}_0^2\Big]+\mathcal{O}(\varepsilon_{i0})\Bigg]$$
$$+\varepsilon_{i0}^{-3}\frac{\mathcal{E}_0^3}{6}+\varepsilon_{i0}^{-2}\mathcal{E}_0^2\frac{\ln(q_0^2)}{2}+\varepsilon_{i0}^{-1}3\Bigg[\ln(q_0^2)+\mathcal{E}_0 q_0^{-2}\Big[1+\frac{\ln^2(q_0^2)}{6}-\frac{\mathcal{E}_0}{2}\Big[1+\frac{\ln^2(q_0^2)}{3}\Big]-\frac{\mathcal{E}_0^2}{3}\Big]\Bigg]$$
$$+\frac{9}{2}q_0^{-2}\ln(q_0^2)+\frac{3}{2}\ln^2(q_0^2)+\frac{\ln^3(q_0^2)}{6}+\frac{9}{2}\mathcal{E}_0 q_0^{-4}\Bigg[1-\frac{\ln(q_0^2)}{3}-\frac{7}{6}\mathcal{E}_0\Big[1+\frac{2}{21}\ln(q_0^2)\Big]$$
$$+\frac{2}{9}\mathcal{E}_0^2\Big[1+2\ln(q_0^2)\Big]-\frac{\mathcal{E}_0^3}{9}\Bigg]+\mathcal{O}(\varepsilon_{i0})\Bigg\}+\mathcal{O}(\lambda^2)\,. \tag{3.92}$$

Next, we obtain the coincident correlation function of the fluctuations up to $\mathcal{O}(\lambda^2)$.

3.4 Coincident Correlation Function of the Fluctuations

Coincident correlation function of the IR truncated fluctuation field, is obtained by adding tree-order (3.82) and one-loop (3.92) correlators. In powers of ε_{i0} and $\mathcal{E}_0$,

$$\langle\Omega|\delta\bar{\varphi}^2(t,\vec{x})|\Omega\rangle_{\text{stoch}} = \frac{H_{i0}^2}{4\pi^2}\frac{q_0^4}{[q_0^2+\varepsilon_{i0}]^2}\Bigg\{\Big[1-\mathcal{E}_0\Big]\Bigg\{\ln(a_0)-\ln\Big(\frac{q_0^2+\varepsilon_{i0}}{q_0^3(1+\varepsilon_{i0})}\Big)\Bigg\}$$
$$\mp\frac{\lambda}{144\pi^2}\Bigg\{\frac{\pi}{GH_{i0}^2}\Bigg\{\varepsilon_{i0}^{-3}\Bigg[1-q_0-\frac{7}{2}\mathcal{E}_0\Big[1-\frac{5}{7}q_0\Big]+\frac{37}{8}\mathcal{E}_0^2\Big[1-\frac{4}{37}q_0\Big]-\frac{9}{4}\mathcal{E}_0^3\Bigg]$$
$$-\varepsilon_{i0}^{-2}q_0^{-2}\Bigg[1-q_0+\frac{15}{2}\Big[1-\frac{2}{15}q_0\Big]\ln(q_0^2)+\frac{9}{2}\mathcal{E}_0\Big[1-\frac{4}{9}q_0-\frac{37}{9}\Big[1-\frac{2}{37}q_0\Big]\ln(q_0^2)\Big]$$
$$-\frac{79}{8}\mathcal{E}_0^2\Big[1-\frac{12}{79}q_0-\frac{117}{79}\ln(q_0^2)\Big]+\frac{37}{8}\mathcal{E}_0^3\Big[1-\frac{29}{37}\ln(q_0^2)\Big]\Bigg]+\varepsilon_{i0}^{-1}q_0^{-4}3\Bigg[1-q_0$$
$$-\frac{5}{3}\Big[1+\frac{3}{5}q_0\Big]\ln(q_0^2)+\frac{\ln^2(q_0^2)}{2}-\frac{17}{3}\mathcal{E}_0\Big[1-\frac{19}{34}q_0-\Big[1+\frac{9}{34}q_0\Big]\ln(q_0^2)+\frac{9}{34}\ln^2(q_0^2)\Big]$$
$$+\frac{121}{12}\mathcal{E}_0^2\Big[1-\frac{20}{121}q_0-\frac{75}{121}\Big[1+\frac{2}{25}q_0\Big]\ln(q_0^2)+\frac{18}{121}\ln^2(q_0^2)\Big]-\frac{95}{12}\mathcal{E}_0^3\Big[1-\frac{27}{95}\ln(q_0^2)$$
$$+\frac{6}{95}\ln^2(q_0^2)\Big]+\frac{29}{12}\mathcal{E}_0^4\Bigg]+q_0^{-6}3\Bigg[1-q_0-\frac{5}{3}\Big[1+\frac{3}{5}q_0\Big]\ln(q_0^2)-\frac{17}{3}\mathcal{E}_0\Big[1-\frac{7}{34}q_0$$
$$-\frac{23}{17}\Big[1+\frac{9}{46}q_0\Big]\ln(q_0^2)\Big]+\frac{155}{12}\mathcal{E}_0^2\Big[1+\frac{12}{155}q_0-\frac{147}{155}\Big[1+\frac{2}{49}q_0\Big]\ln(q_0^2)\Big]$$
$$-\frac{175}{12}\mathcal{E}_0^3\Big[1+\frac{8}{175}q_0-\frac{99}{175}\ln(q_0^2)\Big]+\frac{179}{24}\mathcal{E}_0^4\Big[1-\frac{48}{179}\ln(q_0^2)\Big]-\frac{29}{24}\mathcal{E}_0^5\Bigg]+\mathcal{O}(\varepsilon_{i0})\Bigg\}$$

$$+\Big[1-\mathcal{E}_0\Big]\Big[\varepsilon_{i0}^{-3}\frac{\mathcal{E}_0^3}{2}+\varepsilon_{i0}^{-2}\frac{3}{2}\mathcal{E}_0^2\ln(q_0^2)\Big]+\varepsilon_{i0}^{-1}9\Bigg[\ln(q_0^2)+\mathcal{E}_0\Bigg[1-\ln(q_0^2)+\frac{\ln^2(q_0^2)}{6}\Bigg]$$

$$-\frac{\mathcal{E}_0^2}{2}\Bigg[1+\frac{\ln^2(q_0^2)}{3}\Bigg]-\frac{\mathcal{E}_0^3}{3}\Bigg]+\frac{27}{2}\ln(q_0^2)+\frac{9}{2}\Big[1-\mathcal{E}_0\Big]\Bigg[\ln^2(q_0^2)+\frac{\ln^3(q_0^2)}{9}\Bigg]+\frac{27}{2}\mathcal{E}_0 q_0^{-2}$$

$$\times\Bigg[1-\frac{\ln(q_0^2)}{3}-\frac{7}{6}\mathcal{E}_0\Big[1+\frac{2}{21}\ln(q_0^2)\Big]+\frac{2}{9}\mathcal{E}_0^2\Big[1+2\ln(q_0^2)\Big]-\frac{\mathcal{E}_0^3}{9}\Bigg]+\mathcal{O}(\varepsilon_{i0})\Bigg\}+\mathcal{O}(\lambda^2)\,. \quad (3.93)$$

which is used to compute the power spectrum, in the following section.

3.5 Power Spectrum of the Fluctuations

Recall Eq. (2.107) that the stochastic contributions to the coincident correlator and the power spectrum $\Delta^2_{\delta\varphi}(k)$ are related as

$$\langle\Omega|\delta\bar{\varphi}^2(t,\vec{x})|\Omega\rangle_{\text{stoch}}\equiv\int_0^\infty\frac{dk}{k}\Theta\Big(\frac{Ha}{1+\varepsilon}-k\Big)\Delta^2_{\delta\bar{\varphi}}(k)=\int_{k_i=\frac{H_i}{1+\varepsilon_i}}^{k=\frac{Ha}{1+\varepsilon}}\frac{dk}{k}\Delta^2_{\delta\bar{\varphi}}(k)\,. \quad (3.94)$$

Taking the time derivative of both sides yields

$$\Delta^2_{\delta\bar{\varphi}}\Big(k=\frac{Ha}{1+\varepsilon}\Big)=\Big[H[1-\varepsilon]-\frac{\dot{\varepsilon}}{1+\varepsilon}\Big]^{-1}\frac{d}{dt}\langle\Omega|\delta\bar{\varphi}^2(t,\vec{x})|\Omega\rangle_{\text{stoch}}\,. \quad (3.95)$$

One can, however, look at the power at *any* time t and that time corresponds to a mode k through the relation $a=\frac{k}{H}(1+\varepsilon)$. Thus, by considering Eq. (3.95) at different times one can access the power for different modes with wave number k. Using $\frac{d}{dt}=-\varepsilon_{i0}q^{-1}H\frac{d}{dq}$, the chain rule $\frac{d}{dq}=-\frac{q}{\varepsilon_{i0}H}\frac{d}{dt}$ and coincident correlator (3.93) in Eq. (3.95) yields

$$\Delta^2_{\delta\bar{\varphi}}\Big(k=\frac{H(t)\,a(t)}{1+\varepsilon(t)}\Big)=-\Big[1-\varepsilon(t)-\frac{\dot{\varepsilon}(t)}{H(t)\,[1+\varepsilon(t)]}\Big]^{-1}\frac{\varepsilon_{i0}}{q}\frac{d}{dq}\langle\Omega|\delta\bar{\varphi}^2(t,\vec{x})|\Omega\rangle_{\text{stoch}}$$

$$=\frac{H_{i0}^2}{4\pi^2}\Bigg\{\frac{q_0^6}{[q_0^2+\varepsilon_{i0}]^2}\Bigg[1+\frac{q_0^2+3\varepsilon_{i0}}{q_0^4-3\varepsilon_{i0}^2}\ln\Big(\frac{q_0^2+\varepsilon_{i0}}{a_0q_0^3(1+\varepsilon_{i0})}\Big)^{2\varepsilon_{i0}}\Bigg]\mp\frac{\lambda}{144\pi^2}\Bigg\{\frac{\pi}{GH_{i0}^2}\Bigg[\varepsilon_{i0}^{-2}q_0^{-1}4$$

$$\times\Bigg[1-\frac{5}{4}q_0-\mathcal{E}_0\Big(1-\frac{7}{2}q_0\Big)-\frac{\mathcal{E}_0^2}{8}\Big(1+25q_0\Big)\Bigg]+\varepsilon_{i0}^{-1}q_0^{-4}4\Big[1+\frac{q_0}{2}+5\Big(1+\frac{q_0}{20}\Big)\ln(q_0^2)$$

$$-\mathcal{E}_0\Big(1+q_0+\frac{27}{2}\Big[1+\frac{5}{108}q_0\Big]\ln(q_0^2)\Big)-\frac{9}{4}\mathcal{E}_0^2\Big(1-\frac{5}{18}q_0-\frac{16}{3}\Big[1+\frac{q_0}{32}\Big]\ln(q_0^2)\Big)$$

$$+\frac{35}{16}\mathcal{E}_0^3\Big(1-\frac{8}{5}\ln(q_0^2)\Big)\Big]-q_0^{-6}5\Big[1-4q_0-\frac{3}{5}\Big(1-\frac{2}{3}q_0\Big)\ln(q_0^2)+\frac{3}{5}\ln^2(q_0^2)+\frac{2}{5}\mathcal{E}_0\Big(1+16q_0$$

$$+\frac{13}{2}\Big[1-\frac{7}{26}q_0\Big]\ln(q_0^2)-\frac{9}{2}\ln^2(q_0^2)\Big)+\frac{21}{10}\mathcal{E}_0^2\Big(1-\frac{17}{21}q_0+\frac{23}{14}\Big[1-\frac{2}{23}q_0\Big]\ln(q_0^2)$$

$$+\frac{6}{7}\ln^2(q_0^2)\Big)-\frac{91}{10}\mathcal{E}_0^3\Big(1+\frac{6}{91}q_0-\frac{29}{182}\ln(q_0^2)+\frac{6}{91}\ln^2(q_0^2)\Big)+\frac{28}{5}\mathcal{E}_0^4\Big]+\mathcal{O}(\varepsilon_{i0})\Bigg]$$

$$
+\varepsilon_{i0}^{-2}3\Big[\mathcal{E}_0^2-\frac{4}{3}\mathcal{E}_0^3\Big]+\varepsilon_{i0}^{-1}6q_0^{-4}\Big[\mathcal{E}_0\ln(q_0^2)-\mathcal{E}_0^2\Big(1+\frac{7}{2}\ln(q_0^2)\Big)+\frac{11}{6}\mathcal{E}_0^3\Big(1+\frac{24}{11}\ln(q_0^2)\Big)
$$

$$
-\frac{5}{6}\mathcal{E}_0^4\Big(1+\frac{9}{5}\ln(q_0^2)\Big)\Big]-18q_0^{-6}\Big[\ln(q_0^2)-\frac{\ln^2(q_0^2)}{6}+\mathcal{E}_0\Big(1-\frac{7}{3}\ln(q_0^2)+\frac{5}{6}\ln^2(q_0^2)\Big)
$$

$$
-\frac{17}{6}\mathcal{E}_0^2\Big(1-\frac{7}{17}\ln(q_0^2)+\frac{9}{17}\ln^2(q_0^2)\Big)+\frac{5}{3}\mathcal{E}_0^3\Big(1+\frac{2}{5}\ln(q_0^2)+\frac{7}{10}\ln^2(q_0^2)\Big)
$$

$$
+\frac{7}{6}\mathcal{E}_0^4\Big(1-\frac{3}{7}\ln(q_0^2)-\frac{2}{7}\ln^2(q_0^2)\Big)-\mathcal{E}_0^5\Big]+\mathcal{O}(\varepsilon_{i0})\Big\}. \tag{3.96}
$$

Through the relations

$$
q_0^2(t_k)=1-\mathcal{E}_0(t_k)=1-2\varepsilon_{i0}\ln\Big(a_0(t_k)\Big)\,, \tag{3.97}
$$

and

$$
a_0(t_k)=\frac{k}{H_0(t_k)}\left[1+\varepsilon_0(t_k)\right]\,, \tag{3.98}
$$

one finds the power for any mode

$$
\frac{k}{H_{i0}}=\frac{a_0(t_k)\,q_0^3(t_k)}{q_0^2(t_k)+\varepsilon_{i0}}\,, \tag{3.99}
$$

which is a monotonically increasing function of a_0. Note that Eqs. (3.98) and (3.99) reduce [56] to $\frac{k}{H_{i0}}=a_0(t_k)$ in de Sitter limit. In the noninteracting limit, $\Delta^2_{\delta\bar{\varphi}_0}(k)\equiv\frac{H_{i0}^2}{4\pi^2}\mathfrak{P}_0(k)$. The function $\mathfrak{P}_0(k)$, that can be read off from Eq. (3.96), is expanded in ε_{i0} as $\mathfrak{P}_0(k)=2q_0^2-1-\varepsilon_{i0}\Big[1+q_0^{-2}+\ln(q_0^2)\Big]+\mathcal{O}(\varepsilon_{i0}^2)$. The $\mathfrak{P}_0(k)$ is positive definite during inflation and decreases monotonically as a_0, i.e., k/H_{i0} increases. Thus, as k decreases, the power $\Delta^2_{\delta\bar{\varphi}_0}$ increases. The amplitude of fluctuations grow toward the larger scales and the spectrum is red tilted.

The $\mathcal{O}(\lambda)$ correction to the power spectrum $\Delta^2_{\delta\bar{\varphi}_\lambda}(k)\equiv\mp\lambda\frac{H_{i0}^2}{576\pi^4}\mathfrak{P}_\lambda(k)$. The function $\mathfrak{P}_\lambda$, that can be read off from Eq. (3.96), is also positive definite and decreases monotonically as a_0 or k/H_{i0} increases. As the scale increases, so does the $\mathfrak{P}_\lambda$. Thus, for the $+$ $(-)$ sign choice in potential (3.3), the $\mathcal{O}(\lambda)$ correction $\Delta^2_{\delta\bar{\varphi}_\lambda}$ reduces (increases) the power in the noninteracting limit, $\Delta^2_{\delta\bar{\varphi}_0}$. Note finally that $\Delta^2_{\delta\bar{\varphi}_\lambda}$ is enhanced by the terms involving huge factors of ε_{i0}^{-2} and ε_{i0}^{-1} that are absent in the one-loop power spectrum of the spectator scalar during de Sitter inflation [56]. In Secs. 3.5.1-3.5.2, we compute the $n_{\delta\bar{\varphi}}$ and $\alpha_{\delta\bar{\varphi}}$ for the inflaton fluctuations and compare our predictions with the cosmological measurements [60].

3.5.1 Spectral Index $n_{\bar{\varphi}}$ of the Inflaton Fluctuations

The spectral index of inflaton fluctuations is defined in Eq. (1.10). Hence, the tilt

$$n_{\delta\varphi}\left(k=\frac{Ha}{1+\varepsilon}\right)-1\equiv\frac{d\ln(\Delta^2_{\delta\bar{\varphi}}(k=\frac{Ha}{1+\varepsilon}))}{d\ln(k)}\ . \tag{3.100}$$

The logarithmic derivative

$$\frac{d}{d\ln(k)}=k\frac{d}{dk}=k\frac{dt}{dk}\frac{d}{dt}=-\left[1-\varepsilon-\frac{\dot{\varepsilon}}{H\,[1+\varepsilon]}\right]^{-1}\frac{\varepsilon_{i0}}{q}\frac{d}{dq}\ . \tag{3.101}$$

Therefore, the tilt

$$\begin{aligned}
&n_{\delta\bar{\varphi}}\left(k=\frac{H(t)\,a(t)}{1+\varepsilon(t)}\right)-1=-\left[1-\varepsilon(t)-\frac{\dot{\varepsilon}(t)}{H(t)\,[1+\varepsilon(t)]}\right]^{-1}\frac{\varepsilon_{i0}}{q}\frac{d}{dq}\ln\left(\Delta^2_{\delta\bar{\varphi}}\left(k=\frac{H(t)\,a(t)}{1+\varepsilon(t)}\right)\right)\\
&=-\frac{4\varepsilon_{i0}}{\mathbf{N}}\Bigg\{q_0^{10}+3\varepsilon_{i0}q_0^6\left[1-\frac{5}{6}\mathcal{E}_0\right]-6\varepsilon_{i0}^2q_0^4\left[1-\frac{5}{4}\mathcal{E}_0\right]-18\varepsilon_{i0}^3q_0^2\left[1-\frac{19}{12}\mathcal{E}_0\right]+9\varepsilon_{i0}^4\left[1+\frac{\mathcal{E}_0}{2}\right]\\
&+27\varepsilon_{i0}^5-\mathbf{M}\Bigg\}\mp\frac{\lambda}{36\pi^2}\frac{q_0^{-3}}{[1-2\mathcal{E}_0]^2}\Bigg\{\frac{\pi}{GH_{i0}^2}5\Bigg[\varepsilon_{i0}^{-1}\Bigg[1-\frac{13}{5}\mathcal{E}_0\left(1+\frac{8}{13}q_0\right)+\frac{91}{40}\mathcal{E}_0^2\left(1+\frac{12}{7}q_0\right)\\
&-\frac{13}{20}\mathcal{E}_0^3\left(1+\frac{46}{13}q_0\right)\Bigg]-\frac{3q_0^{-3}}{1-2\mathcal{E}_0}\Bigg[1-\frac{9}{5}q_0-\frac{8}{15}\left(1+\frac{19}{16}q_0\right)\ln(q_0^2)-\frac{25}{6}\mathcal{E}_0\Bigg[1-\frac{363}{250}q_0-\frac{88}{125}\\
&\times\left(1+\frac{261}{352}q_0\right)\ln(q_0^2)\Bigg]+\frac{49}{8}\mathcal{E}_0^2\Bigg[1-\frac{296}{245}q_0-\frac{664}{735}\times\left(1+\frac{41}{83}q_0\right)\ln(q_0^2)\Bigg]-\frac{119}{40}\mathcal{E}_0^3\Bigg[1-\frac{67}{51}q_0\\
&-\frac{520}{357}\left(1+\frac{177}{520}q_0\right)\ln(q_0^2)\Bigg]-\frac{2}{3}\mathcal{E}_0^4\Bigg[1+\frac{49}{40}q_0+\frac{17}{10}\left(1+\frac{q_0}{4}\right)\ln(q_0^2)+\frac{7}{10}\mathcal{E}_0^5\left(1-\frac{2}{21}\ln(q_0^2)\right)\Bigg]\Bigg]\\
&+\mathcal{O}(\varepsilon_{i0})\Bigg]+\varepsilon_{i0}^{-1}3q_0\left[\mathcal{E}_0-4\mathcal{E}_0^2+\frac{17}{3}\mathcal{E}_0^3-\frac{8}{3}\mathcal{E}_0^4\right]+\frac{3q_0^{-3}}{1-2\mathcal{E}_0}\Bigg[\Big[1-7\mathcal{E}_0\Big]\ln(q_0^2)+3\mathcal{E}_0^2\left[1+\frac{22}{3}\ln(q_0^2)\right]\\
&-\frac{32}{3}\mathcal{E}_0^3\left[1+\frac{29}{8}\ln(q_0^2)\right]+\frac{41}{3}\mathcal{E}_0^4\left[1+\frac{117}{41}\ln(q_0^2)\right]-\frac{22}{3}\mathcal{E}_0^5\left[1+\frac{63}{22}\ln(q_0^2)\right]+\frac{4}{3}\mathcal{E}_0^6\left[1+\frac{7}{2}\ln(q_0^2)\right]\Bigg]\\
&\qquad\qquad\qquad+\mathcal{O}(\varepsilon_{i0})\Bigg\},
\end{aligned} \tag{3.102}$$

where

$$\mathbf{N}(q_0,\varepsilon_{i0})=\left[q_0^4-3\varepsilon_{i0}^2\right]^3\left\{1+\frac{q_0^2+3\varepsilon_{i0}}{q_0^4-3\varepsilon_{i0}^2}\ln\left(\frac{q_0^2+\varepsilon_{i0}}{a_0q_0^3(1+\varepsilon_{i0})}\right)^{2\varepsilon_{i0}}\right\}\ , \tag{3.103}$$

$$\mathbf{M}(q_0,\varepsilon_{i0})=\varepsilon_{i0}^2\left[q_0^6+3\varepsilon_{i0}q_0^4+21\varepsilon_{i0}^2q_0^2+27\varepsilon_{i0}^3\right]\ln\left(\frac{q_0^2+\varepsilon_{i0}}{q_0^3(1+\varepsilon_{i0})}\right)\ . \tag{3.104}$$

Recall that $q_0(t_k)$ and k are related via Eq. (3.99). In the noninteracting limit, the spectral index

$$n_{\delta\bar{\varphi}_0}(k)\equiv\mathfrak{N}_0(k)=1-\frac{4\varepsilon_{i0}}{1-2\mathcal{E}_0}+\mathcal{O}(\varepsilon_{i0}^2)\ , \tag{3.105}$$

whose exact form can be read off from Eq. (3.102), is nonsingular for $\mathcal{E}_0 < 1/2$ which implies

$$\varepsilon_{i0} < \frac{1}{4\ln(a_0)} \; . \tag{3.106}$$

During an inflation which lasts 60 e-foldings, for example, Eq. (3.106) implies $\varepsilon_{i0} < 0.0041$. The dimensionless function $\mathfrak{N}_0(k)$, for an ε_{i0} satisfying Eq. (3.106), is negative definite and decreases monotonically as, a_0, i.e., k/H_{i0} increases. Thus, the tree-order tilt is red.

The $\mathcal{O}(\lambda)$ correction to the spectral index

$$n_{\bar{\varphi}_\lambda}(k) \equiv \mp \frac{\lambda}{36\pi^2} \mathfrak{N}_\lambda(k) \; ,$$

where the $\mathfrak{N}_\lambda(k)$ is given in Eq. (3.102), is also nonsingular for an $\varepsilon_{i0} < 1/4\ln(a_0)$. The $\mathfrak{N}_\lambda$ is positive definite and increases monotonically as a_0, hence k/H_{i0}, increases. Thus, for the $+$ $(-)$ sign choice in potential (3.3), the $\mathcal{O}(\lambda)$ correction $n_{\bar{\varphi}_\lambda}$ enhances (reduces) the red tilt.

3.5.2 Running of the Spectral Index $\alpha_{\bar{\varphi}}$ of the Inflaton Fluctuations

Another physical quantity that can be computed and compared with measurements is the running of the spectral index, defined in Eq. (1.12),

$$\alpha_{\delta\bar{\varphi}}\left(k = \frac{Ha}{1+\varepsilon}\right) \equiv \frac{dn_{\delta\bar{\varphi}}\left(k = \frac{Ha}{1+\varepsilon}\right)}{d\ln(k)} \; . \tag{3.107}$$

Substituting Eq. (3.102) into Eq. (3.107), we obtain the running of the inflaton fluctuations, up to $\mathcal{O}(\lambda^2)$, as

$$\begin{aligned}
\alpha_{\delta\bar{\varphi}}\left(k = \frac{H(t)\,a(t)}{1+\varepsilon(t)}\right) &= -\left[1 - \varepsilon(t) - \frac{\dot{\varepsilon}(t)}{H(t)\,[1+\varepsilon(t)]}\right]^{-1} \frac{\varepsilon_{i0}}{q} \frac{d}{dq} n_{\delta\bar{\varphi}}\left(k = \frac{H(t)\,a(t)}{1+\varepsilon(t)}\right) \\
&= -\frac{4\varepsilon_{i0}^2}{\left[q_0^2 + 3\varepsilon_{i0}\right]^2} \left\{ \frac{4}{\mathbf{N}^2} \left[q_0^4 - 3\varepsilon_{i0}^2\right]^2 \left[q_0^8 + \frac{13}{2}\varepsilon_{i0} q_0^6 + \frac{15}{2}\varepsilon_{i0}^2 q_0^4 - \frac{15}{2}\varepsilon_{i0}^3 q_0^2 - \frac{27}{2}\varepsilon_{i0}^4\right]^2 \right. \\
&+ \frac{\varepsilon_{i0} q_0^2 \left[q_0^2 + \varepsilon_{i0}\right]}{q_0^4 - 3\varepsilon_{i0}^2} \left[\frac{1}{\mathbf{N}} \left[q_0^{10} + 3\varepsilon_{i0} q_0^8 + 66\varepsilon_{i0}^2 q_0^6 + 198\varepsilon_{i0}^3 q_0^4 + 153\varepsilon_{i0}^4 q_0^2 + 27\varepsilon_{i0}^5\right] - \frac{2}{\left[q_0^4 - 3\varepsilon_{i0}^2\right]^3} \right. \\
&\left.\left. \times \left[q_0^{10} + 6\varepsilon_{i0} q_0^8 + 54\varepsilon_{i0}^2 q_0^6 + 180\varepsilon_{i0}^3 q_0^4 + 189\varepsilon_{i0}^4 q_0^2 + 54\varepsilon_{i0}^5\right] \right] \right\} \mp \frac{\lambda}{6\pi^2} \frac{1}{\left[1 - 2\mathcal{E}_0\right]^3} \left\{ \frac{\pi}{GH_{i0}^2} q_0^{-5} \frac{37}{6} \right. \\
&\times \left[1 - \frac{24}{37} q_0 - \frac{255}{74} \mathcal{E}_0 \left[1 - \frac{32}{51} q_0\right] + \frac{1305}{296} \mathcal{E}_0^2 \left[1 - \frac{736}{1305} q_0\right] - \frac{183}{74} \mathcal{E}_0^3 \left[1 - \frac{80}{183} q_0\right] \right. \\
&\left.\left. + \frac{\mathcal{E}_0^4}{2} \left[1 - \frac{8}{37} q_0\right] + \mathcal{O}(\varepsilon_{i0}) \right] + 1 - 4\mathcal{E}_0 + 8\mathcal{E}_0^2 - \frac{16}{3}\mathcal{E}_0^3 + \mathcal{O}(\varepsilon_{i0}) \right\} \; .
\end{aligned} \tag{3.108}$$

In the noninteracting limit, the running $\alpha_{\delta\bar{\varphi}_0}(k)\equiv\mathfrak{A}_0(k)$, whose exact form is given in Eq. (3.108), can be expanded in powers of ε_{i0} as

$$\mathfrak{A}_0(k)=-\frac{16\varepsilon_{i0}^2}{(2q_0^2-1)^2}+\mathcal{O}(\varepsilon_{i0}^3)\ . \tag{3.109}$$

The dimensionless function $\mathfrak{A}_0(k)$ is negative definite and decreases monotonically as a_0, i.e., k/H_{i0}, increases. The $\mathcal{O}(\lambda)$ correction to the running is

$$\alpha_{\delta\bar{\varphi}_\lambda}(k)\equiv\mp\frac{\lambda}{6\pi^2}\mathfrak{A}_\lambda(k)\ ,$$

where the dimensionless function $\mathfrak{A}_\lambda(k)$, which can be read off from Eq. (3.102), is positive definite and increases monotonically as a_0, hence k/H_{i0}, increases. Thus, for the $+$ $(-)$ sign choice in potential (3.3), the $\mathcal{O}(\lambda)$ correction $\alpha_{\delta\bar{\varphi}_\lambda}(k)$ enhances (reduces) the $\alpha_{\delta\bar{\varphi}_0}(k)$, the negative running in the noninteracting limit.

3.6 Comparison of Our Predictions for the $n_{\delta\varphi}$ and $\alpha_{\delta\varphi}$ with Measurements

In this section, we compare the measurements for the n and α given by the Planck 2018 Collaboration presented in Table 2.1 of Sec. 2 with our predictions for the $n_{\delta\varphi}$ and $\alpha_{\delta\varphi}$ of the inflaton fluctuations. We estimate the $n_{\delta\bar{\varphi}}$ and $\alpha_{\delta\bar{\varphi}}$ for the inflaton using Eqs. (3.102) and (3.108) for $a_0(t_k)=e^{50}$ and three different ε_{i0} given in Table 3.1. The values for ε_{i0}, which are typical for slow-roll inflation, are chosen to yield the

Table 3.1 : Predictions for the $n_{\delta\varphi}$ and $\alpha_{\delta\varphi}$ of the inflaton.

	Predictions	
Parameter ε_{i0}	$n_{\delta\bar{\varphi}}$	$\alpha_{\delta\bar{\varphi}}$
0.003164	$0.9647\mp\lambda\left(13.762\frac{\pi}{GH_{i0}^2}+2.013\right)$	$-0.0012\mp\lambda\left(0.701\frac{\pi}{GH_{i0}^2}+0.125\right)$
0.003189	$0.9639\mp\lambda\left(13.957\frac{\pi}{GH_{i0}^2}+2.049\right)$	$-0.0013\mp\lambda\left(0.730\frac{\pi}{GH_{i0}^2}+0.130\right)$
0.003128	$0.9658\mp\lambda\left(13.499\frac{\pi}{GH_{i0}^2}+1.963\right)$	$-0.0012\mp\lambda\left(0.661\frac{\pi}{GH_{i0}^2}+0.119\right)$

same measured mean values for the $n_{\delta\bar{\varphi}}$ given in Table 2.1. [Recall that $\lambda<10^{-14}$.] The predicted values for the $\alpha_{\delta\bar{\varphi}}$ in Table 3.1, corresponding to the chosen ε_{i0} values, are within the measured range provided by the Planck 2018 Collaboration, given in the corresponding column of Table 2.1. Considering the fact that the values for ε_{i0} that would yield the measured lower and upper bounds of $n_{\delta\bar{\varphi}}$ extend the range of prediction for the $\alpha_{\delta\bar{\varphi}}$ in each data set we safely conclude that the predictions for $\alpha_{\delta\bar{\varphi}}$ are in accordance with the observations. [Consider the first data set which allows an $n_{\delta\varphi}\in[0.9603,0.9691]$. This constraint, when imposed in Eq. (3.102), implies

$\varepsilon_{i0} \in [0.00301, 0.00329]$. This range of ε_{i0}, when used in Eq. (3.108), predicts an $\varepsilon_{i0} \in [-0.00158, -0.00095]$. The intersection of this predicted range with the observed constraint on the $\alpha_{\delta\varphi_0}$ is the nonempty set $\alpha_{\delta\bar{\varphi}_0} \in [-0.00158, -0.0012]$. The subset $\varepsilon_{i0} \in [0.00301, 0.00329]$ yields such an interval for the $\alpha_{\delta\bar{\varphi}_0}$ via Eq. (3.108).] Thus, compared to the spectator scalar model of Sec. 2, data favor the inflaton model.

The next section is on some unclarified issues that we have attempted to solve related to the content of this thesis. Recall that, to compute the quantum corrected two-point correlation function, we used Starobinsky's formalism which gives the leading dominant terms at each perturbative order, but misses the suppressed subdominant terms. Estimating the deviation of our two-point correlation function—and hence, of our power spectrum—from the yet unknown exact result is an open problem that we address first, in the next section. We suggest to obtain the deviation in a simpler model, considering a MMC scalar with a quartic self-interaction in de Sitter spacetime which, however, as it turnes out, still to be hard enough to reach a conclusion. Hence, we are unable to give the fully renormalized quantum corrected power spectrum using the first definition (1.2) as a Fourier transform of the quantum corrected two-point correlation function, even in this simpler model. We, however, in this model, compute the fully renormalized one-loop corrected power spectrum using the second definition (1.4) as the norm square of the one-loop corrected mode function, and compare it with our stochastic power spectrum which is based, however, on the first—not the second—definition.

4. OPEN ISSUES RELATED TO THE CONTENT OF THE THESIS

Recall that, as pointed out in the Introduction, the quantum corrected power spectrum can be defined in two different ways: either (i) via the Fourier transform the quantum corrected two-point correlation function (Eq. (1.2)) or (ii) via the norm square of the quantum corrected mode function (Eq. (1.4)). However, computing the fully renormalized, quantum corrected, two-point correlation function or mode function applying the SK formalism in the models we consider in Secs. 2 [56] and 3 [57] are, yet unaccomplished, difficult problems. We, therefore, applied the Starobinsky's stochastic formalism to compute the quantum corrected two-point correlation function and adapted definition (i) to get the stochastic contributions to the quantum corrected power spectrum. Starobinsky's formalism is an approximation which gives the leading dominant terms but misses the suppressed subdominant terms, at each perturbative order. To estimate deviations of the stochastic two-point correlation function and the stochastic power spectrum from the exact results are open problems that we attempted to solve. Because, the models we considered are complicated enough due to the notorious mass term (and also due to the time dependent H in the inflaton model in Sec. 3) we consider a simpler model: MMC scalar with a quartic self-interaction during de Sitter inflation, in this section. To estimate deviation of the stochastic two-point correlation function in this simpler model [67] from the exact result, we attempt to compute the fully renormalized one-loop correlator using the SK formalism in Sec. 4.2. We succeed in reducing the computation into the evaulation of four integrals and evaulated one of them. The result however is too long to give in this thesis. Actually, this example explicitly shows how hard it is to compute the exact fully renormalized correlation function using the SK formalism and explains why nobody has calculated it in the models we considered in this thesis. Another open issue, that we address in Sec. 4.2 is an explicit computation which shows the difference between the two alternative definitions of the quantum corrected power spectrum. As we pointed out, it is too difficult to obtain the exact fully renormalized quantum corrected power spectrum, even for a MMC scalar with a quartic self-interaction via the first definition which involves the fully renormalized two-point correlation function. We, however, obtain the one-loop corrected power spectrum for the MMC using the second definition which involves the norm square of the quantum corrected mode function and compare it with the stochastic power spectrum [56] which is based, however, on the first—not on the second—definition.

4.1 The Model

We consider a MMC scalar with a quartic self-interaction in a locally de Sitter background. It is more convenient to work in conformal coordinates $(\eta,\vec{x})$ for which the components of the metric tensor $g_{\mu\nu}(\eta,\vec{x})=a^2(\eta)\eta_{\mu\nu}$ where $a(\eta)=-\frac{1}{H\eta}$ and $\eta_{\mu\nu}$ denotes the components of Minkowski metric. Since $a(\eta)=a(t)=e^{Ht}$, the conformal time η is related to comoving time t as $\eta=-\frac{e^{-Ht}}{H}$, hence, $t=\frac{\ln(a(\eta))}{H}$. The bare Lagrangian density of the model

$$\mathcal{L}=-\frac{1}{2}\partial_\mu\Phi_0\partial_\nu\Phi_0 g^{\mu\nu}\sqrt{-g}-\frac{\xi_0}{2}\Phi_0^2R\sqrt{-g}-\frac{\lambda_0}{4!}\Phi_0^4\sqrt{-g}, \tag{4.1}$$

where Φ is the bare field and $R=D(D-1)H^2$ is the Ricci scalar. The ξ_0 denotes bare conformal coupling constant which we force to vanish upon renormalization so that the coupling of the scalar is minimal, and the λ_0 stands for the bare four-point coupling constant. The renormalization procedure begins by expressing the bare field in terms of the renormalized field as $\Phi\equiv\sqrt{Z}\phi$. Inserting this into bare Lagrangian (4.1) gives

$$\mathcal{L}=-\frac{Z}{2}\partial_\mu\phi\,\partial_\nu\phi\,g^{\mu\nu}\sqrt{-g}-\frac{Z\xi_0}{2}\phi^2R\sqrt{-g}-\frac{\lambda_0Z^2}{4!}\phi^4\sqrt{-g}\,. \tag{4.2}$$

Next, we enforce the condition that the renormalized scalar ϕ should have no conformal coupling: $Z\xi_0\equiv 0+\delta\xi$. Note that even though the renormalized conformal coupling is zero, a conformal counterterm $\delta\xi$ is required. We also define $Z^2\lambda_0\equiv\lambda+\delta\lambda$, where λ is the renormalized four-point coupling and $\delta\lambda$ is the associated counterterm and $Z\equiv 1+\delta Z$, where δZ is the field strength counterterm. The renormalized Lagrangian density is achieved when we express the $\mathcal{L}$ in Eq. (4.2) in terms of the renormalized parameters and counterterms:

$$\mathcal{L}=-\frac{1+\delta Z}{2}\partial_\mu\phi\,\partial_\nu\phi\,g^{\mu\nu}\sqrt{-g}-\frac{\delta\xi}{2}\phi^2R\sqrt{-g}-\frac{\lambda+\delta\lambda}{4!}\phi^4\sqrt{-g}\,. \tag{4.3}$$

In the next section, we attempt to compute the fully renormalized one-loop corrected correlation function using the SK formalism.

4.2 Exact Quantum Corrected Power Spectrum via the Correlation Function

Recall that, the first definition of the quantum corrected power spectrum via the quantum corrected correlation function is given in Eq. (1.2) which implies

$$P_{\phi}(\eta,k) = \int d^3x e^{i\vec{k}(\vec{x}-\vec{0})} \langle\Omega|\phi(\eta,\vec{x})\phi(\eta,\vec{0})|\Omega\rangle. \tag{4.4}$$

Therefore, to compute the power spectrum at one-loop order we need the one-loop corrected two-point correlation function

$$\begin{aligned} &\langle\Omega|\phi(x)\phi(x')|\Omega\rangle \\ &= \langle\Omega|\phi(x)\phi(x')|\Omega\rangle_{\text{tree}} + \langle\Omega|\phi(x)\phi(x')|\Omega\rangle_{1-\text{loop}} + \mathcal{O}(\lambda^2). \end{aligned} \tag{4.5}$$

We obtain the tree-order correlator in Sec. 4.2.1 and work out the one-loop correlator in Sec. 4.2.2 applying the SK formalism.

4.2.1 Tree-Order Correlator

The tree-order correlator

$$\langle\Omega|\phi(x)\phi(x')|\Omega\rangle_{\text{tree}} = \langle\Omega|\phi_0(x)\phi_0(x')|\Omega\rangle, \tag{4.6}$$

is expressed, using the free field mode expansion (2.29) in Eq. (4.6), as

$$\langle\Omega|\phi_0(x)\phi_0(x')|\Omega\rangle = \int \frac{d^{D-1}k}{(2\pi)^{D-1}} u_0(\eta,k) u_0^*(\eta',k) e^{i\vec{k}.(\vec{x}-\vec{x}')}. \tag{4.7}$$

In $D=4$, upon azimuthal angular integration, Eq. (4.7) yields

$$\begin{aligned} \langle\Omega|\phi_0(x)\phi_0(x')|\Omega\rangle &= \int_0^{\infty} \frac{dk}{(2\pi)^2} k^2 u_0(\eta,k) u_0^*(\eta',k) \int_{-1}^{1} d(\cos\theta) e^{ik\Delta x\cos(\theta)}, \\ &= \int_0^{\infty} \frac{dk}{k} \frac{k^3}{2\pi^2} u_0(\eta,k) u_0^*(\eta',k) \frac{\sin(k\Delta x)}{k\Delta x}, \end{aligned} \tag{4.8}$$

where the mode function in the massless limit is

$$u_0(\eta,k) = \frac{H}{\sqrt{2k^3}}(1+ik\eta)e^{-ik\eta}. \tag{4.9}$$

Therefore,

$$\begin{aligned} &\langle\Omega|\phi_0(x)\phi_0(x')|\Omega\rangle \\ &= \frac{H^2}{4\pi^2}\frac{1}{\Delta x}\left[\eta\eta'\int_0^{\infty} dk e^{-ik|\Delta\eta|}\sin(k\Delta x) + \int_0^{\infty}\frac{dk}{k^2}(1+ik|\Delta\eta|)e^{-ik|\Delta\eta|}\sin(k\Delta x)\right], \end{aligned} \tag{4.10}$$

where $\Delta\eta \equiv \eta - \eta'$ and $\Delta x \equiv ||\vec{x} - \vec{x}'||$. The results of the integrals in Eq. (4.10) are given in Ref. [69].

The first integral in Eq. (4.10) can be evaluated by replacing $|\Delta\eta| \to |\Delta\eta| - i\varepsilon$ to ensure the convergence of the integral at $k = \infty$—due to the damping factor $e^{-\varepsilon k}$—and using the Euler's formula $\sin(k\Delta x) = \frac{1}{2i}[e^{ik\Delta x} - e^{-ik\Delta x}]$ in the integrand. The result of the first integral is

$$\int_0^\infty dk e^{-ik(|\Delta\eta| - i\varepsilon)} \sin(k\Delta x) = \frac{\Delta x}{(x - x')^2}, \tag{4.11}$$

where [69]

$$(x - x')^2 \equiv \Delta x^2 - (|\Delta\eta| - i\varepsilon)^2. \tag{4.12}$$

The second integral in Eq. (4.10) can again be evaluated by replacing $|\Delta\eta| \to |\Delta\eta| - i\varepsilon$ in the exponential and using the technique of integration by parts. Note that the IR divergence coming from the lower limit of the integration $k = 0$ is not physical. It is due to the infinite size universe imposed by the continuous integral approximation to the mode sum over discrete momenta we discussed in Sec. 2. The lower limit is, therefore, regulated to k_0 in the integral approximation to the mode sum. The value of k_0 can be taken as the curvature scale $1/R$. The result of the second integral is

$$\begin{aligned} &\int_{k_0}^\infty \frac{dk}{k^2}(1 + ik|\Delta\eta|) e^{-ik(|\Delta\eta| - i\varepsilon)} \sin(k\Delta x) \\ &= \Delta x \left[1 - \frac{1}{2}\Big[\mathrm{Ei}[ik_0(\Delta x - |\Delta\eta| + i\varepsilon)] + \mathrm{Ei}[-ik_0(\Delta x + |\Delta\eta| - i\varepsilon)]\Big]\right], \end{aligned} \tag{4.13}$$

where $\mathrm{Ei}(x)$ is the exponential integral function defined in Eq. (A.1). In obtaining Eq. (4.13), we used

$$\int \frac{dk}{k} e^{-ik(|\Delta\eta| - i\varepsilon)} \cos(k\Delta x) = \frac{1}{2}\Big[\mathrm{Ei}[ik(\Delta x - |\Delta\eta| + i\varepsilon)] + \mathrm{Ei}[-ik(\Delta x + |\Delta\eta| - i\varepsilon)]\Big]. \tag{4.14}$$

Employing the small argument limit (A.2) of the exponential integral function in Eq. (4.13), we obtain the tree-order correlator, in this limit, as

$$\begin{aligned} &\langle\Omega|\phi_0(x)\phi_0(x')|\Omega\rangle \\ &= \frac{H^2}{4\pi^2}\left[\frac{\eta\eta'}{(x - x')^2} - \frac{1}{2}\ln\Big[{k_0}^2(x - x')^2\Big] - \gamma + 1\right]. \end{aligned} \tag{4.15}$$

Employing large argument limit (A.3) of the exponential integral function, we obtain the tree-order correlator, in this limit, as

$$
\begin{aligned}
&\langle\Omega|\phi_0(x)\phi_0(x')|\Omega\rangle \\
&=\frac{H^2}{4\pi^2}\Bigg[\frac{\eta\eta'}{(x-x')^2}-\frac{1}{2}\Big[\frac{\sin(k_0(\Delta x-|\Delta\eta|+i\varepsilon))}{k_0(\Delta x-|\Delta\eta|+i\varepsilon)}+\frac{\sin(k_0(\Delta x+|\Delta\eta|-i\varepsilon))}{k_0(\Delta x+|\Delta\eta|-i\varepsilon)} \\
&\quad -i\Big(\frac{\cos(k_0(\Delta x-|\Delta\eta|+i\varepsilon))}{k_0(\Delta x-|\Delta\eta|+i\varepsilon)}-\frac{\cos(k_0(\Delta x+|\Delta\eta|-i\varepsilon))}{k_0(\Delta x+|\Delta\eta|-i\varepsilon)}\Big)\Big]+1\Bigg]. \qquad (4.16)
\end{aligned}
$$

Next, we compute the one-loop quantum correction to the tree-order correlator.

4.2.2 One-Loop Correlator

The one-loop correlator is depicted in the Feynman diagram given in Fig. 4.1.

Figure 4.1 : One-loop two-point correlator. The $\otimes$ stands for the conformal counterterm vertex. For the $\pm$ polarity it is $\mp\delta\xi R$, respectively.

In the SK formalism the end points of the lines in a Feynman diagram acquire either a + or a − polarity hence, the Feynman propagator $i\Delta(x;x')$ generalizes to four SK propagators: $i\Delta_{++}(x;x')$, $i\Delta_{+-}(x;x')$, $i\Delta_{-+}(x;x')$ and $i\Delta_{--}(x;x')$. Each propagator is obtained from the Feynman propagator by replacing the de Sitter conformal coordinate interval

$$\Delta x^2(x;x')\equiv\Delta x^2_{++}(x;x')=||\vec{x}-\vec{x}'||^2-(|\eta-\eta'|-i\delta)^2, \qquad (4.17)$$

where δ is a small real parameter, in the de Sitter length function

$$y(x;x')=aa'H^2\Delta x^2(x;x'), \qquad (4.18)$$

in the propagator, where $a\equiv a(\eta)$ and $a'\equiv a(\eta')$, with the appropriate coordinate interval

$$
\begin{aligned}
\Delta x^2_{+-}(x;x')&\equiv||\vec{x}-\vec{x}'||^2-(\eta-\eta'+i\delta)^2=(\Delta x^2_{-+}(x;x'))^*, \\
\Delta x^2_{--}(x;x')&=(\Delta x^2_{++}(x;x'))^*. \qquad (4.19)
\end{aligned}
$$

A vertex can either have a $+$ or a $-$ polarity. A $+$ vertex is the usual one of the Feynman formalism, whereas the $-$ vertex is its conjugate. To apply the dimensional regularization, we express the arbitrary dimension D of spacetime in term of its deviation ε from 4 hence, $D=4-\varepsilon$. The propagator [63, 64] for a MMC scalar can be given as

$$i\Delta(x;x') = A + B + C, \tag{4.20}$$

$$A \equiv \frac{\Gamma(1-\frac{\varepsilon}{2})}{4\pi^{2-\frac{\varepsilon}{2}}} \frac{(aa')^{-1+\frac{\varepsilon}{2}}}{\Delta x^{2-\varepsilon}}, \tag{4.21}$$

$$B \equiv \frac{H^{2-\varepsilon}}{(4\pi)^{2-\frac{\varepsilon}{2}}} \left\{ -\frac{2\Gamma(3-\frac{\varepsilon}{2})}{\varepsilon} \left(\frac{y}{4}\right)^{\frac{\varepsilon}{2}} + \pi \cot\left(\frac{\pi\varepsilon}{2}\right) \frac{\Gamma(3-\varepsilon)}{\Gamma(2-\frac{\varepsilon}{2})} + \frac{\Gamma(3-\varepsilon)}{\Gamma(2-\frac{\varepsilon}{2})} \ln(aa') \right\}, \tag{4.22}$$

$$C \equiv \frac{H^{2-\varepsilon}}{(4\pi)^{2-\frac{\varepsilon}{2}}} \sum_{n=1}^{\infty} \left[\frac{1}{n} \frac{\Gamma(3-\varepsilon+n)}{\Gamma(2-\frac{\varepsilon}{2}+n)} \left(\frac{y}{4}\right)^{n} - \frac{1}{n+\frac{\varepsilon}{2}} \frac{\Gamma(3-\frac{\varepsilon}{2+n})}{\Gamma(2+n)} \left(\frac{y}{4}\right)^{n+\frac{\varepsilon}{2}} \right]. \tag{4.23}$$

The ultimate source of the UV divergences is the powers of $A(x;x')$ term. The $B(x;x')$ term, on the other hand, is not UV divergent by itself: $\lim_{\varepsilon\to 0} B(x;x') = -\frac{H}{8\pi^2} \ln(\frac{\sqrt{e}}{4} H^2 \Delta x^2)$. We must retain $\varepsilon \neq 0$ whenever $B(x;x')$ multiplies at least two powers of $A(x;x')$. The $C(x;x')$ term vanishes for $\varepsilon = 0$. We only need it when it is multiplied by more than two powers of $A(x;x')$ which does not happen in this computation since the maximum number of propagators we have in Fig. 4.1 is three. The one-loop correlator in the SK formalism can, therefore, be expressed as a spacetime integral in terms of the propagators $i\Delta$ and the conformal counterterm vertex $\delta\xi$ with appropriate polarities as,

$$\langle\Omega|\phi(x)\phi(x')|\Omega\rangle_{1-\text{loop}} = \int d^D z a^D(z) \left\{ \begin{array}{l} i\Delta_{++}(x;z) \left[\frac{(-i\lambda)}{2} i\Delta_{++}(z;z) - i\delta\xi R \right] i\Delta_{++}(z;x') \\ -i\Delta_{+-}(x;z) \left[\frac{(-i\lambda)}{2} i\Delta_{--}(z;z) - i\delta\xi R \right] i\Delta_{-+}(z;x') \end{array} \right\}. \tag{4.24}$$

The coincidence limit of propagator (4.20) for any polarity is

$$i\Delta(x';x') = \lim_{x\to x'} i\Delta(x;x') = \frac{H^{2-\varepsilon}}{(4\pi)^{2-(\varepsilon/2)}} \frac{\Gamma(3-\varepsilon)}{\Gamma(2-(\varepsilon/2))} \left\{ 2\ln(a) + \pi \cot(\frac{\pi\varepsilon}{2}) \right\}. \tag{4.25}$$

The conformal counterterm is chosen as

$$\delta\xi = -\frac{\lambda H^{2-\varepsilon}}{2^{5-\varepsilon}\pi^{2-(\varepsilon/2)}} \frac{\Gamma(3-\varepsilon)}{\Gamma(2-(\varepsilon/2))} R^{-1} \pi \cot(\frac{\pi\varepsilon}{2}), \tag{4.26}$$

to absorb the one-loop coincident UV divergence of the $\frac{-i\lambda}{2} i\Delta(z,z)$ terms in the limit $\varepsilon \to 0$. Substituting Eq. (4.26) into Eq. (4.24), yields

$$\langle\Omega|\varphi(x)\varphi(x')|\Omega\rangle_{1-\text{loop}} = -i\lambda \frac{H^{2-\varepsilon}}{(4\pi)^{2-\frac{\varepsilon}{2}}} \frac{\Gamma(3-\varepsilon)}{\Gamma(2-\frac{\varepsilon}{2})} \int d^D z a^D(z) \ln(a(z)) \left\{ \begin{array}{l} i\Delta_{++}(x;z) i\Delta_{++}(z;x') \\ -i\Delta_{+-}(x;z) i\Delta_{-+}(z;x') \end{array} \right\}, \tag{4.27}$$

which can be recast, employing Eq. (4.20), as

$$\langle\Omega|\varphi(x)\varphi(x')|\Omega\rangle_{1-\mathrm{loop}}=-i\lambda\frac{H^{2-\varepsilon}}{(4\pi)^{2-\frac{\varepsilon}{2}}}\frac{\Gamma(3-\varepsilon)}{\Gamma(2-\frac{\varepsilon}{2})}\sum_{n=1}^{4}I_n(x;x'), \tag{4.28}$$

where,

$$I_n(x;x')\equiv\int d\eta_z a^{4-\varepsilon}(\eta_z)\ln a(\eta_z)\int d^3z F_n(x;x';z). \tag{4.29}$$

The functions $F_n(x;x';z)$ are defined as follows:

$$F_1(x;x')\equiv\frac{\Gamma^2(1-\frac{\varepsilon}{2})}{2^4\pi^{4-\varepsilon}}\frac{(aa')^{-1+\frac{\varepsilon}{2}}}{a(\eta_z)^{2-\varepsilon}}$$
$$\times\Big[\frac{1}{\Delta x_{++}^{2-\varepsilon}(x;z)}\frac{1}{\Delta x_{++}^{2-\varepsilon}(z;x')}-\frac{1}{\Delta x_{+-}^{2-\varepsilon}(x;z)}\frac{1}{\Delta x_{-+}^{2-\varepsilon}(z;x')}\Big], \tag{4.30}$$

$$F_2(x;x')\equiv\frac{-H^2\Gamma(1-\frac{\varepsilon}{2})}{2^5\pi^{4-\frac{\varepsilon}{2}}}\frac{a^{-1+\frac{\varepsilon}{2}}}{a(\eta_z)^{1-\frac{\varepsilon}{2}}}\Big[\frac{\ln(\mu^2\Delta x_{++}^2(z;x'))}{\Delta x_{++}^{2-\varepsilon}(x;z)}-\frac{\ln(\mu^2\Delta x_{-+}^2(z;x'))}{\Delta x_{+-}^{2-\varepsilon}(x;z)}\Big], \tag{4.31}$$

$$F_3(x;x')\equiv\frac{-H^2\Gamma(1-\frac{\varepsilon}{2})}{2^5\pi^{4-\frac{\varepsilon}{2}}}\frac{a'^{-1+\frac{\varepsilon}{2}}}{a(\eta_z)^{1-\frac{\varepsilon}{2}}}\Big[\frac{\ln(\mu^2\Delta x_{++}^2(x;z))}{\Delta x_{++}^{2-\varepsilon}(z;x')}-\frac{\ln(\mu^2\Delta x_{+-}^2(x;z))}{\Delta x_{-+}^{2-\varepsilon}(z;x')}\Big], \tag{4.32}$$

$$F_4(x;x')\equiv\frac{H^4}{2^6\pi^4}\Big[\ln(\mu^2\Delta x_{++}^2(x;z))\ln(\mu^2\Delta x_{++}^2(z;x'))$$
$$-\ln(\mu^2\Delta x_{+-}^2(x;z))\ln(\mu^2\Delta x_{-+}^2(z;x'))\Big], \tag{4.33}$$

where we define $\mu^2\equiv\frac{\sqrt{e}}{4}H^2$. In this section, we consider the integral $I_4(x;x')$ in one-loop correlator (4.27). The final result—even in the equal time limit—however, is too long to give in this thesis.

Since $\Delta x_{++}^2(z;x')=\Delta x_{++}^2(x';z)$ and $\Delta x_{-+}^2(z;x')=\Delta x_{+-}^2(x';z)$, we have

$$I_4(x;x')=\frac{H^4}{2^6\pi^4}\int d\eta_z a^{4-\varepsilon}(\eta_z)\ln(a(\eta_z))\int d^3z\Big[\ln(\mu^2\Delta x_{++}^2(x;z))\ln(\mu^2\Delta x_{++}^2(x';z))$$
$$-\ln(\mu^2\Delta x_{+-}^2(x;z))\ln(\mu^2\Delta x_{+-}^2(x';z))\Big]. \tag{4.34}$$

Using the identity

$$\ln(x\pm i\varepsilon)=\ln(|x|)\pm i\pi\Theta(-x), \tag{4.35}$$

we expand the logarithms in Eq. (4.34) as

$$\ln(\mu^2\Delta x_{++}^2(x;z))=\ln(\mu^2|(\eta-\eta_z)^2-||\vec{x}-\vec{z}||^2|)+i\pi\Theta((\eta-\eta_z)^2-||\vec{x}-\vec{z}||^2), \tag{4.36}$$

$$\ln(\mu^2\Delta x_{++}^2(x';z))=\ln(\mu^2|(\eta'-\eta_z)^2-||\vec{x}'-\vec{z}||^2|)+i\pi\Theta((\eta'-\eta_z)^2-||\vec{x}'-\vec{z}||^2), \tag{4.37}$$

$$\ln(\mu^2\Delta x_{+-}^2(x;z))=\ln(\mu^2|(\eta-\eta_z)^2-||\vec{x}-\vec{z}||^2|)-i\pi\Theta((\eta-\eta_z)^2-||\vec{x}-\vec{z}||^2)$$
$$\times\mathrm{sgn}(\eta-\eta_z), \tag{4.38}$$

$$\ln(\mu^2\Delta x_{+-}^2(x';z))=\ln(\mu^2|(\eta'-\eta_z)^2-||\vec{x}'-\vec{z}||^2|)-i\pi\Theta((\eta'-\eta_z)^2-||\vec{x}'-\vec{z}||^2)$$
$$\times\mathrm{sgn}(\eta'-\eta_z), \tag{4.39}$$

where sgn(x) is the sign function. Substituting Eqs. (4.36)–(4.39) into Eq. (4.34) yields

$$I_4(x;x') = \frac{H^4}{2^6\pi^4}\int_{-\frac{1}{H}}^{0} d\eta_z a^4(z)\ln(a(z))\int d^3z\Big[i\pi\Theta((\eta-\eta_z)^2-||\vec{x}-\vec{z}||^2)$$
$$\times\ln(\mu^2|(\eta'-\eta_z)^2-||\vec{x}'-\vec{z}||^2|)(1+\text{sgn}(\eta-\eta_z))+i\pi\Theta((\eta'-\eta_z)^2-||\vec{x}'-\vec{z}||^2)$$
$$\times\ln(\mu^2|(\eta-\eta_z)^2-||\vec{x}-\vec{z}||^2|)(1+\text{sgn}(\eta'-\eta_z)-\pi^2\Theta((\eta-\eta_z)^2-||\vec{x}-\vec{z}||^2)$$
$$\times\Theta((\eta'-\eta_z)^2-||\vec{x}'-\vec{z}||^2)(1-\text{sgn}(\eta-\eta_z)\text{sgn}(\eta'-\eta_z))\Big]. \tag{4.40}$$

Recall that definition (4.4) of the quantum corrected power spectrum involves only a simultaneous quantum corrected correlation function. We, therefore, consider the equal time limit of $I_4(x;x')$,

$$I_4(x;x') = \frac{iH^4}{2^5\pi^3}\int_{-\frac{1}{H}}^{0} d\eta_z a^4(\eta_z)\ln(a(\eta_z))\Theta(\eta-\eta_z)\int d^3z$$
$$\times\Big[\Theta((\eta-\eta_z)^2-||\vec{x}-\vec{z}||^2)\ln(\mu^2|(\eta-\eta_z)^2-||\vec{x}'-\vec{z}||^2|)+\Theta((\eta-\eta_z)^2-||\vec{x}'-\vec{z}||^2)$$
$$\times\ln(\mu^2|(\eta-\eta_z)^2-||\vec{x}-\vec{z}||^2|)\Big], \tag{4.41}$$

which is simpler to evaulate. Let us start with the first spatial integral. Notice that the second spatial integral is obtained from the first by simply replacing $\vec{x}$ with $\vec{x}'$ and $\vec{x}'$ with $\vec{x}$. Making a change of variable, $\vec{x}-\vec{z}\equiv-\vec{\tilde{z}}$ implies $\vec{x}'-\vec{z}=-\vec{\tilde{z}}-(\vec{x}-\vec{x}')$ and yields

$$\int d^3\tilde{z}\,\Theta((\eta-\eta_z)^2-||\vec{\tilde{z}}||^2)\ln(\mu^2|\,||\vec{\tilde{z}}+(\vec{x}-\vec{x}')||^2-(\eta-\eta_z)^2|). \tag{4.42}$$

To evaluate the angular integrals we take the third axis (i.e., the "z"-axis) of $\vec{\tilde{z}}$ coordinate system parallel to $\vec{x}-\vec{x}'$ hence, the azimuthal integral becomes trivial. Defining $||\vec{\tilde{z}}||=r$ and denoting the angle between the third axis of $\vec{\tilde{z}}$ and $\vec{x}-\vec{x}'$ with the polar angle θ gives

$$2\pi\int dr\,r^2\Theta((\eta-\eta_z)^2-r^2)\int d\theta\sin(\theta)\ln(\mu^2|r^2+\Delta x^2+2r\Delta x\cos(\theta)-(\eta-\eta_z)^2|). \tag{4.43}$$

The absolute value in the argument of the logarithm implies two cases for the polar integration: (i) $\cos(\theta)\geq\frac{(\eta-\eta_z)^2-(r^2+\Delta x^2)}{2r\Delta x}\equiv A$ and (ii) $\cos(\theta)<A$. Hence, the polar integral in Eq. (4.43) can be expressed as

$$\int d\theta\sin(\theta)\Bigg[\Theta\Big(\cos(\theta)-A\Big)\ln(\mu^2(r^2+\Delta x^2+2r\Delta x\cos(\theta)-(\eta-\eta_z)^2))$$
$$+\Theta\Big(A-\cos(\theta)\Big)\ln(-\mu^2(r^2+\Delta x^2+2r\Delta x\cos(\theta)-(\eta-\eta_z)^2))\Bigg]. \tag{4.44}$$

In this thesis, we evaluate the first part in polar integral (4.44) and leave the second part, which can be evaluated similarly, to the reader. Notice that if $A<-1 \Rightarrow \theta_{\min}=0, \theta_{\max}=\pi$ and $\Theta(\cos(\theta)-A)=1$. If, on the other hand, $-1<A<1 \Rightarrow \theta_{\min}=0, \theta_{\max}=\arccos(A)$ and $\Theta(\cos(\theta)-A)=1$. If, however, $A>1 \Rightarrow \Theta(\cos(\theta)-A)=0$. Although we consider the cases separately, we remind the reader that they should be combined via Θ functions.

If $A<-1$, then $(r-\Delta x)^2>(\eta-\eta_z)^2$. Hence, the first part in polar integral (4.44), when combined with the radial integration in Eq. (4.43), becomes

$$2\pi\left[\Theta(\Delta x-2|\eta-\eta_z|)\int_0^{\eta-\eta_z} dr\, r^2+\Theta(\Delta x-(\eta-\eta_z))\Theta(2(\eta-\eta_z)-\Delta x)\int_0^{\Delta x-(\eta-\eta_z)} dr\, r^2\right]$$
$$\times\int_0^{\pi} d\theta \sin(\theta)\ln(\mu^2\left[r^2+\Delta x^2+2r\Delta x\cos(\theta)-(\eta-\eta_z)^2\right]), \tag{4.45}$$

where we used

$$\begin{aligned}\Theta(|\eta-\eta_z|-r)\Theta((r-\Delta x)^2-(\eta-\eta_z)^2)&=\Theta(|\eta-\eta_z|-r)\Theta(\Delta x-|\eta-\eta_z|-r)\\ &=\Theta(\Delta x-2|\eta-\eta_z|)\Theta(|\eta-\eta_z|-r)+\Theta(\Delta x-|\eta-\eta_z|)\Theta(2|\eta-\eta_z|-\Delta x)\\ &\quad\times\Theta(\Delta x-|\eta-\eta_z|-r).\end{aligned} \tag{4.46}$$

The polar and radial integrations in Eq. (4.45) yield

$$\begin{aligned}&-2\pi\Theta(\Delta x-(\eta-\eta_z))\Theta(2(\eta-\eta_z)-\Delta x)\Bigg[\frac{7}{9}(\Delta x-(\eta-\eta_z))\left[\Delta x^2-\frac{17}{7}\Delta x(\eta-\eta_z)+\frac{16}{7}\right.\\ &\left.\times(\eta-\eta_z)^2\right]+\frac{1}{3}(\eta-\eta_z)^3\ln\left(\frac{\eta-\eta_z}{\Delta x}\right)^2-\frac{2}{3}\left[(\Delta x-(\eta-\eta_z))^3\ln\left(4\mu^2\Delta x(\Delta x-(\eta-\eta_z))\right)\right]\Bigg]\\ &+2\pi\Theta(\Delta x-2(\eta-\eta_z))\Bigg[\frac{(\eta-\eta_z)}{6}\left[\Delta x^2-\frac{32}{3}(\eta-\eta_z)^2\right]+\frac{\Delta x}{24}\left[\Delta x^2-12(\eta-\eta_z)^2\right]\\ &\times\ln\left(\frac{\Delta x-2(\eta-\eta_z)}{\Delta x+2(\eta-\eta_z)}\right)+\frac{2}{3}(\eta-\eta_z)^3\ln\left(\mu^2((\Delta x)^2-4(\eta-\eta_z)^2)\right)\Bigg].\end{aligned} \tag{4.47}$$

We obtained the temporal integration of this result, as required in Eq. (4.43). The result however, is too long to give here.

If $-1\le A\le 1$, then the first part in polar integral (4.44), when combined with the radial integration in Eq. (4.43) becomes

$$2\pi\left[\Theta(\Delta x-(\eta-\eta_z))\Theta(2(\eta-\eta_z)-\Delta x)\int_{\Delta x-(\eta-\eta_z)}^{\eta-\eta_z} dr\, r^2+\Theta((\eta-\eta_z)-\Delta x)\right.$$
$$\left.\times\int_{(\eta-\eta_z)-\Delta x}^{\eta-\eta_z} dr\, r^2\right]\int_0^{\arccos(A)} d\theta\sin(\theta)\ln(\mu^2\left[r^2+\Delta x^2+2r\Delta x\cos(\theta)-(\eta-\eta_z)^2\right]), \tag{4.48}$$

where we used

$$\Theta((\eta-\eta_z)-r)\Theta((\eta-\eta_z)^2-(r-\Delta x)^2)\Theta((r+\Delta x)^2-(\eta-\eta_z)^2)$$
$$=\Theta(\Delta x-(\eta-\eta_z))\Theta(2(\eta-\eta_z)-\Delta x)\Theta((\eta-\eta_z)-r)\Theta(r-(\Delta x-(\eta-\eta_z)))$$
$$+\Theta((\eta-\eta_z)-\Delta x)\Theta((\eta-\eta_z)-r)\Theta(r-((\eta-\eta_z)-\Delta x)), \tag{4.49}$$

and

$$\int_0^{\arccos(A)} d\theta\,\sin(\theta)\ln[\mu^2(r^2+\Delta x^2+2r\Delta x\cos(\theta)-(\eta-\eta_z)^2)]$$
$$=-A\ln\left[\frac{\mu^2}{e}((r+\Delta x)^2-(\eta-\eta_z)^2)\right]. \tag{4.50}$$

The polar and radial integrations in Eq. (4.48) yield

$$-2\pi\Theta(\Delta x-(\eta-\eta_z))\Bigg[(2(\eta-\eta_z)-\Delta x)\Big(\frac{125}{144}\Delta x^2-\frac{61}{72}\Delta x(\eta-\eta_z)+\frac{8}{9}(\eta-\eta_z)^2\Big)$$
$$+\frac{2}{3}(\eta-\eta_z)^3\ln(2\mu^2\Delta x^2)+\frac{2}{3}(\Delta x-(\eta-\eta_z))^3\ln\Big(4\mu^2\Delta x(\Delta x-(\eta-\eta_z))\Big)$$
$$-\frac{1}{24}(4(\eta-\eta_z)-\Delta x)(\Delta x+2(\eta-\eta_z))^2\ln\Big(\mu^2\Delta x(\Delta x+2(\eta-\eta_z))\Big)\Bigg]$$
$$+2\pi\Theta((\eta-\eta_z)-\Delta x)\Bigg[\Delta x\Big(\frac{13}{144}\Delta x^2+\frac{1}{12}\Delta x(\eta-\eta_z)-\frac{13}{12}(\eta-\eta_z)^2\Big)$$
$$+\frac{1}{24}(4(\eta-\eta_z)-\Delta x)(\Delta x+2(\eta-\eta_z))^2\ln\Big(\mu^2\Delta x(\Delta x+2(\eta-\eta_z))\Big)$$
$$-\frac{1}{3}(\eta-\eta_z)^3\ln\Big(4\mu^4\Delta x^2(\eta-\eta_z)^2\Big)\Bigg]. \tag{4.51}$$

We also obtained the temporal integration of this result, as required in Eq. (4.43). As for Eq. (4.41), the result is too long to give here. (Note that if $A>1$, the integral vanishes as we pointed out already.)

We have not yet evaulated the integrals I_1, I_2 and I_3 in the one-loop correlator. The computation of I_4 that we outlined in this section shows how tedious and lengthy it is to compute the one-loop correlator and hence, the power spectrum defined via the correlation function (Eq. (4.4)) applying the SK formalism. The method we introduced in Secs. 2 and 3 to obtain the stochastic contributions to the quantum corrected correlation function and power spectrum is a shortcut which gives the leading terms at each loop order, bypassing the difficulties of the exact computation. In the next section, we compute the exact one-loop corrected power spectrum via the alternative definition in terms of the norm square of the one-loop corrected mode function.

4.3 Exact Quantum Corrected Power Spectrum via the Mode Function

As is pointed out in the Introduction, there is an alternative measure of quantum corrected power spectrum as an amplitude (norm of the mode function) square of the fluctuations. Recall that both definitions agree with each other at tree-order: they both measure the dependence of amplitude square of fluctuations on the wavelengths of the fluctuations. However, the alternative definitions yield different quantum corrections. As we have shown in Sec. 4.2, the computation of exact quantum corrected power spectrum—even in a simple model like MMC scalar with quartic self-interaction in de Sitter spacetime—via the first definition, i.e., as a Fourier transform of quantum corrected correlation function, is too difficult to obtain. The second definition of quantum corrected power spectrum via the quantum corrected mode function given in Eq. (1.4),

$$P_{\phi}(t,k) = |u(t,k)|^2 \; , \tag{4.52}$$

therefore, provides an opportunity to compute the exact quantum corrected power spectrum for the MMC scalar we consider in this section. Let us note here that computing the power spectrum for the massive scalar fields we consider in Secs. 2 and 3 via the second definition is not an easy task since one needs to compute the quantum corrected mode functions for the scalars.

The quantum corrected mode function for the MMC scalar [59] is the amplitude of the spatial plane wave solution of the linearized effective field equation

$$\partial_{\mu}(\sqrt{-g}g^{\mu\nu}\partial_{\nu}\phi_0(x)) = \int_{\eta_i}^{0} d\eta' \int d^3x' \mathrm{M}^2(x;x')\phi_0(x',\vec{k}) \; , \tag{4.53}$$

of the form

$$\phi(x,\vec{k}) = u(\eta,k)e^{i\vec{k}.\vec{x}} = \sum_{\ell=0}^{\infty} \lambda^{\ell} u_{\ell}(\eta,k) e^{i\vec{k}.\vec{x}} \; . \tag{4.54}$$

The self-mass squared in Eq. (4.53),

$$\mathrm{M}^2(x;x') = \sum_{\ell=0}^{\infty} \lambda^{\ell} \mathcal{M}^2_{\ell}(x;x') \; , \tag{4.55}$$

where

$$\mathcal{M}^2_0(x;x') = 0 \; , \tag{4.56}$$

and

$$\mathcal{M}_1^2(x;x') = \frac{H^2}{8\pi^2} a^4 \ln(a) \delta^4(x-x') \; . \tag{4.57}$$

Substituting Eqs. (4.53) and (4.54) into Eq. (4.55) yields

$$a^2(\partial_0^2 + 2Ha\partial_0 + k^2) u_\ell(\eta,k) = -\sum_{n=0}^{\ell} \int_{\eta_i}^{0} d\eta' \int d^3x' \mathcal{M}_n^2(x;x') u_{\ell-n}(\eta',k) e^{i\vec{k}.(\vec{x}-\vec{x}')} \; . \tag{4.58}$$

Converting Eq. (4.58) from conformal time to comoving time we find

$$\Big[\frac{\partial^2}{\partial t^2} + 3H\frac{\partial}{\partial t} + \frac{k^2}{a^2}\Big] u_\ell = -\frac{1}{a^4} \sum_{n=0}^{\ell} \int_{\eta_i}^{0} d\eta' \int d^3x' \mathcal{M}_n^2(x;x') u_{\ell-n}(\eta',k) e^{-i\vec{k}.(\vec{x}-\vec{x}')} \; . \tag{4.59}$$

We give the tree-order mode function u_0 in Sec. 4.3.1 and obtain the one-loop mode function u_1 in Sec. 4.3.2.

4.3.1 Tree-Order Mode Function

The tree-order mode function is the solution of Eq. (4.59) for $\ell = 0$:

$$u_0(t,k) = \frac{H}{\sqrt{2k^3}} \Big[1 - \frac{ik}{Ha}\Big] e^{\frac{ik}{Ha}} \; , \tag{4.60}$$

which is the well known Bunch-Davies mode function given in Eq. (4.60).

4.3.2 One-Loop Mode Function

The one-loop mode function is the solution of Eq. (4.58) for $\ell = 1$, that is

$$\Big[\frac{\partial^2}{\partial t^2} + 3H\frac{\partial}{\partial t} + \frac{k^2}{a^2}\Big] u_1 = -\frac{H^2}{8\pi^2} u_0(\eta,k) \ln(a') \; . \tag{4.61}$$

A solution [59] of Eq. (4.61) can be given as

$$u_1(t,k) = -\frac{H^2}{8\pi^2} \int_0^t dt' G(t,t';k) u_0(\eta',k) \ln(a(\eta')) \; , \tag{4.62}$$

where the retarded Green's function

$$G(t,t',k) = \frac{\Theta(t-t')}{W(t',k)} \Big[u_0(t,k) u_0^*(t',k) - u_0^*(t,k) u_0(t',k)\Big]. \tag{4.63}$$

Here, the Wronskian

$$W(t',k) = u_0(t',k) \dot{u}_0^*(t',k) - u_0^*(t',k) \dot{u}_0(t',k) = -\frac{i}{a'^3}. \tag{4.64}$$

Hence, the one-loop correction can be given as

$$u_1(t,k) = -\frac{iH^3}{16\pi^2 k^3} \Big[u_0(t,k) \mathcal{F}(a,k) - u_0^*(t,k) \mathcal{G}(a,k)\Big], \tag{4.65}$$

where we define

$$\mathcal{F}(a,k) \equiv \int_1^a da' \ln a' \left[a'^2 + \frac{k^2}{H^2}\right] = \frac{a^3}{3}\left[\ln a - \frac{1}{3}\right] + \frac{1}{9} + \left(\frac{k}{H}\right)^2 [a \ln a - a + 1], \quad (4.66)$$

$$\mathcal{G}(a,k) \equiv \int_1^a da' \ln a' \left[a' - \frac{ik}{H}\right]^2 e^{\frac{i2k}{Ha'}} \quad (4.67)$$

$$\begin{aligned} &\equiv \frac{a}{3} e^{\frac{i2k}{Ha}} \left[a\left[\ln a - \frac{1}{3}\right]\left[a - i\frac{2k}{H}\right] + \left(\frac{k}{H}\right)^2 \left[\ln a - \frac{7}{3}\right]\right] + \frac{1}{9} e^{\frac{i2k}{H}} \left[1 - i\frac{2k}{H} + 7\left(\frac{k}{H}\right)^2\right] \\ &\quad - \frac{i}{3}\left(\frac{k}{H}\right)^3 \left[\ln^2 a + 2\ln a\left[\mathrm{ci}\left(\frac{2k}{aH}\right) - \ln\left(\frac{2k}{H}\right) - \gamma + i\left[\frac{\pi}{2} + \mathrm{si}\left(\frac{2k}{aH}\right)\right]\right]\right. \\ &\quad \left. - \frac{14}{3}\left[\mathrm{ci}\left(\frac{2k}{aH}\right) - \mathrm{ci}\left(\frac{2k}{H}\right) + i\left(\mathrm{si}\left(\frac{2k}{aH}\right) - \mathrm{si}\left(\frac{2k}{H}\right)\right)\right]\right] \\ &\quad + \frac{4}{3}\left(\frac{k}{H}\right)^4 \left[\frac{1}{a}\, {}_3\mathcal{F}_3\left(1,1,1;2,2,2;\frac{i2k}{aH}\right) - {}_3\mathcal{F}_3\left(1,1,1;2,2,2;\frac{i2k}{H}\right)\right]. \end{aligned} \quad (4.68)$$

Hence, the one-loop corrected mode function $u(t,k) = u_0(t,k) + \lambda u_1(t,k) + \mathcal{O}(\lambda^2)$ implies

$$P_\phi(t,k) = |u(t,k)|^2 = |u_0(t,k)|^2 + \lambda\left[u_0(t,k)u_1^*(t,k) + u_0^*(t,k)u_1(t,k)\right] + O(\lambda^2). \quad (4.69)$$

Using Eqs. (4.60) and (4.65) in Eq. (4.69), we find

$$P_\phi(t,k) = |u_0(t,k)|^2 - \lambda\frac{H^3}{8\pi^2 k^3}\mathrm{Im}\left[u_0^{*2}(t,k)\mathcal{G}(a,k)\right] + \mathcal{O}(\lambda^2). \quad (4.70)$$

Thus, the one-loop corrected normalized power spectrum

$$\Delta_\phi^2(t,k) = \frac{k^3}{2\pi^2} P_\phi(t,k) = \frac{k^3}{2\pi^2}|u(t,k)|^2, \quad (4.71)$$

is obtained as

$$\begin{aligned} \Delta_\phi^2(t,k) &= \frac{H^2}{4\pi^2}\left\{1 + z^2 - \frac{\lambda}{6\pi^2}\left[\ln(a) - \frac{4}{3} + \frac{a^{-1}}{6}\left(7 + a^{-1} + (1-a)a^{-2}z^{-2}\right)\cos[2(1-a)z]\right.\right. \\ &\quad - \frac{a^{-1}z^{-1}}{12}\left(7(1-z^2) + 4a^{-1} - a^{-2}(1-z^{-2})\right)\sin[2(1-a)z] + \left[\left(\frac{1-z^2}{2}\right)\cos[2z]\right. \\ &\quad \left. + z\sin[2z]\right]\left[\frac{\ln^2(a)}{2} - \ln(a)\left(\mathrm{ci}(2z) - \ln(2z) - \gamma\right) - \frac{7}{3}\left(\mathrm{ci}(2az) - \mathrm{ci}(2z)\right) - 2az\right. \\ &\quad \left. \times\left[\left(g(2az) - \frac{g(2z)}{a}\right) - \left(h(2az) - \frac{h(2z)}{a}\right)\right]\right] - \left[\left(\frac{1-z^2}{2}\right)\sin(2z) - z\cos(2z)\right]\left[\ln(a)\right. \\ &\quad \left.\left.\left. \times\left(\mathrm{si}(2z) + \frac{\pi}{2}\right) + \frac{7}{3}(\mathrm{si}(2az) - \mathrm{si}(2z)) - 2az\left(f(2az) - \frac{f(2z)}{a}\right)\right]\right]\right\} + \mathcal{O}(\lambda^2), \end{aligned} \quad (4.72)$$

where we define $z \equiv \frac{k}{aH}$ and

$$
\begin{aligned}
f(z) &= \sum_{n=0}^{\infty} \frac{(-1)^n}{(2n+1)^3} \frac{z^{2n}}{(2n)!} = {}_2\mathcal{F}_3\left(\frac{1}{2}, \frac{1}{2}; \frac{3}{2}, \frac{3}{2}, \frac{3}{2}; -\left(\frac{z}{2}\right)^2\right), \\
g(z) &= \sum_{n=0}^{\infty} \frac{1}{(4n+2)^3} \frac{z^{4n+1}}{(4n+1)!} = \frac{z}{8}\, {}_2\mathcal{F}_5\left(\frac{1}{2}, \frac{1}{2}; \frac{3}{4}, \frac{5}{4}, \frac{3}{2}, \frac{3}{2}, \frac{3}{2}; \left(\frac{z}{4}\right)^4\right), \\
h(z) &= \sum_{n=0}^{\infty} \frac{1}{(4n+4)^3} \frac{z^{4n+3}}{(4n+3)!} = \frac{4}{3}\left(\frac{z}{8}\right)^3 {}_3\mathcal{F}_6\left(1, 1, 1; \frac{5}{4}, \frac{3}{2}, \frac{7}{4}, 2, 2, 2; \left(\frac{z}{4}\right)^4\right) .
\end{aligned}
\tag{4.73}
$$

Note that for the superhorizon modes $k_{\text{phys}} = \frac{k}{a} < H$ we have $z < 1$. Therefore, using the small argument expansions of the $\text{ci}(x)$ and $\text{si}(x)$ functions given in Eqs. (A.10) and (A.12) in Eq. (4.72) yields the power spectrum of the superhorizon modes at late times (large a), up to $\mathcal{O}(\lambda^2)$, as

$$
\begin{aligned}
\Delta^2_\phi(t,k) \to \frac{H^2}{4\pi^2} \Bigg\{ 1 - \frac{\lambda}{24\pi^2} \Bigg[& \ln^2(a) - \frac{2\ln(a)}{3} - \frac{16}{3} - \frac{14}{3}\left(\text{ci}\left(\frac{2k}{H}\right) - \ln\left(\frac{2k}{H}\right) - \gamma\right) + \frac{2}{3}\left(\frac{k}{H}\right)^{-1} \\
\times \left[\frac{1}{2}\left(7 + \left(\frac{k}{H}\right)^{-2}\right) \sin\left(\frac{2k}{H}\right) - \left(\frac{k}{H}\right)^{-1} \cos\left(\frac{2k}{H}\right)\right] & - 4\frac{k}{H}\left(g\left(\frac{2k}{H}\right) - h\left(\frac{2k}{H}\right)\right)\Bigg]\Bigg\} .
\end{aligned}
\tag{4.74}
$$

Equation (4.72) is the exact one-loop corrected power spectrum, defined as the norm square of one-loop corrected mode function, for the MMC scalar in our model. Since we have not yet completed the computation of the one-loop corrected power spectrum defined as the Fourier transform of the one-loop corrected two-point correlation function in the same model, estimating the numerical difference between the two definitions remains as an unsolved issue to be investigated further. The conclusions we reached in this thesis are outlined in the following section.

5. CONCLUSIONS

According to modern cosmology, the origin of structure (galaxies, stars, planets, us, etc.) is the quantum fluctuations of a scalar field during an inflationary phase of cosmic expansion when the universe was about $10^{-36}-10^{-34}$ sec. old. In such a brief time, our observable universe expanded by at least e^{60} folds. Meanwhile, the virtual particles of the scalar field that emerged out of vacuum persisted longer and, therefore, caused random fluctuations in the field strength in different regions of spacetime, displaying enhanced quantum effects. The fluctuations in the field strength, and hence in energy density, in different regions caused different local expansion rates and, therefore, created wrinkles (potential wells) in the fabric of spacetime which later served as a scaffolding for the structure formation in the universe. First, cold dark matter clumped in the wrinkles and then, after recombination, pulled in baryons and CMB photons by gravitational attraction to form structure in the universe. The observed large scale CMB anisotropy on the sky is, in fact, the amplified imprint of the inflationary scalar field fluctuations. Therefore, it is important to study the correlations and power spectrum of the fluctuations—basically the origin of everything—to predict the cold dark matter distribution and understand the large scale structure in the universe. In this thesis, we computed the quantum corrected two-point correlation function and power spectrum Δ^2 of self-interacting spectator scalar and inflaton fields. We also calculated the spectral index n and the running of the spectral index α in the two models and compared our numerical predictions with the cosmological measurements of the Planck 2018 collaboration obtained by analyzing the CMB data.

In Sec. 2, we considered an IR truncated, massive, spectator scalar field $\bar{\phi}(t,\vec{x})$ with a quartic self-interaction $\frac{\lambda}{4!}\phi^4$ during a cosmological constant driven inflation where the expansion rate H is a constant and the background is, therefore, de Sitter spacetime. We were motivated by the fact that the model, on one hand, provides an opportunity to predict the observational characterictics of a scalar that may have existed during inflation without participating in driving the inflation and, on the other hand, it qualitatively mimics the behaviour of a self-interacting inflaton field that actually drives the inflation. The tree-order correlator is positive. At a fixed comoving separation, it asymptotes to a constant at late times, in the massless limit. As the mass increases the constant limits to zero. For a fixed physical distance, it grows like $\ln(a)$ at late times, in the massless limit. This logarithmic growth is suppressed for the massive scalars. As the mass increases, the suppression gets stronger; see Fig. 2.1. Physically, this means that inflationary particle production, which is suppressed as the mass increases, does not continue forever. It comes to a halt eventually, implying that the fluctuations are not of large amplitude that would yield proliferation of ever newer pocket universes. The fluctuations of small amplitude, as in this model, engender the density perturbations, as the scalar rolls down its potential. The one-loop correlator is negative. At a fixed comoving separation, it grows like $-\lambda\ln^2(a)$ at late times, in the massless limit. As the mass increases it limits to zero. For a fixed physical distance, on the other hand, it grows like $-\lambda\ln^2(a)\ln(a')$ at late times, in the massless limit. This growth, however, is suppressed for massive scalars. The suppression is very sensitive to an increase in mass; see Fig. 2.2. In fact, for $m > \frac{H}{2}$, the one-loop correlator asymptotes to zero. Coincidence limit (2.99) of quantum corrected two-point correlation function of the IR truncated field is used to obtain the leading terms in the induced self-mass squared by the curvature of the potential. We estimated upper bounds for the effective mass $m_{\rm eff}$ for the bare masses $m=\frac{H}{2}$ and $m=0$ in Eqs. (2.101) and (2.104), respectively. We also used coincident correlator (2.99) to introduce a method to compute the stochastic contributions to the quantum corrected Δ^2_ϕ, n_ϕ and α_ϕ. They imply that the spectrum of fluctuations is red tilted at tree and one-loop order. The tilt decreases as the mass decreases. In the massless limit, although the tilt vanishes at tree-order and hence, the spectrum is scale invariant, at this order, the one-loop correction red tilts it. Physically, this means that the amplitudes of fluctuations grow toward the larger scales in both the massive and massless cases. We compared our numerical predictions for the n_ϕ and α_ϕ with the measurements of Planck 2018 Collaboration in Sec. 2.6. The observations do not seem to favor the spectator scalar model compared to the inflaton model we consider in Sec. 3. Finally, in Sec. 2.7, we computed the variance of field variation. The tree-order spatial variance, at a fixed comoving separation, grows logarirthmically in the massless limit at late times whereas it grows like $\frac{1-a^{-\delta}}{\delta}$ in the massive case. Because $\frac{1-a^{-\delta}}{\delta} \leq \ln(a)$, where the equality holds in the massless limit, the growth is suprressed in the massive case. The larger the mass, the stronger the suppression. The positive growth implies that the magnitude of the spatial variation increases with time. This fact is the main reason for some cosmologists to doubt the implications of expectation values. They argue that any local observer perceives either an increase or a decrease in the field strength as fluctuations happen. An expectation value is only a measure of average effect and, therefore, can be misleading. We showed that the tree-order variance of the field variation decreases if the quantum corrections are taken into account. Thus, the difference between the actual effect perceived by a local observer and the average effect, as the field fluctuates, is not as large as the tree-order variance implies.

In Sec. 3, we considered an IR truncated, massive inflaton field $\bar{\varphi}(t,\vec{x})=\bar{\varphi}(t)+\delta\bar{\varphi}(t,\vec{x})$, where $\bar{\varphi}(t)$ is the background field and $\delta\bar{\varphi}(t,\vec{x})$ is the fluctuation field, with a $\pm\frac{\lambda}{4!}\varphi^4$ self-interaction which drives the inflation. The background spacetime is, therefore, Friedmann-Robertson-Walker spacetime. We compute the parameters $a(t)$, $H(t)$, $\varepsilon(t)$ and the background field $\bar{\varphi}(t)$ in terms of initial values H_{i0} and ε_{i0} with $\mathcal{O}(\lambda)$ corrections that arise as a backreaction of interactions. The correlation function is evaluated at the full solution of the effective field equation, therefore, the tree-order and one-loop correlators get $\mathcal{O}(\lambda)$ and $\mathcal{O}(\lambda^2)$ corrections due to the $\mathcal{O}(\lambda)$ corrections to the parameters. The tree-order correlator in the $\lambda \to 0$ limit, for a fixed physical distance, grows at early times and asymptotes to a constant at late times; see Fig. 3.1. The growth is reduced as the ε_{i0} increases. For the $+$ $(-)$ sign choice in the interaction potential, the $\mathcal{O}(\lambda)$ correction at tree-order enhances (reduces) the growth (Fig. 3.2) whereas the $\mathcal{O}(\lambda)$ correction at one-loop order reduces (enhances) the growth (Figs. 3-4). The amplitudes of fluctuations do not grow forever and the inflaton, therefore, cannot continue rolling up its potential, which would lead to proliferation of ever fewer pocket universes. The inflaton comes to a halt eventually and, as the classical restoring force pushes it back down its potential, the fluctuations engender the density inhomogeneties required for structure formation. Generalizing the method we introduced in Sec. 2, we computed the stochastic contributions to the $\Delta^2_{\delta\bar{\varphi}_\lambda}(k)$ of the inflaton fluctuations. In the $\lambda \to 0$ limit, the $\Delta^2_{\delta\bar{\varphi}_0}$ is positive definite and decreases as k increases. The $\mathcal{O}(\lambda)$ correction to the spectrum of inflaton fluctuations, however, is enhanced significantly due to the terms with the huge factors of ε_{i0}^{-2} and ε_{i0}^{-1} that are not present in the $\mathcal{O}(\lambda)$ correction to the spectrum of the spectator scalar during de Sitter inflation. We also computed the $n_{\delta\bar{\varphi}}$ and $\alpha_{\delta\bar{\varphi}}$ for the inflaton fluctuations. The $\mathcal{O}(\lambda)$ correction the spectral index of inflaton fluctuations is enhanced by the terms involving by the factor ε_{i0}^{-1}. In the $\lambda \to 0$ limit, the tilt $n_{\delta\bar{\varphi}}-1$ is negative definite and decreases as k increases. Hence, the power spectrum is red tilted. The $\mathcal{O}(\lambda)$ correction to the $n_{\delta\bar{\varphi}}$ enhances (reduces) the red tilt for the $+$ $(-)$ sign choice in the self-interaction potential. Our numerical predictions for the $n_{\delta\varphi}$ and $\alpha_{\delta\varphi}$ are in accordance with the measurements of Planck 2018 Collaboration.

Sec. 4 is on the problems that are left open in this thesis. The Starobinsky's stochastic formalism that we applied to compute the quantum corrected two-point correlation function and the method we introduced to obtain the stochastic contributions to the quantum corrected power spectrum give the leading terms at each perturbative order. To estimate the deviation of the stochastic formalism from the exact result due to the missing subleading terms, we considered a simple model: a MMC scalar with a quartic self-interaction in de Sitter spacetime, and attempted to compute the exact fully renormalized one-loop corrected two-point correlation function applying the SK formalism. We reduced the computation to the evaluations of four integrals and succeeded in evaluating one of them. The evaluations of the remaining integrals have not been completed and hence, we have not yet computed the deviation of the stochastic correlation function from the exact result. The deviation of stochastic power spectrum, which is defined using the stochastic correlation function, from the exact power spectrum, which is defined as the Fourier transform of the exact correlation function, is therefore an unresolved issue. We, however, succeeded in computing the fully renormalized one-loop corrected power spectrum, in this simpler model, using the alternative definition of the power spectrum as the norm square of the quantum corrected mode function.

REFERENCES

[1] **Brout, R.**, **Englert, F. and Gunzig, E.** (1978). The creation of the universe as a quantum phenomenon, *Annals of Physics*, *115*(1), 78–106, https://www.sciencedirect.com/science/article/pii/0003491678901768.

[2] **Starobinsky, A.** (1980). A new type of isotropic cosmological models without singularity, *Physics Letters B*, *91*(1), 99–102, https://www.sciencedirect.com/science/article/pii/037026938090670X.

[3] **Kazanas, D.** (1980). Dynamics of the universe and spontaneous symmetry breaking, *Astrophysical Journal*, *241*, L59–L63.

[4] **Sato, K.** (1981). First-order phase transition of a vacuum and the expansion of the Universe, *Monthly Notices of the Royal Astronomical Society*, *195*, 467–479.

[5] **Mukhanov, V.F. and Chibisov, G.V.** (1981). Quantum Fluctuations and a Nonsingular Universe, *JETP Lett.*, *33*, 532–535.

[6] **Guth, A.H.** (1981). Inflationary universe: A possible solution to the horizon and flatness problems, *Phys. Rev. D*, *23*, 347–356, https://link.aps.org/doi/10.1103/PhysRevD.23.347.

[7] **Guth, A.H. and Weinberg, E.J.** (1983). Could the universe have recovered from a slow first-order phase transition?, *Nuclear Physics B*, *212*(2), 321–364, https://www.sciencedirect.com/science/article/pii/0550321383903073.

[8] **Hawking, S.W.**, **Moss, I.G. and Stewart, J.M.** (1982). Bubble collisions in the very early universe, *Phys. Rev. D*, *26*, 2681–2693, https://link.aps.org/doi/10.1103/PhysRevD.26.2681.

[9] **Hawking, S.** (1982). The development of irregularities in a single bubble inflationary universe, *Physics Letters B*, *115*(4), 295–297, https://www.sciencedirect.com/science/article/pii/0370269382903732.

[10] **Starobinsky, A.A.** (1982). Dynamics of phase transition in the new inflationary universe scenario and generation of perturbations, *Physics Letters B*, *117*(3), 175–178, https://www.sciencedirect.com/science/article/pii/037026938290541X.

[11] **Guth, A.H. and Pi, S.Y.** (1982). Fluctuations in the New Inflationary Universe, *Phys. Rev. Lett.*, *49*, 1110–1113, `https://link.aps.org/doi/10.1103/PhysRevLett.49.1110`.

[12] **Bardeen, J.M.**, **Steinhardt, P.J. and Turner, M.S.** (1983). Spontaneous creation of almost scale-free density perturbations in an inflationary universe, *Phys. Rev. D*, *28*, 679–693, `https://link.aps.org/doi/10.1103/PhysRevD.28.679`.

[13] **Vilenkin, A.** (1983). Birth of inflationary universes, *Phys. Rev. D*, *27*, 2848–2855, `https://link.aps.org/doi/10.1103/PhysRevD.27.2848`.

[14] **Albrecht, A. and Steinhardt, P.J.** (1982). Cosmology for Grand Unified Theories with Radiatively Induced Symmetry Breaking, *Phys. Rev. Lett.*, *48*, 1220–1223, `https://link.aps.org/doi/10.1103/PhysRevLett.48.1220`.

[15] **Linde, A.** (1982). A new inflationary universe scenario: A possible solution of the horizon, flatness, homogeneity, isotropy and primordial monopole problems, *Physics Letters B*, *108*(6), 389–393, `https://www.sciencedirect.com/science/article/pii/0370269382912199`.

[16] **Linde, A.D.** (1986). Eternal Chaotic Inflation, *Mod. Phys. Lett. A*, *1*, 81.

[17] **Linde, A.** (1987). Eternally Existing Self-Reproducing Inflationary Universe, *Physica Scripta*, *1987*(T15), 169.

[18] **Goncharov, A.S.**, **Linde, A.D. and Mukhanov, V.F.** (1987). The Global Structure of the Inflationary Universe, *International Journal of Modern Physics A*, *2*(3), 561–591, `https://doi.org/10.1142/S0217751X87000211`.

[19] **Aryal, M. and Vilenkin, A.** (1987). The fractal dimension of the inflationary universe, *Physics Letters B*, *199*(3), 351–357, `https://www.sciencedirect.com/science/article/pii/0370269387909324`.

[20] **Borde, A. and Vilenkin, A.** (1994). Eternal inflation and the initial singularity, *Physical Review Letters*, *72*(21), 3305–3308, `https://doi.org/10.1103%2Fphysrevlett.72.3305`.

[21] **Tryon, E.P.** (1973). Is the Universe a Vacuum Fluctuation?, *Nature*, *246*(5433), 396–397.

[22] **Vilenkin, A.** (1982). Creation of universes from nothing, *Physics Letters B*, *117*(1-2), 25–28.

[23] **Hartle, J.B. and Hawking, S.W.** (1983). Wave function of the Universe, *Phys. Rev. D*, *28*, 2960–2975, `https://link.aps.org/doi/10.1103/PhysRevD.28.2960`.

[24] **Woodard, R.P.** (2003). Quantum effects during inflation, *6th Workshop on Quantum Field Theory under the Influence of External Conditions (QFEXT03)*, pp.325–330, https://doi.org/10.48550/arxiv.astro-ph/0310757.

[25] **Woodard, R.P.** (2014). Perturbative quantum gravity comes of age, *International Journal of Modern Physics D*, *23*(09), 1430020, https://doi.org/10.1142%2Fs0218271814300201.

[26] **Starobinsky, A.A.** (1986). *In Field Theory, Quantum Gravity and Strings*, Springer-Verlag.

[27] **Starobinsky, A.A. and Yokoyama, J.** (1994). Equilibrium state of a self-interacting scalar field in the de Sitter background, *Phys. Rev. D*, *50*, 6357–6368, https://link.aps.org/doi/10.1103/PhysRevD.50.6357.

[28] **Brunier, T.**, **Onemli, V.K. and Woodard, R.P.** (2004). Two-loop scalar self-mass during inflation, *Classical and Quantum Gravity*, *22*(1), 59–84, http://dx.doi.org/10.1088/0264-9381/22/1/005.

[29] **Kahya, E.O. and Onemli, V.K.** (2007). Quantum stability of a $w < -1$ phase of cosmic acceleration, *Physical Review D*, *76*(4), http://dx.doi.org/10.1103/PhysRevD.76.043512.

[30] **Miao, S.P. and Woodard, R.P.** (2006). Leading log solution for inflationary Yukawa theory, *Phys. Rev. D*, *74*, 044019, https://link.aps.org/doi/10.1103/PhysRevD.74.044019.

[31] **Woodard, R.P.** (2007). Generalizing Starobinskĭs Formalism to Yukawa Theory & to Scalar QED, *Journal of Physics: Conference Series*, *68*, 012032, https://doi.org/10.1088/1742-6596/68/1/012032.

[32] **Prokopec, T.**, **Tsamis, N.C. and Woodard, R.P.** (2006). Two loop scalar bilinears for inflationary SQED, *Classical and Quantum Gravity*, *24*(1), 201–230, http://dx.doi.org/10.1088/0264-9381/24/1/011.

[33] **Prokopec, T.**, **Tsamis, N. and Woodard, R.** (2008). Stochastic inflationary scalar electrodynamics, *Annals of Physics*, *323*(6), 1324–1360, http://dx.doi.org/10.1016/j.aop.2007.08.008.

[34] **Woodard, R.** (2005). A Leading Log Approximation for Inflationary Quantum Field Theory, *Nuclear Physics B - Proceedings Supplements*, *148*, 108–119, https://www.sciencedirect.com/science/article/pii/S0920563205005530, dPU 2004.

[35] **Tsamis, N. and Woodard, R.** (2005). Stochastic quantum gravitational inflation, *Nuclear Physics B*, *724*(1-2), 295–328, http://dx.doi.org/10.1016/j.nuclphysb.2005.06.031.

[36] **Miao, S.P. and Woodard, R.P.** (2008). A simple operator check of the effective fermion mode function during inflation, *Classical and Quantum Gravity*, *25*(14), 145009, https://doi.org/10.1088/0264-9381/25/14/145009.

[37] **Schwinger, J.** (1961). Brownian Motion of a Quantum Oscillator, *Journal of Mathematical Physics*, *2*(3), 407–432.

[38] **Keldysh, L.V.** (1965). Diagram technique for nonequilibrium processes, *Soviet Physics JETP*, *20*(4), 1018.

[39] **Markkanen, T.**, **Rajantie, A.**, **Stopyra, S. and Tenkanen, T.** (2019). Scalar correlation functions in de Sitter space from the stochastic spectral expansion, *Journal of Cosmology and Astroparticle Physics*, *2019*(08), 001–001, `http://dx.doi.org/10.1088/1475-7516/2019/08/001`.

[40] **Tokuda, J. and Tanaka, T.** (2018). Statistical nature of infrared dynamics on de Sitter background, *Journal of Cosmology and Astroparticle Physics*, *2018*(02), 014–014, `http://dx.doi.org/10.1088/1475-7516/2018/02/014`.

[41] **Akhmedov, E.**, **Moschella, U.**, **Pavlenko, K. and Popov, F.** (2017). Infrared dynamics of massive scalars from the complementary series in de Sitter space, *Physical Review D*, *96*(2), `http://dx.doi.org/10.1103/PhysRevD.96.025002`.

[42] **Akhmedov, E.**, **Moschella, U. and Popov, F.** (2019). Characters of different secular effects in various patches of de Sitter space, *Physical Review D*, *99*(8), `http://dx.doi.org/10.1103/PhysRevD.99.086009`.

[43] **Moss, I. and Rigopoulos, G.** (2017). Effective long wavelength scalar dynamics in de Sitter, *Journal of Cosmology and Astroparticle Physics*, *2017*(05), 009–009, `http://dx.doi.org/10.1088/1475-7516/2017/05/009`.

[44] **Rigopoulos, G.** (2016). Thermal interpretation of infrared dynamics in de Sitter, *Journal of Cosmology and Astroparticle Physics*, *2016*(07), 035–035, `http://dx.doi.org/10.1088/1475-7516/2016/07/035`.

[45] **Boyanovsky, D.** (2016). Effective field theory during inflation. II. Stochastic dynamics and power spectrum suppression, *Phys. Rev. D*, *93*, 043501, `https://link.aps.org/doi/10.1103/PhysRevD.93.043501`.

[46] **Wetterich, C.** (2016). Primordial cosmic fluctuations for variable gravity, *Journal of Cosmology and Astroparticle Physics*, *2016*(05), 041–041, `https://doi.org/10.1088/1475-7516/2016/05/041`.

[47] **Chen, X.**, **Wang, Y. and Xianyu, Z.Z.** (2016). Loop Corrections to Standard Model fields in inflation, *Journal of High Energy Physics*, *2016*(8), `https://doi.org/10.1007%2Fjhep08%282016%29051`.

[48] **Assadullahi, H.**, **Firouzjahi, H.**, **Noorbala, M.**, **Vennin, V. and Wands, D.** (2016). Multiple fields in stochastic inflation, *Journal of Cosmology and Astroparticle Physics*, *2016*(06), 043–043, `http://dx.doi.org/10.1088/1475-7516/2016/06/043`.

[49] **Gautier, F. and Serreau, J.** (2015). Scalar field correlator in de Sitter space at next-to-leading order in a $1/N$ expansion, *Phys. Rev. D*, *92*, 105035, https://link.aps.org/doi/10.1103/PhysRevD.92.105035.

[50] **Boyanovsky, D.** (2015). Effective field theory during inflation: Reduced density matrix and its quantum master equation, *Phys. Rev. D*, *92*, 023527, https://link.aps.org/doi/10.1103/PhysRevD.92.023527.

[51] **Pattison, C.**, **Vennin, V.**, **Assadullahi, H. and Wands, D.** (2019). Stochastic inflation beyond slow roll, *Journal of Cosmology and Astroparticle Physics*, *2019*(07), 031–031, https://doi.org/10.1088/1475-7516/2019/07/031.

[52] **Guilleux, M. and Serreau, J.** (2015). Quantum scalar fields in de Sitter space from the nonperturbative renormalization group, *Phys. Rev. D*, *92*, 084010, https://link.aps.org/doi/10.1103/PhysRevD.92.084010.

[53] **Jain, R.K.**, **Sandora, M. and Sloth, M.S.** (2015). Radiative corrections from heavy fast-roll fields during inflation, *Journal of Cosmology and Astroparticle Physics*, *2015*(06), 016–016, https://doi.org/10.1088/1475-7516/2015/06/016.

[54] **Onemli, V.K.**, (2015), Quantum corrected power spectra of massless minimally coupled scalars during inflation: Effects of Yukawa coupling versus quartic self-interaction, https://arxiv.org/abs/1510.02272.

[55] **Boyanovsky, D.** (2016). Fermionic influence on inflationary fluctuations, *Phys. Rev. D*, *93*, 083507, https://link.aps.org/doi/10.1103/PhysRevD.93.083507.

[56] **Karakaya, G. and Onemli, V.** (2018). Quantum effects of mass on scalar field correlations, power spectrum, and fluctuations during inflation, *Physical Review D*, *97*(12), http://dx.doi.org/10.1103/PhysRevD.97.123531.

[57] **Karakaya, G. and Onemli, V.K.** (2019). Quantum Fluctuations of a Self-interacting Inflaton, arXiv:1912.07963, https://arxiv.org/abs/1912.07963.

[58] **Miao, S.P. and Park, S.** (2014). Alternate definitions of loop corrections to the primordial power spectra, *Phys. Rev. D*, *89*, 064053, https://link.aps.org/doi/10.1103/PhysRevD.89.064053.

[59] **Onemli, V.K.** (2014). Quantum corrected mode function and power spectrum for a scalar field during inflation, *Phys. Rev. D*, *89*, 083537, https://link.aps.org/doi/10.1103/PhysRevD.89.083537.

[60] **Akrami, Y.**, **Arroja, F.**, **Ashdown, M.**, **Aumont, J.**, **Baccigalupi, C.**, **Ballardini, M... Zonca, A.** (2020). Planck2018 results, *Astronomy Astrophysics*, *641*, A10, http://dx.doi.org/10.1051/0004-6361/201833887.

[61] **Tsamis, N.**, **Tzetzias, A. and Woodard, R.** (2010). Stochastic samples versus vacuum expectation values in cosmology, *Journal of Cosmology and Astroparticle Physics*, *2010*(09), 016–016, https://doi.org/10.1088/1475-7516/2010/09/016.

[62] **Tegmark, M.** (2012). How unitary cosmology generalizes thermodynamics and solves the inflationary entropy problem, *Phys. Rev. D*, *85*, 123517, https://link.aps.org/doi/10.1103/PhysRevD.85.123517.

[63] **Onemli, V.K. and Woodard, R.P.** (2002). Super-acceleration from massless, minimally coupled ϕ^4, *Classical and Quantum Gravity*, *19*(17), 4607–4626, https://doi.org/10.1088/0264-9381/19/17/311.

[64] **Onemli, V.K. and Woodard, R.P.** (2004). Quantum effects can render $w < -1$ on cosmological scales, *Phys. Rev. D*, *70*, 107301, https://link.aps.org/doi/10.1103/PhysRevD.70.107301.

[65] **Kahya, E.O.**, **Onemli, V.K. and Woodard, R.P.** (2010). Completely regular quantum stress tensor with $w < -1$, *Phys. Rev. D*, *81*, 023508, https://link.aps.org/doi/10.1103/PhysRevD.81.023508.

[66] **Kahya, E.**, **Onemli, V. and Woodard, R.** (2010). The $\zeta - \zeta$ correlator is time dependent, *Physics Letters B*, *694*(2), 101–107, http://dx.doi.org/10.1016/j.physletb.2010.09.050.

[67] **Onemli, V.** (2015). Vacuum fluctuations of a scalar field during inflation: Quantum versus stochastic analysis, *Physical Review D*, *91*(10), http://dx.doi.org/10.1103/PhysRevD.91.103537.

[68] **Finelli, F.**, **Marozzi, G.**, **Vacca, G.P. and Venturi, G.** (2002). Energy-momentum tensor of field fluctuations in massive chaotic inflation, *Phys. Rev. D*, *65*, 103521, https://link.aps.org/doi/10.1103/PhysRevD.65.103521.

[69] **Iliopoulos, J.**, **Tomaras, T.**, **Tsamis, N. and Woodard, R.** (1998). Perturbative quantum gravity and Newtons law on a flat Robertson-Walker background, *Nuclear Physics B*, *534*(1-2), 419–446, https://doi.org/10.1016%2Fs0550-3213%2898%2900528-8.

APPENDICES

APPENDIX A : The Case of Spectator Field

A.1 Special Functions

In this appendix, we describe various special functions that we use.

A.1.1 Exponential Integral $E_\beta(z)$ and Incomplete Gamma $\Gamma(\beta,z)$ Functions

The exponential integral function is

$$E_\beta(z) \equiv \int_1^\infty dt\, t^{-\beta}\, e^{-tz}\ , \tag{A.1}$$

where β and z are c-numbers. The small argument limit of exponential function

$$\mathrm{Ei}[ix] = \mathrm{Ci}[x] - [\frac{\pi}{2} - \mathrm{Si}[x]], \tag{A.2}$$

and the large argument of the exponential function

$$\mathrm{Ei}[ix] = \frac{\sin(x)}{x} + i\frac{\cos(x)}{x}. \tag{A.3}$$

The incomplete gamma function is defined as

$$\Gamma(\beta,z) \equiv \int_z^\infty dt\, t^{\beta-1}\, e^{-t}\ , \tag{A.4}$$

which satisfies the recurrence relation

$$\Gamma(\beta+1,z) = \beta\Gamma(\beta,z) + z^\beta e^{-z}\ . \tag{A.5}$$

We express the incomplete gamma function in terms of the ordinary gamma function plus an alternating power series as

$$\Gamma(\beta,z) = \Gamma(\beta) - \sum_{n=0}^{\infty} \frac{(-1)^n z^{\beta+n}}{n!(\beta+n)}\ . \tag{A.6}$$

The right side of Eq. (A.6) is replaced by its limiting value if β is a negative integer or zero.

Asymptotic expansion of the $\Gamma(\beta,z)$, as $|z| \to \infty$, and for $-\frac{3\pi}{2} < \arg(z) < \frac{3\pi}{2}$, can be represented as

$$\Gamma(\beta,z) \ \to \ z^{\beta-1} e^{-z} \sum_{n=0}^{\infty} \frac{(-1)^n \Gamma(1-\beta+n)}{z^n \Gamma(1-\beta)}\ . \tag{A.7}$$

A.1.2 Generalized Hypergeometric Function ${}_p\mathcal{F}_q(\alpha_1,\ldots,\alpha_p;\beta_1,\ldots,\beta_q;z)$

Generalized hypergeometric function is given as

$${}_p\mathcal{F}_q(\alpha_1,\ldots,\alpha_p;\beta_1,\ldots,\beta_q;z) = \frac{\Gamma(\beta_1)\cdots\Gamma(\beta_q)}{\Gamma(\alpha_1)\cdots\Gamma(\alpha_p)} \sum_{n=0}^{\infty} \frac{\Gamma(\alpha_1+n)\cdots\Gamma(\alpha_p+n)}{\Gamma(\beta_1+n)\cdots\Gamma(\beta_q+n)} \left(\frac{z^n}{n!}\right)\ , \tag{A.8}$$

where p and q are integers, α_i, β_j and z are c-numbers.

A.1.3 Cosine Integral Function $ci(z)$

The cosine integral function is defined as

$$\mathrm{ci}(z) \equiv -\int_z^\infty dt \frac{\cos(t)}{t} = \gamma + \ln(z) + \int_0^z dt \frac{\cos(t)-1}{t} , \tag{A.9}$$

where $\gamma \approx 0.577$ is the Euler-Mascheroni number. The following identity involving $\mathrm{ci}(z)$ and $\sin(z)$ is useful

$$\mathrm{ci}(z) - \frac{\sin(z)}{z} = \gamma - 1 + \ln(z) + \sum_{n=1}^\infty \frac{(-1)^n z^{2n}}{2n(2n+1)!} . \tag{A.10}$$

The asymptotic expansion of the function $\mathrm{ci}(z)$

$$\mathrm{ci}(z) \longrightarrow \frac{\sin(z)}{z} \sum_{n=0}^\infty \frac{(-1)^n \Gamma(2n+1)}{z^{2n}} - \frac{\cos(z)}{z} \sum_{n=0}^\infty \frac{(-1)^n \Gamma(2n+2)}{z^{2n+1}} , \tag{A.11}$$

for large argument, as $|z| \to \infty$, and for $-\frac{3\pi}{2} < \arg(z) < \frac{3\pi}{2}$.

A.1.4 Sine Integral Function $si(z)$

The power series expansion of function $\mathrm{si}(x)$ can be found similarly. By definition,

$$\mathrm{si}(z) = -\int_z^\infty dt \frac{\sin(t)}{t} = -\int_0^\infty dt \frac{\sin(t)}{t} + \int_0^x dt \frac{\sin(t)}{t} = -\frac{\pi}{2} + \int_0^x dt \frac{\sin(t)}{t} . \tag{A.12}$$

The asymptotic form of function $\mathrm{si}(x)$ for large argument can be found similarly

$$\mathrm{si}(z) = -\int_x^\infty dt \frac{\sin(t)}{t} = -\frac{\cos(z)}{z} - \frac{\sin(z)}{z^2} + 2\int_z^\infty dt \frac{\sin(t)}{t^3} . \tag{A.13}$$

Hence

$$\begin{aligned} \mathrm{si}(z) &= -\frac{\sin(z)}{z}\left(\frac{1}{z} - \frac{3!}{z^3} + \frac{5!}{z^5} - \frac{7!}{z^7} \dots\right) - \frac{\cos(z)}{z}\left(1 - \frac{2!}{z^2} + \frac{4!}{z^4} - \frac{6!}{z^6} \dots\right) \\ &\longrightarrow -\frac{\cos(z)}{z} . \end{aligned} \tag{A.14}$$

A.2 Massless Limit of the Tree-Order Correlator

Massless limit of Eq. (2.51) gives

$$\lim_{m\to 0} \langle \Omega | \bar{\phi}_0(t,\vec{x}) \bar{\phi}_0(t',\vec{x}') | \Omega \rangle \simeq \frac{\Gamma(D-1)}{\Gamma(\frac{D}{2})} \frac{H^{D-2}}{2^{D-1}\pi^{\frac{D}{2}}} \lim_{m\to 0} f_0(t,t',\Delta x) , \tag{A.15}$$

where

$$\begin{aligned} &\lim_{m\to 0} f_0(t,t',\Delta x) \\ &= \frac{1}{2}\Big\{\Gamma\big(-1, i\alpha(t')\big) + \Gamma\big(-1, -i\alpha(t')\big) - \Big[\Gamma(-1, iH\Delta x) + \Gamma(-1, -iH\Delta x)\Big]\Big\} . \end{aligned} \tag{A.16}$$

Recurrence relation (A.5) for $\beta=-1$ and $z=\pm iy$ with $y\in\mathbb{R}$ yields

$$\Gamma(-1,iy)+\Gamma(-1,-iy)=-\Gamma(0,iy)-\Gamma(0,-iy)-2\,\frac{\sin(y)}{y}\,. \tag{A.17}$$

Using the identity

$$\mathrm{ci}(z)=\ln(z)-\frac{1}{2}\Big[\Gamma(0,iz)+\Gamma(0,-iz)+\ln(iz)+\ln(-iz)\Big]\,, \tag{A.18}$$

for purely real $z=\alpha(t')$ and $z=H\Delta x$ in Eq. (A.17) we obtain

$$\lim_{m\to 0} f_0(t,t',\Delta x)=\mathrm{ci}(\alpha(t'))-\frac{\sin(\alpha(t'))}{\alpha(t')}-\mathrm{ci}(H\Delta x)+\frac{\sin(H\Delta x)}{H\Delta x}\,. \tag{A.19}$$

We obtain the power series representation of the tree-order correlator for the massless scalar using Eq. (A.10) in Eq. (A.19) as

$$\begin{aligned}&\lim_{m\to 0}\langle\Omega|\bar{\phi}_0(t,\vec{x})\bar{\phi}_0(t',\vec{x}')|\Omega\rangle\\ &\simeq\frac{\Gamma(D-1)}{\Gamma\left(\frac{D}{2}\right)}\frac{H^{D-2}}{2^{D-1}\pi^{\frac{D}{2}}}\left[\ln(a(t'))+\sum_{n=1}^{\infty}\frac{(-1)^n(H\Delta x)^{2n}}{(2n+1)!}\frac{a^{2n}(t')-1}{2n}\right]\,.\end{aligned} \tag{A.20}$$

This massless limit agrees with the massless limits of Eqs. (2.52) and (2.59).

A.3 Asymptotic Form of the Tree-Order Correlator

Asymptotic form of tree-order correlator (2.51)-(2.54), for a fixed comoving separation, can be calculated using Eq. (A.7) in the time dependent terms inside the curly brackets of Eq. (2.53),

$$\begin{aligned}&\big[-\alpha(t)\,\alpha(t')\big]^{-\frac{\delta}{2}}\Big\{\Gamma\big(-1+\delta,i\alpha(t')\big)+(-1)^{-\delta}\Gamma\big(-1+\delta,-i\alpha(t')\big)\Big\}\\ &\to-\frac{2}{\Gamma(2-\delta)}\left[\frac{a(t')}{a(t)}\right]^{\frac{\delta}{2}}\sum_{n=0}^{\infty}\frac{(-1)^n\Gamma(2n+2-\delta)}{\alpha^{2n}(t')}\left[\frac{\cos(\alpha(t'))}{\alpha^2(t')}\right.\\ &\qquad\left.+(2n+2-\delta)\frac{\sin(\alpha(t'))}{\alpha^3(t')}\right]\,.\end{aligned} \tag{A.21}$$

It asymptotes to zero for both massive and massless cases. (For $a(t')<a(t)$, the larger the mass, the faster it approaches to zero.) In fact, as $m\to 0$, Eq. (A.21) limits to

$$2\left[\mathrm{ci}(\alpha(t'))-\frac{\sin(\alpha(t'))}{\alpha(t')}\right]\longrightarrow 0+\mathcal{O}\left(\alpha^{-2}(t')\right)\,. \tag{A.22}$$

We used Eq. (A.11) in obtaining Eq. (A.22). Hence, at late times, tree-order correlator (2.51),

$$\begin{aligned}&\langle\Omega|\bar{\phi}_0(t,\vec{x})\bar{\phi}_0(t',\vec{x}')|\Omega\rangle\\ &\to-\frac{\mathcal{A}}{2}\Big[-\alpha(t)\alpha(t')\Big]^{-\frac{\delta}{2}}\Big\{\Gamma(-1+\delta,iH\Delta x)+(-1)^{-\delta}\Gamma(-1+\delta,-iH\Delta x)\Big\}.\end{aligned} \tag{A.23}$$

Equation (A.23) asymptotes to zero for the massive case with an increasing rate as the mass increases. In the massless case, however, it asymptotes to a nonzero constant,

$$\lim_{m\to 0}\langle\Omega|\bar{\phi}_0(t,\vec{x})\bar{\phi}_0(t',\vec{x}')|\Omega\rangle \longrightarrow \frac{\Gamma(D-1)}{\Gamma\left(\frac{D}{2}\right)}\frac{H^{D-2}}{2^{D-1}\pi^{\frac{D}{2}}}\left\{\frac{\sin(H\Delta x)}{H\Delta x}-\mathrm{ci}(H\Delta x)\right\}. \quad (A.24)$$

We used Eqs. (A.17) and (A.18) in obtaining Eq. (A.24).

A.4 Computing the Two-Loop Contribution to the Two-Point Correlation Function $\langle\Omega|\bar{\phi}(t,\vec{x})\bar{\phi}(t',\vec{x}')|\Omega\rangle$

Two-loop contribution (2.45) to the two-point correlation function consists of three terms each of which is proportional to a VEV. The VEVs are computed in Sec. 2.4.3. We give the details of the computation in each of the VEVs in sections A.4.1, A.4.2 and A.4.3, respectively.

A.4.1 The VEV $\langle\Omega|\bar{\phi}_0(t,\vec{x})\int_0^{t'}d\tilde{t}\,\bar{\phi}_0^2(\tilde{t},\vec{x}')\int_0^{\tilde{t}}d\tilde{\tilde{t}}\,a^{\frac{\delta}{2}}(\tilde{\tilde{t}})\bar{\phi}_0^3(\tilde{\tilde{t}},\vec{x}')|\Omega\rangle$

In Eq. (2.89) computation of the first VEV in two-loop correlator (2.45) is reduced to the evaluations of three double integrals. The first double integral is given as

$$\int_0^{t'}d\tilde{t}\left[a^{2n}(\tilde{t})-a^{-\delta}(\tilde{t})\right]\int_0^{\tilde{t}}d\tilde{\tilde{t}}\left[a^{\delta}(\tilde{\tilde{t}})+a^{-\delta}(\tilde{\tilde{t}})-2\right]$$
$$=-H^{-2}\left\{\left[\frac{a^{2n}(t')}{n}+2\frac{a^{-\delta}(t')}{\delta}+\frac{1}{\delta}\right]\ln(a(t'))+\frac{1}{\delta}\left[\frac{1-a^{2n+\delta}(t')}{2n+\delta}\right]+\frac{1}{n}\left[\frac{1-a^{2n}(t')}{2n}\right]\right.$$
$$\left.-\frac{1}{\delta}\left[\frac{1-a^{2n-\delta}(t')}{2n-\delta}\right]-\frac{2}{\delta}\left[\frac{1-a^{-\delta}(t')}{\delta}\right]-\frac{1}{\delta}\left[\frac{1-a^{-2\delta}(t')}{2\delta}\right]\right\}. \quad (A.25)$$

The second double integral in Eq. (2.89) is given as

$$\frac{1}{2}\int_0^{t'}d\tilde{t}\left[1-a^{-\delta}(\tilde{t})\right]\int_0^{\tilde{t}}d\tilde{\tilde{t}}\left[a^{2n+\delta}(\tilde{\tilde{t}})-a^{2n}(\tilde{\tilde{t}})+a^{-\delta}(\tilde{\tilde{t}})-1\right]=-\frac{H^{-2}}{4}\left\{\ln^2(a(t'))\right.$$
$$-2\left[\frac{1-a^{-\delta}(t')}{\delta}+\frac{1}{2n}-\frac{1}{2n+\delta}\right]\ln(a(t'))+\frac{2}{2n+\delta}\left[\frac{1-a^{2n+\delta}(t')}{2n+\delta}\right]-\left[\frac{1}{n}+\frac{2}{2n+\delta}\right]$$
$$\times\left[\frac{1-a^{2n}(t')}{2n}\right]+\frac{1}{n}\left[\frac{1-a^{2n-\delta}(t')}{2n-\delta}\right]+\left[\frac{2}{\delta}+\frac{1}{n}-\frac{2}{2n+\delta}\right]\left[\frac{1-a^{-\delta}(t')}{\delta}\right]$$
$$\left.-\frac{2}{\delta}\left[\frac{1-a^{-2\delta}(t')}{2\delta}\right]\right\}. \quad (A.26)$$

The third double integral in Eq. (2.89) is given as

$$\int_0^{t'}d\tilde{t}a^{-\delta}(\tilde{t})\int_0^{\tilde{t}}d\tilde{\tilde{t}}\left[a^{2n}(\tilde{\tilde{t}})-a^{-\delta}(\tilde{\tilde{t}})\right]\left[a^{\delta}(\tilde{\tilde{t}})-1\right]^2=-H^{-2}\left\{\left[2\frac{a^{-\delta}(t')}{\delta}+\frac{1}{\delta}\right]\ln(a(t'))\right.$$
$$+\frac{1}{2(n+\delta)}\left[\frac{1-a^{2n+\delta}(t')}{2n+\delta}\right]-\frac{2}{2n+\delta}\left[\frac{1-a^{2n}(t')}{2n}\right]+\frac{1}{2n}\left[\frac{1-a^{2n-\delta}(t')}{2n-\delta}\right]$$
$$\left.-\left[\frac{2}{\delta}-\frac{1}{2n}-\frac{1}{2(n+\delta)}+\frac{2}{2n+\delta}\right]\left[\frac{1-a^{-\delta}(t')}{\delta}\right]-\frac{1}{\delta}\left[\frac{1-a^{-2\delta}(t')}{2\delta}\right]\right\}. \quad (A.27)$$

Employing Eqs. (A.25), (A.26) and (A.27) in Eq. (2.89) yields the first VEV in two-loop correlator (2.45), given in Eq. (2.90). Notice that the infinite sum in Eq. (2.90) runs from $n=0$ and includes terms proportional to n^{-1} and n^{-2}. The $n=0$ term in the summand of infinite sum,

$$\frac{3}{2\delta}\ln^2(a(t'))+\frac{6}{\delta^2}\left[a^{-\delta}(t')+\frac{3}{4}\right]\ln(a(t'))-\frac{2}{\delta^3}\left[a^{\delta}(t')-3a^{-\delta}(t')\right.$$
$$\left.-\frac{5}{8}a^{-2\delta}(t')+\frac{21}{8}\right]\,, \tag{A.28}$$

however, is finite.

A.4.2 The VEV $\langle\Omega|\int_0^t dt''\bar{\phi}_0^2(t'',\vec{x})\int_0^{t''}dt'''a^{\frac{\delta}{2}}(t''')\bar{\phi}_0^3(t''',\vec{x})\bar{\phi}_0(t',\vec{x}')|\Omega\rangle$

In Eq. (2.92) computation of this VEV is reduced to the evaluations of three double integrals. Let us evaluate the first one. Because $t'\leq t$, we can break up the double integral into two [to be able to use Eqs. (2.51), (2.52) and (2.55)]:

$$\int_0^t dt''\int_0^{t''}dt'''=\int_0^{t'}dt''\int_0^{t''}dt'''+\int_{t'}^t dt''\int_0^{t''}dt'''\,. \tag{A.29}$$

In the first double integral on the right we have $0\leq t''\leq t'$, whereas $t'\leq t''\leq t$ in the second. Thus, using Eqs. (2.51), (2.52), (2.55) and (A.29) we express the first double integral in Eq. (2.92) as

$$\mathcal{A}a^{-\frac{\delta}{2}}(t')\sum_{n=0}^{\infty}\frac{(-1)^n(H\Delta x)^{2n}}{(2n+1)!(2n+\delta)}\left\{\int_0^{t'}dt''a^{-\delta}(t'')\Big[a^{2n+\delta}(t'')-1\Big]\int_0^{t''}dt'''\Big[a^{\delta}(t''')-1\Big]\right.$$
$$\times\Big[1-a^{-\delta}(t''')\Big]+\Big[a^{2n+\delta}(t')-1\Big]\int_{t'}^t dt''a^{-\delta}(t'')\int_0^{t''}dt'''\Big[a^{\delta}(t''')-1\Big]$$
$$\left.\times\Big[1-a^{-\delta}(t''')\Big]\right\}. \tag{A.30}$$

Evaluating the integrals we obtain,

$$-\frac{\mathcal{A}}{H^2}a^{-\frac{\delta}{2}}(t')\sum_{n=0}^{\infty}\frac{(-1)^n(H\Delta x)^{2n}}{(2n+1)!(2n+\delta)}\left\{\Big[1+2a^{-\delta}(t)\Big]\left[\frac{1-a^{2n+\delta}(t')}{\delta}\right]\ln(a(t))\right.$$
$$+\left[\frac{a^{\delta}(t')}{\delta}+\frac{1}{n}+\frac{2}{\delta}\right]a^{2n}(t')\ln(a(t'))+\left[\frac{1}{2n+\delta}+\frac{2a^{-\delta}(t)}{\delta}+\frac{a^{-2\delta}(t)}{2\delta}\right]\left[\frac{1-a^{2n+\delta}(t')}{\delta}\right]$$
$$\left.+\left[\frac{\delta}{2n^2}-\frac{2}{\delta}\right]\left[\frac{1-a^{2n}(t')}{\delta}\right]-\left[\frac{1}{2n-\delta}+\frac{1}{2\delta}\right]\left[\frac{1-a^{2n-\delta}(t')}{\delta}\right]\right\}. \tag{A.31}$$

Let us now evaluate the second double integral in Eq. (2.92). Breaking up the integrals as

$$\int_0^t dt''\int_0^{t''}dt'''=\int_0^{t'}dt''\int_0^{t''}dt'''+\int_{t'}^t dt''\int_0^{t'}dt'''+\int_{t'}^t dt''\int_{t'}^{t''}dt'''\,, \tag{A.32}$$

and using Eqs. (2.51), (2.52) and (2.55) the second double integral in Eq. (2.92) can be written as

$$\frac{\mathcal{A}}{2}a^{-\frac{\delta}{2}}(t')\sum_{n=0}^{\infty}\frac{(-1)^n(H\Delta x)^{2n}}{(2n+1)!(2n+\delta)}\left\{\int_0^{t'}dt''\left[1-a^{-\delta}(t'')\right]\int_0^{t''}dt'''\left[a^{2n+\delta}(t''')-a^{2n}(t''')\right.\right.$$
$$\left.+a^{-\delta}(t''')-1\right]+\int_{t'}^{t}dt''\left[1-a^{-\delta}(t'')\right]\int_0^{t'}dt'''\left[a^{2n+\delta}(t''')-a^{2n}(t''')+a^{-\delta}(t''')-1\right]$$
$$\left.+\left[a^{2n+\delta}(t')-1\right]\int_{t'}^{t}dt''\left[1-a^{-\delta}(t'')\right]\int_{t'}^{t''}dt'''\left[1-a^{-\delta}(t''')\right]\right\}. \qquad \text{(A.33)}$$

Evaluating the integrals in Eq. (A.33), it is obtained as

$$-\frac{\mathcal{A}}{2H^2}a^{-\frac{\delta}{2}}(t')\sum_{n=0}^{\infty}\frac{(-1)^n(H\Delta x)^{2n}}{(2n+1)!(2n+\delta)}\left\{\left[\frac{1-a^{2n+\delta}(t')}{2}\right]\ln^2(a(t))+a^{2n+\delta}(t')\ln(a(t))\right.$$
$$\times\ln(a(t'))-\frac{a^{2n+\delta}(t')}{2}\ln^2(a(t'))+\left[\frac{1-a^{2n+\delta}(t')}{\delta}\left[a^{-\delta}(t)+\frac{\delta}{2n+\delta}\right]-\frac{1-a^{2n}(t')}{\delta}\right.$$
$$\left.\times\left[1+\frac{\delta}{2n}\right]\right]\ln(a(t))+\left[\frac{a^{2n+\delta}(t')}{\delta}\left[a^{-\delta}(t)+\frac{\delta}{2n+\delta}\right]-\frac{a^{2n}(t')}{\delta}\left[1+\frac{\delta}{2n}\right]\right]\ln(a(t'))$$
$$+\frac{1-a^{2n+\delta}(t')}{\delta}\left[\frac{a^{-\delta}(t)}{2n+\delta}+\frac{a^{-2\delta}(t)}{2\delta}-\frac{a^{-\delta}(t)\,a^{-\delta}(t')}{\delta}-\frac{a^{-\delta}(t')}{2n+\delta}+\frac{a^{-2\delta}(t')}{2\delta}\right.$$
$$\left.+\frac{\delta}{(2n+\delta)^2}\right]-\frac{1-a^{2n}(t')}{2n}\left[\frac{a^{-\delta}(t)}{\delta}-\frac{a^{-\delta}(t')}{\delta}+\frac{1}{2n}+\frac{1}{2n+\delta}\right]+\frac{1-a^{2n-\delta}(t')}{2n-\delta}\frac{1}{2n}$$
$$\left.-\frac{1-a^{-\delta}(t')}{\delta}\left[\frac{a^{-\delta}(t)}{\delta}-\frac{1}{2n}+\frac{1}{2n+\delta}\right]+\frac{1-a^{-2\delta}(t')}{2\delta^2}\right\}. \qquad \text{(A.34)}$$

The third double integral in Eq. (2.92) is calculated similarly. Employing Eqs. (2.51), (2.52), (2.55) and (A.32) we express it as

$$\mathcal{A}a^{-\frac{\delta}{2}}(t')\sum_{n=0}^{\infty}\frac{(-1)^n(H\Delta x)^{2n}}{(2n+1)!(2n+\delta)}\left\{\int_0^{t'}dt''a^{-\delta}(t'')\int_0^{t''}dt'''a^{-\delta}(t''')\left[a^{2n+\delta}(t''')-1\right]\right.$$
$$\times\left[a^{\delta}(t''')-1\right]^2+\int_{t'}^{t}dt''a^{-\delta}(t'')\int_0^{t'}dt'''a^{-\delta}(t''')\left[a^{2n+\delta}(t''')-1\right]\left[a^{\delta}(t''')-1\right]^2$$
$$\left.+\left[a^{2n+\delta}(t')-1\right]\int_{t'}^{t}dt''a^{-\delta}(t'')\int_{t'}^{t''}dt'''a^{-\delta}(t''')\left[a^{\delta}(t''')-1\right]^2\right\}. \qquad \text{(A.35)}$$

Evaluating the integrals in Eq. (A.35), it is obtained as

$$-\frac{\mathcal{A}}{H^2}a^{-\frac{\delta}{2}}(t')\sum_{n=0}^{\infty}\frac{(-1)^n(H\Delta x)^{2n}}{(2n+1)!(2n+\delta)}\left\{\left[1-a^{2n+\delta}(t')\right]\left[\frac{1+2a^{-\delta}(t)}{\delta}\right]\ln(a(t))\right.$$
$$+a^{2n+\delta}(t')\left[\frac{1+2a^{-\delta}(t)}{\delta}\right]\ln(a(t'))-\frac{1-a^{2n+2\delta}(t')}{\delta}\left[a^{-\delta}(t)\left[\frac{1}{2(n+\delta)}-\frac{1}{\delta}\right]\right.$$

$$-\frac{a^{-\delta}(t')}{2(n+\delta)}\Bigg]+\frac{1-a^{2n+\delta}(t')}{\delta}\Bigg[a^{-\delta}(t)\Big[\frac{2}{2n+\delta}+\frac{2}{\delta}\Big]-\frac{1-a^{-2\delta}(t)}{2\delta}-\frac{2a^{-\delta}(t')}{2n+\delta}$$
$$-\frac{1-a^{-2\delta}(t')}{2\delta}+\frac{\delta}{2(n+\delta)(2n+\delta)}\Bigg]-\frac{1-a^{2n}(t')}{\delta}\Bigg[a^{-\delta}(t)\Big[\frac{1}{2n}+\frac{1}{\delta}\Big]-\frac{a^{-\delta}(t')}{2n}$$
$$+\frac{\delta}{n(2n+\delta)}+\frac{2}{\delta}\Bigg]+\frac{1-a^{2n-\delta}(t')}{2n(2n-\delta)}+\frac{1-a^{-\delta}(t')}{\delta}\Bigg[\frac{1}{2n}+\frac{1}{2(n+\delta)}-\frac{2}{2n+\delta}\Bigg]$$
$$+\frac{1-a^{-2\delta}(t')}{2\delta^2}\Bigg\}. \tag{A.36}$$

Combining (A.31), (A.34) and (A.36) in Eq. (2.92) yields the second VEV in two-loop correlator (2.45) as a power series expansion. The outcome is given in Eq. (2.93). Notice that the infinite sum in Eq. (2.93) runs from $n=0$ and includes terms proportional to n^{-1} and n^{-2}. However, the $n=0$ term in the summand in Eq. (2.93) is finite. In fact, it is

$$\Bigg[\frac{1-a^{\delta}(t')}{\delta}\Bigg]\frac{\ln^2(a(t))}{2}+\Bigg[\frac{1+a^{\delta}(t')}{\delta}\Bigg]\ln(a(t))\ln(a(t'))+\Bigg[\frac{1-a^{\delta}(t')}{\delta}+\frac{2}{\delta}\Bigg]\frac{\ln^2(a(t'))}{2}$$
$$+\Bigg\{\frac{1-a^{\delta}(t')}{\delta}\Bigg[5\Bigg[\frac{1+a^{-\delta}(t)}{\delta}\Bigg]+4\frac{a^{-\delta}(t)}{\delta}\Bigg]\Bigg\}\ln(a(t))+\Bigg\{\frac{1+a^{-\delta}(t)}{\delta}\Bigg[3\Bigg[\frac{1+a^{\delta}(t')}{\delta}\Bigg]$$
$$+2\frac{a^{\delta}(t')}{\delta}\Bigg]+\frac{5}{\delta^2}\Bigg\}\ln(a(t'))+\frac{5}{\delta^2}\Bigg[\frac{1+a^{-2\delta}(t)}{2\delta}\Bigg]+\frac{a^{-\delta}(t)}{\delta^2}\Bigg[13\Bigg[\frac{1-a^{\delta}(t')}{\delta}\Bigg]+\frac{1-a^{2\delta}(t')}{\delta}$$
$$-\frac{5}{2\delta}a^{-\delta}(t)a^{\delta}(t')\Bigg]-\frac{a^{\delta}(t')}{\delta^2}\Bigg[\frac{1-a^{-2\delta}(t')}{2\delta}+\frac{5}{2\delta}\Bigg]. \tag{A.37}$$

A.4.3 The VEV $\langle\Omega|\int_0^t dt'' a^{\frac{\delta}{2}}(t'')\bar{\phi}_0^3(t'',\vec{x})\int_0^{t'} d\tilde{t}\, a^{\frac{\delta}{2}}(\tilde{t})\bar{\phi}_0^3(\tilde{t},\vec{x}')|\Omega\rangle$

In Eq. (2.96) computation of this VEV is reduced to the evaluations of four double integrals. The first double integral in Eq. (2.96) gives

$$\int_0^{t'} d\tilde{t}\Big[1-a^{-\delta}(\tilde{t})\Big]\int_0^{\tilde{t}} dt''\Big[1-a^{-\delta}(t'')\Big]\Big[a^{2n+\delta}(t'')-1\Big]=-H^{-2}\Bigg\{\frac{\ln^2(a(t'))}{2}$$
$$-\Bigg[\frac{1-a^{-\delta}(t')}{\delta}+\frac{1}{2n}-\frac{1}{2n+\delta}\Bigg]\ln(a(t'))+\frac{1-a^{2n+\delta}(t')}{(2n+\delta)^2}-\frac{1-a^{2n}(t')}{2n}\Bigg[\frac{1}{2n}+\frac{1}{2n+\delta}\Bigg]$$
$$+\frac{1-a^{2n-\delta}(t')}{(2n-\delta)2n}+\frac{1-a^{-\delta}(t')}{\delta}\Bigg[\frac{1}{2n}-\frac{1}{2n+\delta}+\frac{1}{\delta}\Bigg]-\frac{1-a^{-2\delta}(t')}{2\delta^2}\Bigg\}. \tag{A.38}$$

The second double integral in Eq. (2.96) gives

$$\int_0^{t'} d\tilde{t}\Big[1-a^{-\delta}(\tilde{t})\Big]\Big[a^{2n+\delta}(\tilde{t})-1\Big]\int_{\tilde{t}}^{t} dt''\Big[1-a^{-\delta}(t'')\Big]=-H^{-2}\Bigg\{\ln(a(t))\ln(a(t'))$$
$$-\frac{\ln^2(a(t'))}{2}+\Bigg[\frac{1-a^{2n+\delta}(t')}{2n+\delta}-\frac{1-a^{2n}(t')}{2n}-\frac{1-a^{-\delta}(t')}{\delta}\Bigg]\ln(a(t))$$

$$+\left[\frac{a^{2n+\delta}(t')}{2n+\delta}-\frac{a^{2n}(t')}{2n}+\frac{a^{-\delta}(t)}{\delta}-\frac{a^{-\delta}(t')}{\delta}\right]\times\ln(a(t'))+\frac{1-a^{2n+\delta}(t')}{2n+\delta}\left[\frac{a^{-\delta}(t)}{\delta}\right.$$
$$\left.+\frac{1}{2n+\delta}\right]-\frac{1-a^{2n}(t')}{2n}\left[\frac{1+a^{-\delta}(t)}{\delta}+\frac{1}{2n}\right]+\frac{1-a^{2n-\delta}(t')}{(2n-\delta)\delta}-\frac{1-a^{-\delta}(t')}{\delta}$$
$$\left.\times\frac{a^{-\delta}(t)}{\delta}+\frac{1-a^{-2\delta}(t')}{2\delta^2}\right\}. \tag{A.39}$$

The third double integral in Eq. (2.96) gives

$$\int_0^{t'}d\tilde{t}\,a^{-\delta}(\tilde{t})\int_0^{\tilde{t}}dt''a^{-\delta}(t'')\left[\sum_{n=0}^{\infty}\frac{(-1)^n(H\Delta x)^{2n}}{(2n+1)!(2n+\delta)}\left[a^{2n+\delta}(t'')-1\right]\right]^3$$
$$=-H^{-2}\sum_{q=0}^{\infty}\sum_{p=0}^{q}\sum_{n=0}^{p}\Gamma_{qpn}(H\Delta x)^{2q}\left\{\frac{1}{2(q+\delta)}\left[\frac{1-a^{2q+\delta}(t')}{2q+\delta}+\frac{1-a^{-\delta}(t')}{\delta}\right]\right.$$
$$-\frac{3}{2p+\delta}\left[\frac{1-a^{2p}(t')}{2p}+\frac{1-a^{-\delta}(t')}{\delta}\right]+\frac{3}{2(q-p)}\left[\frac{1-a^{2(q-p)-\delta}(t')}{2(q-p)-\delta}+\frac{1-a^{-\delta}(t')}{\delta}\right]$$
$$\left.+\frac{1}{\delta}\left[\frac{1-a^{-\delta}(t')}{\delta}-\frac{1-a^{-2\delta}(t')}{2\delta}\right]\right\}, \tag{A.40}$$

where we define the coefficients

$$\Gamma_{qpn}\equiv\frac{(-1)^q}{[2(q-p)+1]![2(q-p)+\delta][2(p-n)+1]![2(p-n)+\delta][2n+1]![2n+\delta]}\,. \tag{A.41}$$

The fourth double integral in Eq. (2.96) gives

$$\int_0^{t'}d\tilde{t}\,a^{-\delta}(\tilde{t})\int_{\tilde{t}}^{t}dt''a^{-\delta}(t'')\left[\sum_{n=0}^{\infty}\frac{(-1)^n(H\Delta x)^{2n}}{(2n+1)!(2n+\delta)}\left[a^{2n+\delta}(\tilde{t})-1\right]\right]^3$$
$$=-\frac{H^{-2}}{\delta}\sum_{q=0}^{\infty}\sum_{p=0}^{q}\sum_{n=0}^{p}\Gamma_{qpn}(H\Delta x)^{2q}\left\{\frac{1-a^{2q+\delta}(t')}{2q+\delta}-3\frac{1-a^{2p}(t')}{2p}+3\frac{1-a^{2(q-p)-\delta}(t')}{2(q-p)-\delta}\right.$$
$$+\frac{1-a^{-2\delta}(t')}{2\delta}-a^{-\delta}(t)\left[\frac{1-a^{2(q+\delta)}(t')}{2(q+\delta)}-3\frac{1-a^{2p+\delta}(t')}{2p+\delta}+3\frac{1-a^{2(q-p)}(t')}{2(q-p)}\right.$$
$$\left.\left.+\frac{1-a^{-\delta}(t')}{\delta}\right]\right\}. \tag{A.42}$$

Employing Eqs. (A.38)-(A.40) and (A.42) in Eq. (2.96) yields the third VEV in two-loop correlator (2.45), given in Eq. (2.97). Notice that the $n=0$ term in the summand of the first infinite sum in Eq. (2.97) is finite. It is

$$-\frac{1}{\delta^2}\left[a^{\delta}(t')-a^{-\delta}(t')\right]\left[\ln(a(t))+\frac{2+a^{-\delta}(t)}{\delta}\right]+\frac{2}{\delta}\ln(a(t))\ln(a(t'))$$
$$+\frac{1}{\delta^2}\left[2a^{-\delta}(t)+a^{\delta}(t')+a^{-\delta}(t')+2\right]\ln(a(t'))\,. \tag{A.43}$$

Notice also that, for $p=0$ (which implies $n=0$) the terms proportional to p^{-1} in the summand of triple infinite sum in Eq. (2.97),

$$\Gamma_{qpn}(H\Delta x)^{2q}\, 3\frac{1-a^{2p}(t')}{2p}\left[\frac{1}{2p+\delta}+\frac{1}{\delta}\right] \longrightarrow -6\frac{(-1)^q(H\Delta x)^{2q}\ln(a(t'))}{\delta^3[2q+1]![2q+\delta]}\ , \quad (A.44)$$

is finite as well. Let us note finally that for $p=q$, the terms proportional to $(q-p)^{-1}$ in the summand of triple infinite sum,

$$\Gamma_{qpn}(H\Delta x)^{2q}\left[\frac{a^{-\delta}(t)}{\delta}\, 3\frac{1-a^{2(q-p)}(t')}{2(q-p)} - 3\frac{1-a^{2(q-p)-\delta}(t')}{2(q-p)-\delta}\frac{1}{2(q-p)} - \frac{1-a^{-\delta}(t')}{\delta}\frac{3}{2(q-p)}\right]$$

$$\longrightarrow -3\frac{(-1)^q(H\Delta x)^{2q}\left\{a^{-\delta}(t')\left[\frac{1-a^{\delta}(t')}{\delta}\right]+\left[a^{-\delta}(t)+a^{-\delta}(t')\right]\ln(a(t'))\right\}}{\delta^2[2(q-n)+1]![2(q-n)+\delta][2n+1]![2n+\delta]}\ , \quad (A.45)$$

are also finite. Combining all the three VEVs, computed in Secs. A.4.1-3, in Eq. (2.45) gives the two-loop correlator.

APPENDIX B : The Case of Inflaton Field

B.1 The Comoving Time t in Terms of $q(t)$, H_{i0} and ε_{i0}

In this Appendix, we express the comoving time t in the interacting theory in terms of $q(t)$ defined in Eq. (3.26) and the initial values H_{i0} and ε_{i0}.

We integrate Eq. (3.24), neglecting the term linear in ε_{i0} among the $\mathcal{O}(\lambda)$-terms as a zeroth order approximation in our iteration, and obtain

$$z^3+Az^2+Bz+C\cong 0\,, \tag{B.1}$$

where we define

$$z\equiv H_{i0}t,\ \rho\equiv\pm\frac{\lambda\xi}{12}\varepsilon_{i0}^{-2},\ A\equiv-\frac{\varepsilon_{i0}^{-1}}{2\rho}\Big[1+3\rho\Big],\ B\equiv\frac{\varepsilon_{i0}^{-2}}{\rho}\Big[1+\frac{\rho}{2}\Big],\ C\equiv-\frac{\varepsilon_{i0}^{-3}}{2\rho}\Big[1-q^2\Big]\,. \tag{B.2}$$

Let

$$Q\equiv\frac{3B-A^2}{9},\ R\equiv\frac{9AB-27C-2A^3}{54},\ S\equiv\sqrt[3]{R+\sqrt{D}},\ T\equiv\sqrt[3]{R-\sqrt{D}}, \tag{B.3}$$

where the discriminant $D\equiv Q^3+R^2$. The roots of the cubic polynomial are

$$z_1=S+T-\frac{A}{3},\ z_2=-\frac{S+T}{2}-\frac{A}{3}+i\frac{\sqrt{3}}{2}(S-T),\ z_3=-\frac{S+T}{2}-\frac{A}{3}-i\frac{\sqrt{3}}{2}(S-T)\,. \tag{B.4}$$

If the discriminant $D>0$, one root is real and two are complex conjugate of each other. If $D=0$, all roots are real and at least two are equal. If $D<0$, as is the case for cubic polynomial (B.1), all roots are real and unequal. The physically relevant root,

$$z_2=H_{i0}t=\varepsilon_{i0}^{-1}\Big[1-q\Big]\Big[1+\frac{\rho}{2}\Big[1-2q\Big]+\mathcal{O}(\lambda^2)\Big]\,, \tag{B.5}$$

yields the comoving time given in Eq. (3.27).

CURRICULUM VITAE

Name Surname: Gülay Karakaya

B.Sc.: June 2010, Kocaeli University, Faculty of Science and Letters, Physics Department

B.Sc.: June 2011, Kocaeli University, Faculty of Science and Letters, Mathematics Department

M.Sc.: January 2014, Istanbul Technical University, Faculty of Science and Letters, Department of Physics Engineering

PROFESSIONAL EXPERIENCE AND REWARDS:

- May 2017 - February 2020 Research Assistant in Department of Physics Engineering, Istanbul Technical University.

PUBLICATIONS AND PRESENTATIONS ON THE THESIS:

- **Karakaya, G.**, Onemli, V. K., 2018. Quantum Effects of Mass on Scalar Field Correlations, Power Spectrum and Fluctuations during Inflation, *P*hys. Rev. D, 97, 123531.
- **Karakaya, G.**, Onemli, V. K., 2019. Quantum Fluctuations of a Self-interacting Inflaton, arXiv:1912.07963.
- **Karakaya, G.**, Onemli, V. K., 2020. Quantum Fluctuations of a Self-interacting Inflaton, Workshop on High Energy Physics, Astrophysics and Cosmology, İstanbul University, Turkey.
- **Karakaya, G.**, Onemli, V. K., 2021. Stochastic power spectrum during inflation, Workshop on High Energy Physics, Astrophysics and Cosmology, İstanbul University, Turkey. (Invited speaker)